INVESTIGATION OF CELLULAR AND MOLECULAR MECHANISMS OF ENDOTHELIAL DYSFUNCTION IN THE KIDNEY

ADELE R. GORDON

Thesis presented for the degree of Doctor of Philosophy

University of Edinburgh

April 2003

DECLARATION

This thesis and the data presented in it are entirely the result of my own efforts. This work contains no material which has been accepted for the award of any other degree or diploma in any university or tertiary institution and, to the best of my knowledge contains no material previously published or written by another person, except where stated in the text.

31st October 2003

Adele Rhona Gordon

ABSTRACT

Many cardiovascular diseases are associated with abnormal function of the endothelium, a condition commonly referred to as endothelial dysfunction (ED). ED is well characterised as the diminished capacity of the endothelium to mediate vasorelaxation that results from a decrease in the availability of nitric oxide (NO). However, additional physiological roles of NO may also be altered. For example, NO plays a vital role in promoting natriuresis/diuresis within the kidney and thus contributes to the maintenance of normal blood pressure. This prompted the hypothesis that diminished availability of NO as a result of ED in the kidney could result in sodium retention and may provide an explanation for the sustained elevation of blood pressure in hypertension. There are several reasons for why NO availability may be decreased during ED. One proposed explanation is altered activity of endothelial nitric oxide synthase (eNOS), the enzyme responsible for generating NO. However, little is known of the mechanisms involved in regulating eNOS activity within the kidney. This thesis describes experiments which aim to further elucidate the cellular and molecular mechanisms involved in the regulation and activation of renal eNOS and discusses how these may be affected during ED.

Subcellular localisation to caveolae and interactions with proteins which reside there (e.g. caveolin-1, bradykinin receptor and endothelin type B receptor) are important features of eNOS regulation. The first approach was to determine if interactions between eNOS and regulatory proteins within the kidney were altered in an animal model of ED, the spontaneously hypertensive rat (SHR). Western blot analysis of isolated caveolae revealed no alterations in eNOS or caveolin expression in SHR compared to normotensive WKY rats. Likewise, no change in caveolin expression was observed in whole kidney homogenates, whereas eNOS expression was slightly increased. Although interactions between caveolin-1 and eNOS in isolated endothelial cells were observed, it was not possible to replicate this within tissue, and raises questions concerning the extent to which these proteins interact *in vivo*. These

data imply that alterations in renal caveolin expression are not altered during ED whereas eNOS may be upregulated.

Experiments then focused on activation of eNOS by endothelin-1. Within the renal medulla this is mediated by the endothelin type B receptor (ET_B) and leads to inhibition of sodium reabsorption. However, the cellular mechanisms remain unknown due to the lack of precise localisation of medullary ET_B. Therefore, localisation of ET_B was investigated by introducing a LacZ reporter gene into the endothelin type B receptor locus (*EDNRB*) by homologous recombination in ES cells, thereby generating *EDNRB*-LacZ mice which expressed LacZ wherever ET_B was expressed. These mice, together with another strain of *EDNRB*-LacZ mice (supplied by Dr. M. Shin), were used to determine renal ET_B localisation. Analysis of LacZ expression in homozygote mice revealed intense staining within the medulla, particularly within endothelial cells of the medullary capillaries. In contrast, renal tubules were negative for transgene expression. Since the vasa recta is also a major site of eNOS expression within the medulla, these results suggest that ET-1 activates eNOS by binding to ET_B located on vasa recta. These observations enhance the understanding of the basic cellular and molecular mechanisms involved in ET_B/eNOS mediated sodium transport and provide a platform for ongoing physiological experiments and investigations into potential pathways which may be associated with renal ED.

TABLE OF CONTENTS

INDEX OF FIGURES AND TABLES

CHAPTER 1

CHAPTER 2

CHAPTER 3

CHAPTER 4

CHAPTER 5

CHAPTER 6

CHAPTER 7

ABBREVIATIONS

ACh	acetylcholine
ADMA	asymmetric dimethyl arginine
ADP	adenosine diphosphate
AP-1, -2	activator protein-1, -2
ATP	adenosine triphosphate
BAEC	bovine aortic endothelial cells
BH_4	tetrahydrobiopterin
BK	bradykinin
BLMEC	bovine lung microvascular endothelial cells
bp	base pair
BSA	bovine serum albumin
CaM	calmodulin
cGMP	cyclic guanosine monophosphate
CSD	caveolin scaffolding domain
Cys	cysteine
DAF-2A	4,5-diaminofluoresceindiacetate
dATP	2'-deoxyadenosine-5'-triphosphate
dCTP	2'-deoxycytidine-5'-triphosphate
dGTP	2'-deoxyguanosine-5'-triphosphate
DMSO	dimethylsulfoxide
DNA	deoxyribonucleic acid
dNTP	deoxynucleotide-5'-triphosphate
DTT	dithiothreitol
dTTP	2'-deoxythymidine-5'-triphosphate
DOCA	deoxycorticosterone acetate
EB	embryoid body
ECL	enhanced chemiluminescent
ED	endothelial dysfunction
EDHF	endothelium-derived hyperpolarizing factor

EDNRA	endothelin type A receptor (gene)
EDNRB	endothelin type B receptor (gene)
EDRF	endothelium-derived relaxing factor
EDTA	ethylenediaminetetra-acetic acid
EGTA	ethyleneglycol-bis(β-aminoethylether)-N,N,N',N'-tetra-acetic acid
En-2	engrailed-2
ENaC	epithelial sodium channel
eNOS	endothelial nitric oxide synthase
ES	embryonic stem
ET-1	endothelin-1
ET_A	endothelin type A receptor
ET_B	endothelin type B receptor
FAD	flavin adenine dinucleotide
FCS	foetal calf serum
FMN	flavin mononucleotide
GFP	green fluorescent protein
Gly	glycine
GMEM	Glasgow's modification of Eagle's Medium
GPCR	G-protein coupled receptor
GST	glutathione-S-transferase
HRP	horseradish peroxidase
Hsp90	heat shock protein 90
HUVEC	human umbilical vein endothelial cell
IMCD	inner medullary collecting duct
iNOS	inducible nitric oxide synthase
IRES	internal ribosome entry site
kb	kilobase
kD	kilodalton
L-arg	L-arginine
Leu	Leucine
LIF	leukaemia inhibitory factor

L-NAME	N-nitro-L-arginine methyl ester
L-NMMA	N-monomethyl-L-arginine
LB	Luria-Bertani
lysoPC	lysophosphatidylcholine
MBS	Mes-buffered saline
MCP	multi-channel pipette
MU	4-methylumbelliferone
NA	noradrenaline
NADPH	nicotinamide adenine dinucleotide phosphate (reduced form)
Neo	neomycin
NF-1	nuclear factor-1
NLS	nuclear localisation signal
nNOS	neuronal nitric oxide synthase
NOS	nitric oxide synthase
NOSIP	eNOS interacting protein
NP-40	Nonidet P-40
O_2^-	superoxide
OD	optical density
OG	octyl-glucoside
oxLDL	oxidised low density lipoprotein
PAGE	polyacrylamide gel electrophoresis
pBS	pBluescript II SK
PBS	phosphate buffered saline
PCR	polymerase chain reaction
PE	phenylephrine
PGS	protein G sepharose
PKB	protein kinase B
PKC	protein kinase C
PKG	protein kinase G
PMSF	phenylmethylsulfonylfluoride
PSS	physiological salt solution

PVDF	polyvinylidene difluoride
RNA	ribonucleic acid
RT-PCR	reverse transcriptase polymerase chain reaction
SDS	sodium dodecyl sulfate
Ser	serine
sGC	soluble guanylate cyclase
SV40polyA	SV40 polyadenylation
SHR	spontaneously hypertensive rat
SHR-SP	spontaneously hypertensive rat – stroke prone
sl	spotting lethal
SOD	superoxide dismutase
Sp1	SV40 virus promoter specific transcription factor protein 1
SSC	saline-sodium citrate buffer
TAE	tris-acetate-EDTA
TBS	tris-buffered saline
TE	tris-EDTA
TEMED	N,N,N',N'-tetramethylethylenediamine
TESPA	aminopropylethoxysilane
TGFβ	transforming growth factor β
Thr	threonine
TNFα	tumour necrosis factor α
UV	ultraviolet
VEGF	vascular endothelial growth factor
WKY	Wistar-Kyoto rat

Standard prefixes:

m	milli (10^{-3})
μ	micro (10^{-6})
n	nano (10^{-9})
p	pico (10^{-12})

PRESENTATIONS

The following poster and oral presentations have arisen from the work described in this thesis.

" Caveolin-1 and eNOS expression in spontaneously hypertensive rats and Wistar-Kyoto rats." Abstract in *Nitric Oxide Biology and Chemistry* 2002; 6, 394. Poster presentation at 2nd International Conference of Biology, Chemistry and Therapeutic Applications of Nitric Oxide, Prague (2002).

" Investigation of eNOS and caveolin interactions as a potential mechanism for endothelial dysfunction." Oral presentation at CVRI Annual Symposium, Edinburgh (2002).

" The regulation of eNOS during endothelial dysfunction." Poster presentation at Wellcome Trust PhD Meeting, Cambridge (2002).

" Endothelin B receptor expression in the kidney – a transgenic approach." Poster presentation at Scottish Cardiovascular Forum, St Andrews (2002).

" Interactions of nitric oxide with the renal endothelin system – localisation of the endothelin type B receptor using a transgenic approach." Oral presentation at Nitric Oxide UK Forum, London (2003).

ACKNOWLEDGEMENTS

I am indebted to my supervisor, Dr. Yuri Kotelevtsev for his constant encouragement and support throughout the duration of my PhD. He must be given the credit for many of the scientific ideas explored in this thesis and provided expert guidance and motivation to see me through to the end. Thanks also to Professor David Webb for his interest and support and for careful editing of this thesis.

I am especially grateful to Dr. Myung Shin at the Fox Chase Cancer Centre, Philadelphia, USA for his generous gift of the *EDNRB*-LacZ knock-in mice.

Thank you to The Wellcome Trust and Cardiovascular Research Initiative for supporting this 4 year PhD.

Thanks also to those who assisted me with practical issues. In particular:
Dr. Andrew Smith and Stephen Meek at the Institute for Stem Cell Research, Edinburgh for invaluable help with gene targeting.
Dr. J. Ure at the Institute for Stem Cell Research, Edinburgh for performing microinjection of ES cells.
Dr. Lesley Forrester, Richard Axton and Helen Taylor at the John Hughes Bennett Laboratories, Edinburgh for help with ES cell differentiation and for useful discussions.
Dr Juliette Hadchouel for her excellent LacZ staining protocols and never tiring from my constant emails.
Professor Stewart Fleming, University of Dundee for help with renal histology.
Fiona Gulliver-Sloan for micro-dissection of mesenteric vessels for use in myography.
Linda Sharp for technical support with the confocal microscope.
Pat, Stan and all the staff in the animal house for help with animal procedures.

And finally a huge thank-you to my family and friends:

To my parents and sisters, who have shown me endless love and support. You'll soon be able to tell people I'm no longer a student!

To my grandparents, for always showing an interest and for supplying me with fish supper money!

To close friends, Sonia and Flora, for long chats and lots of laughs.

And to Jamie, for helping me through the difficult times, for encouraging me and for persuading me I could do it. Thanks for being there.

CHAPTER 1

GENERAL INTRODUCTION

1.1 THE ENDOTHELIUM AND ENDOTHELIAL DYSFUNCTION — AN OVERVIEW

The historical view of the endothelium as merely an inert single layer of cells lining the blood vessels has radically changed in the last 20 years. It is now clear that the vascular endothelium controls many important physiological functions including control of vascular tone through the production of vasodilator (e.g. nitric oxide, prostacyclin, endothelium-derived hyperpolarizing factor (EDHF)) and vasoconstrictor (e.g. endothelin, angiotensin II, thromboxane A_2, prostaglandin H_2) substances. Therefore, it is of no surprise that the endothelium is a major target for cardiovascular risk factors such as hypertension. Indeed, hypertension is associated with an imbalance in relaxing and contracting factors resulting in abnormal function of the endothelium, a condition commonly referred to as endothelial dysfunction (ED).

In addition to altered vascular tone, other roles of the endothelium may be affected during ED. These include inhibition of platelet aggregation and smooth muscle cell proliferation and prevention of leukocyte adhesion to the vessel wall. As depicted in figure 1-1 alterations in these actions may result in pro-atherogenic consequences. ED is therefore thought to be a key initial event in the development of hypertension, atherosclerosis and other cardiovascular diseases.

Although associated with alterations in several endothelial factors (e.g. decreased EDHF and increased thromboxane A_2 or prostaglandin H_2), ED is most commonly characterised as the diminished bioavailability of endothelium-derived nitric oxide (NO). This free radical gas mediates the actions described above as well as many other physiological processes throughout the cardiovascular system and other regions of the body. However, the molecular mechanisms associated with decreased NO bioavailability remain largely unknown. Elucidation of such mechanisms may prove extremely important in the understanding of the pathologic processes involved in ED and hypertension. One conclusion that can be drawn from the vast array of studies on

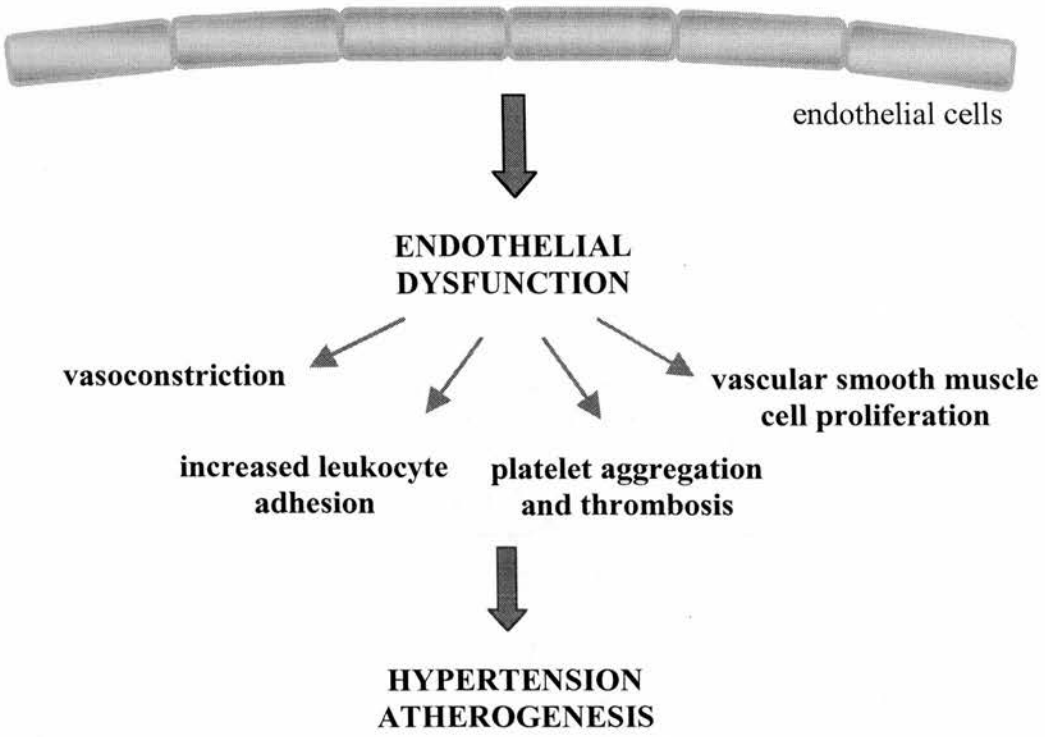

Figure 1-1. Endothelial dysfunction is associated with the development and progression of hypertension and atherosclerosis.

ED is that the mechanisms involved vary in different models of hypertension and in different vascular beds. Furthermore, given the importance of the kidney in the control of long term blood pressure and development of hypertension and the recently described role of NO as a regulator of natriuresis and diuresis, it is surprising that little is known of whether this is affected by ED.

Endothelium-derived NO production is tightly regulated on several levels, any of which may be affected during ED. One proposed explanation to account for the reduction of NO bioavailability is altered activity of endothelial nitric oxide synthase (eNOS), the enzyme responsible for generating NO within the endothelium. Recent data imply that alterations in interactions with regulatory proteins, such as caveolin-1, may be involved.

Moreover, with regard to the kidney, regulatory information for eNOS is almost absent despite the crucial role of eNOS in normal renal physiology. Several recent studies suggest that the endothelin system may be involved and that endothelin-1 (ET-1) may be a major physiological activator of eNOS and NO production within the kidney. However, the mechanisms involved are only beginning to be unravelled.

Therefore, the subject of this thesis is to explore regulation of eNOS within the kidney by investigating whether eNOS activity is altered during ED and by examining interactions with the ET-1 system. In particular, it focuses on interactions of eNOS with receptors (e.g. endothelin type B receptor (ET_B)) and regulatory proteins (e.g. caveolin-1) that are known to play a role in activation and control of this enzyme.

1.2 PHYSIOLOGICAL ROLES OF NO

In 1980, Furchgott and Zawadzki (Furchgott & Zawadzki, 1980) demonstrated that vascular relaxation in response to acetylcholine (ACh) was dependent on the presence of the endothelium and named the factor responsible as endothelium-derived relaxing factor (EDRF). Several years later, the actions of EDRF were attributed to that of the free radical gas, NO (Ignarro *et al.*, 1986; Furchgott *et al.*, 1987; Ignarro *et al.*, 1987; Palmer *et al.*, 1987). Now, 20 years on, NO is considered a major, widespread effector molecule in cardiovascular, renal and brain physiology as well a key regulator in the immune response (Moncada *et al.*, 1991). Although the roles and regulation of NO in the kidney are the focus of this thesis, many of the pathways and mechanisms involved in NO synthesis and regulation were first established within the vasculature. Therefore, vascular derived NO will also be reviewed.

1.2.1 NO in the vasculature

Within the vasculature, NO is produced by endothelial cells and induces relaxation of vascular smooth muscle cells. In addition, NO has a regulatory effect on platelets and circulating monocytes. The pathways involved in physiological stimulation and production of NO and the effects NO has within the vasculature have been the source of much interest within the cardiovascular field.

1.2.1.1 NO release by blood vessels

Physiologically, shear stress appears to be the main stimulus for the tonic release of NO. However, endothelial cells may also be stimulated to produce NO by circulating, autocrine and paracrine substances.

Shear stress is caused by the friction of rapid blood flow on the endothelium. Rubanyi *et al* were first to observe that the NO concentration released from endothelial cells and subsequent vasorelaxation of smooth muscle cells of a perfused artery increased with perfusion rate (Rubanyi *et al.*, 1986) suggesting that NO is a mediator of flow-dependent vasodilatation. Shear stress is now known to be one of the most important physiological regulators of NO production (Pohl *et al.*, 1986; Cooke *et al.*, 1990; Joannides *et al.*, 1995).

However, NO synthesis and release is also stimulated by a variety of agonists (e.g. bradykinin (BK), endothelin-1 (ET-1), adenosine diphosphate (ADP) and thrombin) which elicit their effects by causing an increase in intracellular calcium ($[Ca^{2+}]_i$) upon binding to specific membrane bound G-protein coupled receptors (GPCRs). *In vitro* and *in vivo* studies show that specific inhibitors of NO synthesis can abolish the effects of these agonists on relaxation of smooth muscle cells (Rees *et al.*, 1989; Vallance *et al.*, 1989; Whittle *et al.*, 1989; Rees *et al.*, 1990). Some exogenous pharmacological agents act in similar ways (e.g. ACh acting via muscarinic receptors and the calcium ionophore, A23187). These activators of NO synthesis have been extensively reviewed elsewhere (Busse *et al.*, 1985; Furchgott & Vanhoutte, 1989).

The intracellular regulatory mechanisms controlling NO-stimulated relaxation of vascular smooth muscle cells are summarised in figure 1-2 producing a simplified picture of NO production. In the endothelium, NO is formed when the amino acid, L-arginine is converted to L-citrulline (Palmer *et al.*, 1988a; Palmer *et al.*, 1988b). This reaction is catalysed by one of three nitric oxide synthases (NOS), eNOS, which is activated in response to increases in $[Ca^{2+}]_i$ and requires the presence of several cofactors. This enzyme and the other NOS isoforms, neuronal NOS (nNOS) and inducible NOS (iNOS), will be discussed in more detail in section 1.3. Downstream, NO diffuses abluminally and induces relaxation of the smooth muscle by increasing cyclic guanosine monophosphate (cGMP) formation via stimulation of the enzyme soluble guanylate cyclase (sGC) (Rapoport *et al.*, 1983). This culminates in activation of cGMP-dependent protein kinases (protein kinase G, PKG), dephosphorylation of myosin light chains, leading to vasodilatation (Draznin *et al.*, 1986; Moncada *et al.*, 1991).

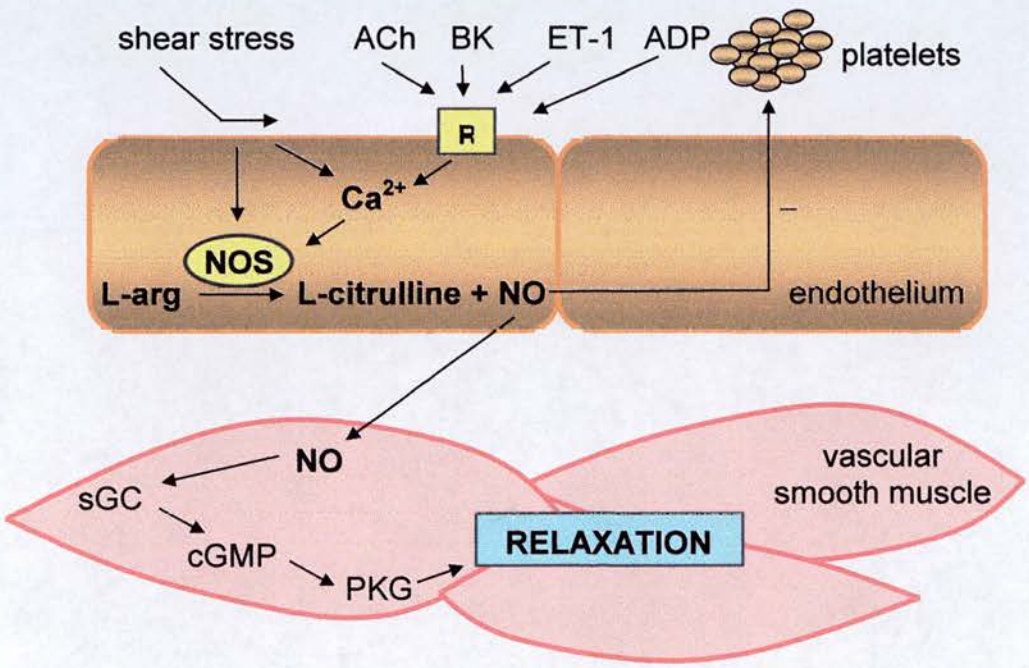

Figure 1-2. Production of NO in vasculature. Abbreviations: ACh, acetylcholine; BK, bradykinin; ET-1, endothelin-1; ADP, adenosine diphosphate; R, receptor; L-arg, L-arginine; NOS, nitric oxide synthase; sGC, soluble guanylate cyclase; cGMP, cyclic guanosine monophosphate; PKG, protein kinase G.

1.2.1.2 Regulation of blood pressure

NO is continuously produced by endothelial cells and acts on underlying vascular smooth muscle cells to maintain a constant state of vasodilatation and thus contributes to maintenance of vascular tone. This effect is unmasked by infusion of isolated arteries with L-NMMA, a specific inhibitor of NO biosynthesis, resulting in abolition of endothelium-dependent relaxation and induction of endothelium-dependent contractions (Palmer *et al.*, 1988b; Rees *et al.*, 1990). *In vivo* studies produced similar results. Acute intravenous infusion of L-NMMA in anaesthetised rabbits induced an increase in blood pressure (Rees *et al.*, 1989), a study which has since been replicated in other species (Aisaka *et al.*, 1989; Whittle *et al.*, 1989; Gardiner *et al.*, 1990; Rees *et al.*, 1990). Furthermore, administration of L-NMMA into the brachial arteries of the human forearm caused a 50% reduction in basal blood flow (Vallance *et al.*, 1989) and an increase in blood pressure (Haynes *et al.*, 1993). Thus, under normal conditions, basal release of NO plays an important role in regulating blood flow and blood pressure. A deficiency in NO would therefore have an adverse effect and may result in the development and maintenance of hypertension.

1.2.1.3 Regulation of smooth muscle cell proliferation

As well as regulating relaxation of vascular smooth muscle cells, the endothelium also plays a role in maintaining vascular structure. In the presence of a healthy, intact endothelium, vascular smooth muscle cells remain in a relatively quiescent state due to the presence of NO and other regulatory factors (Garg & Hassid, 1989). However, removal of the endothelium and hence a deficiency in NO release, results in smooth muscle cell proliferation (Clowes *et al.*, 1983), a common feature in the development of atherosclerotic lesions.

1.2.1.4 Regulation of platelet aggregation and adhesion

NO has an inhibitory effect on platelet aggregation and adhesion to the vessel wall (Furlong *et al.*, 1987; Radomski *et al.*, 1987b; Radomski *et al.*, 1987a). Aside from the stimulated endothelial generation of NO described above, platelets themselves

can induce production of NO from the endothelium by releasing ADP (see figure 1-2). In addition, platelets also possess their own L-arginine/NO pathway similar to that described above and synthesise NO when activated by ADP, collagen and thrombin (Radomski *et al.*, 1987b). This autocrine and paracrine generation of NO may represent a negative feedback mechanism of anti-aggregation. However, during ED this mechanism may be altered and favour platelet aggregation and adhesion to the vessel wall.

1.2.1.5 Regulation of leukocyte adhesion

NO also inhibits leukocyte adhesion to the vessel wall by altering expression of cell surface adhesion molecules (Kubes *et al.*, 1991; Niu *et al.*, 1994). Alteration of physiological NO release can lead to infiltration of monocytes to the endothelium, a key initial step in the development of foam cells and progression of atherosclerosis.

Therefore, endothelium-derived NO has multiple effects within the vasculature. By controlling blood pressure and protecting the vessel wall from platelet adhesion and infiltration of monocytes and smooth muscle cells, NO plays a key role in prevention of hypertension and atherosclerosis.

1.2.2 NO in the kidney

It is well known that the kidney plays a major role in the long-term regulation of blood pressure. This is largely controlled through changes in extracellular fluid volume by pressure natriuresis/diuresis where an increase in blood pressure is compensated by an increase in renal excretion of salt and water (Guyton *et al.*, 1990). It is also widely recognised that the kidney may be the key to understanding hypertension. This is highlighted by the observation that all genetic disorders currently identified as contributing to or causing hypertension involve mutations in genes which control renal sodium handling (Lifton, 1996). One of the major regulators of blood pressure and salt/water homeostasis is the renin-angiotensin system which plays an important role in the process of pressure natriuresis (reviewed

in (Guyton & Hall, 2000a)). More recently, the NO system has also been shown to contribute to the control of pressure natriuresis/diuresis.

1.2.2.1 Control of natriuresis/diuresis

The diuretic and natriuretic effects of NO were first described by Lahera *et al* who studied the contribution of NO to renal function in the absence of changes in blood pressure. Intrarenal infusion of rats with ACh and BK significantly increased renal blood flow, urinary volume and sodium excretion without changes in blood pressure (Lahera *et al.*, 1990; Lahera *et al.*, 1991a). Intravenous infusions of low doses (0.1-1.0μg/kg/min) of L-NAME, an inhibitor of NO release, to rats resulted in decreased urine volume and sodium excretion again without affecting systemic blood pressure and glomerular filtration rate. In contrast, infusion of higher doses (10-50μg/kg/min) resulted in significantly increased blood pressure and after an initial fall in urinary volume and sodium excretion, these parameters were normalised through pressure natriuresis (Lahera *et al.*, 1991b). The primary determinant of glomerular filtration and the amount of sodium excreted is renal perfusion pressure. By inducing increases in renal perfusion pressure in anaesthetised dogs, Salom *et al*, described the involvement of NO in pressure natriuresis. Intrarenal infusion of L-NAME (1.0μg/kg/min) abolished the increase in urinary sodium excretion and diuresis produced by increasing renal perfusion pressure from 100 to 150mmHg. Again, blood pressure and glomerular filtration rate did not change (Salom *et al.*, 1992). Therefore, together these studies indicate that NO plays a role in sodium and water excretion in response to changes in renal perfusion pressure by mechanisms which are independent of vascular and glomerular events.

Enzymatic studies have shown that the kidney medulla, in particular the inner medulla, has a greater capacity to produce NO than the renal cortex (Mattson & Wu, 2000a). Furthermore western blotting revealed the highest levels of NOS expression are found in the medulla (Mattson & Higgins, 1996b) suggesting that medullary produced NO may be responsible for the effects described above. Indeed, NO increases medullary blood flow, which is known to promote sodium and water

excretion (reviewed in (Mattson & Wu, 2000a)). Another potential mechanism may involve inhibition of renin secretion although there is much controversy on this subject (Kurtz & Wagner, 1998).

More recent studies indicate that NO may induce natriuresis by inhibiting sodium reabsorption within the medulla directly. Using isolated cortical collecting ducts, Stoos *et al* reported the inhibition of sodium transport following addition of ACh and NO donors. (Stoos *et al.*, 1995). Likewise a similar study using isolated thick ascending loops of Henle reported a decrease in chloride transport following addition of a NO donor. Endogenous NO was also investigated. Upon addition of L-arginine, a similar decrease in chloride flux was observed via an L-NAME sensitive pathway (Plato *et al.*, 1999). L-arginine was subsequently shown, through the use of NOS knockout mice, to function through the activation of eNOS as opposed to nNOS and iNOS (Plato *et al.*, 2000b). Furthermore, eNOS -/- mice are hypertensive (Huang *et al.*, 1995; Shesely *et al.*, 1996; Stauss *et al.*, 2000) whereas nNOS -/- animals have slightly lower blood pressure than wild types (Plato *et al.*, 2000b). However, at present there are no data correlating changes in blood pressure with salt sensitivity in eNOS -/- mice.

It should be clear from the information above that the role of NO as a diuretic/natriuretic agent has been well described for some time. However the mechanisms involved, particularly those which regulate renal NO release, are only beginning to be unravelled. As described above, eNOS appears to be the major isoform involved in regulating sodium transport. However, although shear stress is the major physiological activator of eNOS within the vasculature (see section 1.2.1.1), it is not known if the same applies to the kidney. Recent data have suggested that renal NO release may be mediated by receptor activation. In particular the endothelin system may be involved and ET-1, acting via the endothelin type B receptor (ET_B), may be a major physiological activator of NO production within the kidney.

1.2.2.2 The renal endothelin system

The endothelin system is well known to play an important role in regulation of vascular tone and control of blood pressure (reviewed in (Rubanyi & Polokoff, 1994; Haynes & Webb, 1998)). The endothelin system within the kidney regulates a wide range of effects, including regulation of renal blood flow, control of glomerular filtration rate and, as alluded to above, control of sodium and water reabsorption.

1.2.2.3 Endothelin synthesis

The endothelin family is made up of three 21 amino acid peptides (ET-1, -2 and -3) with ET-1 being the major renal isoform (reviewed in (Kohan, 1997)). ET-1 was originally identified as a substance released from endothelial cells that caused potent, sustained vasoconstriction in isolated coronary vessels (Yanagisawa *et al.*, 1988). ET-1 is synthesised from inactive precursors by successive rounds of proteolysis. PreproET-1 is cleaved by a furin-like endopeptidase to form big ET-1. Big ET-1 is then cleaved to form ET-1. This step is catalysed by endothelin converting enzymes (ECE) (see figure 1-3).

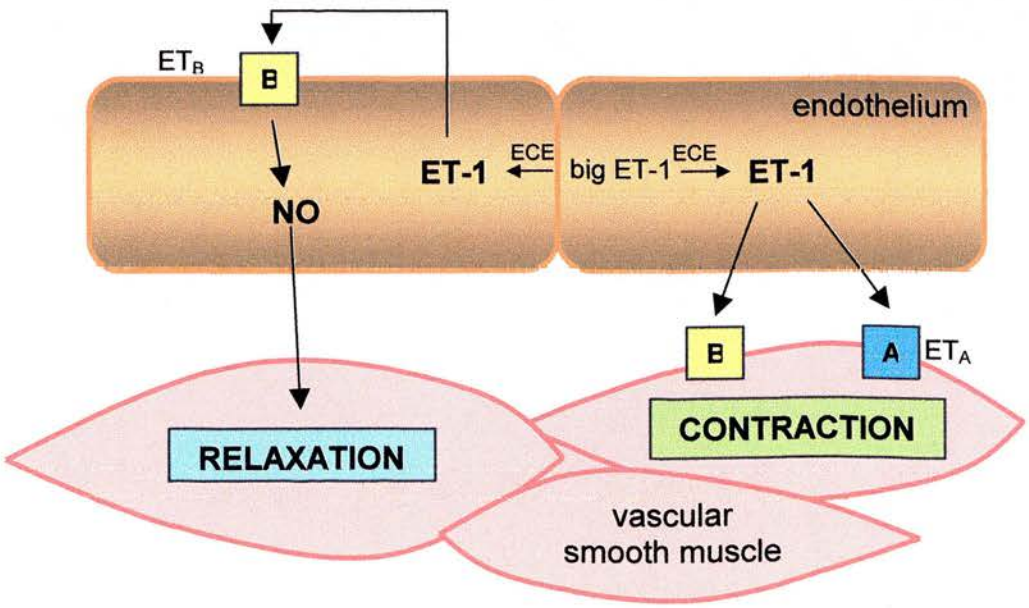

Figure 1-3. The autocrine and paracrine mechanisms of the endothelin system in the vasculature. Abbreviations: ET_B, endothelin type B receptor; ET_A, endothelin type A receptor; ECE, endothelin converting enzyme; ET-1, endothelin-1.

1.2.2.4 Endothelin receptors

Endothelin elicits vasoconstriction of blood vessels via increased $[Ca^{2+}]_i$ resulting from binding to two subtypes of endothelin receptors, termed endothelin type A (ET_A) and endothelin type B (ET_B), located on smooth muscle cells (Sakamoto *et al.*, 1991; Hosoda *et al.*, 1992). ET_A and ET_B are encoded by *EDNRA* and *EDNRB* genes respectively. Both receptors are 7 transmembrane GPCRs and activate an overlapping set of G proteins. ET_A binds endothelins with different affinities (ET-1>2>3) whereas ET_B binds all endothelins with equal affinity. ET-1 can also induce vasodilatation of smooth muscle cells via activation of ET_B located on endothelial cells resulting in prostaglandin and NO production (de Nucci *et al.*, 1988; Filep *et al.*, 1991).

1.2.2.5 Renal expression of ET-1 and endothelin receptors

The renal vasculature is one of the most sensitive vascular beds to ET-1-induced vasoconstriction probably due to the high abundance of endothelin receptors found on vascular smooth muscle cells in renal resistance vessels. ET-1 is produced within the renal vasculature and contributes to control of renal blood flow through constriction of glomerular afferent and efferent arterioles and control of glomerular filtration rate.

However, the highest concentrations of immunoreactive ET-1 are in fact found within the inner medulla (Kitamura *et al.*, 1989a; Kitamura *et al.*, 1989b), interestingly corresponding to the highest levels of eNOS expression and NO production (see section 1.2.2.1). This has been confirmed by *in vitro* autoradiography and [^{125}I]-ET-1 binding (Dean *et al.*, 1994; Yukimura *et al.*, 1996; Zhuo *et al.*, 1998). These studies also showed, using ET_B and ET_A specific antagonists, high expression of the receptors within the medulla. In particular cultured inner medullary collecting duct cells (IMCD) release high amounts of ET-1 (Kohan & Fiedorek, 1991; Kohan & Padilla, 1992) and express ET_A and ET_B (Kohan *et al.*, 1992). However, this observation remains to be confirmed *in vivo* (refer to section 1.2.2.8).

The main stimulus for ET-1 production from epithelial cells appears to be increased osmolality, in particular increases in sodium (Yang *et al.*, 1993; Migas *et al.*, 1995). Renal ET-1 expression is increased during salt loading. Both ET-1 mRNA and protein expression were reported to be upregulated in mice fed an 8% NaCl diet compared with mice on a normal or sodium deficient diet (Melo *et al.*, 1998; Ohuchi *et al.*, 1999b). These observations, together with high expression of the endothelin system in the medulla, suggest a role in sodium handling and homeostasis.

1.2.2.6 Endothelin system and control of Na^+ transport

There is now considerable evidence supporting the role of ET-1 as a diuretic/natriuretic hormone. Intravenous infusion of low doses of ET-1 in the rat caused natriuresis due to reduced sodium transport in the proximal and distal tubules, whereas higher doses resulted in sodium retention due to glomerular vasoconstriction (Harris *et al.*, 1991). ET_A and ET_B specific antagonists revealed that ET_B was mainly responsible for the diuretic/natriuretic effect whilst ET_A mediated vasoconstriction (Clavell *et al.*, 1995; Hoffman *et al.*, 2000).

The role of the endothelin system in natriuresis has been confirmed using transgenic animal models. Although ET-1 -/- homozygous mice die from respiratory failure, ET-1 +/- heterozygous mice develop elevated blood pressure despite ET-1 being a potent vasoconstrictor (Kurihara *et al.*, 1994; Morita *et al.*, 1998). Furthermore, collecting duct specific knockouts of ET-1 are hypertensive, have reduced urine volume and excrete less sodium (Ahn *et al.*, 2002).

Similar results were reported using animals deficient in ET_B. Spotting lethal (sl) rats carry a naturally occurring 301 base pair deletion in the *EDNRB* gene which die soon after birth from aganglionic megacolon (Gariepy *et al.*, 1996). Genetic "rescue" of these rats with an *EDNRB* transgene under the control of a dopamine-β-hydroxylase promoter results in viable animals which express ET_B only in ganglionic cells of the intenstine but are deficient in ET_B elsewhere (Gariepy *et al.*, 1998). When administered a high salt diet (8% NaCl), these animals developed severe

hypertension which was reversed by amiloride, the specific epithelial sodium channel (ENaC) blocker (Gariepy *et al.*, 2000). These results implicate a role of ET_B in inhibition of sodium reabsorption via ENaC. This has been supported by *in vitro* studies using cultured IMCD cells to demonstrate that ET-1, acting via ET_B, downregulates ENaC activity (Gallego & Ling, 1996). However, the rats above also exhibited significantly increased plasma ET-1 levels, which may have caused an increase in vascular resistance and therefore complicates the interpretation of these results. Mouse models of ET_B deficiency also exist. Since homozygous ET_B knockout mice also die from aganglionic megacolon (Hosoda *et al.*, 1994), a similar "rescue" strategy to that described above was adopted by Ohuchi *et al* (Ohuchi *et al.*, 1999b). These mice also develop salt-sensitive hypertension. However, no data on plasma ET-1 levels were reported. In addition another ET_B mouse mutant was developed by the same group by breeding ET_B +/- heterozygotes to piebald (s) mutants which harbour a naturally occurring mutant *EDNRB* allele (Ohuchi *et al.*, 1999a). The offspring (s/-) had ET_B levels 1/8 of normal expression and had significantly higher blood pressure than s/+ or wild type animals, without elevated plasma ET-1 levels. Taken together the findings from these transgenic studies consolidate the physiological role of the endothelin system in sodium transport.

1.2.2.7 Interaction of renal NO and endothelin system in Na^+ transport

The same group that demonstrated a decrease in chloride transport in isolated ascending loops of Henle following addition of NO donors and L-arginine (see section 1.2.2.1), also showed a similar effect following addition of ET-1 (Plato *et al.*, 2000a). Furthermore L-NAME inhibited the ET-1-induced decrease in chloride transport. Removal of L-arginine resulted in a similar effect. These findings suggest that ET-1 exerts its natriuretic effect through an NOS-dependent pathway. Again this was shown to be mediated by ET_B. Hoffman *et al* also reported an equivalent effect *in vivo* in anaesthetised rats. Following big ET-1 infusion, urinary flow rate and sodium excretion were significantly increased with no change in blood pressure, glomerular filtration rate or renal blood flow (Hoffman *et al.*, 2000). However, pre-treatment with L-NAME abolished the natriuretic effect of ET-1.

Downstream, NO is thought to inhibit sodium reabsorption through a cGMP-kinase dependent mechanism which phosphorylate and block sodium channels (Light *et al.*, 1990; Lahera *et al.*, 1993). The observation that ET-1/ ET_B increased cGMP production in cultured rat IMCD cells provides indirect evidence further supporting a link between NO, the ET system and sodium transport (Wong *et al.*, 2000). As described in section 1.2.2.6, ET-1 may inhibit sodium reabsorption by downregulating ENaC activity. There is also evidence that ET-1 can inhibit Na^+-K^+-ATPase activity (Zeidel *et al.*, 1989). In addition, it was reported that ET-1 inhibited reabsorption of sodium and water in isolated cortical collecting ducts and IMCD by blocking the action of anti-diuretic hormone (also known as vasopressin) (Tomita *et al.*, 1990; Nadler *et al.*, 1992). A similar finding was reported for NO (Stoos *et al.*, 1995).

This array of studies provides evidence that renal ET-1, acting via the ET_B, is a major activator of eNOS and NO production and together they regulate sodium transport resulting in diuresis/natriuresis (Plato & Garvin, 1999; Kotelevtsev & Webb, 2001). However, from these studies it is not possible to identify the precise cellular and molecular mechanisms involved. Localisation data may provide some answers.

1.2.2.8 Localisation of eNOS and ET system in the kidney

To help describe the localisation of eNOS and the ET system within the renal medulla, a schematic diagram of a juxtamedullary nephron is shown in figure 1-4. Much of the evidence to date would suggest that renal ET-1 acts in an autocrine fashion where ET-1 is produced by IMCD cells and binds to ET_B on the same cell resulting in eNOS stimulation and NO production (figure 1-5a). However, despite the presence of ET_B on cultured IMCD cells (Kohan & Padilla, 1992), *in vitro* and *in vivo* radioligand ($[^{125}I]$-ET-1) electron microscopy revealed either low or no expression in cells of the renal tubules (Dean *et al.*, 1994; Yukimura *et al.*, 1996; Zhuo *et al.*, 1998).

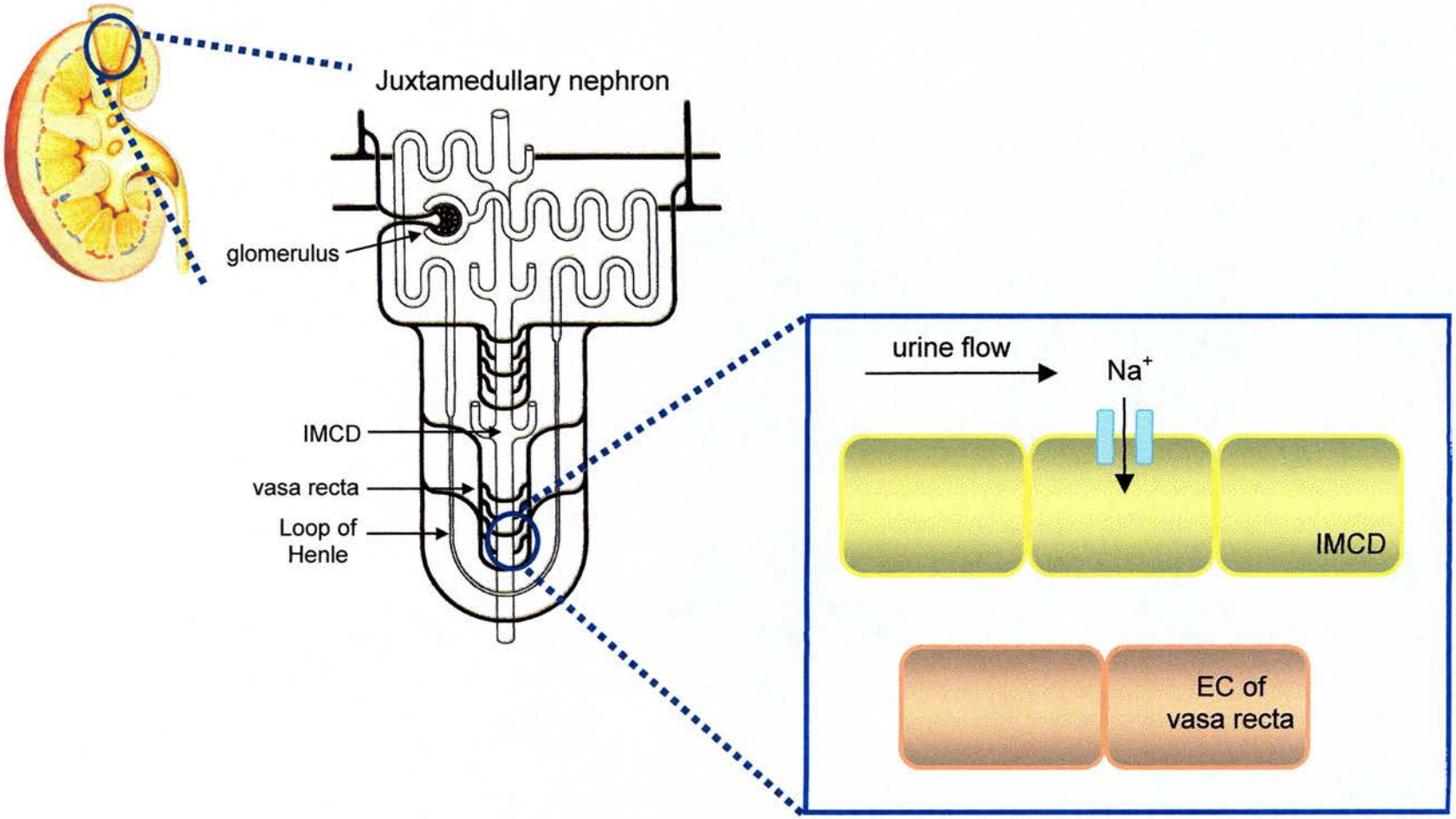

Figure 1-4. Localisation of IMCD cells and vasa recta within the kidney. Schematic diagram of juxtamedullary nephron and location of IMCD cells and EC of vasa recta which are involved in sodium transport. Abbreviations: IMCD, inner medullary collecting duct; EC, endothelial cell.

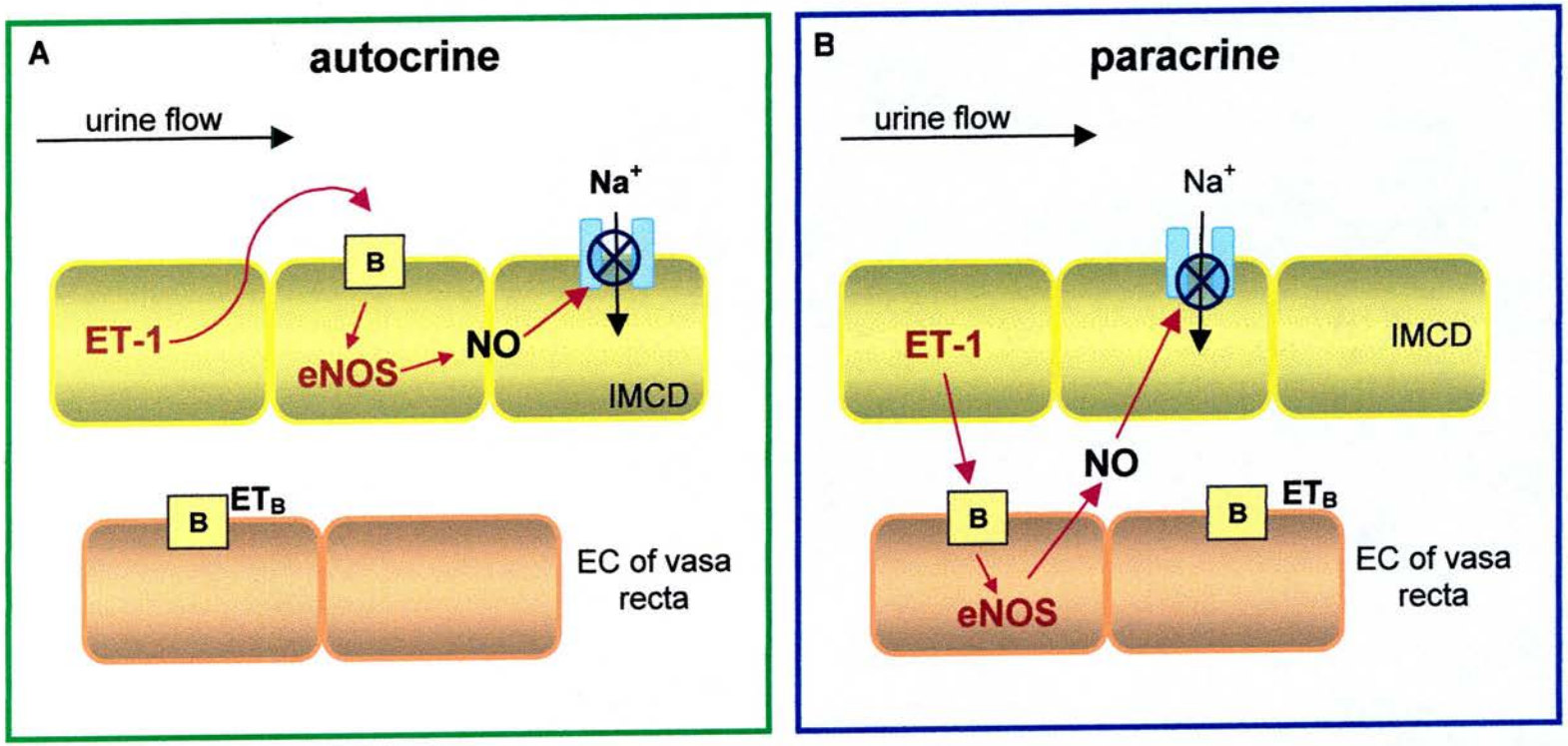

Figure 1-5. The proposed autocrine and paracrine mechanisms of the endothelin system during inhibition of sodium reasorption in the kidney. Abbreviations: ET-1, endothelin-1; ET_B, endothelin type B receptor; eNOS, endothelial nitric oxide synthase; NO, nitric oxide; IMCD, inner medullary collecting duct; EC, endothelial cell.

Instead the majority of binding was localised to glomerular capillaries and vasa recta, the peritubular capillaries found deep within the medulla. However, it is difficult to distinguish between cells using this method and binding sites may be inaccessible to intravascularly administered [^{125}I]-ET-1 (Dean *et al.*, 1994; Zhuo *et al.*, 1998). Furthermore, no indication is given regarding receptor subtypes. Therefore, it is clear that further precise localisation is required.

As for eNOS, the highest levels of calmodulin-dependent NOS activity were found in micro-dissected vasa recta compared to other renal vessels (Mattson & Wu, 2000b). This was confirmed by precise staining using a nuclear localised reporter gene (LacZ) under the control of the eNOS promoter (Teichert *et al.*, 2000). Teichert *et al* reported strong staining within the endothelial cells of the vasa recta but no expression within renal tubules. Likewise, no eNOS expression was detected in renal tubules by immunohistochemical analysis using an anti-eNOS antibody compared to strong staining within renal vessels (Bachmann *et al.*, 1995). Nevertheless, Wu *et al* reported high NOS activity within micro-dissected IMCD segments compared to moderate activity within isolated glomeruli and vasa recta and low activity in other regions of the nephron (Wu *et al.*, 1999). The same study used RT-PCR to reveal that nNOS was the major isoform in IMCD cells whilst eNOS was the predominant isoform in isolated vasa recta. In contrast, RT-PCR performed by Terada *et al* reported high expression in isolated IMCD segments compared to a small signal obtained from vasa recta, glomeruli and other renal tubules (Terada *et al.*, 1992b). These discrepancies may be a consequence of cross-contamination resulting from the microdissection procedure. Therefore, histological analysis appears to yield more accurate results.

Morphological analysis suggests that the main site of ET_B and eNOS expression is the endothelium of the vasa recta. Given that these cells lie in close proximity to IMCD cells, separated only by a basal membrane and together with the physiological experiments described earlier, it is hypothesised that ET-1, released from IMCD cells, acts in a paracrine fashion by binding to ET_B on the vasa recta where eNOS is

activated and NO produced (figure 1-5b). In turn, NO acts on IMCD cells to reduce sodium transport thereby promoting natriuresis/diuresis. This hypothesis assumes that the vasa recta is the major site of ET_B expression. However, as described above this remains to be confirmed.

1.2.3 Endothelial dysfunction in the kidney

ED was first characterised as impaired endothelium-dependent vasorelaxation by Konishi and Su by measuring aortic responses to ACh in spontaneously hypertensive rats (SHR) compared to normotensive Wistar-Kyoto rats (WKY) (Konishi & Su, 1983). Since then impaired endothelium-dependent vasorelaxation has been reported in several other models of ED and in other vascular beds.

Given the importance of the endothelium in kidney physiology, it is of little surprise that the renal vascular bed is also a target for ED and may contribute to the development and/or maintenance of hypertension. In fact, patients with hypertension have impaired endothelium-dependent vasorelaxation in renal arteries manifested as decreased renal blood flow and abnormal renal vascular resistance in response to L-arginine infusion (Higashi *et al.*, 1995; Higashi *et al.*, 1996). Impaired renal NO release and decreased renal perfusion pressure were also observed in stroke-prone SHR (SHRSP) animals in response to ACh infusion (Hirata *et al.*, 1996). Similar attenuation of ACh-induced vasorelaxation has also been reported in deoxycorticosterone acetate (DOCA) salt-hypertensive rats and Dahl salt-sensitive rats (Hayakawa *et al.*, 1993).

However, it should be clear from the physiological roles of NO described in the previous section that vasorelaxation is not the only parameter that may be affected during ED. In particular, NO-induced inhibition of sodium reabsorption may be a target. Dahl salt-sensitive rats and SHR have blunted pressure-natriuresis curves compared to their normotensive counterparts. Administration of L-arginine to these rats is associated with increased urinary sodium excretion and normalisation of pressure-natriuresis (Ikenaga *et al.*, 1993; Patel *et al.*, 1993; Hu & Manning Jr, 1995;

Larson & Lockhart, 1995). Furthermore, urinary excretion of NO metabolites (NO_2 and NO_3) were significantly lower in hypertensive patients (Sierra *et al.*, 1998). Therefore, it is hypothesised that the diminished ability of NO to inhibit sodium reabsorption within the renal medulla may result in sodium retention and subsequently lead to sustained elevation of blood pressure through the resetting of pressure natriuresis.

As described above, locally produced medullary ET-1 can be major activator of NO. Therefore, it is of interest that in hypertensive patients daily urinary excretion of ET-1 was significantly decreased compared to normotensive subjects (Hoffman *et al.*, 1994). This ET-1 was of renal origin and implies that these patients had impaired ET-1 production in the kidney, particularly in the renal medulla. Urinary ET-1 excretion was also lower in SHR, reflected by reduced levels of ET-1 mRNA (Hughes *et al.*, 1992) and decreased immunoreactive ET-1 in the inner medulla (Kitamura *et al.*, 1989b). Moreover, cultured IMCD cells isolated from SHR had lower ET-1 mRNA and released less ET-1 compared to the normotensive, WKY (Hughes *et al.*, 1992). It should also not be overlooked that in some animal models of salt sensitive hypertension the renal endothelin system appears to be activated. PreproET-1 mRNA levels were increased in kidneys from Dahl salt-sensitive rats (Ikeda *et al.*, 1999) and renal ET-1 mRNA expression was enhanced in DOCA-salt hypertensive rats (Deng *et al.*, 1996). Whereas Ikeda *et al* did not specify intrarenal sites of increased expression, the latter report documented the increase in ET-1 only within the renal vasculature and glomeruli implying that ET_A-mediated vasoconstriction may be activated and be the cause of increased systemic blood pressure. Therefore, this should be regarded independently of ET_B -mediated effects of ET-1 within the medulla.

ET_B expression is also altered in animals models of hypertension. Hirata *et al* reported that the DOCA-salt sensitive rat expressed less ET_B mRNA and produced less NO in response to ET-1 perfusion compared to controls (Hirata *et al.*, 1995b). Likewise, expression of ET_B was decreased in Dahl salt-sensitive rats, although this

was reported in large renal arteries. No data were described for IMCD or vasa recta (Kakoki *et al.*, 1999).

Taken together, these observations imply that impairment of the renal medullary ET system is associated with hypertension. Decreased ET-1 induced NO production via eNOS may lead to an inability to block sodium reabsorption resulting in diminished salt and water excretion. Thus, renal ED may play an important role in the maintenance and development of hypertension. In order to address this, the molecular mechanisms underlying the pathways involved need to be unravelled.

Several explanations have been given for why NO bioavailability is altered during ED. One of these, as alluded to above, may be impairment of NO production by the ET system. However, most likely it is a complex, multi-factorial process. Due to the pivotal role of eNOS in both the vasculature and within the kidney, as described above, it is hypothesised that eNOS activity may be altered during ED. Since eNOS is a tightly regulated enzyme, its activity can potentially be altered on a number of different levels. The following section describes some of the factors involved in eNOS regulation and how these may be altered during ED. eNOS regulation within the kidney will also be reviewed although data on this area are limited.

The other isoforms of NOS, nNOS and iNOS may also play a role in ED. However, since these isoforms are not thought to regulate ET-1 induced NO production within the kidney, they have not been considered further.

1.3 REGULATION OF eNOS AND ALTERATIONS DURING ED

eNOS was first described in vascular endothelial cells by Palmer and Moncada in 1989 (Palmer & Moncada, 1989), a finding which sparked an entire new era in NO research. The enzyme was soon purified (Pollock *et al.*, 1991) and cloned (Janssens *et al.*, 1992; Lamas *et al.*, 1992; Sessa *et al.*, 1992) and since then an enormous amount of research has been dedicated to this enzyme. It rapidly became obvious that

eNOS-mediated NO generation is a highly regulated cellular event involving tight control of eNOS activity. Regulatory mechanisms include transcriptional regulation, post-translational modifications (e.g. phosphorylation and acylation), cellular localisation and interactions with regulatory proteins. This complex regulation of eNOS activity will be discussed below.

1.3.1 Synthesis of NO – an overview

NO is synthesised from the oxidation of amino acid, L-arginine (Palmer *et al.*, 1988a; Palmer *et al.*, 1988b) (see figure 1-6). The enzymes responsible for catalysing this reaction are the NO synthases (NOS), of which three isoforms have been described (reviewed in (Stuehr, 1999)). These isoforms are expressed in different tissues and carry out distinct biological roles. Two of the NOS, endothelial NOS (eNOS) and neuronal NOS (nNOS), are constitutively expressed in cells and generally synthesise NO in response to calcium-releasing agonists and fluid shear stress. However, Ca^{2+} - independent pathways also exist. eNOS and nNOS are named after the cell types in which they were originally identified (i.e. endothelial cells and neurons) although they are now known to be expressed in a variety of cell types. The third NOS, inducible NOS (iNOS), was originally identified as being inducible by cytokines in macrophages and synthesises NO via Ca^{2+} - independent mechanisms. nNOS, iNOS and eNOS are also commonly referred to as NOS I, II and III respectively.

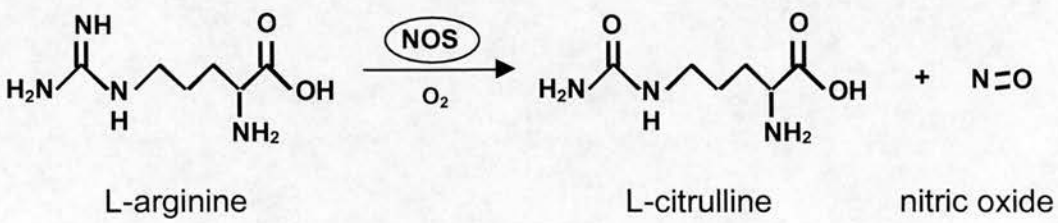

Figure 1-6. NOS-catalysed NO synthesis from L-arginine.

1.3.2 Structure of eNOS

The reaction described in figure 1-6 is a greatly simplified account of NOS-catalysed NO synthesis. Instead the reaction relies on a number of cofactors which are essential for eNOS activity (reviewed in (Fleming & Busse, 1999; Stuehr, 1999)). eNOS is a 140kDa protein comprised of an N-terminal oxygenase domain (1-491 amino acids) and a C-terminal reductase domain (492-1205 amino acids) (see figure 1-7). Within the oxygenase domain are binding sites for heme, cofactor tetrahydrobiopterin (BH_4) and the substrate L-arginine thus forming the active site for NO synthesis. The reductase domain contains sites for cofactors flavin mononucleotide (FMN) and flavin adenine dinucleotide (FAD) and the co-substrate nicotinamide adenine dinucleotide phosphate (NADPH). There is also a binding site for the Ca^{2+} - binding protein, calmodulin (CaM). Upon binding of calcium-loaded CaM, electrons pass from NADPH, through the CaM-binding domain and towards the heme located in the oxygenase domain which allows the heme to bind oxygen and catalyse NO synthesis. The functional eNOS is formed only when two subunits dimerize to form a homodimer and it is thought that electrons transfer from the reductase domain of one subunit to the oxygenase domain of the other (domain swapping). In addition to containing binding sites for substrates and cofactors, the oxygenase domain is also

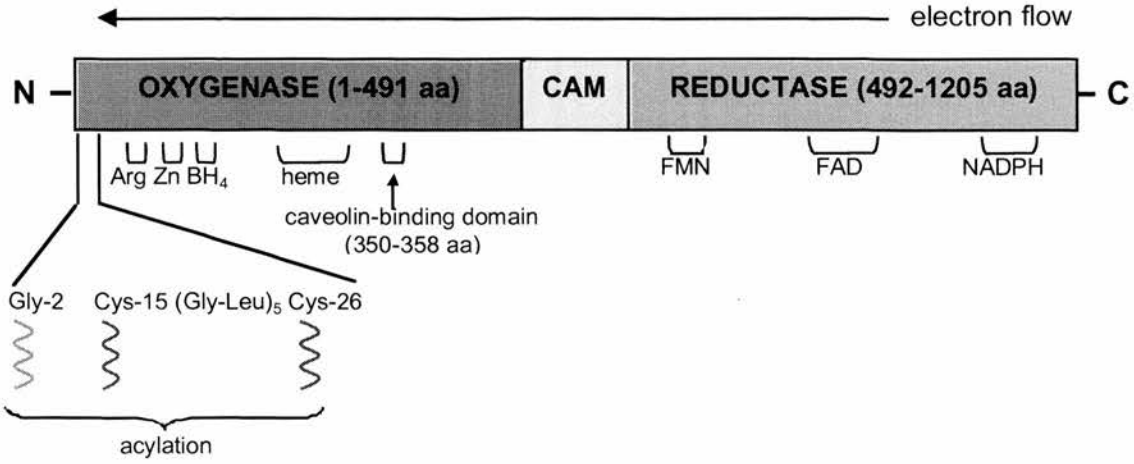

Figure 1-7. Diagram of eNOS structure. Abbreviations: Arg, L-arginine; Zn, zinc; BH_4, tetrahydrobiopterin; FMN, flavin mononucleotide; FAD, flavin adenine dinucleotide; NADPH, nicotinamide adenine dinucleotide phosphate; Gly, glycine; Cys, cysteine; Leu, leucine.

subject to acylation. Co-translational N-myristoylation and post-translational cysteine palmitoylation of the N-terminus are required for correct subcellular targeting of eNOS (refer to section 1.3.5).

1.3.3 Transcriptional regulation of eNOS expression

Despite being designated a constitutively expressed enzyme, basal eNOS expression is also regulated by a number of factors (refer to table 1-1). However, the mechanisms involved and the physiological significance of the effects of these factors are not yet fully established (reviewed in (Forstermann *et al.*, 1998)). These factors may modulate transcription directly via binding of transcription factors (e.g. Sp1 (SV40 virus promoter specific transcription protein 1), AP-1, -2 (activator protein-1, -2), NF-1 (nuclear factor-1) and GATA). The eNOS promoter also contains consensus sequences for regulatory *cis* elements (e.g. shear stress response elements and estrogen response elements (Venema *et al.*, 1994)). However, the functional relevance of these potential regulatory binding sites has not been proven. mRNA stability (i.e. the balance between gene transcription and mRNA degradation) may also be a potential mechanism for altered transcript levels. VEGF (vascular endothelial growth factor), hydrogen peroxide and proliferation have all been shown to stabilise eNOS mRNA, whereas TNF-α (tumor necrosis factor-α), hypoxia, high concentrations of oxidised low density lipoprotein (oxLDL) and lipopolysaccharide decrease mRNA stability (Yoshizumi *et al.*, 1993; Arnal *et al.*, 1994; McQuillan *et al.*, 1994; Liao *et al.*, 1995; Lu *et al.*, 1996; Bouloumie *et al.*, 1999; Drummond *et al.*, 2000). Physiologically, shear stress is one of the major regulators of NO production and therefore it is appropriate that induction of eNOS transcription is controlled by this factor (Nishida *et al.*, 1992). The significance of the other factors described here remain to be elucidated. Atherogenic substances (e.g. lysophosphatidylcholine and oxLDL) which increase eNOS expression may be involved in a pathological defence mechanism against atherosclerotic lesion formation (Hirata *et al.*, 1995a; Cieslik *et al.*, 1999). On the other hand, TNF-α which is commonly found in atherogenic vessels, downregulates eNOS expression

and may provide an explanation as to why NO availability is diminished in atherosclerosis (Yoshizumi *et al.*, 1993; Alonso *et al.*, 1997).

Table 1-1. Factors which modulate eNOS expression

Upregulates eNOS expression	Downregulates eNOS expression
exercise (Sessa *et al.*, 1994)	TNF-α (Yoshizumi *et al.*, 1993; Alonso *et al.*, 1997)
shear stress (Nishida *et al.*, 1992)	erythropoietin (Wang & Vaziri, 1999)
estrogen (via Sp1) (Kleinert *et al.*, 1998)*	hypoxia (McQuillan *et al.*, 1994)*
proliferation (Arnal *et al.*, 1994)*	high oxLDL (Liao *et al.*, 1995)
H_20_2 (Drummond *et al.*, 2000)	lipopolysaccharide (Lu *et al.*, 1996)
VEGF (Bouloumie *et al.*, 1999)	NO (negative feedback via cGMP mediated processes) (Vaziri & Wang, 1999)
TGF-β (Inoue *et al.*, 1995)	
low oxLDL (Hirata *et al.*, 1995a)	
lysoPC (via Sp1) (Cieslik *et al.*, 1999)	

Abbreviations: H_2O_2, hydrogen peroxide; VEGF, vascular endothelial growth factor; TGF-β, transforming growth factor-β; oxLDL, oxidised low density lipoprotein; lysoPC, lysophosphatidylcholine; TNF-α, tumor necrosis factor-α.
* contradictory findings by some groups. Refer to (Flowers *et al.*, 1995; Arnal *et al.*, 1996; Arnet *et al.*, 1996)

1.3.4 Regulation of eNOS by phosphorylation

Phosphorylation may also be an important regulator of eNOS activity (reviewed by (Fleming & Busse, 2003)). eNOS is primarily phosphorylated on serine residues and to a lesser extent on threonine and tyrosine residues (Michel *et al.*, 1993; Corson *et al.*, 1996; Garcia-Cardena *et al.*, 1996a). Although tyrosine phosphorylation has been reported, little is known of the residues and kinases involved. On the other hand, serine-1177 (Ser-1177) phosphorylation occurs in response to shear stress (Dimmeler *et al.*, 1999; Gallis *et al.*, 1999) and a variety of calcium mobilizing agents (e.g. VEGF, estrogen, insulin and BK (Fulton *et al.*, 1999; Michell *et al.*, 1999; Fleming *et al.*, 2001; Kim *et al.*, 2001)) mediated by different kinases depending on the stimulus. For example, shear stress and VEGF induce

phosphorylation via protein kinase B (PKB), whereas insulin appears to activate both PKB and AMP-activated protein kinase (AMPK). Phosphorylation is also thought to be dependent on intracellular localisation of eNOS (Gonzalez *et al.*, 2002). Phosphorylation of Ser-1177 increases eNOS activity by increased electron flow through the reductase domain (McCabe *et al.*, 2000). On the contrary, threonine-495 (Thr-495) is a negative phosphorylation site and is constitutively phosphorylated by protein kinase C (PKC) thus decreasing eNOS activity (Fleming *et al.*, 2001). This is thought to inhibit eNOS by sterically preventing binding of calmodulin. Dephosphorylation of Thr-495 by protein phosphatase 1, in response to BK and other agonists that increase $[Ca^{2+}]_i$, significantly increases eNOS activity (Fleming *et al.*, 2001). Therefore, changes in phosphorylation state play a crucial role in regulating eNOS activity.

1.3.5 Intracellular localisation of eNOS

It is now known that eNOS subcellular localisation plays a vital role in eNOS regulation. Incorrect localisation negatively affects enzyme activity (see below). Within the cell, eNOS is found predominantly within the Golgi apparatus and also at the plasma membrane, in particular caveolae (Hecker *et al.*, 1994). Acylation of the enzyme has been shown to be an important determinant of eNOS localisation (Liu *et al.*, 1997).

1.3.5.1 Myristoylation

The glycine residue (Gly-2) at the N-terminus of eNOS is myristoylated, an irreversible co-translational modification (see figure 1-7). Site-directed mutagenesis of this residue to produce non-myristoylated eNOS (myr^-) resulted in an abnormal localisation profile. Wild type eNOS was associated primarily with the particulate or membrane cellular fraction whereas mutation of Gly-2 resulted in complete cytosolic localisation and decreased enzyme activity (Busconi & Michel, 1993; Sessa *et al.*, 1993; Sakoda *et al.*, 1995). More precise localisation revealed that myristoylation was required for targeting to the Golgi apparatus. Cells transfected with mutant eNOS did not colocalise with the Golgi marker, mannosidase. Moreover, despite

retaining the catalytic properties of the enzyme, these cells produced markedly less stimulated production of NO than cells transfected with wild type eNOS (Sessa *et al.*, 1995). It has also been reported that myristoylation is required for palmitoylation (see below) (Sessa *et al.*, 1993; Liu *et al.*, 1996) and lack of myristoylation affects localisation of eNOS to caveolae on the plasma membrane by attenuating palmitoylation. Thus myristoylation is required for optimal eNOS activity through correct intracellular targeting to the membrane, Golgi apparatus and caveolae (via palmitoylation).

1.3.5.2 Palmitoylation

The N-terminal of eNOS is also subject to palmitoylation on cysteine residues 15 and 26 (Cys-15 and Cys-26, see figure 1-7). Mutation of these residues or the unique $(Gly\text{-}Leu)_5$ repeat lying between these residues results in attenuated palmitoylation ($palm^-$). Transfection of these mutants revealed altered cellular distribution with markedly reduced membrane association however myristoylation was not affected (Robinson & Michel, 1995; Liu *et al.*, 1997). Compared to the cytosolic distribution of eNOS myr^-, eNOS $palm^-$ had a more diffuse perinuclear localisation pattern indicating that palmitoylation may be involved in stabilising the membrane interaction conferred by myristoylation alone. This is supported by Shaul *et al* who reported that the decrease in eNOS activity of $palm^-$ mutant cells in membrane fractions was not as great as in myr^- mutant cells (Shaul *et al.*, 1996).

The same group of researchers used biochemical subfractionation methods to show that eNOS also resides in specialised domains of the plasma membrane termed caveolae. By measuring eNOS activity in caveolae isolated from cells transfected with $palm^-$ mutants they report that palmitoylation is important for caveolar targeting (Shaul *et al.*, 1996). Compared to wild type eNOS, the $palm^-$ mutant eNOS did not colocalise with the main component of caveolae, caveolin-1 (Garcia-Cardena *et al.*, 1996b). However, more recent studies imply that palmitoylation alone is not sufficient to target eNOS to caveolae. Instead, eNOS requires additional signals, found within eNOS itself, to enhance caveolar localisation. At present the nature of

these sequences are unknown (Prabhakar *et al.*, 2000). Targeting of eNOS to caveolae also involves additional post-translational modifications (e.g. phosphorylation, and protein-protein interactions, refer to section 1.3.6). As with myr$^-$ mutant cells, palm$^-$ produced significantly reduced NO upon stimulation with ionomycin confirming that mislocalisation of eNOS results in suboptimal NO release (Liu *et al.*, 1996).

1.3.5.3 Two distinct intracellular pools of eNOS

The majority of reports agree that eNOS is compartmentalised into two distinct intracellular pools. These pools may be differentially regulated and respond to different stimuli as implicated by Govers *et al* (Govers *et al.*, 2002). O'Brien *et al* and Sessa *et al* were first to show by electron and immunofluoresence microscopy respectively, that the majority of cellular eNOS is found within the Golgi apparatus (O'Brien *et al.*, 1995; Sessa *et al.*, 1995). However, several years on, the function of Golgi-localised eNOS remains a mystery. Much of the data suggest that this pool contains potentially active eNOS. Resting levels of $[Ca^{2+}]_i$, one of the main stimuli for eNOS, are high in the perinuclear and Golgi regions of the cell which rise further upon activation of surface receptors and shear stress (Geiger *et al.*, 1992; Burnier *et al.*, 1994). Furthermore, disruption of the Golgi apparatus with brefeldin A inhibited eNOS activity (Stanboli & Morin, 1994). However, this has not been supported elsewhere (Bauersachs *et al.*, 1997). Until recently there was no evidence of direct activation of Golgi-localised eNOS. Using an NO sensitive dye, DAF-2 DA (4,5-diaminofluorescein diacetate), Fulton *et al* reported that basal and VEGF-stimulated NO synthesis were present in the perinuclear area (Fulton *et al.*, 2002) thus concluding that the Golgi apparatus contains a pool of active eNOS. This is in agreement with the early palmitoylation mutagenesis studies. Even though the palm$^-$ mutants produced less NO, it was not abolished altogether suggesting that Golgi-localised eNOS was capable of NO synthesis. However, the question of physiological stimulation and the relative amounts of NO produced in this subcellular compartment remain unanswered.

In recent years, the focus has turned from Golgi to caveolar localised eNOS. Biochemical subfractionation methods used to isolate caveolae revealed highest eNOS protein content and activity in caveolar fractions compared to non-caveolar fractions (Shaul *et al.*, 1996). However, these findings have not been confirmed by immunostaining. Although several studies show intracellular colocalisation of eNOS with caveolin-1, a caveolar marker protein, the extent of this localisation is inconsistent with the biochemical data (Garcia-Cardena *et al.*, 1996b). Whereas the biochemical data implies that most cellular eNOS resides in caveolae, immunostaining clearly shows only a small fraction of eNOS co-localised with caveolin-1, with the majority being localised to the Golgi apparatus described above (Liu *et al.*, 1997). Despite these inconsistencies, caveolar-localised eNOS has received much attention and it is generally accepted that this form of regulation is necessary for optimal, stimulated NO release.

The localisation of eNOS to these two distinct pools is by no means static. eNOS – green fluorescent protein (GFP) fusion proteins have been used to visualise intracellular movement of eNOS and report dynamic movement of eNOS cycling between the two compartments (Sowa *et al.*, 1999). By photobleaching sections of the Golgi apparatus and the plasma membrane and measuring fluorescence recovery, Sowa *et al* reported that eNOS-GFP translocates to and from the Golgi apparatus at high speed and suggest a role in eNOS activation and de-activation.

Taken together, the data imply that during translation eNOS is myristoylated and is targeted to the Golgi apparatus where it is consequently palmitoylated and translocates to caveolae. Upon stimulation, eNOS can recycle back to the Golgi apparatus by mechanisms involving depalmitoylation or changes in protein-protein interactions (see below).

1.3.6 eNOS - caveolin interactions

Much of the recent research in the eNOS regulatory field has focused on its localisation to caveolae and interaction with the resident caveolar protein, caveolin-1.

Until recently most of the studies described were performed *in vitro* and the role of caveolin-1 with regard to eNOS regulation *in vivo* was unknown. *In vivo* immunohistochemical studies have shown that eNOS and caveolin-1 are codistributed to the endothelium of the carotid artery, aorta, vena cava and femoral artery of the hamster (Segal *et al.*, 1999) and in the rat myocardial capillary endothelium as shown by immunogold labelling and electron microscopy (Reiner *et al.*, 2001). However, only with the recent generation of caveolin-1 knockout mice has the physiological regulatory role of caveolin-1 started to be unravelled.

1.3.6.1 Localisation of eNOS to caveolae

As described above, several studies have localised eNOS to specialised microdomains of the plasma membranes known as caveolae (Garcia-Cardena *et al.*, 1996b; Shaul *et al.*, 1996). Caveolae were first described by electron microscopists in the 1950s when they were given the name plasmalemmal vesicles by Palade (Palade, 1953). Two years later Yamada proposed the name *caveolae intracellularis* or "little caves" to describe these flask-shaped invaginations (Yamada, 1955).

Originally studied for their involvement in transcytosis, caveolae are now thought to play an important role in signal transduction (reviewed in (Anderson, 1998)). In addition to eNOS, they contain a variety of signal transduction molecules. These include GPCRs (e.g. ET_A (Chun *et al.*, 1994), m2 ACh (Raposo *et al.*, 1987) and BK receptors (de Weerd & Leeb-Lundberg, 1997)), G-proteins (Gα and Gβ) (Lisanti *et al.*, 1994), CaM (Shaul *et al.*, 1996), adenyl cyclases (Toya *et al.*, 1998), cationic amino acid transporter (CAT-1) which transports L-arginine into the cell (McDonald *et al.*, 1997) and the calcium pump (Fujimoto, 1993) suggesting that many of the components required for optimal eNOS function are concentrated within caveolae and therefore may function as signal transduction centres.

Caveolae are present in most cells and are extremely abundant in certain cell types such as capillary endothelial cells (Simionescu *et al.*, 1972), fibroblasts (Bretscher & Whytock, 1977) and smooth muscle cells (Forbes *et al.*, 1979). Structurally, they

consist predominantly of cholesterol and glycosphingolipids which form the lipid core and accounts for the detergent insolubility of caveolae at low temperature, a characteristic property which is exploited during purification procedures (reviewed in (Anderson, 1998)). In addition to the lipid core, caveolae contain the characteristic protein, caveolin.

1.3.6.2 Caveolin

Caveolin-1 was first identified as a 22-kDa protein which is tyrosine phosphorylated upon transformation with the Rous sarcoma viral oncogene (Glenney, 1989). A few years later caveolin was shown to be a major component of caveolae (Rothberg *et al.*, 1992) and was soon cloned by two independent groups (Glenney & Soppet, 1992; Kurzchalia *et al.*, 1992). Glenney and Soppet's study revealed an unusually large (33 amino acids) hydrophobic domain suggesting that caveolin is an integral membrane protein (see figure 1-8). It is thought that this domain forms a hairpin structure within the membrane with both the N-terminal (residues 1-101) and C-terminal (residues 135-178) remaining in the cytoplasm (Dupree *et al.*, 1993). This protein is now more accurately referred to as caveolin-1α, as a shorter isoform, caveolin-1β, also exists which lacks the N-terminal sequence (1-32 amino acid residues) as a result of two translation start sites (Scherer *et al.*, 1995). In addition to caveolin-1, are caveolin-2 (2α, 2β and 2γ) and caveolin-3 (Way & Parton, 1995;

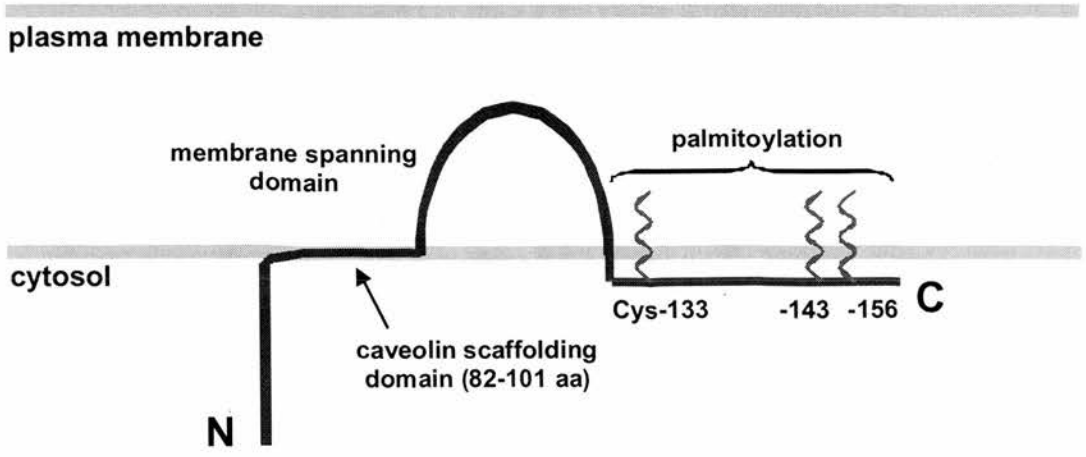

Figure 1-8. Diagram of caveolin-1 structure.

Scherer *et al.*, 1996; Tang *et al.*, 1996) which show similar protein structures. Whilst caveolin-1 and -2 have similar tissue distributions, caveolin-3 is strongly associated with expression in muscle. Initial reports suggested that caveolins played a structural role in caveolae formation as transfection of 2B2318 lymphocytes, which lack caveolae, with caveolin-1 resulted in the *de novo* formation of caveolae (Fra *et al.*, 1995). However, other groups report that caveolae-like structures can exist in the absence of caveolin-1 (Anderson, 1998). More recently the focus has turned to the ability of caveolin-1 to interact with many other caveolar proteins, in particular eNOS, thus suggesting a role in signal transduction.

Like eNOS, caveolin-1 is palmitoylated on three cysteine residues (Cys-133, Cys-143, Cys-156, see figure 1-8) (Dietzen *et al.*, 1995). However, unlike eNOS, palmitoylation is not required for caveolar localisation. Instead, a region in the N-terminus of caveolin-1, residues 82-101 appears important for membrane localisation due to the high content of basic and aromatic residues in this region (Schlegel *et al.*, 1999; Schlegel & Lisanti, 2000). This region is known as the caveolin-scaffolding domain (CSD) as it is also involved in mediating interactions with other caveolar-localised proteins (Li *et al.*, 1996) and caveolin itself (Sargiacomo *et al.*, 1995). Amongst these proteins are adenylyl cyclase (Toya *et al.*, 1998), heterotrimeric G proteins (G_s, G_o, G_i) (Li *et al.*, 1995) and, of course, eNOS (see below). In addition, each of these molecules contains a caveolin-binding motif characterised as $\phi x\phi xxxx\phi$ and $\phi xxxx\phi xx\phi$, where ϕ is aromatic amino acid Trp, Tyr or Phe and x is any residue) (Couet *et al.*, 1997).

1.3.6.3 eNOS interacts with caveolin-1

The localisation of eNOS to caveolae renders the enzyme inactive. This has been attributed to the dynamic interaction between eNOS and caveolin-1 in which caveolin negatively regulates eNOS activity (Michel *et al.*, 1997a). This interaction, first identified by co-immunoprecipitation using antibodies against caveolin, revealed that the majority of eNOS is found in association with caveolin-1 in cultured endothelial cells (Feron *et al.*, 1996; Garcia-Cardena *et al.*, 1996a). Conversely, co-

immunoprecipitations performed using antibodies against eNOS, did not significantly affect the total pool of caveolin suggesting that only a small fraction of the caveolin pool is associated with eNOS. However, the extent to which eNOS and caveolin are complexed is controversial considering that immunostaining clearly shows that not all eNOS co-localises with caveolin at an intracellular level (refer to section 1.3.5.3).

The eNOS-caveolin interaction was subsequently shown to be regulated by Ca^{2+}-CaM (Michel *et al.*, 1997a). In the presence of Ca^{2+}, eNOS-caveolin complexes from endothelial cell lysates were disrupted. In contrast, eNOS-CaM complexes were observed which did not form in the absence of Ca^{2+}. Co-transfection of COS-7 cells with eNOS and caveolin led to marked inhibition of eNOS activity demonstrating for the first time the negative regulatory properties of caveolin on eNOS activity. Upon addition of Ca^{2+}-CaM, the interaction was disrupted and eNOS activity restored.

In 1998, the same group examined the intracellular localisation of eNOS-caveolin complexes in endothelial cells following treatment with the Ca^{2+} ionophore A23187 and provided evidence for the eNOS-caveolin regulatory cycle (Feron *et al.*, 1998b). In the absence of A23187, the majority of eNOS in association with caveolin, was detected in the particulate (i.e. membrane) fraction. Upon treatment with the Ca^{2+} ionophore caveolin-eNOS complexes were disrupted and eNOS was found in both the particulate and soluble (i.e. cytosolic) fractions. This suggests that during activation eNOS is translocated to the cytosol. When performed in the presence of EGTA, a Ca^{2+} chelator, eNOS relocated back to the membrane fraction bound to caveolin. They also reported that eNOS dissociation from caveolin was agonist induced using COS cells transfected with eNOS and the muscarinic ACh receptor. Addition of the agonist, carbachol, resulted in rapid disruption of eNOS-caveolin complexes, quickly followed by reassociation of the proteins. Agonist induced translocation of eNOS has been reported elsewhere (Michel *et al.*, 1993; Fukuda *et al.*, 1995; Prabhakar *et al.*, 1998). In addition, this pattern of recycling of eNOS-caveolin complexes was shown to be palmitoylation dependent, probably as a result

of targeting of eNOS back to caveolae (Feron *et al.*, 1998b). Palmitoylation and de-palmitoylation of eNOS is also regulated by agonists (Robinson *et al.*, 1995).

Since agonist induced activation of eNOS is not a particularly physiological regulator of NO production, attention turned to the potential association of caveolar regulation of eNOS and shear stress. Acute changes in shear stress or pressure induce rapid release of NO from the vascular endothelium resulting in vasodilatation. Recently Rizzo *et al* proposed that these haemodynamic forces may transmit through caveolae (Rizzo *et al.*, 1998). Using isolated caveolae from lung exposed to different vascular flow *in situ*, they reported that increased flow enhanced caveolar eNOS activity compared to other cellular membrane fractions. In parallel, increased flow induced eNOS-caveolin dissociation as shown by co-immunoprecipitation. Conversely a greater amount of eNOS-CaM complexes appeared after enhanced flow. Thus shear stress induced activation of eNOS is associated with release of eNOS from its inhibitory association with caveolin.

In summary, in resting cells eNOS is tonically inhibited by caveolin-1 (figure 1-9). Activation is initiated by increases in $[Ca^{2+}]_i$ in response to agonist binding to cell surface receptors or increased shear stress. The rise in $[Ca^{2+}]_i$ causes CaM to displace caveolin resulting in translocation of eNOS to the cytosol where it is free to generate NO. As the levels of $[Ca^{2+}]_i$ drop below a threshold level, CaM dissociates and the inhibitory eNOS-caveolin complex reforms.

As described in section 1.3.6.3 eNOS and caveolin interact directly. Using glutathione S-transferase (GST)-caveolin-1 fusion proteins and the yeast two-hybrid system, Ju *et al* mapped the regions of interaction to the oxygenase domain of eNOS (see figure 1-7) and the CSD of caveolin (see figure 1-8). Incubation of purified eNOS with synthetic peptides corresponding to 82-101 amino acids of caveolin-1 (cav82-101) inhibited binding of eNOS to CaM-sepharose and resulted in significantly attenuated eNOS activity. This inhibition could be competitively reversed by addition of excess Ca^{2+}-CaM (Ju *et al.*, 1997). Furthermore, incubation

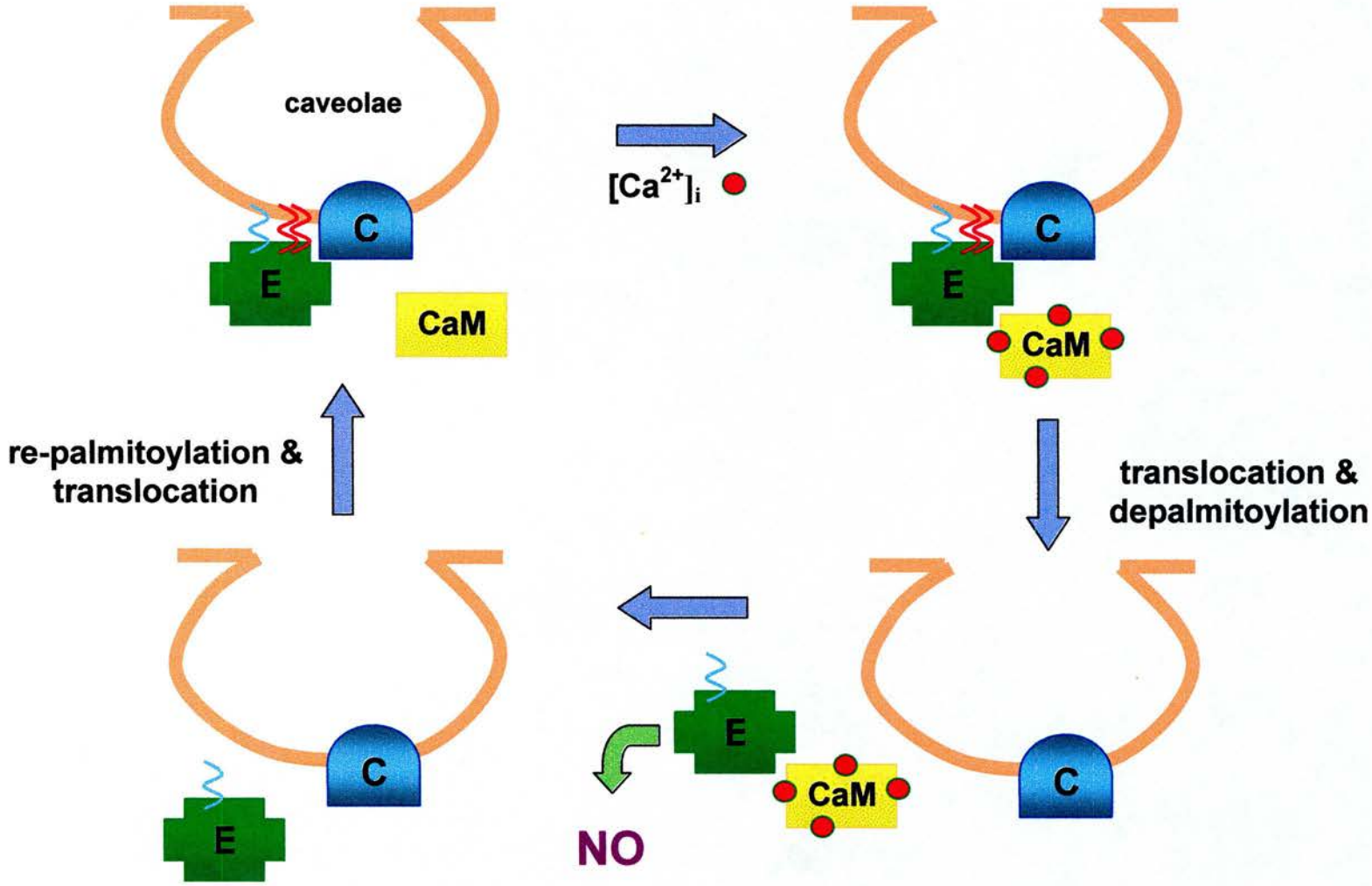

Figure 1-9. The eNOS-caveolin regulatory cycle. Abbreviations: E, eNOS; C, caveolin-1; CaM, calmodulin. Acylation is indicated by zig-zag lines.

of endothelial cell lysates with cav82-101 abolished co-immunoprecipitation of the eNOS-caveolin complexes. In comparison, a scrambled peptide bearing 60% homology to cav82-101 had no effect on eNOS-caveolin co- immunoprecipitation (Michel *et al.*, 1997b). Caveolin also directly interacts with eNOS, albeit to a lesser extent, via its C-terminal cytoplasmic tail (Garcia-Cardena *et al.*, 1997; Ju *et al.*, 1997). However, present data suggest that the CSD is alone sufficient to interact with eNOS and inhibit its activity.

Garcia-Cardena *et al* further characterised the interaction using site-directed mutagenesis to mutate the putative caveolin-binding motif of eNOS (**F**$_{350}$SAAP**F**SG**W** to **A**$_{350}$SAAP**A**SG**A**). Cells transfected with both mutant eNOS and caveolin released the equivalent amount of NO as cells transfected with eNOS alone. In contrast co-transfection of wild type eNOS and caveolin resulted in marked inhibition of NO release (Garcia-Cardena *et al.*, 1997).

Although Ju *et al* reported no interaction between caveolin-1 and the reductase domain of eNOS by the yeast two-hybrid system (Ju *et al.*, 1997), Ghosh *et al* clearly showed the presence of such an interaction. They demonstrated interactions between the purified reductase domain of eNOS and GST-caveolin-1 as well as interaction within the oxygenase domain. Furthermore, by measuring cytochrome c activity, an artificial acceptor of electrons transferred from the reductase domain, they demonstrated the inhibition of eNOS reductase domain-specific activity by caveolin 82-101 amino acid peptides, again reversed by addition of excess CaM. They concluded that caveolin inhibition of eNOS is the result of diminished electron transfer between reductase and oxygenase domains (Ghosh *et al.*, 1998).

1.3.6.4 Physiological consequences of eNOS-caveolin interactions

The physiological importance of eNOS-caveolin interactions has only become clear within the last couple of years. Two independent reports provided strong *in vivo* evidence supporting the role of caveolin as a negative regulator of eNOS. These studies report the generation of caveolin-1 null mice by gene targeting which lack

caveolae and have similar phenotypes (Drab *et al.*, 2001; Razani *et al.*, 2001). Aortic rings from these mice were used to assess vascular tone. Compared to wild-type, the knockout mice exhibited an impaired vasoconstrictor response to phenylephrine and an enhanced relaxation response to ACh. NOS inhibitor, L-NAME, restored the proper vasoconstrictor response and it was concluded that the changes in vascular responses in caveolin-1 knockout mice were a consequence of increased eNOS activity. In addition, NO production was measured in aortic vascular smooth muscle cells isolated from caveolin -/-. Basal NO release was significantly higher in knockouts complemented by an increase in cGMP content (Drab *et al.*, 2001).

Another *in vivo* study has been described which also illustrates the physiological importance of eNOS-caveolin interactions. In the study by Bucci *et al*, a chimeric peptide comprised of the caveolin scaffolding domain (amino acids 82-101) fused to a cellular internalisation sequence was incubated with mouse aortic rings (Bucci *et al.*, 2000). The peptide blocked ACh-induced vasorelaxations suggesting that the peptide is a potent inhibitor of eNOS. A scrambled version of the peptide had no effect. Together these studies have confirmed the *in vitro* data and established that caveolin-1 is a negative regulator of eNOS activity *in vivo*.

1.3.7 Additional protein interactions

As well as interacting with CaM and caveolin-1, eNOS interacts with a variety of other proteins, including heat shock protein 90 (hsp90), kinases, eNOS interacting protein (NOSIP) and, of particular interest, GPCRs (reviewed in (Fulton *et al.*, 2001; Fleming & Busse, 2003)). As described above (refer to section 1.3.6.1), caveolae contain a variety of signal transduction molecules, many of which are needed to make up the eNOS "signalling complex" (see figure 1-10). This colocalisation of molecules may facilitate enzyme activity and subsequently NO production by bringing all the necessary components for eNOS activation (e.g. GPCRs and CaM) and downstream NO production (e.g. G proteins and adenyl cyclases) into close proximity. At present there is no direct evidence localising ET_B to caveolae. However, it is likely to follow the pattern of expression of other GPCRs. For

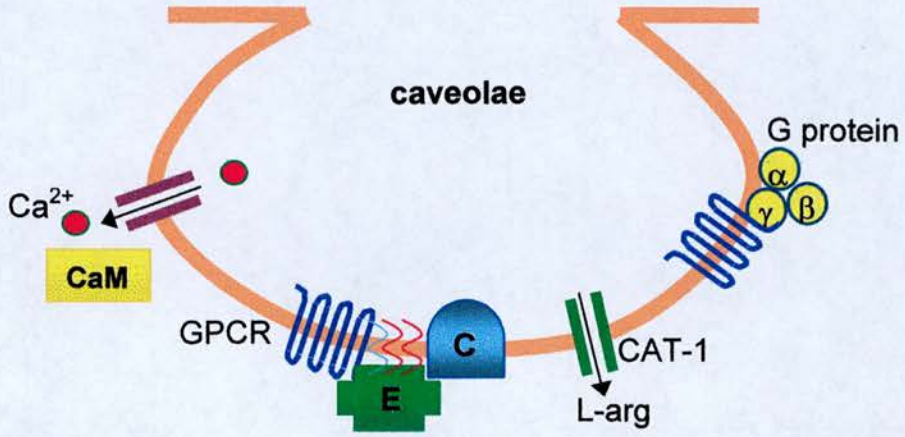

Figure 1-10. eNOS signalling complex. Abbreviations: CaM, calmodulin; GPCR, G protein coupled receptor (e.g. receptors for acetylcholine, bradykinin and endothelin); E, eNOS; C, caveolin-1, L-arg, L-arginine, CAT-1, cationic amino acid transporter.

example, the presence of bradykinin B2 receptors within caveolae has been reported (de Weerd & Leeb-Lundberg, 1997) and have been shown to physically interact with eNOS via the intracellular domain 4 (ID4) by *in vitro* binding assays (Ju *et al.*, 1998). Likewise ID4 of the angiotensin II AT1 receptor and the ET_B physically interact with eNOS *in vitro* (Marrero *et al.*, 1999). Although no *in vivo* studies have been published to support this observation, ET_A was localised to caveolae by immunofluoresence and was found to co-immunoprecipitate with caveolin-1 (Chun *et al.*, 1994) implying that ET_B may also reside there. Interaction of eNOS with bradykinin B2 receptors is reported to inhibit eNOS activity (Ju *et al.*, 1998). Furthermore, eNOS and GPCRs are reported to be associated in unstimulated cells. Upon stimulation with BK, the proteins dissociate.

1.3.8 Regulation of renal eNOS

NO has several effects within the kidney including control of medullary blood flow, regulation of acid-base balance and inhibition of sodium reabsorption (see section 1.2.2.1). However, despite the well-defined roles of NO within the kidney, little is

known of the mechanisms involved. Much of the evidence suggests that eNOS is the main isoform controlling these processes and although the published data on eNOS regulation is extensive, much of this has been performed *in vitro* and has not yet been reproduced *in vivo*. Furthermore, it is quite plausible that eNOS is differentially regulated depending on the type of tissue or vascular bed (Andries *et al.*, 1998; Piech *et al.*, 2003). Therefore mechanisms involved in regulation of eNOS in the heart cannot simply be extrapolated to the kidney. In fact, with regard to the kidney, eNOS regulatory information is almost absent and requires further investigation.

Since eNOS is thought to have a crucial role in promoting natriuresis, it is interesting that eNOS proteins levels were dramatically increased in the inner medulla of rats fed on high salt compared to those on low salt (Mattson & Higgins, 1996). However, hyperosmolality has been reported to decrease eNOS mRNA and protein levels in cultured IMCD (Chen *et al.*, 2002).

As described in section 1.3.6.1, subcellular localisation to caveolae is an important regulatory feature of eNOS. However, it is not known if this occurs within the vascular and epithelial structures of the kidney. Evidence regarding caveolin-1 localisation may provide some clues. Although protein analysis show that the kidney expresses very low amounts of caveolin compared to the lung (Lisanti *et al.*, 1994), precise immunohistochemical analysis revealed expression within the glomerulus, mesangial cells, collecting duct and endothelial cells of the efferent and afferent arterioles (Breton *et al.*, 1998; Tamai *et al.*, 2001). Of particular interest was the high expression within the descending vasa recta corresponding to large numbers of caveolae as shown by immunogold labelling and electron microscopy (Breton *et al.*, 1998). This vascular bed is also a major site of renal eNOS and ET_B expression as described in section 1.2.2.8. Therefore, this circumstantial evidence suggests that caveolin may be a potential regulatory mechanism controlling renal eNOS production.

1.3.9 Alterations in eNOS regulation during ED

It should be clear from the complexity of eNOS regulation described above that there are many possible ways in which eNOS activity could be potentially altered during ED. Like ED itself, it probably involves a combination of different factors. Some of these factors are described below. Of particular interest is the emerging evidence indirectly suggesting that the pathogenic mechanism underlying ED may involve alterations in eNOS-caveolin interactions within caveolae.

1.3.9.1 Alterations in substrate and cofactor availability

Despite the fact that intracellular levels of L-arginine can be between 100 and 1000μM and that the K_m for NOS is only ~ 5μM, several studies have demonstrated the beneficial effects of L-arginine in conditions such as hypertension, hypercholesterolemia and diabetes and in experimental animal models of these disorders (Chen & Sanders, 1991; Creager *et al.*, 1992; Pieper & Peltier, 1995). However, the mechanisms involved are unclear. Some suggestions include antagonism of NOS by endogenous asymmetric dimethyl arginine (ADMA) or breakdown of L-arginine by arginase expressed within the endothelium (Vallance *et al.*, 1992; Buga *et al.*, 1996). Furthermore, it is not known if the concentrations of L-arginine within caveolae reflect that within the rest of the cell (McDonald *et al.*, 1997). Indeed caveolar concentrations may be significantly lower due to reduced transport of L-arginine into these regions and may be a rate-limiting factor.

Deficient levels of the cofactor BH_4, will trigger eNOS to produce superoxide (O_2^-) instead of NO (see section 1.3.9.4) (Pou *et al.*, 1992). Recent studies suggest that BH_4 levels may be decreased in conditions such as diabetes and hypercholesterolemia (Pieper, 1997; Stroes *et al.*, 1997).

1.3.9.2 Alterations in NOS expression

As described in section 1.3.3 eNOS transcription is modulated by a number of factors, including several substances associated with atherosclerotic lesion formation. In animal models of hypertension, alterations in NOS protein expression are also

detected. In the SHR, increased calcium-dependent NOS activity is reflected by increased eNOS protein expression and higher levels of cGMP, despite these animals exhibiting impaired endothelium-dependent relaxations (Mourlon-Le Grand *et al.*, 1992; Nava *et al.*, 1996; Bauersachs *et al.*, 1998; Nava *et al.*, 1998; Vaziri *et al.*, 1998). This probably signifies an upregulation in the NO pathway to compensate for increased blood pressure. However, these observations have not always been confirmed elsewhere (Ruetten *et al.*, 1999). Increased aortic eNOS expression is also observed in a model of ED induced by aortic banding (Bouloumie *et al.*, 1997) but is decreased in the kidneys of the two-kidney, one clip model of hypertension (Wickman *et al.*, 2001). Polymorphisms of the eNOS gene linked to hypertension have been reported in a number of separate Japanese studies (Nakayama *et al.*, 1997; Miyamoto *et al.*, 1998; Uwabo *et al.*, 1998). In particular, a variable number of tandem repeats in intron 4 and an exon 7 variant that leads to an amino acid change (Glu298Asp) have been identified. However, these polymorphisms have not been observed in other populations (Bonnardeaux *et al.*, 1995; Benjafield & Morris, 2000).

1.3.9.3 Uncoupling of GPCR and G proteins

Activation of eNOS may be altered in ED. Some reports describe defects in activation of GPCRs or the signalling pathways activated by these receptors, for example uncoupling of GPCRs and G proteins. In several models of ED, endothelium-dependent vasorelaxation in response to a calcium ionophore is less altered than responses to receptor mediated agonists (Bossaller *et al.*, 1987). Indeed, the endothelin system within the kidney medulla is impaired in hypertensive patients and in several animal models of hypertension (refer to section 1.2.3) and may result in diminished eNOS activation and NO production. However, Panza *et al* reported that abnormalities in signal transduction did not relate to impaired agonist-induced vasorelaxation responses in hypertensive patients (Panza *et al.*, 1995).

1.3.9.4 Destruction of NO by superoxide

Although not affecting eNOS activity directly, inactivation of NO by increased concentrations of O_2^- is probably one of the major factors accounting for reduced NO bioavailability in ED. Treatment of rabbits, that had been maintained on a cholesterol rich diet, with superoxide dismutase (SOD) increased endothelium-dependent vasorelaxation and infusion of ascorbic acid in hypertensive patients improved vascular responses to ACh (Mugge *et al.*, 1991; Solzbach *et al.*, 1997). Augmented O_2^- was also observed in SHR and aortic-banding induced hypertension (Bouloumie *et al.*, 1997; Bauersachs *et al.*, 1998).

1.3.9.5 Alterations in eNOS-caveolin interactions

The first report to investigate eNOS-caveolin interactions in a pathogenic situation was by Feron *et al* (Feron *et al.*, 1999). They demonstrated that incubation of bovine aortic endothelial cells with hypercholesterolemic human serum was associated with upregulation of caveolin-1 levels and impairment of basal NO release. This was paralleled by an increase in the formation of inhibitory eNOS-caveolin complexes, despite no increase in eNOS levels. Higher Ca^{2+}-CaM levels were required to disrupt the increased number of complexes. However, it is puzzling as to why a small increase in caveolin protein levels should result in the formation of more complexes since the same group previously published that the majority of eNOS is already found in association with caveolin (Feron *et al.*, 1996).

A similar study, using oxLDL-treated porcine pulmonary artery endothelial cells, revealed that eNOS and caveolin were displaced from caveolae to the cytosol. Incubation with oxLDL also significantly reduced eNOS activity in response to ACh. Removal of oxLDL was followed by redistribution of eNOS and caveolin to caveolar membrane fractions (Blair *et al.*, 1999).

Only one study to date has investigated alterations in eNOS-caveolin interactions during hypertension. Following confirmation of decreased NO production from pulmonary arteries isolated from pulmonary hypertensive rats, Murata *et al* measured

protein-protein interactions of eNOS with caveolin-1, CaM and hsp90. Aortas from hypertensive rats contained increased eNOS-caveolin complexes compared to normotensive rats and complexes were not disrupted upon carbachol treatment. Furthermore CaM and hsp90 binding to eNOS were reduced in hypertensive animals (Murata *et al.*, 2002).

Alterations in caveolar structure, although not specifically eNOS-caveolin interactions, were also observed during ED in the SHR. Scanning electron microscopy revealed that in 10 week old SHR (i.e. the onset of hypertension) there were significantly increased numbers of caveolae compared with aged matched WKY and 5 week old prehypertensive SHR suggesting that structural changes may be associated with hypertension (Goto *et al.*, 1990). However, these observations were not supported by McGuire *et al* who reported no changes in caveolar density in SHR at 4, 10 and 24 weeks (McGuire & Twietmeyer, 1985).

Finally acute changes in shear stress, which are proposed to transmit through caveolae as described in section 1.3.6.3 and by Rizzo *et al*, may also be affected during ED (Rizzo *et al.*, 1998). Increases in shear stress as a consequence of higher blood pressure during hypertension may alter caveolar structure and eNOS-caveolin interactions. Together, these studies suggest that there is a high probability that during ED eNOS protein-protein interactions may be disturbed and pose a potential pathogenic mechanism either in causing or maintaining ED.

In summary, eNOS plays a pivotal role in normal renal physiology, in particular control of natriuresis/diuresis. ET-1, acting via ET_B, is thought to be one of the major regulators of eNOS activity within the kidney. However, eNOS activity is also tightly regulated in a number of different ways. During ED renal eNOS activation and regulation may be altered and physiological outcomes disturbed.

1.4 HYPOTHESES AND AIMS

General hypotheses

Together the renal ET and NO systems play a vital role in the inhibition of sodium and water reabsorption and thus contribute to the maintenance of normal blood pressure and the prevention of hypertension. It is hypothesised that the inability of eNOS to generate NO as a result of ED in the kidney results in sodium retention and the sustained elevation of blood pressure. There are several reasons for why eNOS activity may be altered. This thesis explores the following two general hypotheses:

(i) ED is associated with alterations in caveolar structure and interactions between eNOS and regulatory proteins such as caveolin and ET_B.

(ii) ED is associated with the inability of ET-1 to activate eNOS via ET_B resulting from either reduced activity of the renal ET system, reduced responsiveness of eNOS to ET-1 activation or a combination of both.

Since these areas are too vast to be fully addressed within the scope of this thesis, I have chosen to address the following specific aims:

Aims

In order to investigate the first hypothesis, I used an animal model of ED, the SHR, to determine if these animals display abnormalities in renal eNOS, caveolin and ET_B protein expression and if interactions between these proteins are altered within the kidney.

In order to address the second hypothesis first requires further knowledge of the fundamental cellular and molecular mechanisms involved in ET-1 induced natriuresis through ET_B and eNOS activation. It is hypothesised that ET-1 acts as a paracrine hormone, released from IMCD cells and activates eNOS by binding to ET_B located on endothelial cells of the vasa recta. To address this hypothesis, precise localisation of ET_B in the kidney medulla is required. This was achieved using an *EDNRB*-LacZ transgene resulting in transgenic animals which express LacZ

wherever *EDNRB* is expressed thereby producing a precise *in vivo* expression profile of ET_B.

The use of these animals was extended to investigate if ET_B expression is altered during salt loading.

CHAPTER 2

MATERIALS & METHODS

2.1 MATERIALS

All chemicals were supplied by Sigma-Aldrich Company Ltd unless otherwise stated. All stock solutions were prepared using reverse osmosis distilled water (Milli-Q50, Millipore UK Ltd) and where necessary were autoclaved before use. Adjustment of pH of solutions was performed using acids supplied by Fisher Scientific UK. Further information on specific materials used is provided within each section. A list of all companies mentioned is found in section 2.7 at the end of the chapter.

2.2 FUNCTIONAL STUDIES ON ISOLATED BLOOD VESSELS

2.2.1 Materials

All drugs were dissolved in distilled water, aliquoted and stored at -20°C until use. The stock concentrations and working concentration range for each drug used are shown in table 2-1. Drugs were diluted in physiological salt solution (PSS) before use (see table 2-2 for composition of PSS).

Table 2-1. Drugs and concentrations used in functional studies

Drug	Stock concentration (M)	Working dose range (M)
Noradrenaline (NA)	$1x10^{-2}$	$1x10^{-8}$ to $1x10^{-5}$
Phenylephrine (PE)	$1x10^{-1}$	$1x10^{-8}$ to $3x10^{-5}$
Acetylcholine (ACh)	$1x10^{-2}$	$1x10^{-9}$ to $1x10^{-5}$

The compositions of solutions used in functional studies are listed in table 2-2.

2.2.2 Animals

Male SHR and WKY rats (16 weeks old) were supplied by Harlan UK Ltd and were housed in the Hugh Robson Building animal house, University of Edinburgh under the Animals (Scientific Procedures) Act 1986 (UK Home Office, project licence number PPL 60/2813). Animals had free access to food (standard commercial animal chow) and water. Animals were sacrificed by dislocation of the neck.

Table 2-2. Composition of solutions used in functional studies

Solution	Composition
PSS	119mM NaCl 4.7mM KCl 2.5mM $CaCl_2.2H_2O$ 1.17mM $MgSO_4.7\ H_2O$ 25mM $NaHCO_3$ 1.18mM KH_2PO_4 0.027mM EDTA 5.5mM glucose (pH 7.4)
KPSS	123.7mM KCl 2.5mM $CaCl_2.2H_2O$ 1.17mM $MgSO_4.7\ H_2O$ 25mM $NaHCO_3$ 1.18mM KH_2PO_4 0.027mM EDTA 5.5mM glucose (pH 7.4)
NAK	10μM NA in KPSS

Abbreviations: PSS, physiological salt solution; KPSS, PSS containing 123.7mM KCl; NAK, KPSS containing 10μM noradrenaline (NA); EDTA, ethylenediaminetetra-acetic acid.

2.2.3 Functional studies using mesenteric arteries

2.2.3.1 Preparation of mesenteric arteries

The mesentery was removed from the animal and placed in cold, oxygenated PSS. Four third order mesenteric arteries were isolated by microdissection, cleaned of connective tissue and suspended between two wires, 40μm in diameter, in a myograph organ bath (Multimyograph Model 610M, Danish Myo Technology A/S). Vessel lengths were 1.82 ± 0.03mm (WKY, n=5) and 1.90 ± 0.04mm (SHR, n=6). The chambers were filled with warmed PSS (37°C), aerated with 95% O_2, 5% CO_2 and vessels were allowed to equilibrate for 15 minutes. A resting stretch of 0.4g was applied to each vessel and maintained for 1 hour during which time the PSS was replaced every 15 minutes. Each chamber was connected to a force transducer and changes in isometric tension were processed by a MacLab/4e analogue-digital converter and recorded by MacLab Chart v3.4 software (ADInstruments).

2.2.3.2 Experimental protocol

Vessels were constricted with NAK (3x), NA (1x) and KPSS (1x) as shown in figure 2-1. Each incubation was for 5 minutes and was separated by 5 minute washes with PSS. Following the wake-up procedure vessels were allowed to rest for 30 minutes – 1 hour with PSS being replaced every 15 minutes. Vessels were then exposed to cumulative additions of PE ($1x10^{-8}$ to $3x10^{-5}$M) followed by washout with PSS. The concentration of PE that produced 80% contraction of the maximum PE dose was used to preconstrict vessels, following which relaxation responses to cumulative additions of ACh ($1x10^{-9}$ to $1x10^{-5}$M) were measured to test for endothelial integrity. Responses to ACh were expressed as the % relaxation of contraction to PE.

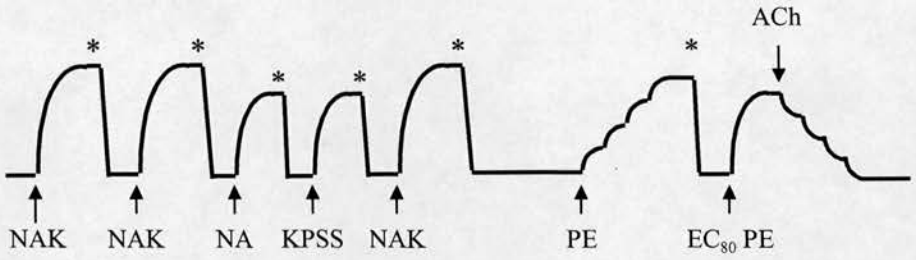

Figure 2-1. Schematic diagram of experimental protocol for mesenteric myography. * denotes washout with PSS. See text for further details.

2.2.4 Functional studies using aorta

2.2.4.1 Preparation of aortic rings

The thoracic aorta was removed from the animal and immediately placed in cold, oxygenated PSS. After removal of connective tissue, the aorta was cut into 4 rings approximately 3mm in length and mounted between two wires in organ bath chambers (Organ bath model 700MO, Danish Myo Technology A/S) which contained PSS (37°C) aerated with 95% O_2, 5% CO_2. Vessels were allowed to equilibrate for 15 minutes. A resting stretch of 1.5g was applied to each vessel and maintained for 1 hour during which time the PSS was replaced every 15 minutes. Changes in isometric tension were recorded as described in section 2.2.3.1.

2.2.4.2 Experimental protocol

Vessels were constricted with NAK (3x) as shown in figure 2-2. Each incubation was for 5 minutes and was separated by 15-20 minute washes with PSS. Following the wake-up procedure vessels were allowed to rest for 30 minutes – 1 hour with PSS being replaced every 15 minutes. Vessels were then exposed to cumulative additions of NA ($1x10^{-8}$ to $1x10^{-5}$M) followed by washout with PSS. The concentration of NA that produced 80% contraction of the maximum NA dose was used to preconstrict vessels, following which relaxation responses to cumulative additions of ACh ($1x10^{-9}$ to $1x10^{-5}$M) were measured to test for endothelial integrity. Responses to ACh were expressed as the % relaxation of contraction to NA.

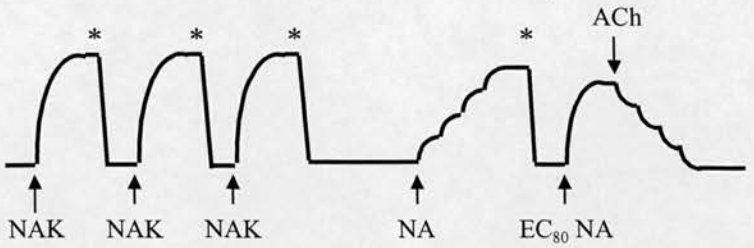

Figure 2-2. Schematic diagram of experimental protocol for functional studies in aortic rings. * denotes washout with PSS. See text for further details.

2.3 BIOCHEMICAL PROCEDURES

2.3.1 Materials

Anti-caveolin polyclonal antibodies were supplied by Autogen Bioclear UK Ltd (cat. no. sc-894). Anti-eNOS monoclonal antibodies (clone 3) were from BD Biosciences UK Ltd (cat. no. 610297). Anti-ET_B polyclonal antibodies were supplied by Biogenesis Ltd (cat. no. 4113-3059), Research Diagnostics Inc (cat. no. RDI-ENDTHLHBRabS) or AbCam Ltd (cat. no. ab1922). Secondary antibodies were purchased from Sigma-Aldrich Company Ltd.

Cell culture reagents were supplied by Invitrogen Ltd (Gibco) and tissue culture plastic-ware by Corning (Bibby Sterilin Ltd).

2.3.2 Preparation of tissue and cellular protein extracts

2.3.2.1 Animals

Animals were as described in section 2.2.2.

2.3.2.2 Preparation and culture conditions for HUVECs

Human umbilical vein endothelial cells (HUVECs) were supplied by Dr. Peter Henriksen, University of Edinburgh prepared using a method described by Jaffe *et al* (Jaffe *et al.*, 1973).

2.3.2.3 Isolation of caveolin-rich domains by sucrose gradient ultracentrifugation

Caveolin-rich domains were isolated from rat lung and kidney using a method described by Lisanti *et al* (Lisanti *et al.*, 1994). 400mg (wet weight) of tissue was minced with scissors in 2ml Mes-buffered saline, MBS (25mM Mes (2-[N-morpholino]ethanesulfonic acid monohydrate), 0.15M NaCl, pH 6.5) containing 1% Triton-X100 and 1mM phenylmethylsulfonylfluoride (PMSF) at 4°C. The tissue was homogenised using a Polytron tissue grinder (two 5 second bursts) followed by 10 strokes of a Dounce homogeniser. Homogenates were incubated on ice for 30 minutes following which 2ml of 80% sucrose prepared in MBS was added to the homogenate to yield a 40% sucrose solution.

5-30% linear sucrose gradients were formed in SW41 centrifuge tubes (Beckman Coulter UK Ltd) using a Bio-Rad gradient former (Bio-Rad Laboratories Ltd). 5ml of 5% and 30% sucrose solutions prepared in MBS were used for each gradient. The homogenates (4ml) were carefully transferred to the bottom of the sucrose gradient using a syringe. Gradients were centrifuged at 39000rpm, 4°C for 20 hours in an L8-55 ultracentrifuge using a SW41 Ti rotor (Beckman Coulter UK Ltd).

Following centrifugation, twelve 1ml fractions were collected, of which fraction 9 corresponded to a visible light scattering band. This was also confirmed by measuring absorbance at 600nm. The insoluble pellet was resuspended in 500µl MBS. All samples were stored at -20°C until protein measurement and western blot analysis was performed.

2.3.2.4 Protein extraction from tissue

Immediately following excision from the animal, tissues were immersed in ice cold Nonidet P-40 (NP-40) lysis buffer (50mM Tris-HCl pH 7.4, 125mM NaCl, 1mM

EDTA, 1mM EGTA, 1% NP-40 (v/v), 1mM PMSF, 1µg/ml pepstatin A). 1g (wet weight) of tissue was transferred to 5ml of fresh lysis buffer and roughly minced with scissors followed by homogenisation using a Polytron tissue grinder (two 5 second bursts) and 10 strokes of a Dounce homogeniser. Homogenates were incubated for 1 hour at 4°C. To remove insoluble material homogenates were centrifuged in a microcentrifuge at 10000rpm, 4°C for 15 minutes. Supernatants were collected and aliquoted into 500µl samples. Pellets were resuspended in 500µl of NP-40 lysis buffer. Samples were stored at -20°C until protein measurements and western blot analysis were performed.

2.3.2.5 Protein extraction from cultured endothelial cells

HUVEC cells were lysed as described by Feron *et al* (Feron *et al.*, 1998b). HUVEC cells were grown to approximately 80% confluency in a 150cm^2 flask. Following aspiration of medium, cells were rinsed in PBS (2.7mM KCl, 137mM NaCl, 1.5mM KH_2PO_4, 4.3mM Na_2HPO_4, pH 7.4) and either 5ml of cold Octyl-Glucoside (OG) lysis buffer (50mM Tris-HCl pH7.4, 125mM NaCl, 2mM dithiothreitol, 0.1mM EGTA, 60mM OG, 1mM PMSF, 1µg/ml pepstatin A, 1µg/ml leupeptin) or NP-40 lysis buffer (see section 2.3.2.4 for composition) was added. Cells were scraped from the flask using a rubber policeman and transferred to a 15ml centrifuge tube. The cell suspension was either homogenised or sonicated (three 10 second bursts at output power 10 microns) using a Soniprep 150 sonicator (Sanyo). Insoluble material was removed by centrifugation at 10000 rpm in a microcentrifuge. Supernatants were aliquoted in 500µl samples and pellets were resuspended in 100µl of the appropriate lysis buffer. Samples were stored at -20°C until protein measurements and western blot analysis were performed.

2.3.3 Measurement of protein concentration

Protein concentration measurements were performed using Bradford's reagent (Bradford, 1976) according to the manufacturer's protocol for micro (0-25µg/ml) or standard (0-1400µg/ml) assays (Sigma-Aldrich Company Ltd). Bovine serum albumin (BSA) was used to prepare the standard curve. Briefly, BSA was diluted

accordingly depending on the type of assay used (micro or standard). 50µl of each standard was mixed with 1.5ml of Bradford's solution, incubated for 5 minutes and absorbance was measured at 595nm using a SmartSpec 3000 spectrophotometer (Bio-Rad Laboratories Ltd). Samples of unknown protein concentration were diluted appropriately in order to obtain an absorbance which would fall within the linear region of the standard curve. 50µl of each sample was mixed with 1.5ml of Bradford's solution, incubated for 5 minutes and absorbance was read at 595nm.

2.3.4 Co-immunoprecipitation of eNOS-caveolin-1 complexes

Co-immunoprecipitation was performed as described by Feron *et al* (Feron *et al.*, 1998b). All incubations were performed at 4°C. Aliquots of cell and tissue homogenates (approximately 100µg total protein) were incubated with 10µg of either anti-caveolin or anti-eNOS antibodies for 2 hours with continuous rotation. In some samples immune antibody was omitted in order to assess non-specific binding. 50µl of a 50% slurry of protein G Sepharose (PGS) (Protein G Sepharose 4 Fast Flow, Amersham Pharmacia Biotech UK Ltd) was added to the samples for a further 1 hour incubation. Prior to use the PGS was washed 3 times by centrifugation in lysis buffer (NP-40 or OG depending on method of protein extraction). Following incubation with PGS, bound immune complexes were washed 3 times by centrifugation (5000rpm for 1 minute at 4°C) in lysis buffer and then once in wash buffer (50mM Tris-HCl, pH 7.4, 150mM NaCl). In all experiments the first supernatant fraction after incubation with protein G Sepharose was kept for analysis. After washing, bound complexes were eluted in 50µl of 2x Laemmli sample buffer by boiling for 5 minutes. Immunoprecipitated samples were stored at -20°C until western blot analysis was performed.

2.3.5 Western blot analysis

2.3.5.1 Solutions

Western blot analysis was performed using standard protocols (Hames & Rickwood, 1990). The composition of common solutions used in SDS-polyacrylamide

electrophoresis (SDS-PAGE), western transfer and subsequent immunodetection are listed in table 2-3.

Table 2-3. Composition of solutions used in western blotting

Buffer	Composition
2x Laemmli sample buffer	0.063M Tris-HCl (pH 6.8) 10% (v/v) glycerol 2% (w/v) SDS 0.05% (w/v) bromophenol blue 5% (v/v) 2-mercaptoethanol (added immediately prior to use)
Electrophoresis running buffer (pH8.3)	0.025M Trizma base 0.19M glycine 0.1% (w/v) SDS
Transfer buffer	0.025M Tris-HCl (pH 8.3) 0.19M glycine 20% (v/v) methanol 0.05% (w/v) SDS
TBS-T (wash buffer)	0.02M Tris-HCl (pH 7.6) 0.14M NaCl 0.1% (v/v) Tween-20 (Bio-Rad Laboratories Ltd.)
Blocking solution	5% (w/v) non-fat dried milk in TBS-T

Abbreviations: SDS, sodium dodecyl sulfate; TBS, tris-buffered saline; T, Tween-20.

2.3.5.2 Separation of proteins by SDS-PAGE

Following extraction, protein samples were denatured in an equal volume of Laemmli sample buffer and incubated at 95°C for 5 minutes. Molecular weight standards (broad range 200-6.5 kDa, Bio-Rad Laboratories Ltd) were also diluted 1:20 in sample buffer and boiled for 5 minutes. Proteins (1µg-100µg) and molecular weight standards (20µl/lane) were separated on denaturing SDS polyacrylamide gels using Bio-Rad Mini-PROTEAN II Cell gel apparatus assembled according to manufacturer's instructions (Bio-Rad Laboratories Ltd). 1mm thick gels were routinely used, the compositions of which are shown in table 2-4. Gels were immersed in electrophoresis running buffer and a voltage of 100V applied for approximately 2 hours or until the dye front had reached the bottom edge of the gel. Following separation, gels were either processed for western blot transfer and

immunodetection (refer to section 2.3.5.3) or used for visualisation of proteins by Coomassie or silver staining (refer to section 2.3.6.1 and 2.3.6.2).

Table 2-4. Composition of SDS-PAGE gels

% gel	Composition
6%	6% acrylamide mix [a] 0.38M Tris-HCl (pH 8.8) 0.1% SDS 0.1% ammonium persulfate 0.08% TEMED
12%	12% acrylamide mix 0.38M Tris-HCl (pH 8.8) 0.1% SDS 0.1% ammonium persulfate 0.04% TEMED
5% (stacking gel)	5% acrylamide mix 0.13M Tris-HCl (pH 6.8) 0.1% SDS 0.1% ammonium persulfate 0.1% TEMED

[a] Acrylamide mix was comprised of acrylamide : N,N'-methylene-bis-acrylamide, 37.5:1 (Bio-Rad Laboratories Ltd)
Abbreviations: SDS, sodium dodecyl sulfate; TEMED, N,N,N',N'-tetramethylethylene diamine

2.3.5.3 Immobilisation of proteins by western transfer

Following electrophoresis, proteins were transferred from the polyacrylamide gel to a positively charged polyvinylidene difluoride (PVDF) membrane (Hybond-P, Amersham Pharmacia Biotech UK Ltd) using a Bio-Rad Mini Trans-Blot Electrophoretic Transfer Cell (Bio-Rad Laboratories Ltd). During western transfer the gel and membrane were sandwiched between two stacks of filter paper and fibre pads with the membrane placed nearest the anode and the gel nearest the cathode so that SDS-coated negatively charged proteins were transferred to the membrane when the current was applied.

Prior to assembly of the gel sandwich, the membrane was pre-wetted in 100% methanol and rinsed in distilled water for 5 minutes. The membrane and all components of the sandwich were equilibrated for 20 minutes in cold transfer buffer (see table 2-3 for composition) following which the electroblotting cassette was

assembled and submerged in cold transfer buffer. A current of 400mA (approximately 100V) was applied for 2 hours.

Following transfer, the cassette was dismantled and the PVDF membrane, now containing immobilised proteins was immediately placed in blocking solution to block non-specific binding sites and incubated overnight at 4°C with continuous shaking. If molecular weight standards were to be visualised, the lane carrying these markers was cut from the membrane and processed by Coomassie staining (refer to section 2.3.6.1).

2.3.5.4 Immunodetection of immobilised caveolin, eNOS and ET_B

After blocking of non-specific binding sites, membranes were incubated with primary antibodies diluted in blocking solution (5ml final volume). Dilutions for all antibodies are listed in table 2-5. Incubations were performed in 50ml centrifuge tubes at room temperature with continuous rotation. After 2 hours, membranes were rinsed briefly in wash buffer and then extensively washed for 15 minutes (x2) followed by three 5 minutes washes to remove non-specifically bound antibody.

Table 2-5. Antibodies, suppliers and working dilutions for western blotting

Antibody	Supplier and catalogue no.	Dilution
anti-caveolin-1 (rabbit polyclonal)	Autogen Bioclear sc-894	1:2500
anti-eNOS (monoclonal IgG1)	BD Biosciences 610297	1:1000
anti-ET_B (sheep polyclonal)	Biogenesis 4113-3059	various
anti-ET_B (sheep polyclonal)	Research Diagnostics Inc RDI-ENDTHLHBRabS	various
anti-ET_B (rabbit polyclonal)	AbCam ab1922	various
anti-rabbit – HRP	Sigma-Aldrich A2074	1:5000
anti-mouse IgG1 – HRP	Sigma-Aldrich A8924	1:5000
anti-sheep – HRP	Sigma-Aldrich A3415	1:5000

After each wash the buffer was removed and fresh buffer applied. Excess wash buffer was removed by blotting on tissue paper and membranes were incubated with horseradish peroxidase (HRP) conjugated secondary antibodies for 2 hours at room temperature. Membranes were washed as described above. Specific antibody binding was detected by Enhanced Chemiluminescent (ECL) reagents according to the manufacturer's protocol (ECL Plus, Amersham Pharmacia Biotech). This method detects immobilised specific antigens conjugated to HRP labelled antibodies which catalyse the oxidation of Lumigen resulting in detectable emission of light. Briefly, excess wash buffer was drained from the membrane and was placed on SaranWrap, protein side up. Solutions A and B were mixed in a ratio of 40:1 and 1-2ml was applied per membrane ensuring that the entire surface of the membrane was covered. Blots were incubated for 5 minutes at room temperature. Excess ECL was removed by blotting on tissue paper and blots were wrapped in Saranwrap and exposed to Hyperfilm ECL autoradiography film (Amersham Pharmacia Biotech UK Ltd). Exposure times ranged from 10 seconds to 30 minutes. Films were processed using a Konica SRX-101 A developer.

2.3.6 Visualisation of proteins on SDS-PAGE gels

2.3.6.1 Coomassie staining

Gels containing 10-100µg of protein were stained with Coomassie staining solution (0.05% (w/v) Coomassie Brilliant Blue R-250 (Bio-Rad Laboratories Ltd), 40% (v/v) methanol, 10% (v/v) glacial acetic acid). Following electrophoresis gels were submerged in the solution for 2 hours with gentle shaking. The stained gels were destained overnight in destaining solution (40% (v/v) methanol, 10% (v/v) glacial acetic acid) and then transferred to distilled water for storage. The same protocol was used for visualising proteins on PVDF membranes (e.g. protein standards).

2.3.6.2 Silver staining

Silver staining was used for gels containing less than 10µg protein (Gottlieb & Chavko, 1987). The Silver Stain Plus kit (Bio-Rad Laboratories Ltd) was used according to the manufacturer's instructions. Following electrophoresis, gels were placed in Fixative Enhancer Solution (50% (v/v) methanol, 10% (v/v) glacial acetic

acid, 10% (v/v) Fixative Enhancer Concentrate) for 20 minutes with gentle shaking after which they were rinsed in distilled water for 20 minutes. During washing the Staining Solution was prepared comprising 50% (v/v) Development Accelerator Solution, 5% (v/v) Silver Complex Solution, 5% (v/v) Reduction Moderator Solution, 5% (v/v) Image Development Reagent. After gels had been washed they were stained in the Staining Solution for 10-20 minutes. The time of incubation was dependant on the quantity of protein present. Once desired staining was reached the reaction was stopped by placing the gels in 5% glacial acetic acid for 15 minutes following which they were stored in distilled water.

2.3.7 Drying of SDS-PAGE gels

Stained gels were vacuum dried using a Hoefer Drygel slab gel dryer (Amersham Pharmacia Biotech UK Ltd). Gels were covered in clingfilm and sandwiched between two pieces of filter paper. The sealing gasket was placed over the gel and the vacuum applied. Gels were dried at 80°C for 40 minutes.

2.3.8 Densitometry and statistical analysis

Gels and western blots were scanned and densitometry was performed using Aida 2.11 2D densitometry (Raytest Scientific Ltd). Comparisons between two groups were made using a Student's unpaired t test. Values are given as mean ± S.E.M. and P values of less than 0.05 were considered significant.

2.3.9 Visualisation of eNOS and caveolin expression by immunofluorescence

eNOS and caveolin expression were analysed in HUVECS using antibodies to eNOS and caveolin and fluorescent conjugated secondary antibodies (see table 2-6). HUVECS were cultured overnight on glass coverslips 13mm in diameter (BDH, VWR International Ltd) in 24-well plates in cell culture medium (DMEM, 10% (v/v) foetal calf serum, 100U/ml penicillin, 100ug/ml streptomycin, 25mM HEPES, 2.0mM glutamine). They were plated at low density to produce an evenly spread population of cells. The following day cells were rinsed in PBS and fixed by incubation for 10 minutes in 4% (w/v) paraformaldehyde, pH 7.4. Fixative was

removed and cells washed twice in PBS followed by permeabilisation in 0.2% (v/v) Triton X100/PBS for 5 minutes. Cells were then washed 4 times in PBS. After blocking in 2% (w/v) BSA/PBS for 1 hour, primary antibody was applied for 1 hour. Antibodies were diluted in blocking solution and a minimal volume applied. See table 2-6 for dilutions used. For controls, samples were incubated with the appropriate non-immune serum to assess for non-specific binding of primary antibodies (e.g. rabbit serum for anti-caveolin and mouse IgG for anti-eNOS). Following 3 washes in PBS, fluorescent secondary antibodies were applied for a further hour. Excess antibody was removed by further washing in PBS. In some cases nuclei were stained using TO-PRO-3 (Molecular Probes Europe BV) by incubation for 5 minutes in 1μM TO-PRO-3 (diluted from 1mM stock dissolved in DMSO) followed by a brief rinse in PBS. After antibody incubations were completed, coverslips were inverted onto glass slides and the edges sealed with nail varnish. Cells were viewed using a Leica TCS-NT 3-channel confocal microscope (Leica Microsystems (UK) Ltd). FITC was detected by green emission and TRITCI by red emission.

Table 2-6. Antibodies, suppliers and working dilutions for immunofluorescence

Antibody (host species)	Supplier and catalogue no.	Dilution
anti-caveolin-1 (rabbit polyclonal)	Autogen Bioclear sc-894	1:100
anti-eNOS (monoclonal IgG1)	BD Biosciences 610297	1:50
anti-rabbit-FITC [a]	Sigma-Aldrich F9887	1:100
anti-mouse-TRITCI [b]	Sigma-Aldrich T2402	1:100

[a] Fluorescein (excitation 495nm, emission 525nm)
[b] Rhodamine (excitation 552nm, emission 570nm)

2.4 MOLECULAR BIOLOGY PROCEDURES

All molecular procedures were carried out using standard techniques (Sambrook *et al.*, 1989).

2.4.1 Materials

2.4.1.1 Chemicals and solutions

Absolute ethanol, chloroform, isoamyl alcohol and phenol were supplied by Fisher Scientific UK. SeaKem LE agarose was supplied by Cambrex Bioscience Ltd. Oligodeoxynucleotide primers were synthesised by MWG Biotech UK Ltd. They were diluted upon arrival in distilled water to 100pmol/µl and stored at -20°C.

Luria-Bertani (LB) medium was prepared from 10g bacto-tryptone, 5g bacto-yeast extract and 10g NaCl per litre. pH was adjusted to 7.5 with 10N NaOH and autoclaved before use. Agar selection plates were prepared from 15g agar/L of LB. Unless otherwise stated, ampicillin (Sigma-Aldrich Company Ltd) was added to LB and agar plates at a final concentration of 100µg/ml. Bacto-tryptone, bacto-yeast extract and agar were supplied by Invitrogen Ltd.

MBI Fermentas DNA molecular weight markers were supplied by Helena Biosciences Europe. Either GeneRuler 100bp DNA ladder (1000-100bp) or Lambda DNA/*Hin*dIII (23130, 9416, 6511, 4361, 2322, 2027, 564bp) were used depending on the size of DNA to be analysed.

2.4.1.2 Enzymes

All restriction enzymes, Klenow, alkaline phosphatase and T4 DNA polymerase were supplied by Roche Diagnostics Ltd. MBI Fermentas T4 polynucleotide kinase and T4 DNA ligase were supplied by Helena Biosciences Europe and M-MLV Reverse Transcriptase and *Pfu* DNA Polymerase were from Promega UK Ltd.

2.4.1.3 Bacterial strains

All plasmids were maintained in *Escherichia coli* strain XL1-blue cells (genotype supE44 hsdR17 recA1 endA1 gyrA46 thi relA1 lac^- F'[$proAB^+$ $lacI^q$ lacZΔM15 Tn10(tet^r)]) (Sambrook *et al.*, 1989).

2.4.1.4 Cloning vectors and plasmids

The vectors and plasmids used during cloning are shown in figures 2-3 – 2-8. Further detailed information will be given in chapter 4.

2.4.2 Preparation of electrocompetent cells

Prior to use all glass- and plastic-ware was thoroughly rinsed in 5% acetic acid followed by several washes with distilled water and stored at 4°C. A single XL1-blue colony from a freshly streaked agar plate (without ampicillin) was incubated at 37°C in 50ml LB medium (without ampicillin) with shaking (200-225rpm) for 12-16 hours. The following day the 50ml culture was used to inoculate 1 litre of LB medium and the culture incubated at 37°C with shaking for approximately 2-3 hours or until the OD_{550} was between 0.5 and 0.6 after which the culture was transferred to two sterile 500ml Sorvall centrifuge bottles and incubated on ice for 30 minutes. All subsequent steps were performed at 4°C. Cells were centrifuged at 5000rpm for 15 minutes at 4°C in a precooled Beckman J2-21 centrifuge, rotor JA14 (Beckman Coulter UK Ltd. The medium was discarded and the cell pellet resuspended in 500ml of cold sterile water. After a further centrifugation the supernatant was discarded and the pellet resuspended in 250ml sterile water and again centrifuged for 15 minutes. Washing of the cells is necessary to ensure that salts are removed to reduce the conductivity of the cell solution. High conductivity may result in arcing during electroporation. The cell pellet was resuspended in 20ml of cold sterile 10% glycerol and centrifuged at 6000rpm for 15 minutes following which the pellet was resuspended in 1ml 10% glycerol. Cells were snap frozen in 1.5ml microcentrifuge tubes (40µl aliquots) in a dry ice/ethanol bath before being transferred to -70°C until required.

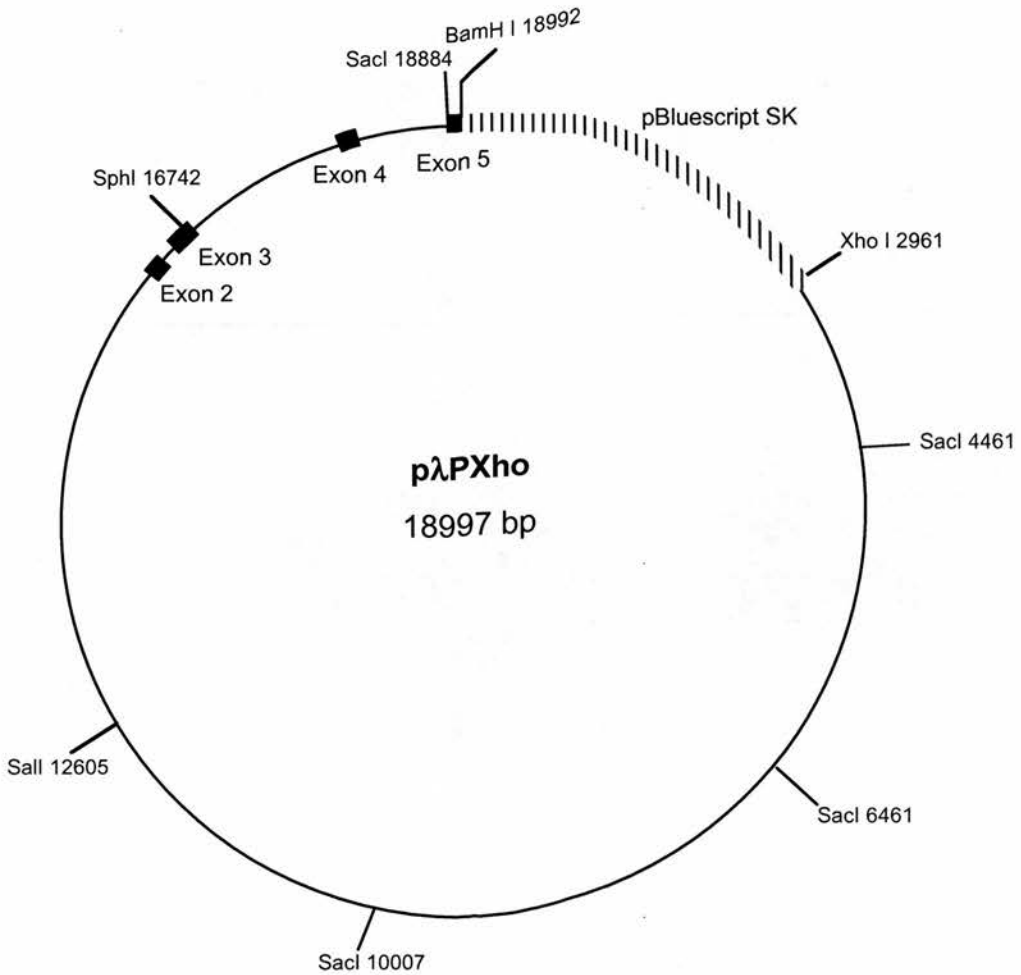

Figure 2-3. Plasmid pλPXho. pλPXho is a genomic clone spanning from the last 12kb of intron 1 to 54bp of exon 5 of the *EDNRB* gene. It was obtained by screening a λphage library (created by Dr. A Smith, Institute for Stem Cell Research, University of Edinburgh) using *EDNRB* cDNA as a probe and cloned into pBluescript II SK (pBS). Only restriction sites of relevance to this thesis are marked.

Reference/Source: a gift from Dr. A. Bagnall, University of Edinburgh. Constructed by Dr. A. Bagnall

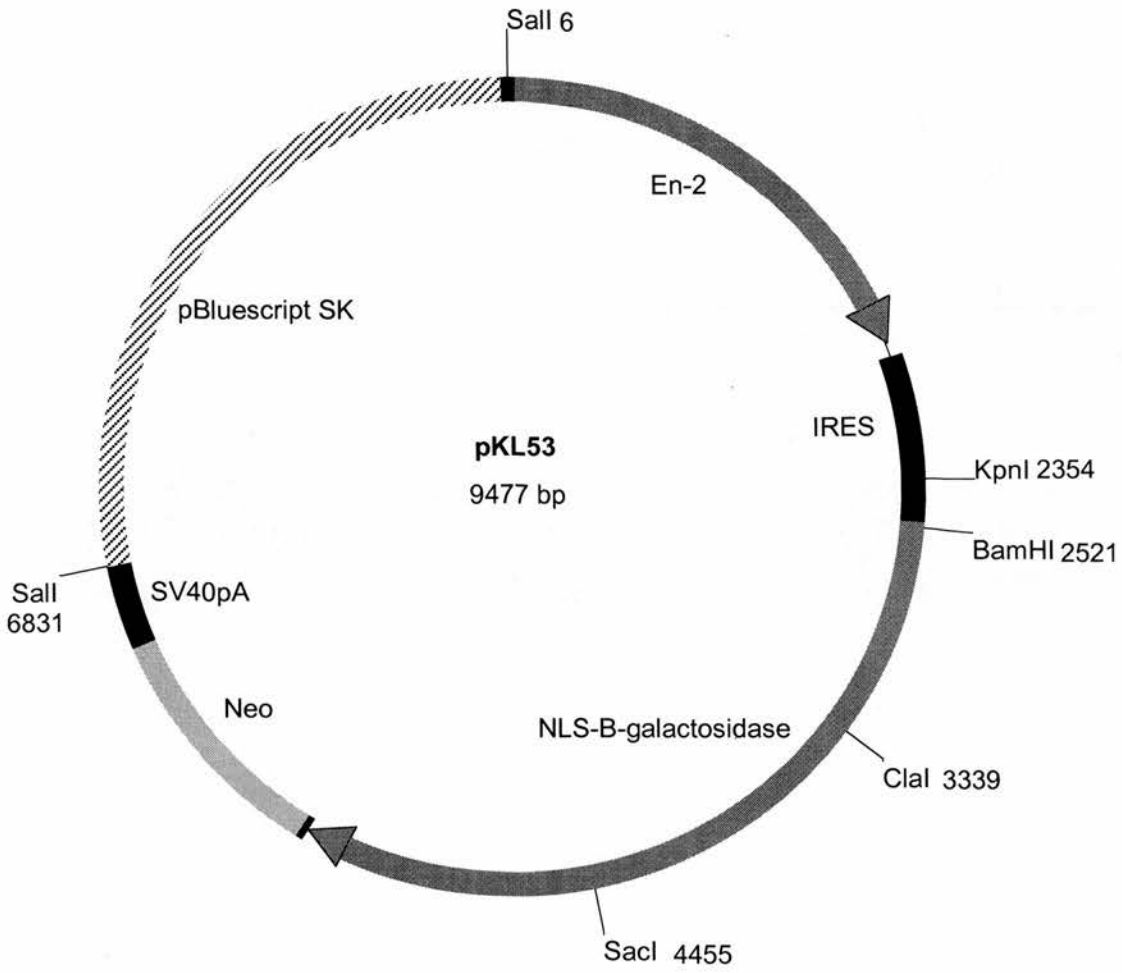

Figure 2-4. Plasmid pKL53. pKL53 contains an internal ribosome entry site (IRES) followed by the LacZ gene (β-galactosidase) cloned into pBS II SK. Preceding LacZ is a 29bp nuclear localisation signal (NLS). There is also the neomycin phosphotransferase resistance gene (neo), simian virus 40 polyadenylation site (SV40 polyA) and engrailed-2 (En-2). Only restriction sites of relevance to this thesis are marked.

Reference/Source: a gift from Dr. M. Sharp, University of Edinburgh. Constructed by Dr K. Lee and Dr. P. Mountford, Institute for Stem Cell Research, University of Edinburgh.

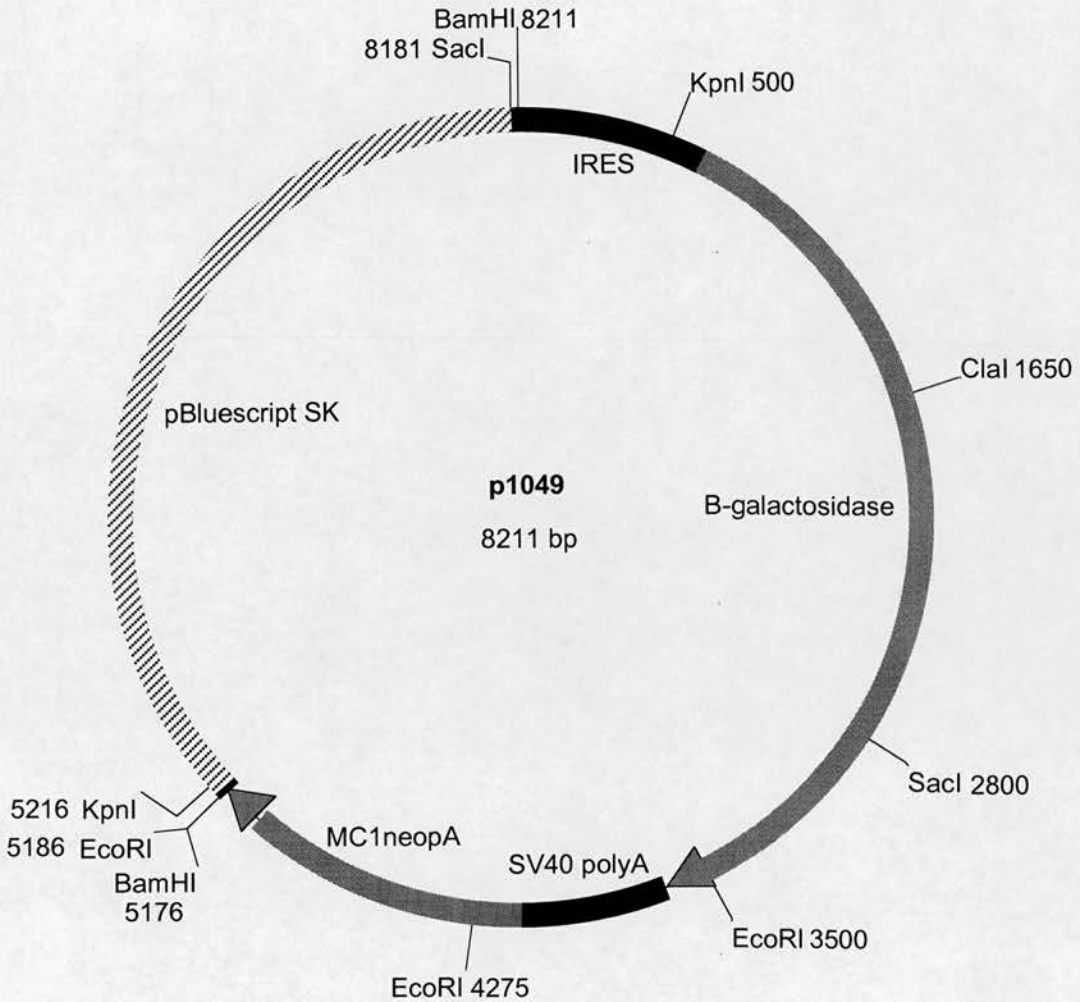

Figure 2-5. Plasmid p1049. p1049 contains an internal ribosome entry site (IRES) followed by the LacZ gene (β-galactosidase) cloned into pBS II SK. There is also the neomycin phosphotransferase resistance gene whose expression is driven by the MC1 promoter (MC1neopA) and a simian virus polyadenylation site (SV40 polyA). Only restriction sites of relevance to this thesis are marked.

Reference/Source: a gift from Dr. Andrew Smith, Institute for Stem Cell Research, University of Edinburgh. Constructed by Dr A. Smith, Institute for Stem Cell Research, University of Edinburgh.

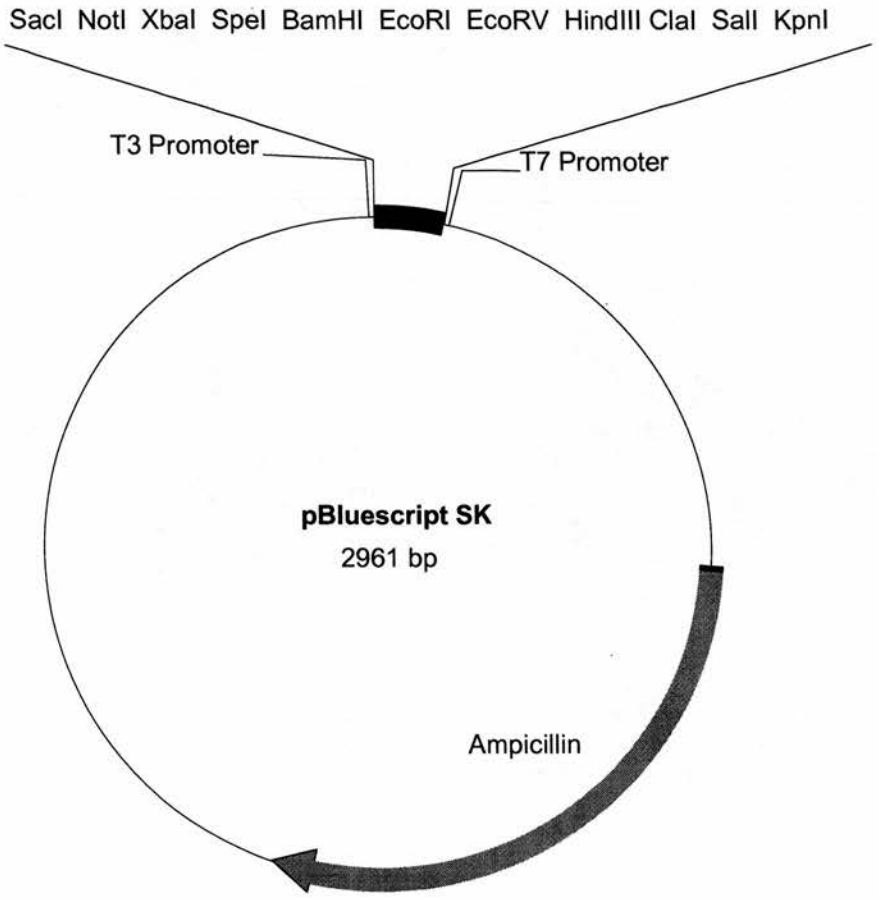

Figure 2-6. Plasmid pBluescript II SK. pBluescript II SK (pBS) is a cloning vector possessing a polylinker site containing 21 unique restriction sites (not all of them are shown here) flanked by T3 and T7 promoters. Also present is the ampicillin resistance gene.

Reference/Source: Stratagene Europe (cat. no. 212206).

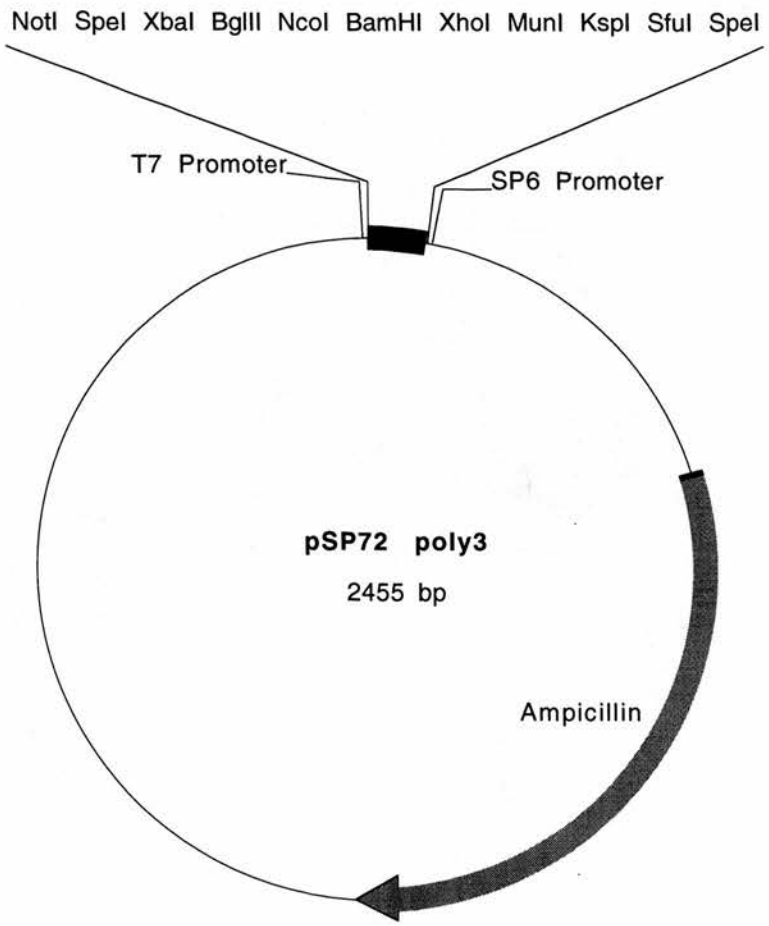

Figure 2-7. Plasmid pSP72poly3. pSP72poly3 is a pSP72 based vector (Promega UK Ltd) containing an altered polylinker flanked by T7 and SP6 promoters. Also present is the ampicillin resistance gene.

Reference/Source: a gift from Professor J. Mullins, University of Edinburgh. Constructed by A. Popplewell and S. Morley.

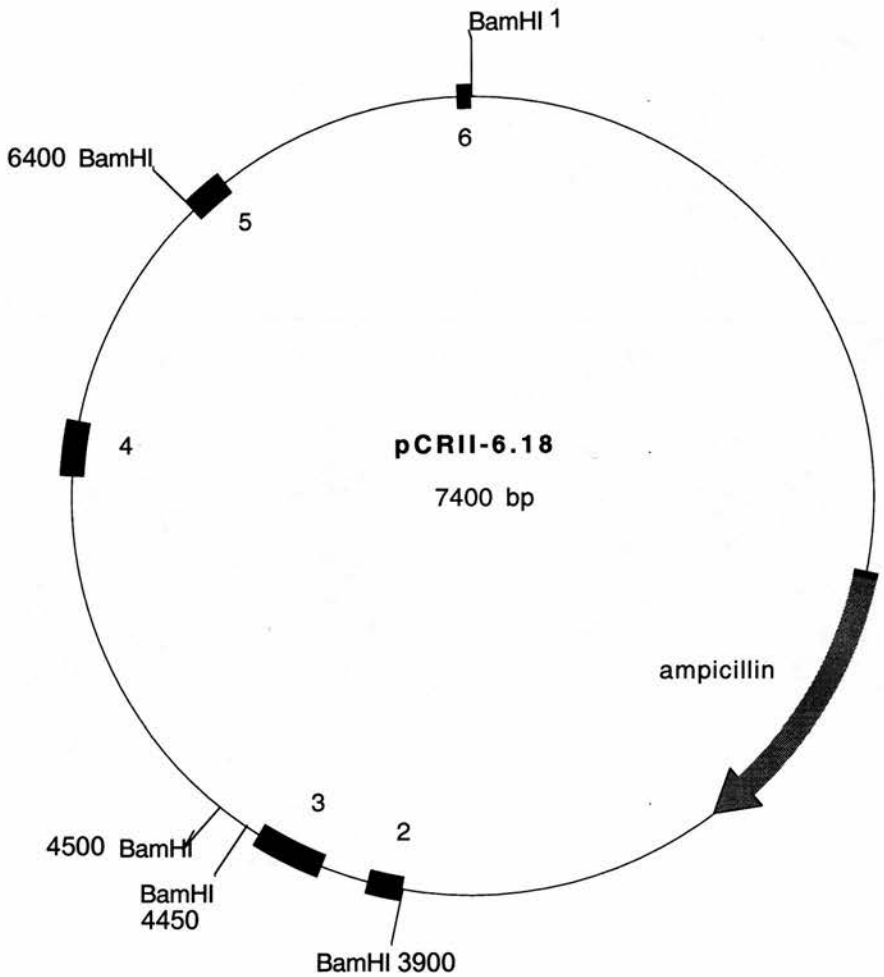

Figure 2-8. Plasmid pCRII-6.18. pCRII-6.18 is a pCRII based vector (Invitrogen Ltd) containing *EDNRB* genomic DNA spanning exon 2 to part of exon 6.

Reference/Source: a gift from Dr. A. Bagnall, University of Edinburgh. Constructed by Dr. A. Bagnall

2.4.3 Transformation of electrocompetent cells

One aliquot (40µl) of competent cells was used per transformation. Frozen aliquots were thawed on ice and between 0.5 and 4µl of plasmid DNA or ligation mix (approximately 10-100ng) were added to the cells and gently mixed by pipetting. The mix was transferred to a prechilled 0.2cm electroporation cuvette pre-washed with 70% ethanol and rinsed with water. Electroporation was performed in a Bio-Rad Gene-Pulser (Bio-Rad Laboratories Ltd) with the capacitor set to 25µF, 2.5KV and the pulse controller unit set to 200Ω. One pulse was applied resulting in a pulse of 12.5KV/cm with a time constant of 4.6-4.8msec. Immediately following electroporation, 300µl of SOC (20g/L bacto-tryptone, 5g/L bacto-yeast extract, 10mM NaCl, 2.5mM KCl, 10mM $MgCl_2$, 10mM $MgSO_4$ and 20mM glucose) was added to the transformation mix and incubated for 30 minutes at 37°C to allow expression of antibiotic resistance. Cells were plated on selection plates with approximately 100-200µl plated per plate. Plates were incubated overnight at 37°C.

2.4.4 Preparation of plasmid DNA

A single bacterial colony containing plasmid DNA of interest was picked from a freshly streaked plate and used to inoculate a starter culture of 2ml LB medium. Cultures were incubated at 37°C for 8 hours with shaking after which the starter culture was diluted 1/1000 in LB medium (final volume 50ml) and incubated overnight at 37°C with shaking. Cells were harvested by centrifugation at 3000rpm (Beckman J-6B, rotor JS 4.2, Beckman Coulter UK (Ltd)) for 15 minutes at 4°C followed by resuspension of the pellet in 50mM Tris-Cl pH 8, 10mM EDTA, 100µg/ml RNaseA.

Plasmid DNA was prepared using HiSpeed Plasmid Midi/Maxi kits supplied by QIAGEN (QIAGEN Ltd). A detailed description of the procedure is given in the manufacturer's instruction manual. This method involved alkaline lysis of the cells in 200mM NaOH, 0.1% SDS followed by neutralisation in 3M potassium acetate pH5.5. Precipitated material (proteins, chromosomal DNA and cellular debris) was removed by filtration and the cleared lysate passed through HiSpeed QIAGEN

columns containing DNA binding resin. RNA and proteins were removed by washing in medium salt wash buffer (1M NaCl, 50mM MOPS pH7, 15% isopropanol). Bound DNA was then eluted from the column in high salt buffer (1.25M NaCl, 50mM Tris-Cl pH8.5, 15% isopropanol) and the resulting eluate precipitated in 0.7 volumes of isopropanol resulting in high quality DNA. The midi and maxi kits routinely yielded approximately 200µg and 750µg plasmid DNA respectively. The DNA concentration was determined by UV spectrophotometry (refer to section 2.4.5) and the identity of the plasmid was confirmed by restriction mapping (refer to 2.4.8).

2.4.5 Quantification of DNA

DNA concentration was determined by measuring the absorbance at 260nm (OD_{260}) in a SmartSpec 3000 spectrophotometer (Bio-Rad Laboratories Ltd) using a quartz cuvette zeroed with TE (10mM Tris-HCl pH8.0, 1mM EDTA). Plasmid DNA was diluted in TE and absorbance measured at 260 and 280nm to obtain a reading which was between 0.1 and 1.0 units. An absorbance of 1 unit at 260nm corresponds to 50µg plasmid DNA/ml. This relationship was used to calculate DNA concentrations taking into account the dilution factor.

2.4.6 Agarose gel electrophoresis

DNA fragments were separated according to size by agarose gel electrophoresis. Agarose gels were 0.8-2.0% (w/v) containing 1x TAE (40mM Tris-acetate, 1mM EDTA) and 0.5µg/ml ethidium bromide. Prior to loading 6x gel loading buffer (0.2% bromophenol blue, 0.2% xylene cyanol FF, 10% glycerol, MBI Fermentas) was added to each sample to give a final concentration of 1x loading buffer. Samples were always run alongside molecular weight markers. Electrophoresis was performed in 1 x TAE running buffer at 100V until the dye front had migrated an appropriate distance. Ethidium bromide – DNA complexes were visualised under UV light (UVP Transilluminator, UVP Inc.) and photographed by a Sony Video Graphic Printer UP-890CE (Sony UK Ltd).

2.4.7 Nucleic acid extraction and precipitation

Phenol:chloroform extraction and alcohol precipitation was used to desalt and concentrate DNA preparations. An equal volume of phenol:chloroform:isoamyl alcohol (25:24:1) was added to the DNA solution, vortexed and centrifuged for 2 minutes at 12000x g at 4°C. The upper phase was transferred to a fresh tube and 2 volumes of ice cold 100% ethanol and 0.1 volumes of 3M sodium acetate pH 5.2 were added to precipitate the DNA. The solution was incubated at -20°C for 30-60 minutes. For the recovery of small quantities of DNA, samples were left overnight at -20°C. DNA was pelleted by centrifugation in a microcentrifuge at maximum speed for 15 minutes at 4°C. The DNA pellets were washed in 70% ethanol to remove co-precipitated salt and respun for 5 minutes. Pellets were air dried and resuspended in a suitable volume of TE.

2.4.8 Restriction enzyme digests

DNA was digested using restriction endonucleases for either analytical or downstream cloning purposes. For analytical purposes 1µg plasmid DNA was digested with 10 units of enzyme in the appropriate restriction buffer made up to a final volume of 20µl with distilled water. Digests were usually incubated at 37°C for 3 hours to ensure complete restriction. However, some enzymes required higher incubation temperatures as indicated on the product data sheet. Following digestion, 15µl of the sample was analysed by agarose gel electrophoresis.

For downstream applications (e.g. ligation) approximately 10µg plasmid DNA was digested with 50 units of enzyme in the appropriate restriction buffer made up to a final volume of 50µl. Digests were incubated overnight at the appropriate temperature. Following digestion, the enzyme was heat-inactivated by incubation at 65°C for 15 minutes. Digested DNA was then used for further manipulations.

2.4.9 Preparation of PCR products for ligation

2.4.9.1 PCR conditions

PCR reactions were performed in 4x 25µl volumes. A "master mix" containing all components except DNA was made for each PCR. The master mix comprised 1x *Pfu* DNA polymerase buffer (20mM Tris-HCl pH 8.8, 10mM KCl, 10mM $(NH_4)_2SO_4$, 2mM $MgSO_4$, 100µg/ml BSA, 0.1% Triton X-100), 200µM dNTP mix, 0.3µM forward and reverse primers and 1.125 units *Pfu* DNA polymerase. Primer sequences are documented in section 4.2.1.3. For the purposes of cloning, PCR was performed using *Pfu* proofreading enzyme to minimise the chance of introducing random mutations. The master mix was aliquoted into PCR tubes and template DNA (approximately 1ng) added. PCR was performed on an MJ Research PTC-200 DNA Engine (Genetic Research Instrumentation) and DNA amplified as follows: initial denaturation at 92°C for 2 minutes, amplification for 30 cycles of denaturation for 30 seconds at 92°C, annealing for 30 seconds at 50°C, extension for 2 minutes at 68°C followed by a final extension period of 10 minutes at 68°C. A heated lid was used to prevent evaporation. 5µl of PCR reaction was checked on an agarose gel before proceeding with Klenow, Kinase, Ligase reactions.

2.4.9.2 Klenow, Kinase, Ligase

The Klenow, Kinase, Ligase reaction creates concatermeric DNA from PCR products by polishing (Klenow), phosphorylating (Kinase) and ligating (Ligase) PCR termini in a single. The concatermeric DNA can then be used for restriction enzyme digestion and ligation to the vector. PCR reactions (4x 25µl) were pooled and phenol:chloroform extracted and precipitated (refer to section 2.4.7). DNA was resuspended in 12.6µl distilled water. Ligase buffer (30mM Tris-HCl pH 7.8, 10mM $MgCl_2$, 10mM DTT, 0.5mM ATP), 0.2mM dNTP mix, 5 units Klenow, 4 units T4 polynucleotide kinase and 2 units T4 DNA ligase were added to give a final reaction volume of 25µl. The reaction was incubated at room temperature for 2 hours followed by another round of phenol:chloroform extraction and precipitation.

2.4.9.3 Restriction enzyme digest of PCR concatamers

Precipitated DNA was redissolved in 36µl distilled water and digested with the appropriate restriction enzymes (20 units) and restriction buffer in a final volume of

50µl and incubated overnight at 37°C. The digested PCR products were phenol:chloroform extracted and precipitated and DNA resuspended in 40µl distilled water ready for ligation.

2.4.10 Purification of DNA fragments from agarose gels

Digested DNA fragments were purified from agarose gels using silica gel based purification. QIAEX II Agarose Gel Extraction kits were used (QIAGEN Ltd) and the supplied protocol followed. Briefly, digested DNA was separated on a 0.8% agarose gel and the DNA band of interest excised under UV light. The gel was solubilised in QX1 buffer (3M NaCl, 4M sodium perchlorate, 10mM Tris-HCl pH 7, 10mM sodium thiosulphate) and DNA bound to QIAEX beads by incubation at 50°C for 10 minutes. The beads were washed by centrifugation once in buffer QX1 and then twice in buffer PE (70% ethanol, 100mM NaCl, 10mM Tris-HCl pH 7.5). Bound DNA was eluted by incubation of the beads in 20µl TE at 50°C for 5 minutes followed by centrifugation and recovery of the purified DNA in the supernatant. In order to increase the yield a second elution step was performed and the supernatants combined.

2.4.11 Conversion of a 3′ -overhang to a blunt end terminus

Before ligation some DNA fragments with incompatible restriction sites had to be blunt-ended using T4 DNA polymerase (e.g. BamHI and SphI). Following purification of DNA (described in section 2.4.10) approximately 2-5µg DNA was used per reaction in a final volume of 50µl. Reactions were performed in 1x incubation buffer (50mM Tris-HCl pH8.8, 15mM $(NH_4)_2SO_4$, 7mM $MgCl_2$, 0.1mM EDTA, 10mM 2-mercaptoethanol, 20µg/ml bovine serum albumin) supplemented with 100µM dNTP and 5 units of T4 DNA polymerase. Reactions were performed at 11°C for 30 minutes before being phenol:chloroform extracted and precipitated (refer to section 2.4.7) ready for ligation.

2.4.12 Ligation of DNA

Ligations were set up with insert:vector molar ratio of 3:1 for sticky ends and 5:1 for blunt ends. Concentrations of vector and insert were estimated by running a sample of each alongside molecular weight standards of known concentration on an agarose gel. Approximately 50-100ng of vector DNA was used in a final reaction volume of 25µl. Reactions were performed in 1x ligase buffer (40mM Tris-HCl pH7.8, 10mM $MgCl_2$, 10mM DTT, 0.5mM ATP) and with 1 unit T4 DNA ligase. A control reaction using vector alone with ligase was set up with every ligation. The ligation reaction was performed on a MJ Research PTC-200 DNA Engine (Genetic Research Instrumentation) using a program cycling between 16°C for 30 seconds and 25°C for 30 seconds repeated 60 times. Following ligation, the ligated DNA was used for transformation of competent cells (refer to section 2.4.3).

2.4.13 Analysis of transformants

Recombinants obtained from ligation reactions were screened by one of the following methods.

2.4.13.1 DNA minipreps and restriction enzyme digest analysis

2ml LB was inoculated with a single bacterial clone picked from the transformation plate and incubated overnight at 37°C with shaking. Approximately 24 colonies were analysed per ligation. 1.5ml aliquots were centrifuged at 12000x g in a microcentrifuge for 1 minute at 4°C. Cell pellets were resuspended in 100µl cell resuspension buffer (50mM glucose, 25mM Tris-HCl pH 8.0, 10mM EDTA) by vortexing and incubated for 5 minutes at room temperature after which 200µl of freshly prepared lysis buffer (0.2N NaOH, 1% SDS) was added and mixed by inversion. Lysates were incubated for 5 minutes on ice before being neutralised by the addition of 150µl ice cold potassium acetate solution pH 4.8 (3M potassium, 5M acetate) and gently vortexed for 10 seconds. Following a further 5 minute incubation on ice, lysates were centrifuged at 12000x g for 5 minutes at 4°C and the supernatant transferred to a fresh tube. DNA was phenol:chloroform extracted and ethanol precipitated (refer to section 2.4.7). DNA was resuspended in 50µl TE containing

20µg/ml RNase A and used for analytical restriction enzyme digest analysis (refer to section 2.4.8).

2.4.13.2 Colony lift and hybridisation

The composition of solutions used in colony lift and hybridisation are listed in table 2-7. Cells were plated to give an optimal density of 200 colonies per 83mm agar plate. After overnight incubation at 37°C, plates were pre-cooled to 4°C for 30 minutes. Colonies were transferred onto Hybond-N nylon membrane discs (Amersham Pharmacia Biotech UK Ltd) by placing the membrane onto the plate for 30-60 seconds. The orientation of the colonies was marked with a needle. The membrane was transferred colony side uppermost onto a fresh agar plate and incubated for 2 hours at 37°C. DNA was liberated from bacteria by placing the membrane on filter paper (colony side up) soaked in denaturation buffer for 4 minutes and then onto filter paper soaked in neutralisation buffer for 2x 3 minutes.

Table 2-7. Composition of solutions used in colony lifts and Southern blotting

Solution	Composition
Denaturation buffer	1.5M NaCl 0.5M NaOH
Neutralisation buffer	1.5M NaCl 1M Tris-HCl pH 7.5
20x SSC	0.3M tri-sodium citrate 3M NaCl pH 7.2
Hybridisation buffer	50% formamide 0.025% (w/v) sodium pyro-phosphate 5x SSC 5x Denhardt's reagent 50µg/ml yeast tRNA
100x Denhardt's reagent	20g/L Ficoll 400 20g/L polyvinylpyrrolidone 20g/L BSA fraction V (filtered and stored at -20°C)
Wash buffer 1	6x SSC 0.1% SDS
Wash buffer 2	2x SSC 0.1% SDS

Membranes were then washed vigorously in 2x SSC to remove any debris and allowed to air dry. DNA was fixed to the membrane by baking at 120°C for 1 hour and stored at 4°C until hybridisation.

For hybridisation, probes were labelled with Redivue [^{32}P] dCTP (Amersham Pharmacia Biotech UK Ltd) using Rediprime II random prime labelling system (Amersham Pharmacia Biotech UK Ltd). Denatured DNA (approximately 25ng of DNA diluted in 45µl TE) was added to the reaction tube (containing dATP, dGTP, dTTP, Klenow and random primers in a dried pellet) along with 5µl of [^{32}P] dCTP and incubated for 30 minutes at 37°C. Unincorporated nucleotides were removed on ProbeQuant G-50 Micro columns (Amersham Pharmacia Biotech UK Ltd) according to the manufacturer's instructions. Membranes, prewet in 2x SSC, were placed in a prewarmed hybridisation bottle (Techne Ltd) and pre-hybridised for one hour in hybridisation buffer at 42°C in a Techne hybridisation oven (Techne Ltd). The labelled probe was denatured by incubation at 100°C, added to the membranes and hybridised overnight at 68°C. Upon completion of hybridisation, the probe was discarded and membranes rinsed briefly in 2x SSC. The blots were then washed for 10 minutes in wash buffer 1 and then a further 10 minutes in wash buffer 2. If necessary a further wash of 10 minutes in 0.2x SSC, 0.1% SDS was performed. Membranes were wrapped in Saran Wrap and placed in a cassette with intensifying screens for autoradiography using Kodak XOMAT XAR-5 film (Sigma-Aldrich Company Ltd). After 24 hours at -70°C films were developed using a Konica SRX-101 A developer and if necessary re-exposed for a suitable amount of time to detect the desired signal. Resulting dark spots on the film were aligned with the original tranformation plate and the corresponding colonies picked and used to inoculate 2ml LB which were grown up overnight at 37°C and analysed by DNA minipreps and restriction enzyme digest as described in section 2.4.13.1.

2.4.14 Sequencing of plasmid DNA

Sequencing was performed by Mrs. N. Kotelevtseva, University of Edinburgh using an ABI Prism sequencer with BigDye Terminator chemistry (Applied Biosystems).

2.4.15 Analysis of DNA sequences

Sequences were analysed with Gene Jockey Sequence Processor software (Biosoft, Cambridge, UK).

2.5 ES CELL CULTURE AND GENERATION OF KNOCK-IN MICE

2.5.1 Materials

All cell culture reagents were supplied by Invitrogen Ltd (Gibco) except for foetal calf serum (FCS) which was from Globepharm (Surrey, UK). Embryonic stem (ES) cells were grown on Corning culture grade plastic-ware (Bibby Sterilin Ltd, Stone, UK). G418 was supplied by Invitrogen Ltd (Gibco). Leukaemia inhibitory factor (LIF) was purified in-house (Institute for Stem Cell Research, University of Edinburgh).

The composition of standard ES cell culture media is shown in table 2-8. Media was prepared under sterile conditions and stored as 500ml aliquots at 4°C. Fresh media was tested for bacterial contamination by incubating 5ml with 5ml tryptose phosphate broth a 37°C for at least 2 days before use.

Table 2-8. Composition of ES cell culture media

Solution	Composition
ES cell culture media	1x GMEM 10% FCS 0.23% (w/v) sodium bicarbonate 1x MEM non-essential amino acids 2mM L-glutamine 1mM sodium pyruvate 0.1μM 2-mercaptoethanol DIA/LIF (100U/ml)

Abbreviations: GMEM, Glasgow minimal essential media; FCS, foetal calf serum; MEM, minimal essential media; DIA, differentiation inhibitory factor; LIF, leukaemia inhibitory factor.

2.5.2 ES cell culture conditions

E14Tg2a ES cells were grown in ES cell culture medium on gelatinised tissue culture flasks (0.1% gelatin) in a humidified incubator (Heraeus model B5060 EC/CO_2) at 37°C, 6-7.5% CO_2. ES cells were maintained in an undifferentiated state by growing

in the presence of leukaemia inhibitory factor (LIF). Manipulations were performed inside a laminar flow sterile hood (Gelair ICN Flow Hood (class 3), ICN Pharmaceuticals Ltd, Thame, UK). Before performing manipulations, all surfaces (including arms and hands) were sterilised with 70% industrial methylated spirits.

2.5.3 Passage of ES cells

ES cells were maintained in 25cm^2 flasks and passaged every 2-3 days. Prior to passaging, media, TVP and PBS were warmed to 37°C. Following aspiration of media, cells were washed twice with 10ml PBS to remove any dead cells. Cells were trypsinised with 5ml TVP (0.025% trypsin, 1% chicken serum, 0.5mM EDTA in PBS) and the flask incubated at 37°C for 1-2 minutes. Cells were dissociated by tapping the flask and by pipetting up and down to obtain a single cell suspension. TVP was neutralised by the addition of 15ml ES cell culture media and cells were transferred to a sterile universal tube. Cells were pelleted by centrifugation at 1300rpm for 5 minutes in a benchtop centrifuge before being resuspended in 5ml PBS and counted in a haemocytometer. 1x10^6 cells were seeded in a 25 cm^2 gelatinised flask.

2.5.4 Freezing and thawing ES cells

Cells were trypsinised and pelleted as described above and resuspended in 1ml freezing medium (10% (v/v) DMSO in ES cell culture medium) before transfer to cryotubes. Cells were immediately frozen at -70°C for 1-2 days before transfer to liquid nitrogen for long term storage. Frozen cells were thawed in a 37°C water bath and diluted in 9ml ES cell culture medium. Cells were seeded in a 25cm^2 gelatinised flask and incubated at 37°C for 8 hours before replacing the media with fresh ES cell culture medium to remove traces of DMSO.

2.5.5 Electroporation of ES cells

150µg and 75µg of DNA construct was linearised with the appropriate restriction enzyme (100 units enzyme), precipitated as described in section 2.4.7 and allowed to air dry. DNA was resuspended in 100µl PBS.

Four 150cm^2 flasks (approximately 1x10^8 cells) were grown to confluency. Approximately 3-4 hours before electroporation the cells were fed with fresh ES cell culture medium. In addition, twenty 100mm round tissue culture plates were gelatinised, 10ml ES cell culture medium added to each plate and stored in the incubator until use. For electroporation, ES cells were trypsinised as described above, pooled and counted. Cells were pelleted and resuspended in an appropriate volume of PBS to give 1x10^8 cells in 600µl. This was equivalent to 5x10^6 cells per plate. At this stage 5µl and 20µl of cells were seeded onto two of the plates to represent non-electroporated controls. To the remainder of the cells, 100µl linearised DNA construct was added and transferred to a sterile 0.4cm cuvette. Electroporation was performed in a Bio-Rad Gene Pulser (Bio-Rad Laboratories Ltd) with the capacitor set to 3µF, 0.8kV. One pulse was applied resulting in a time constant of 0.1msec. Cells were immediately transferred to 10ml ES cell culture medium. Cells were plated either neat (undiluted) or diluted (1:2, 4 and 8). In each case, 1ml of cells was added to each plate. Twenty-four hours after electroporation, selection was started by adding 160µg/ml G418 to the medium. Selection medium was replaced every 2 days or more frequently depending on the number of dead cells.

2.5.6 Expansion of G418 ES cell colonies

After selection in G418 for 7-8 days, clones were picked and expanded for either freezing (storage, refer to section 2.5.7) or DNA preparation (screening, refer to section 2.5.8). Media was aspirated and ES cells rinsed in PBS. Individual colonies were picked by scraping the colony with a P20 tip fitted to a P20 pipette. Colonies, along with 20µl PBS, were transferred to individual wells containing 150µl selection medium per well, in a round bottomed 96 well plate. Once 96 colonies had been picked, cells were dispersed by pipetting up and down with a multi-channel pipette (MCP) and then transferred to a gelatinised 96 well plate containing 150µl selection medium/well (final volume of medium was 300µl). 960 colonies were picked resulting in a total of ten 96 well plates. Clones were grown to confluence and were fed every 1-2 days before being processed for freezing (section 2.5.7) or DNA preparation (section 2.5.8).

2.5.7 Splitting and freezing of 96 well plates

Cells were split 1:2 onto replica 96 well plates, one of which was gelatinised. Medium was aspirated from the wells and 150µl PBS added using a MCP. 30µl of TVP was added to each well and the plate incubated for 3-5 minutes at 37°C after which cells were dissociated by pipetting up and down. Following trypsinisation, 70µl of quench medium (50% (v/v) medium, 50% (v/v) FCS) was added to each well to neutralise the trypsin. From this plate, 50µl was seeded onto the fresh gelatinised 96 well plate and 150µl of selection medium added. This plate, termed the "DNA plate", was returned to the incubator and grown to confluency for DNA preparation (refer to section 2.5.8). The remainder of the trypsinised cells were used for "freezing plates" by the addition of 50µl 2x freezing medium (25% (v/v) DMSO in ES cell culture medium) to each well. Plates were immediately sealed with adhesive tape and stored at -70°C.

2.5.8 ES cell DNA preparation

Once cells in the "DNA plate" had reached confluency they were processed for DNA extraction. Medium was aspirated and cells lysed overnight at 37°C in 50µl of lysis buffer (100mM Tris-HCl pH8.5, 200mM NaCl, 5mM EDTA, 0.2% (w/v) SDS, 100µg/ml Proteinase K). After transfer of the lysates to a fresh 96 well plate, 50µl of room temperature isopropanol was added to precipitate DNA and incubated for 10 minutes on a plate shaker. DNA was pelleted by centrifugation at 2700rpm for 15 minutes in a 96 well plate bench top centrifuge and washed in 70% ethanol. Excess ethanol was removed by incubation at room temperature for 5-10 minutes and DNA redissolved in 50µl TE by incubation on a heated (55°C) plate shaker for 2 hours. To ensure all DNA was resuspended, the solution was pipetted up and down several times. DNA was frozen at -20°C in the 96 well plate until screening was performed (refer to section 2.5.9).

2.5.9 Screening by Southern blotting

Southern blotting was performed from a modified version of the original method of Southern (Southern, 1975).

2.5.9.1 Restriction enzyme digest and electrophoresis

Restriction enzyme digests were set up using approximately 10µg ES cell DNA, 1x BSA, 1x restriction buffer and 20 units of the appropriate restriction enzyme in a final volume of 25µl. Digests were performed in round bottomed 96 well plates and incubated at 37°C overnight. A further 10 units of enzyme was added the following morning and the plate incubated for 2-3 hours to ensure complete digestion.

Digested DNA, alongside lambda DNA/*Hin*dIII ladder, was separated on 0.8% agarose gels (refer to section 2.4.6) using Bio-Rad Sub-Cell Model 96 Cell electrophoresis apparatus (Bio-Rad Laboratories Ltd). This apparatus is designed for running 96 samples simultaneously enabling gels to be loaded using a MCP. Ethidium bromide was not included in the gel since electrophoresis was carried out overnight at 10V. Ethidium bromide migrates in the opposite direction of current and would not produce an even staining pattern if included in the gel during prolonged electrophoresis. Instead gels were stained in an ethidium bromide bath (0.5µg/ml in TAE) for 10 minutes with shaking after electrophoresis was complete. After photographing, gels were denatured in denaturation buffer (refer to table 2-7) for 2x 10 minutes with shaking, rinsed in distilled water and neutralised in neutralisation buffer (refer to table 2-7) for 30 minutes.

2.5.9.2 Transfer of DNA by Southern blotting

A Pyrex dish containing transfer buffer (20x SSC, refer to table 2-7) with a glass plate on top was set up with two sheets of Whatman 3mm paper acting as a wick into the SSC solution. The inverted gel was positioned on top and surrounded by Parafilm. Hybond-N nylon membrane (Amersham Pharmacia Biotech UK Ltd), cut to the size of the gel, was soaked in transfer buffer for 10 minutes and placed on top of the gel ensuring there were no trapped air bubbles, followed by two pieces of 3mm paper soaked in transfer buffer (cut to gel size) and a stack of paper towels. Finally a glass plate was placed on top and the whole apparatus weighted down with a 500g weight and left overnight to allow capillary transfer to take place. After

blotting the membrane was rinsed briefly in 2x SSC and baked between two sheets of dry 3mm paper for 40 minutes at 120°C.

2.5.9.3 Hybridisation

Hybridisation and washing was performed as described in section 2.4.13.2 with the following modifications. Hybridisation buffer was 5x SSC, 0.2mM Dextran sulphate, 0.5% SDS, 4x Denhardt's reagent and 200µg/ml denatured sheared salmon sperm DNA and hybridisation was performed at 68°C. The lambda DNA/*Hin*dIII ladder was also detected using labelled lambda DNA (supplied with Rediprime kit). 25ng of lambda DNA was used for this purpose and labelled using 1µl of [^{32}P] dCTP and 9µl of cold dCTP.

2.5.10 Screening by 96-well Expand PCR

ES cell colonies were also screened by PCR using Expand Long Template PCR System (Roche Diagnostics Ltd). This system uses two thermostable DNA polymerases, *Taq* and *Pwo* specifically designed to amplify genomic DNA (i.e. long templates up to 20kb) (Cheng *et al.*, 1994). PCR was performed in a 96 well format in a final reaction volume of 25µl. A "master mix" containing all components except DNA, comprised 1x PCR buffer 3 (exact composition unknown, final Mg^{2+} concentration was 2.25mM), 500µm dNTP mix, 0.3µM forward and reverse primers and 1.3 units Expand enzyme mix. Primer sequences are documented in section 4.3.2.3. The master mix was aliquoted into thin-walled PCR tubes (Robbins Strip-Ease-8 PCR tubes, Genetic Research Instrumentation), using an MCP and 1µl of ES cell DNA added and mixed thoroughly. PCR was performed on an MJ Research PTC-200 DNA Engine (Genetic Research Instrumentation) with a 96 well block. DNA was amplified as follows: initial denaturation at 92°C for 2 minutes, amplification for 10 cycles of denaturation for 10 seconds at 92°C, annealing for 30 seconds at 60°C, extension for 3 minutes at 68°C followed by 25 cycles of denaturation for 10 seconds at 92°C, annealing for 60 seconds at 30°C and extension at 68°C for 3 minutes + 20 seconds/cycle. The program was completed with a final elongation step of 7 minutes at 68°C. A heated lid was used to prevent evaporation.

After PCR reactions were completed, 20µl of each reaction was analysed on an agarose gel.

2.5.11 Expansion of positive clones

Once positive homologously targeted clones had been identified by Southern blotting or by PCR screening, the replica "freezing" plate was defrosted and the appropriate clone revived. 96-well plates were removed from the -70°C freezer and were immediately thawed by floatation in a 37°C water bath for 30 seconds. Cells were then transferred to a gelatinised 96-well plate containing 250µl medium/well and incubated at 37°C for 8 hours or until the cells had adhered to the plate. The medium was replaced with fresh ES cell culture medium to remove traces of DMSO and dead cells. Cells were then cultured at 37°C until confluent, replacing medium when required. Once confluent, cells were seeded in $25cm^2$ flasks where they were maintained for use in further analysis (e.g. Southern blotting, *in vitro* analysis) and for blastocyst microinjection.

2.5.12 ES cell differentiation

To confirm expression of the knocked-in gene in homologously targeted clones, ES cells were differentiated into endothelial cells using one of the following methods.

2.5.12.1 Differentiation of ES cells in hanging drops

ES cells were cultured in hanging drops as previously described (Bloch *et al.*, 1997; Gustafsson *et al.*, 2000). ES cells were trypsinised and counted as described in section 2.5.3. $6x10^5$ cells were diluted in 20ml ES cell culture medium and transferred to a sterile trough. Using a MCP set to dispense 10µl, cells were grown in rows on ten $100mm^2$ bacteriological grade square plates each containing 8ml of sterile water and incubated in an inverted position (i.e. drops hanging down) for 2 days at 37°C during which time ES cells develop into embryoid bodies (EB). To harvest the EB, the plates were gently tapped and cells collected into a centrifuge tube. Cells were centrifuged for 3 minutes on a low speed (800rpm) in a benchtop centrifuge, resuspended in 20ml ES cell culture medium and transferred to a bacteriological grade petri dish. At this point penicillin (100U/ml) and streptomycin

(100µg/ml) was added to prevent bacterial contamination. EB were incubated for a further 4 days at 37°C with medium being replaced after 2 days. At this stage EB were either disaggregated into single cells or kept as EB (4-5 EB per well). In both cases cells were cultured on gelatin (0.1%) coated 6 well plates in the absence of LIF to initiate differentiation.

For disaggregation, EB were collected into a centrifuge tube and allowed to settle by gravity. After washing in PBS, cells were incubated with shaking for 1 hour at 37°C in dispase solution (1.2U/ml dispase (Roche Diagnostics Ltd), 70µg/ml DNase in PBS). Cells were dissociated by passing through a blue needle several times. After addition of 4ml ES cell culture medium cells were incubated for 5-10 minutes at room temperature followed by centrifugation at 1000rpm for 5 minutes. Finally, cells were washed once in PBS by centrifugation and resuspended in 1ml medium before transfer to a fresh plate containing 5ml medium (with penicillin/streptomycin). Cells were incubated at 37°C and medium changed when required before being processed for LacZ staining (refer to section 2.6.1).

2.5.12.2 Differentiation of ES cells on collagen IV plates

Differentiation of ES cells on collagen IV plates was performed as described by Nishikawa *et al* (Nishikawa *et al.*, 1998). ES cells were maintained as described in section 2.5.2. Once confluent, cells were trypsinised and counted as described in section 2.5.3. $1x10^4$ cells were plated per well on a 6 well plate coated with mouse collagen IV (BD Biosciences UK Ltd) in 2ml of ES cell culture medium with or without LIF (refer to chapter 4 for further details). Medium was replaced every 2 days. Cells were grown for 5-6 days after which they were processed for either FACS analysis (refer to section 2.5.12.3) or LacZ staining (refer to section 2.6.1).

2.5.12.3 Flow cytometry of differentiated ES cells

ES cells were trypsinised and counted as described in section 2.5.3 before being washed twice in PBS (supplemented with 0.1% BSA, 0.1% sodium azide). Cells were resuspended in PBS at a concentration of $2x10^6$ cells/ml and aliquots of $2x10^5$ cells were incubated with phycoerythrin (PE) conjugated antibodies (anti-mouse - Flk-1, -Sca-1, -ICAM-1, all supplied by Caltag Medsystems Ltd) for 40 minutes at 4°C. Following removal of unbound antibody by washing twice in PBS, cells were

resuspended in PBS and positively stained cells counted using FACSCaliber and CellQuest software (BD Biosciences UK Ltd). Data for 10000-40000 cells were acquired. Unstained cells were included as negative controls.

2.5.13 Microinjection of ES cells, generation of chimeric mice and germline transmission

ES cells which were found to contain the targeted gene, were expanded as described in section 2.5.11 and used in the microinjection of blastocysts and production of transgenic mice. Microinjection of ES cells and all steps involved in production of chimeric mice were performed by Dr. J. Ure (Institute for Stem Cell Research, University of Edinburgh) according to the method described by Bradley *et al* (Bradley *et al.*, 1984).

Blastocysts were obtained from the fallopian tubes of C57BL/6J female mice on day 4 of pregnancy by flushing with PB1 medium supplemented with 10% (v/v) FCS (140mM NaCl, 3mM KCl, 21.1mM Na_2HPO_4, 1.5mM KH_2PO_4, 5.8mM glucose, 0.4mM sodium pyruvate, 0.2mM penicillin, 0.1mM $CaCl_2$, 0.1mM $MgCl_2$, 0.01% (v/v) phenol red, pH 7.0-7.2) and were immediately transferred to ES cell culture medium and incubated at 37°C to promote expansion of the blastocoel cavity. They were then transferred to pre-prepared hanging drops of PB1 medium/10% FCS on siliconised coverslips (Repelcote, BDH) suspended over a custom-made manipulation chamber. Trypsinised ES cells were also placed in the hanging drops. The chamber was filled with liquid paraffin and chilled at 4°C for 10 minutes. Injection of blastocysts was performed using an IMT2 image-corrected microscope (Olympus Optical Company (UK) Ltd). Blastocysts were held in place by suction to a rounded holding pipette (20μm internal diameter) and ES cells injected using a flat-ended injection pipette (15μm internal diameter). Between 15 and 20 ES cells were injected into each blastocyst. Both the holding and injection pipettes were prepared in-house by stretching glass capillary tubing (100μm internal diameter) on an electrode puller (Camden Instruments). Before use, the pipettes were heat polished with a microforge (Micro Instruments Ltd). Pipettes were attached to instrument holders and controlled by Leica manipulators (Leica Microsystems (UK) Ltd).

Vacuum pressure was controlled by injectors connected to pipettes via paraffin-filled plastic tubes (Narashige International Ltd for holding pipette and Micro Instruments Ltd for injection pipette).

Following injection, blastocysts were transferred to ES cells culture medium and incubated at 37°C for 2-3 hours before implantation into pseudopregnant MF1 female mice. The recipient females had been mated with vasectomised DBA/2J males 2.5 days prior to implantation. Between 5 and 10 blastocysts were transferred to one uterine horn of each recipient. The resulting pups were assessed by coat colour. Chimeric pups were identified by the presence of beige-coloured patches, derived from ES cell derived 129 cells, amongst the host blastocyst derived black fur. Germline transmission of targeted ES cell DNA was assessed by crossing chimeras with BKW mice. Again, resulting pups were assessed by coat colour and germline transmission was confirmed by PCR genotyping (see section 2.5.14).

2.5.14 Maintenance of transgenic colonies

All transgenic animals were housed in the Hugh Robson Building animal house, University of Edinburgh and maintained under the Animals (Scientific Procedures) Act 1986 (UK Home Office, project licence number PPL 60/2813). Animals had free access to food (standard commercial animal chow) and water. Animals were genotyped by PCR of tail tip DNA.

2.5.14.1 Extraction of tail DNA

For each animal, approximately 0.5cm of tail was removed under anaesthetic (halothane). Tails were digested in 600µl tail buffer (50mM Tris-HCl pH 8.0, 100mM EDTA pH 8.0, 100mM NaCl, 1% (w/v) SDS) supplemented with 35µl of 10mg/ml proteinase K and incubated overnight at 55°C. The following day, 20µl of 20µg/ml RNAse was added to each sample and incubated for a further 1 hour at 37°C. Samples were placed on ice for 10 minutes before being centrifuged at 12000rpm for 2 minutes. DNA was precipitated by adding an equal volume of isopropanol to the resulting supernatants and rotating for 20 minutes at room temperature. DNA was pelleted by centrifugation and the pellet washed in 70%

ethanol. Pellets were allowed to air-dry briefly before being resuspended in 200µl of TE buffer. To aid resuspension, samples were incubated at 37°C for 1 hour.

2.5.14.2 Genotyping of transgenic animals by PCR analysis

Tail DNA was analysed by PCR. PCR was performed in a final reaction volume of 25µl. A "master mix" containing all components except DNA comprised 1x NH_4 PCR buffer, 500µM dNTP mix, 0.3µM forward and reverse primers, 2.25mM Mg^{2+} and 1 unit DNA polymerase (Bioline (UK) Ltd). Primer sequences are documented in section 4.2.4 and 4.2.5. The master mix was aliquoted into thick-walled 0.5ml microcentrifuge tubes, 1µl of mouse tail DNA added and mixed thoroughly. PCR was performed on an MJ Research PTC-200 DNA Engine (Genetic Research Instrumentation) and DNA amplified as follows: initial denaturation at 92°C for 2 minutes, amplification for 30 cycles of denaturation for 30 seconds at 92°C, annealing for 30 seconds at 57°C, extension for 1 minute at 72°C followed by a final extension period of 10 minutes at 72°C. A heated lid was used to prevent evaporation. After PCR reactions were completed, 20µl of each reaction was analysed on an agarose gel.

2.6 LACZ STAINING AND HISTOLOGY

LacZ gene expression can be visualised by the formation of a blue precipitate resulting from hydrolysis of substrate 5-bromo-4-chloro-indolyl-B-D-galactoside (X-gal) (Pearson *et al.*, 1961; Horwitz *et al.*, 1964). X-gal was therefore utilised to analyse β-gal activity in targeted ES cells and in tissues obtained from knock-in animals (Fire, 1992). X-gal was supplied by Invitrogen Ltd.

2.6.1 Staining of differentiated ES cells

Cells were washed twice in PBS before fixation in fix buffer (0.2% (v/v) gluteraldehyde, 5mM EDTA pH 7.4, 2mM $MgCl_2$ in PBS pH 7.4) for 10 minutes at room temperature. Fixative was removed and cells were washed thoroughly in wash buffer (0.004% (v/v) NP-40, 0.002% (v/v) sodium deoxycholate, 2mM $MgCl_2$ in PBS pH 7.4) before being stained overnight at 37°C in X-gal staining solution. The

staining solution was prepared in wash buffer with the addition of 1mg/ml X-gal (from stock solution of 25mg/ml X-gal in DMSO), 4mM potassium ferrocyanide and 4mM potassium ferricyanide. Following staining, cells were washed in wash buffer, viewed under a Zeiss Axiovert 25 inverted microscope (Carl Zeiss Ltd) and photographed using a Zeiss Axiocam with Axiovision 3.1 software (Carl Zeiss Ltd).

2.6.2 Staining of tissues

Tissues from knock-in animals were removed, rinsed in PBS and fixed at 4°C in 4% (w/v) paraformaldehyde in PBS pH 7.4. Fixation times differed depending on the type of tissue and the level of LacZ expression. Since β-gal activity is inactivated by paraformaldehyde fixation, the optimal fixation time had to be determined at the outset. For kidney samples, fixation was for 1 hour. For lung samples, fixation was for 15 minutes. For further information refer to chapter 5. Tissues were then washed thoroughly in PBS pH 7.4 and equilibrated in 30% (w/v) sucrose in PBS overnight at 4°C. The following day tissues were snap-frozen in liquid nitrogen and stored at -70°C until use. For frozen sections, tissues were placed in the cryostat (Model OFT, Bright Instruments Co Ltd) for at least 30 minutes prior to sectioning to allow the tissue to reach the chamber temperature of -20°C. Samples were mounted in CRYO-M-BED embedding compound (Bright Instruments Co Ltd) and 10-15μm sections cut. Sections were collected onto TESPA coated slides and allowed to air-dry for 1 hour before being stored at -20°C until use. TESPA coated slides were prepared as follows. Slides were cleaned by immersion in 10% HCl/70% ethanol followed by rinsing in water and then acetone. Slides were allowed to air-dry before further immersion in 2% (v/v) aminopropylethoxysilane (TESPA)/acetone for 10 seconds. After two final rinses in 100% acetone, slides were again allowed to air-dry and were ready to use.

For staining, sections were briefly rinsed in PBS pH 7.4 and transferred to X-gal staining solution (1mg/ml X-gal (from stock solution of 25mg/ml X-gal in DMSO), 4mM potassium ferrocyanide and 4mM potassium ferricyanide, 2mM $MgCl_2$, 0.02% (v/v) NP-40 prepared in PBS pH 7.4). Tissues were stained overnight at 37°C. Following a final rinse in PBS for 20 minutes, sections were counterstained with

eosin to allow visualisation of individual cells. This involved immersion of slides in eosin for 3 minutes followed by washing in tap water for 20-60 seconds. Sections were then mounted and photographed using a Kontron Elektronik ProgRes 3012 camera attached to a Zeiss Axioskop microscope (Carl Zeiss Ltd). Images were manipulated using Prog Res 3012 v3.05 software (Carl Zeiss Ltd). Renal localisation was verified by an independent kidney histologist (Professor Stewart Fleming, University of Dundee).

2.6.3 Quantification of β-gal activity

β-gal activity was quantified in tissue extracts using an assay based on the methylumbelliferone fluorescence method which measures the hydrolysis of 4-methylumbelliferyl-β-D-galactoside catalysed by β-gal (Braell, 1991). This reaction yields 4-methylumbelliferone (MU), a fluorescent product that emits fluorescence at 460nm when excited at 365nm. 4-methylumbelliferyl- β-D-galactoside was supplied by Sigma-Aldrich Company Ltd.

Tissues from knock-in animals were removed and rinsed in PBS, pH 7.4. Kidney and lung were routinely used. Whole kidneys (approximately 0.2g) and 0.2g (wet weight) of lung were homogenised in 2ml of ice cold 1x reporter lysis buffer (Promega UK Ltd, exact composition unknown) supplemented with 1mM PMSF. Tissue homogenates were centrifuged at 12000g for 5 minutes at 4°C and supernatants stored at -20°C until use. Protein concentration was determined by the Bradford's assay (see section 2.3.3) and approximately 100μg used for quantification of β-gal activity.

Prior to measurement of β-gal activity in tissues, the fluorometer (TKO 100 mini-fluorometer, Hoeffer Scientific Instruments) was calibrated according to the manufacturer's instructions with a standard 50nM MU solution to give a reading of 400 fluorescence units. Linearity of fluorescence was checked with a set of MU standards (0-200nM MU). A typical standard curve is shown in figure 2-9a. The assay was also performed using known quantities of *E. Coli.* β-gal enzyme (Promega UK Ltd) to produce the standard curve shown in figure 2-9b.

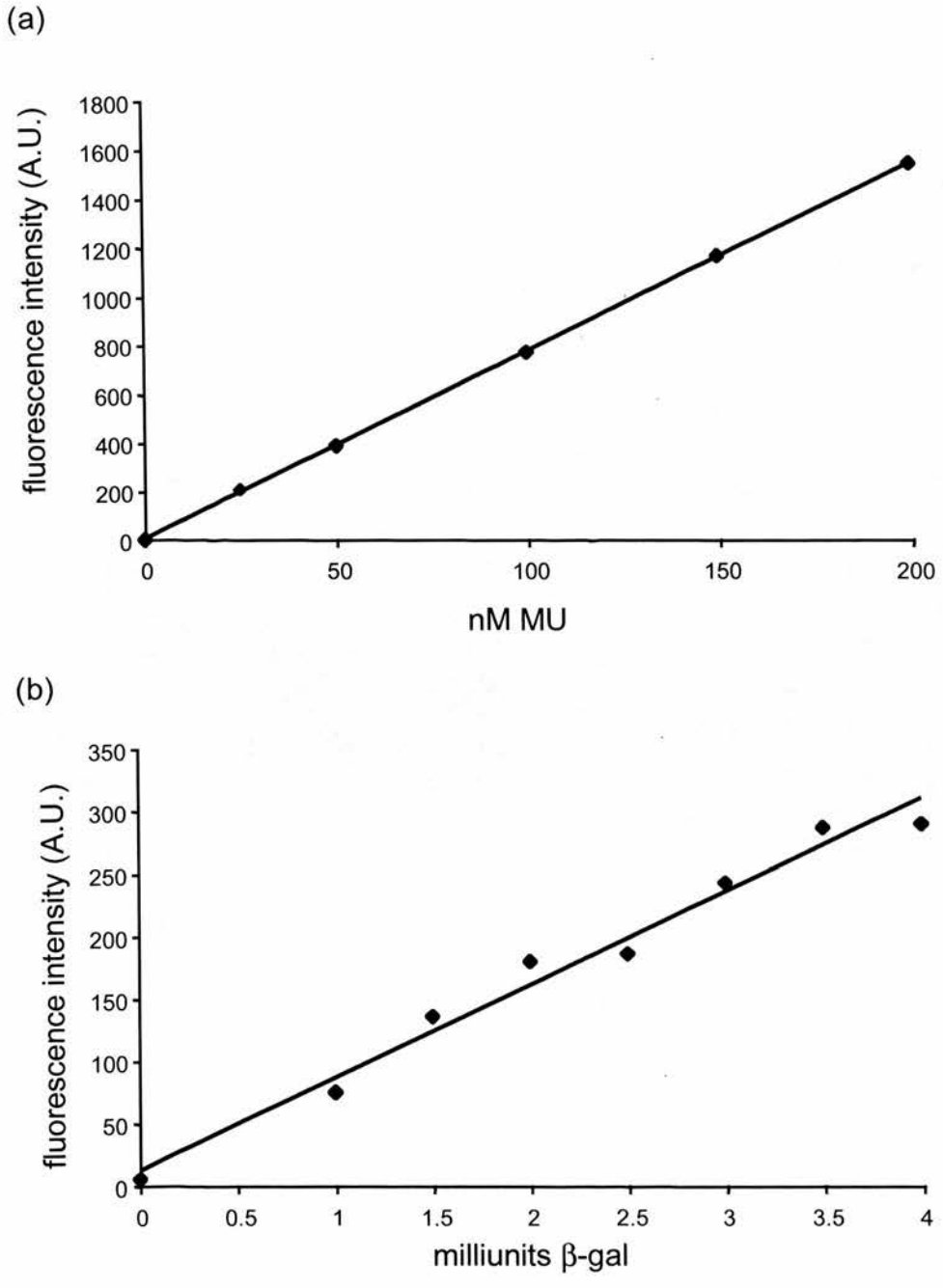

Figure 2-9. β-gal fluorescence assay. (a) Fluorescent standard curve of 0-200nM MU. (b) Linear relationship between amount of fluorescence produced from increasing amounts of β-gal (0-4 mU).

100µg of tissue homogenate was diluted to 40µl in 1x reporter lysis buffer. This was added to 160µl of reaction buffer (25mM Tris-HCl pH 7.5, 125mM NaCl, 2mM $MgCl_2$, 12mM 2-mercaptoethanol, 0.3mM 4-methylumbelliferyl- βD-galactoside (dissolved in dimethyl formamide)) and incubated at 37°C for 30 minutes. The reaction was stopped by adding 50µl of 25% (w/v) trichloroacetic acid and cooled on ice. The solution was clarified by centrifugation for 2 minutes following which 100µl of clear supernatant was added to 1.9ml glycine-carbonate reagent (133mM glycine, 83mM Na_2CO_3 pH 10.7) and mixed. The mixture was transferred to a 3ml glass cuvette and fluorescence determined using the Hoeffer mini-fluorometer. If fluorescence levels in 100µl were too high (i.e. greater than 1000 units), the samples were diluted (x10 or x100 depending on the level of β-gal activity) and fluorescence re-measured.

2.6.4 Salt loading of transgenic mice

Male knock-in mice (aged 10 weeks) were maintained on either a normal (0.3%) or high (3%) sodium diet for 3 weeks. Food was supplied in powdered form from B. S. and S. (Scotland) Ltd and was given to the mice by means of custom made feeding pots. The amount of food and water consumed each day was recorded. At the end of 3 weeks animals were transferred to metabolic cages for urine collection. Urine was collected over 12 hours, during which time animals had free access to water but not to food. After 12 hours, mice were sacrificed and β-gal activity determined in kidneys and lungs as described in sections 2.6.2 and 2.6.3.

Comparisons between two groups were made using a Student's unpaired t test. Values are given as mean ± S.E.M. and P values of less than 0.05 were considered significant.

2.7 LIST OF SUPPLIERS

AbCam Ltd	Cambridge, UK
AD Instruments	Sussex, UK
Amersham Pharmacia Biotech UK Ltd	Little Chalfont, UK
Applied Biosystems	Warrington, UK
Autogen Bioclear UK Ltd	Calne, UK
BD Biosciences UK Ltd	Oxford, UK
BDH (VWR International Ltd)	Poole, UK
Beckman Coulter UK Ltd	High Wycombe, UK
Bibby Sterilin Ltd	Stone, UK
Biogenesis Ltd	Poole, UK
Bioline (UK) Ltd	London, UK
Bio-Rad Laboratories Ltd	Hemel Hempstead, UK
Biosoft	Cambridge, UK
Bright Instruments Co Ltd	Huntingdon, UK
B. S. and S. (Scotland) Ltd	Edinburgh, UK
Caltag-Medsystems Ltd	Silverstone, UK
Cambrex Bioscience Ltd	Wokingham, UK
Camden Instruments	Loughborough, UK
Carl Zeiss Ltd	Welwyn Garden City, UK
Danish Myo Technology A/S	Copenhagen, Denmark
Dynal UK Ltd	Bromborough, UK
Fisher Scientific UK	Loughborough, UK
Genetic Research Instrumentation	Essex, UK
Harlan UK Ltd	Oxford, UK
Helena BioSciences Europe	Sunderland, UK
Hoeffer Scientific Instruments	San Francisco, California, USA
Invitrogen Ltd	Paisley, UK
Leica Microsystems (UK) Ltd	Milton Keynes, UK
Micro Instruments Ltd	Witney, UK

Millipore UK Ltd	Watford, UK
Molecular Probes Europe BV	Leiden, The Netherlands
MWG Biotech UK Ltd	Milton Keynes, UK
Narashige International Ltd	London, UK
Olympus Optical Company (UK) Ltd	London, UK
Promega UK Ltd	Southampton, UK
QIAGEN Ltd	Crawley, UK
Raytest Scientific Ltd	Sheffield, UK
Research Diagnostics Inc	Flanders, New Jersey, USA
Roche Diagnostics Ltd	Lewes, UK
Sigma-Aldrich Company Ltd	Poole, UK
Stratagene Europe	Amsterdam, The Netherlands
Techne Ltd	Cambridge, UK
UVP Inc	San Gabriel, California, USA
Vector Laboratories Inc	Peterborough, UK

CHAPTER 3

ALTERATIONS IN CAVEOLAR STRUCTURE DURING ENDOTHELIAL DYSFUNCTION

3.1 INTRODUCTION

Given the importance of the kidney in the control of blood pressure and the physiological role of NO as an important mediator of natriuresis/diuresis, it is surprising that little is known of whether renal endothelial cells are affected by ED. Perhaps even more surprising is the lack of data on eNOS regulation within the kidney. It is hypothesised that ET-1 is one of the major physiological activators of NO production within the kidney eliciting its effects via the activation of ET_B and eNOS (refer to section 1.2.2.8 and (Kotelevtsev & Webb, 2001)). Alterations in this pathway that lead to decreased NO availability, for example through changes in eNOS regulation, may result in sodium retention and elevation of blood pressure.

One of the potential reasons for altered eNOS regulation may be abnormalities in interactions with regulatory proteins. eNOS is negatively regulated by caveolin-1 (refer to section 1.3.6.3). However, this relationship has not been investigated within the kidney. Although western blot analysis demonstrated that the kidney expresses very low amounts of caveolin compared to the lung (Lisanti *et al.*, 1994), precise immunohistochemical analysis revealed high expression within the descending vasa recta corresponding to large numbers of caveolae as shown by immunogold labelling and electron microscopy (Breton *et al.*, 1998). Interestingly, this vascular bed is also a major site of renal eNOS expression (Teichert *et al.*, 2000). Therefore, this circumstantial evidence suggests that caveolin may be a potential regulatory mechanism controlling renal eNOS activity.

eNOS has also recently been reported to interact with GPCRs (see section 1.3.7). *In vitro* binding studies revealed that eNOS directly binds ET_B (Marrero *et al.*, 1999). This interaction most likely mimics the interaction of eNOS with other GPCRs (e.g. the BK receptor) in which eNOS activity is inhibited. However, as yet no *in vivo* studies have been published to support this observation and there are no direct data localising ET_B to caveolae by conventional biochemical methods.

There is now emerging evidence suggesting that the pathogenic mechanisms associated with ED may involve alterations in eNOS protein-protein interactions within caveolae (refer to section 1.3.9.5). Incubation of bovine aortic endothelial cells with hypercholesterolemic human serum was associated with upregulation of caveolin-1 levels, increased numbers of inhibitory eNOS-caveolin complexes and impairment of basal NO release (Feron *et al.*, 1999). Increased eNOS-caveolin complexes were also observed in aortas from pulmonary hypertensive rats compared to their normotensive counterparts (Murata *et al.*, 2002). The SHR also experiences changes in caveolar architecture. Goto *et al* reported that in 10 week old SHR (i.e. the onset of hypertension) there were significantly increased numbers of caveolae in intracellular membranes of cardiac muscles compared with aged matched WKY (Goto *et al.*, 1990). Although caveolin protein levels were not measured in this study, circumstantial evidence demonstrating a structural role for caveolin in caveolae formation (Fra *et al.*, 1995), predicts that caveolin levels may be elevated, potentially resulting in increased eNOS-caveolin complex formation.

Based on these studies it is hypothesised that alterations in caveolar structure may occur in ED associated with hypertension. In particular, it is proposed that increased protein-protein interactions of eNOS with inhibitory proteins (e.g. caveolin and ET_B) will reduce eNOS activity and may be a potential mechanism behind diminished NO availability in ED. Therefore, the aim of this chapter was to investigate whether ED is associated with alterations in caveolar structure, particularly within the kidney. Firstly, I wanted to investigate whether eNOS, caveolin-1 and ET_B reside in the same subcellular fraction (i.e. isolated caveolae) and then determine whether expression within these fractions is altered during ED using western blot analysis. I also endeavoured to demonstrate the physical interactions between eNOS and caveolin, and eNOS and ET_B, using co-immunoprecipitation with an ultimate goal to identify alterations within these interactions in animals with ED. In order to address these aims, an animal model of ED, the SHR, was used.

Developed in Japan in 1963, the SHR remains the most commonly used animal model of hypertension. By inbreeding WKY rats with elevated blood pressure, Okamoto *et al* generated a strain of rat which is characterised by sustained high blood pressure throughout adulthood (Okamoto & Aoki, 1963). Following a pre-hypertensive phase at 6 to 8 weeks of age where systolic blood pressures (SBPs) are around 100-120mmHg, the SHR develops spontaneous hypertension between 12 to 14 weeks of age, with SBPs reaching up to 200mmHg. From 14 to 30 weeks blood pressure remains constant after which it continues to climb to around 220mmHg in animals up to the age of 50 weeks (figure 3-1). In contrast, the WKY control animals remain normotensive with blood pressures reaching around 130mmHg. Konishi and Su were first to observe impaired endothelium-dependent relaxations to ACh in aortic rings isolated from SHR compared to WKY (Konishi & Su, 1983), an observation that has since been confirmed in other vascular beds (Luscher *et al.*, 1990). The SHR also develop other features of hypertensive end-organ damage (e.g. hypertrophy, cardiac failure and renal failure) (Pinto & Ganten, 1998). For these reasons, as well as the morphological observations regarding caveolae and SHR described above, it was decided that the SHR would provide a good animal model to investigate if alterations in caveolar structure are associated with ED.

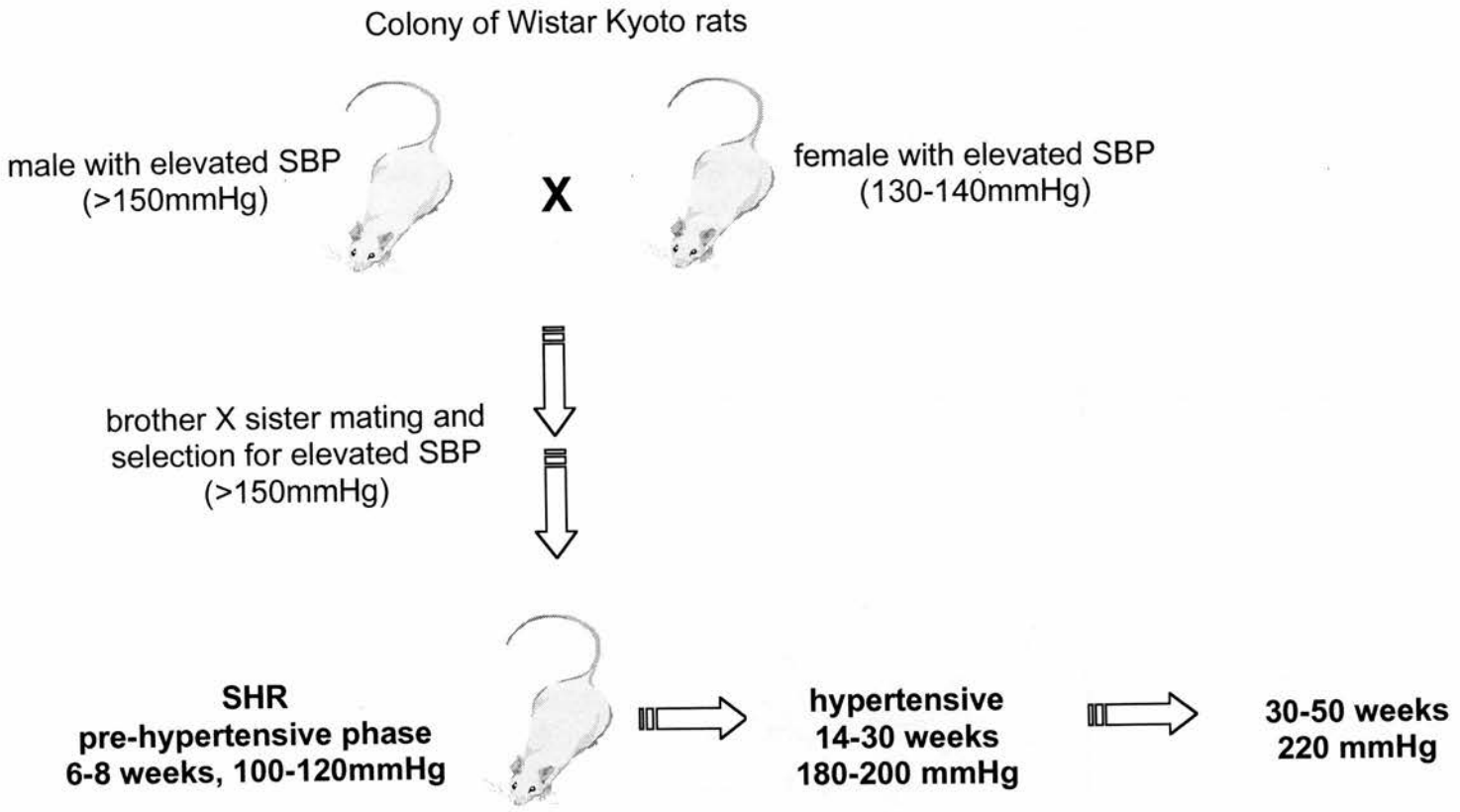

Figure 3-1. Generation of SHR and progession of hypertension.

3.2 RESULTS

3.2.1 General parameters of SHR and WKY

General parameters of WKY and SHR rats are shown in table 3-1. Ages and body weights were similar between groups (n=6 in each group). See section 3.2.4 for further information regarding animal numbers.

Table 3-1. Characteristics of WKY and SHR rats.

Rat strain	Age (weeks)	Body weight (g)
WKY	23.2 ± 0.7	401.3 ± 17.4
SHR	23.5 ± 0.6	375.2 ± 11.8

3.2.2 Confirmation of ED in SHR

Endothelial integrity was assessed by measuring responses of isolated vessels to ACh (refer to section 2.2). In both mesenteric arteries and aorta, SHR animals responded differently to ACh compared to WKY (figure 3-2). In mesenteric vessels, there was a rapid relaxation followed by a marked contractile response at higher doses of ACh. The early and complete relaxation of these arteries, though surprising, has been reported elsewhere (Luscher *et al.*, 1990). In contrast, vessels from WKY animals relaxed to the baseline and remained there. In the aorta, relaxation was impaired by around 20% of WKY at low doses of ACh. Again, vessels from SHR animals contracted at higher concentrations of ACh compared to WKY. Figure 3-3 shows an example of an original trace in which the biphasic response of relaxation followed by constriction can be seen more clearly. As previously reported contractile responses to PE or NA did not differ between groups (figure 3-4). These alterations in response to ACh confirm that the SHR displayed characteristics of ED.

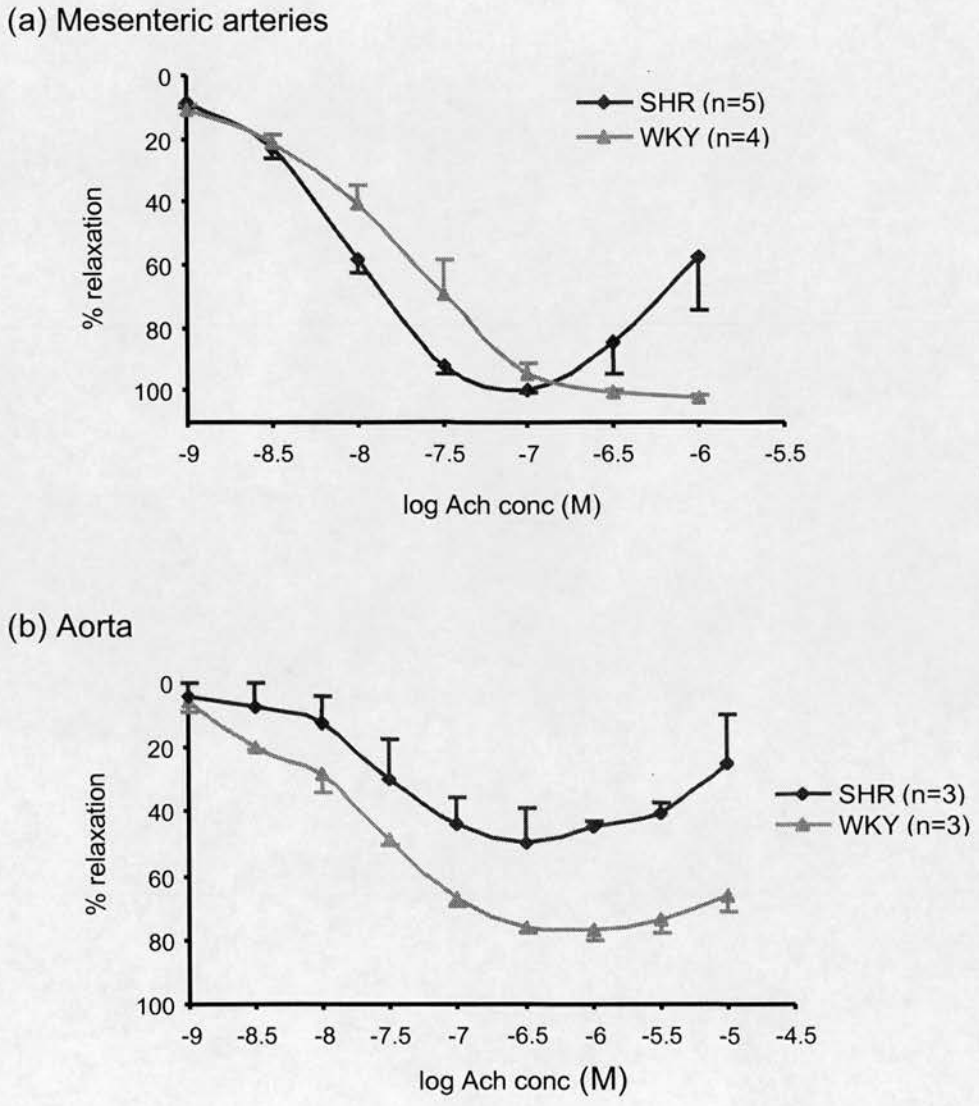

Figure 3-2. ACh-induced relaxation of vessels isolated from SHR and WKY. Mesenteric arteries (a) and aortas (b) were preconstricted with phenylephrine and noradrenaline respectively followed by relaxation in response to increasing doses of ACh. Values are expressed as % relaxation of maximal contraction to preconstrictor and are displayed as the mean ± S.E.M.

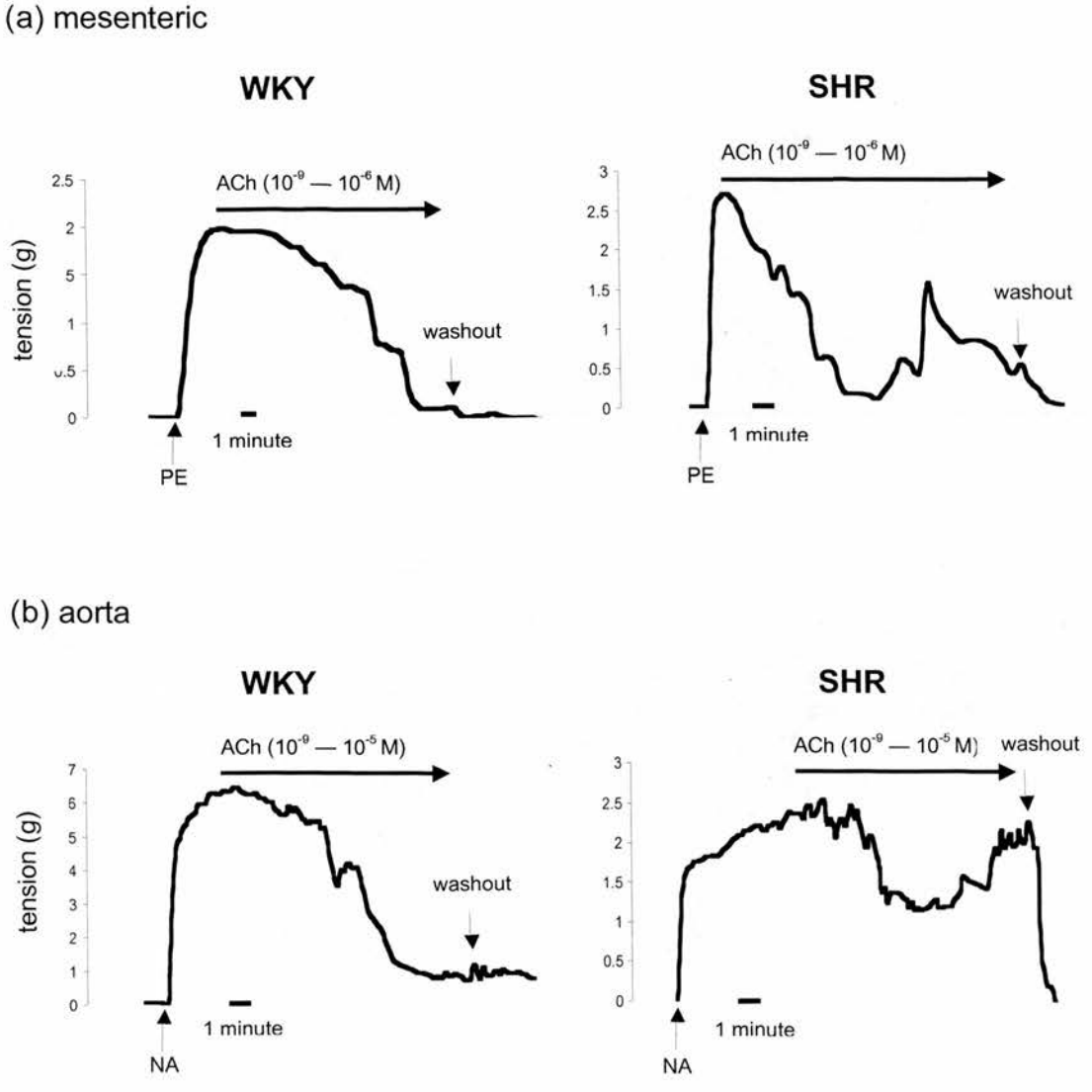

Figure 3-3. Myograph traces of vessel responses to ACh. Examples of original traces showing responses to ACh following pre-constriction in (a) mesenteric and (b) aortic vessels isolated from WKY and SHR. Note the biphasic response in SHR vessels. Abbreviations: PE, phenylephrine; NA, noradrenaline.

(a) Mesenteric arteries

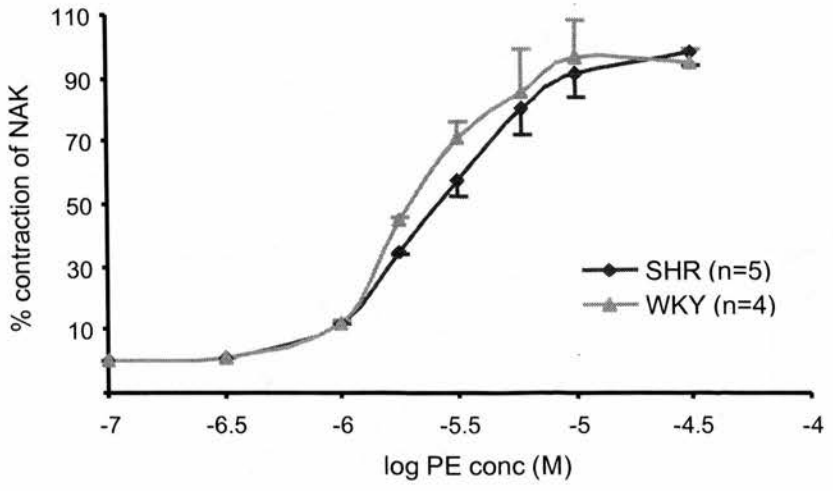

(b) Aorta

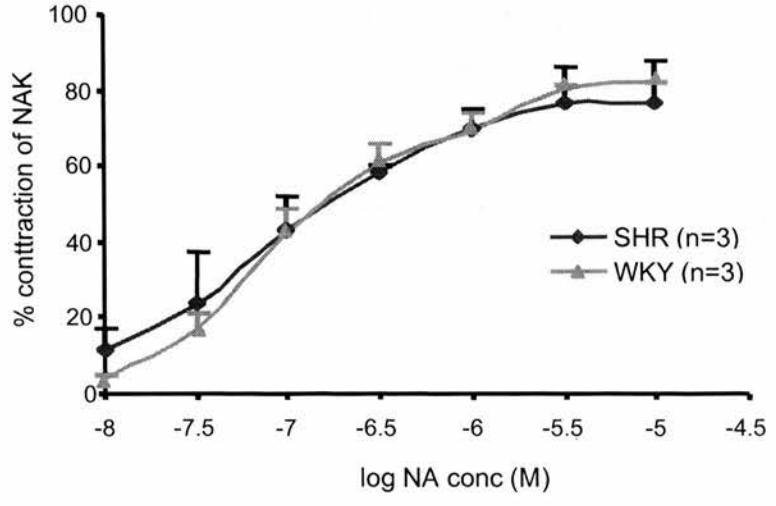

Figure 3-4. Contractile responses of vessels isolated from SHR and WKY. Mesenteric arteries (a) and aorta (b) were constricted with increasing doses of PE and NA respectively. Results are expressed as a percentage of the maximal NAK response. Values are mean ± S.E.M. Abbreviations: PE, phenylephrine; NA, noradrenaline; NAK, 10μM NA in KPSS.

3.2.3 eNOS, caveolin and ET_B expression in caveolin-rich domains

3.2.3.1 Isolation of caveolin-rich domains from lung tissue

To investigate whether eNOS, caveolin-1 and ET_B reside in the same subcellular fraction, caveolin-rich domains were isolated from rat tissue using sucrose density ultracentrifugation (refer to section 2.3.2.3). As the name suggests, these fractions are rich in caveolin and represent isolated caveolae. This method of isolation, first described by Lisanti *et al* (Lisanti *et al.*, 1994), relies on two properties of caveolae; (1) resistance to solubilisation by Triton X-100 and (2) buoyancy at a specific density in sucrose gradients. Due to the abundance of endothelial cells and caveolae, the lung was initially used in order to optimise this method of subcellular fractionation.

A single light scattering band (fraction 8) corresponded to the low-density Triton-insoluble complex (figure 3-5a). Analysis of protein content revealed that these fractions excluded most of the cellular protein which remained within the pellet (P) (figure 3-5b). Western blot analysis using antibodies against caveolin-1 clearly demonstrated that fractions 7-9 were enriched with caveolin-1 (figure 3-5c). Furthermore, when compared to equal amounts of whole lung homogenate, caveolin levels were around 1.5 times higher in caveolin-rich domains as determined by densitometry (figure 3-5d), a considerable increase taking into account the low protein concentration of the caveolin-rich domain samples.

Caveolin-rich domains were also analysed for the presence of eNOS and ET_B. As with caveolin, high levels of eNOS were observed in fraction 8 and in the insoluble pellet compared to the other fractions (figure 3-6a). Again, when compared to equal amounts of whole lung homogenate, eNOS was approximately 3 fold higher in caveolin-rich domains (figure 3-6b). Analysis of ET_B expression proved to be more problematic largely resulting from the inaccessibility of good commercial ET_B antibodies. Three different ET_B antibodies were used (refer to table 2-5). However, on no occasion was satisfactory staining achieved. All three antibodies resulted in consistently high non-specificity and therefore made it impossible to analyse ET_B by this method.

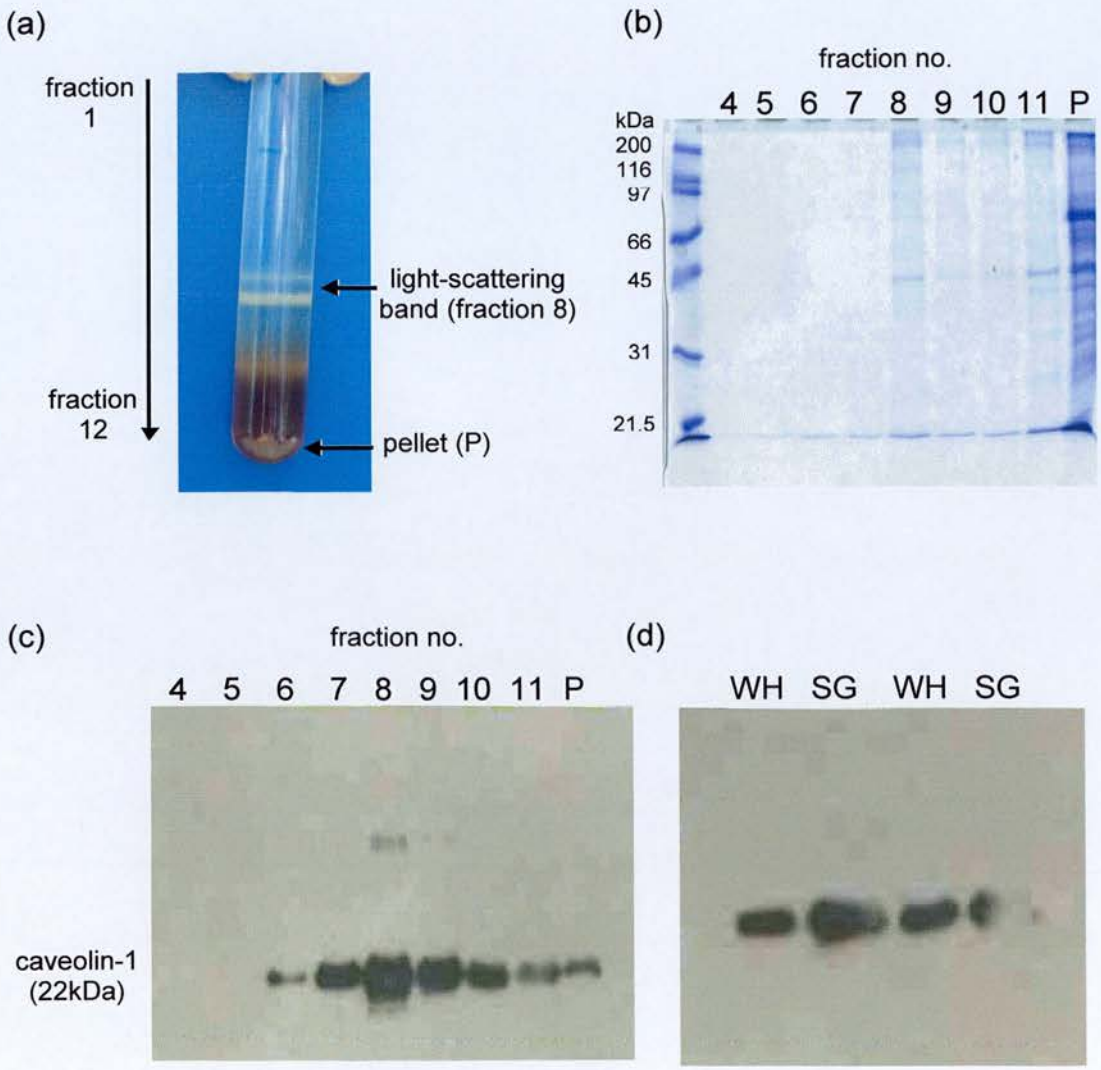

Figure 3-5. Isolation of lung caveolin-rich domains. (a) Isolation of caveolin-rich domains by sucrose gradient centrifugation produces a light scattering band (fraction 8). (b) Coomassie protein stain of fractions 4-11 and pellet (P). An equal volume of each fraction was loaded. (c) Western blot of caveolin expression in fractions 4-11 and pellet. An equal volume of each fraction was loaded. (d) Comparison of caveolin expression in whole lung homogenates (WH) and sucrose gradient fractions (SG). An equal amount was loaded for each sample.

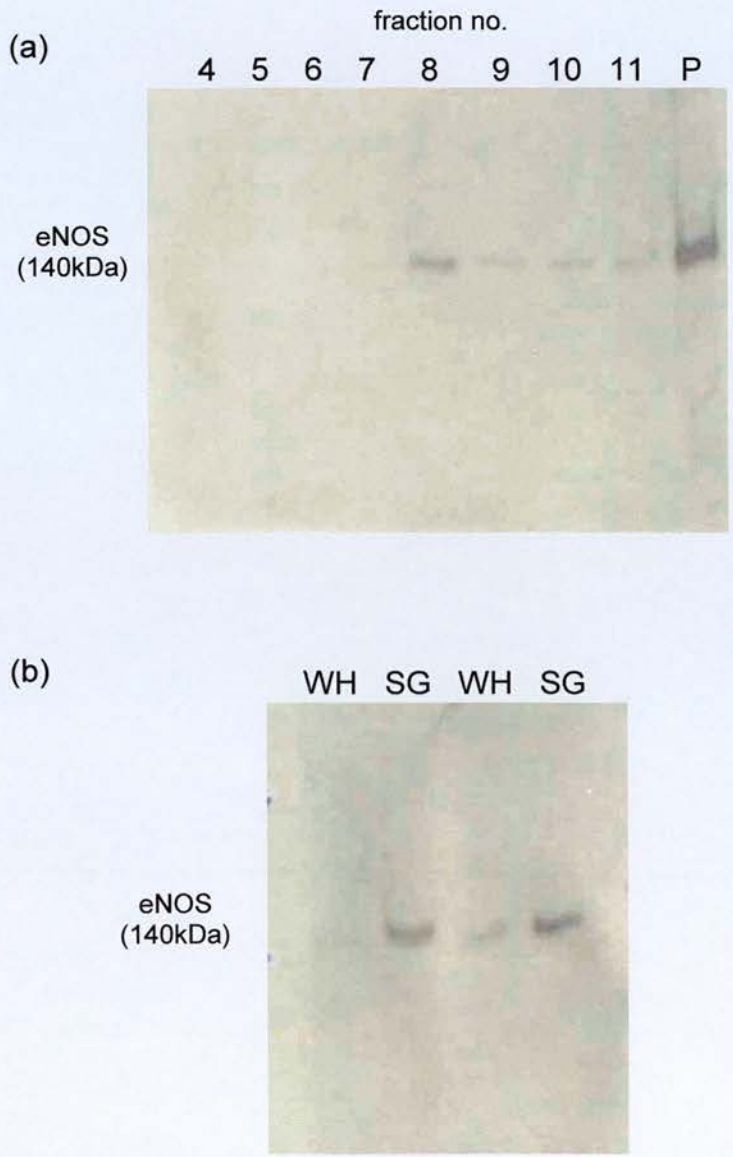

Figure 3-6. eNOS expression in lung caveolin-rich domains. (a) Western blot of eNOS expression in fractions 4-11 and pellet. An equal volume of each fraction was loaded. (b) Comparison of eNOS expression in whole lung homogenates (WH) and sucrose gradient fractions (SG). An equal amount of protein was used in each sample.

Therefore, although it was not possible to detect ET_B expression in these samples, they do represent subcellular fractions highly enriched in both caveolin-1 and eNOS.

3.2.3.2 Isolation of caveolin-rich domains from kidney tissue

Preparation of similar caveolin-rich domains was then attempted using the kidney. Firstly, to illustrate the low level of caveolin expression in the kidney, renal homogenates were compared to lung, a source of abundant endothelial cells. Figure 3-7 shows significantly higher caveolin-1 expression in the lung compared to the kidney. Densitometric analysis revealed that caveolin-1 was expressed almost 10 fold more in the lung.

Therefore, since the kidney expresses such low amounts of caveolin-1, I did not expect to be able to reproduce similar data to those observed from caveolin-rich domains of the lung. However a similar pattern for caveolin-1 expression was obtained, albeit at a much lower signal (figure 3-8). As with the lung, a light scattering band was visible and this sample corresponded to increased caveolin-1 expression (fraction 8). However, when the same fractions were analysed for eNOS expression, no eNOS protein was detected probably resulting from the limitations of the detection system.

3.2.4 Caveolin-1 and eNOS expression are not altered in caveolin-rich domains isolated from SHR

In order to investigate whether changes in caveolin and eNOS expression are associated with ED, caveolin-rich domains were isolated from lungs and kidneys of WKY and SHR animals and analysed for caveolin-1 and eNOS protein expression. Within the lung, there were no significant differences in caveolin-1 (figure 3-9) and eNOS (figure 3-10) expression between groups. Likewise, caveolin protein levels were similar in caveolin-rich domains isolated from kidneys of SHR and WKY (figure 3-11). Equal loading was confirmed by coomassie protein stains.

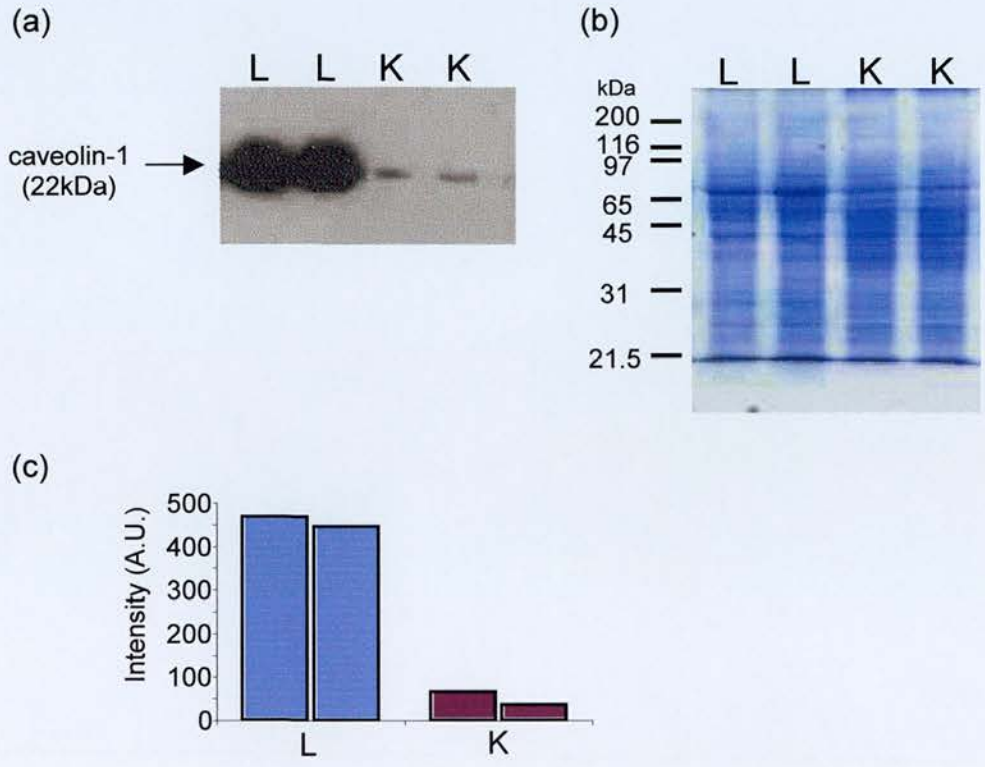

Figure 3-7. Expression of lung and renal caveolin-1. (a) Representative western blot of renal caveolin-1 (K) versus lung caveolin-1 (L) expression in WKY rat. 40μg of protein from each sample was loaded. (b) Coomassie stain of identical gel to demonstrate equal loading. (c) Densitometric analysis of western blot.

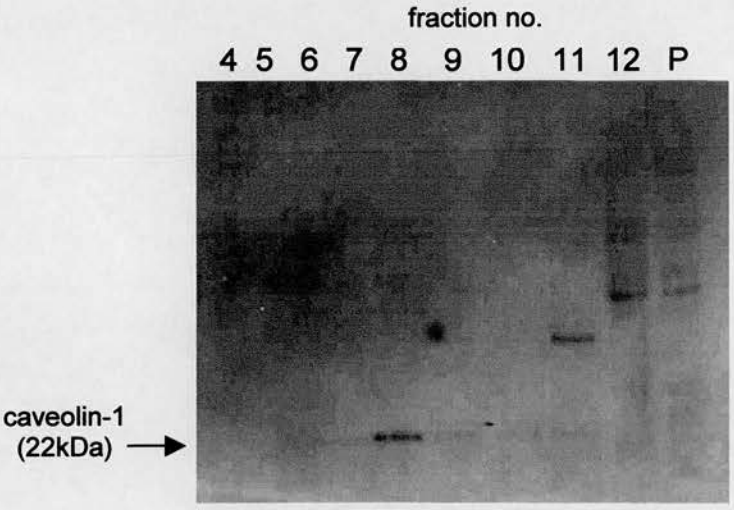

Figure 3-8. Isolation of renal caveolin-rich domains. Western blot of caveolin-1 expression in caveolin-rich domains (fractions 4-12 and pellet (P)) isolated from kidney. An equal volume of each fraction was loaded.

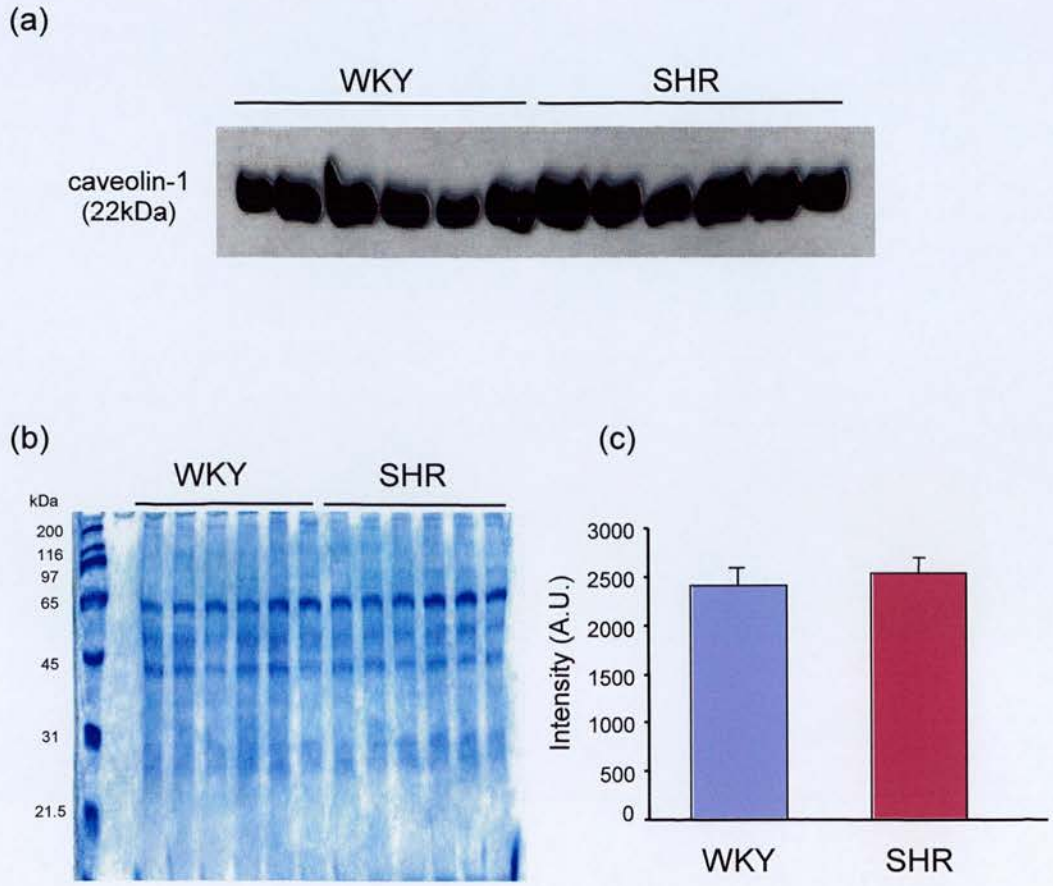

Figure 3-9. Caveolin-1 expression in lung caveolin-rich domains from SHR and WKY. (a) Representative western blot of caveolin-1 expression in caveolin-rich domains isolated from lung. 1μg of protein was loaded for each sample. (b) Coomassie staining of an identical gel demonstrates equal loading (c) Densitometric analysis of western blot. n=6 in each group.

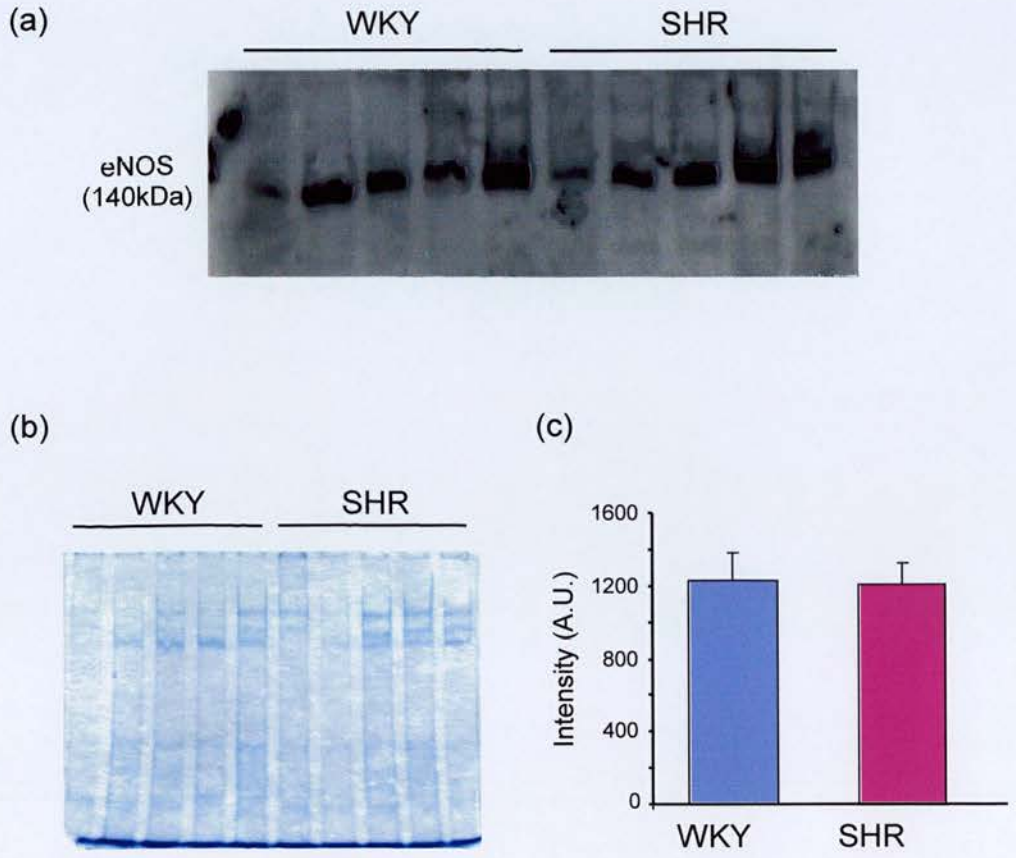

Figure 3-10. eNOS expression in lung caveolin-rich domains from SHR and WKY. (a) Representative western blot of eNOS expression in caveolin-rich domains isolated from lung. 10μg of protein was loaded for each sample. (b) Coomassie staining of an identical gel demonstrates equal loading (c) Densitometric analysis of western blot. n=6 in each group.

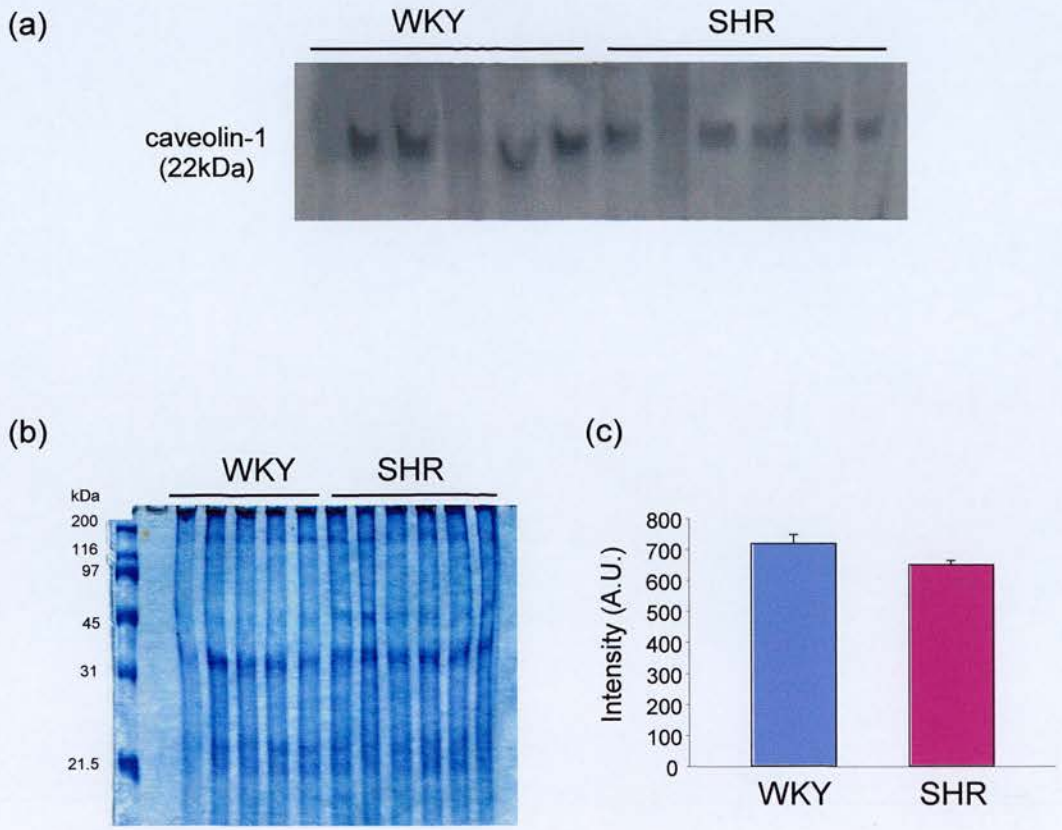

Figure 3-11. Caveolin-1 expression in kidney caveolin-rich domains from SHR and WKY. (a) Representative western blot of caveolin-1 expression in caveolin-rich domains isolated from kidney. 10μg of protein was loaded for each sample. (b) Coomassie staining of an identical gel demonstrates equal loading (c) Densitometric analysis of western blot. n=6 in each group. This experiment was performed on one set of animals only (see section 3.2.4 for details).

It should be noted at this point that in all SHR/WKY comparative experiments, six animals were analysed in each group. However, in all cases, except where indicated, experiments were repeated on a secondary set of animals, again with six in each group. Due to the nature of western blotting, it was not possible to directly compare protein expression between these groups since only samples that have been loaded on the same gel can be compared directly. Therefore, these sets of animals were analysed separately. Since there were no obvious differences between experimental sets, only one group of data has been shown.

3.2.5 Renal eNOS expression is increased in SHR

Due to the inability of being able to measure eNOS expression in caveolin-rich domains isolated from kidney, whole kidney homogenates were analysed for eNOS expression instead. Kidneys from SHR exhibited a modest increase in eNOS levels (figure 3-12). Although significance was not reached, eNOS expression was almost 2 times higher in SHR kidneys compared to WKY. In contrast, caveolin expression was not altered in SHR kidneys (n=6, one group only). Due to high background, this blot has not been shown. Finally, to confirm that eNOS expression is upregulated during ED, heart tissue was used as a positive control. Elevated eNOS expression in the heart has been previously reported in SHR (Nava *et al.*, 1998). As with the kidney, eNOS expression was increased in SHR hearts compared to WKY (figure 3-13). However, although caveolin-1 was highly expressed in the heart, expression levels were comparable between WKY and SHR (figure 3-14).

These results suggest that ED in the SHR is not associated with alterations in caveolin-1 or eNOS expression within caveolin-rich domains. On the other hand, eNOS expression in the kidney and heart is upregulated in SHR and may therefore be associated with ED.

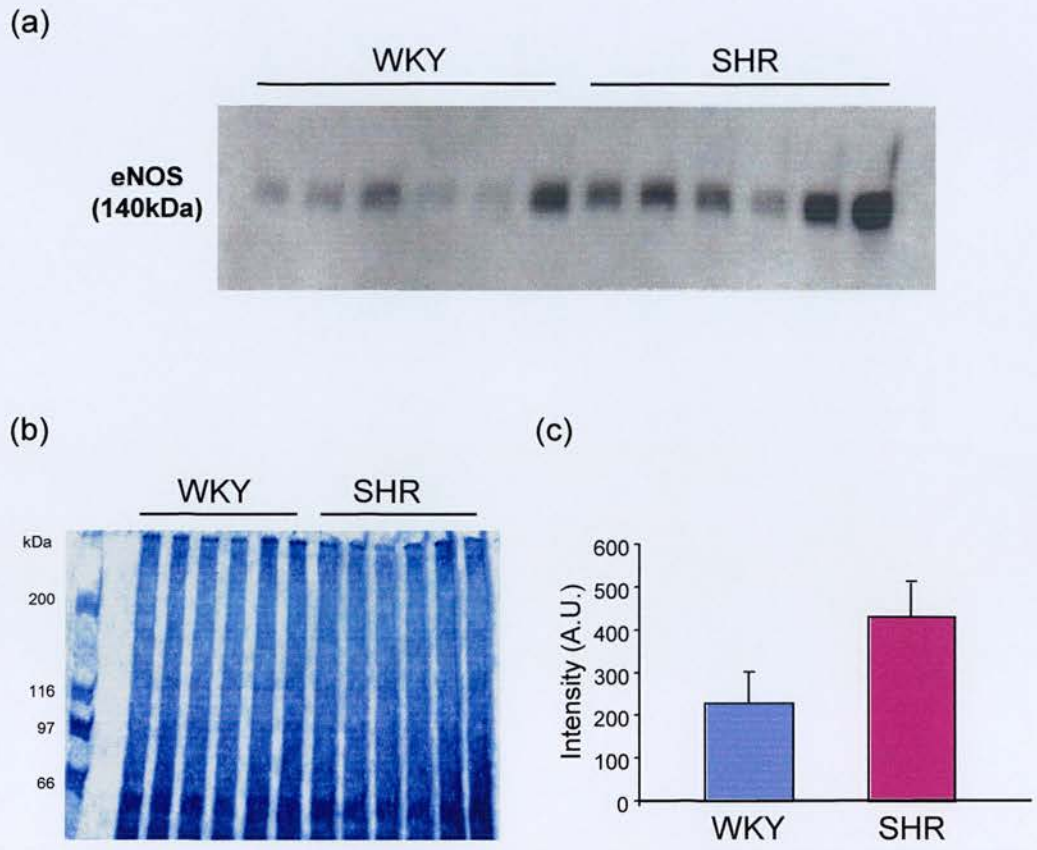

Figure 3-12. Renal eNOS expression in SHR and WKY. (a) Representative western blot of renal eNOS expression from WKY and SHR kidney whole homogenates. 100μg of protein was loaded for each sample. (b) Coomassie stain of identical gel confirms equal loading. (c) Densitometric analysis of western blots. n=6 in each group.

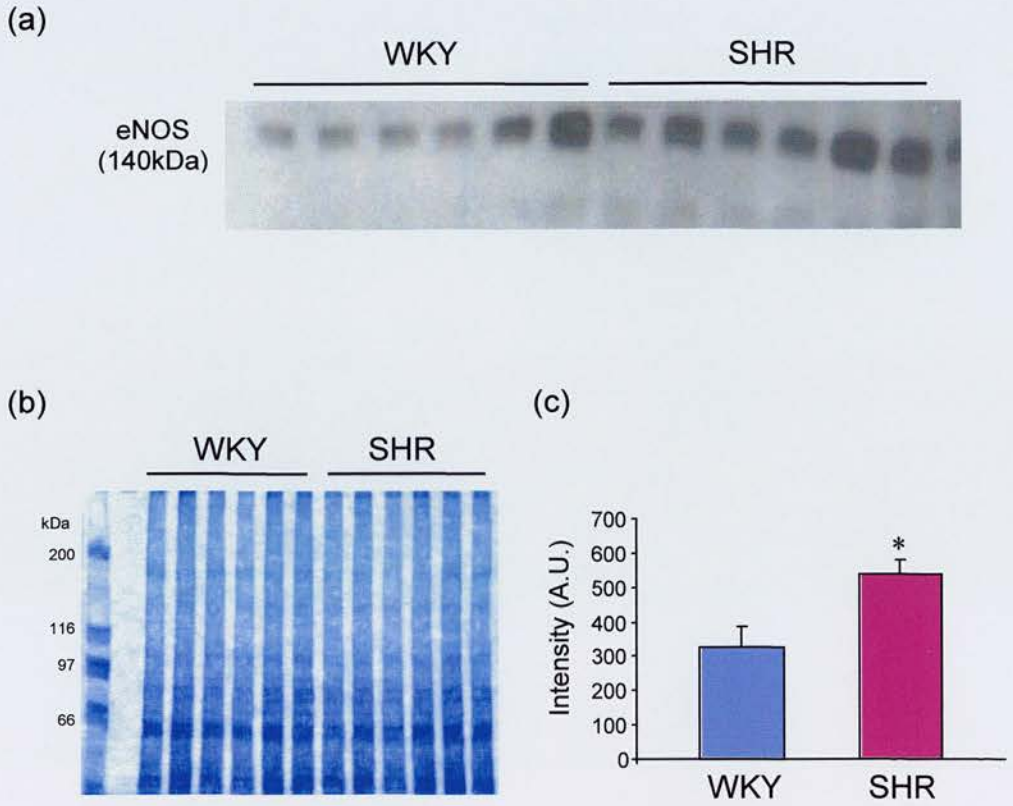

Figure 3-13. eNOS expression in hearts from SHR and WKY. (a) Representative western blot of eNOS expression in whole heart homogenates from WKY and SHR. 100μg of protein from each sample was loaded. (b) Coomassie stain of identical gel confirms equal loading. (c) Densitometric analysis of western blots. n=6 in each group.* $P<0.05$ versus WKY.

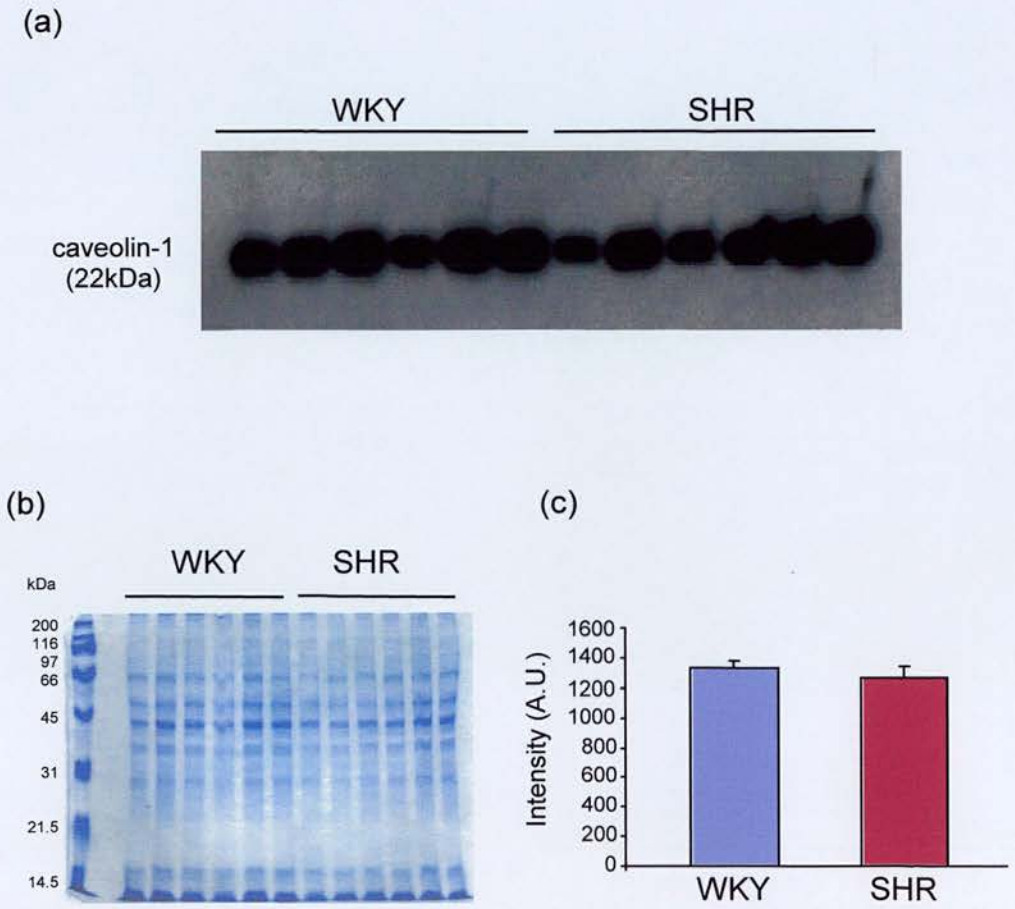

Figure 3-14. Caveolin-1 expression in hearts from SHR and WKY. (a) Representative western blot of caveolin-1 expression in whole heart homogenates from WKY and SHR. 1μg of protein from each sample was loaded. (b) Coomassie stain of identical gel confirms equal loading. (c) Densitometric analysis of western blots. n=6 in each group.

3.2.6 Analysis of eNOS-caveolin protein interactions

Although no differences in caveolin expression levels in caveolin-rich domains or whole tissue were observed between SHR and WKY, this did not eliminate the possibility of changes in caveolin-1 - eNOS protein interactions. Therefore, co-immunopreciptation was performed to investigate whether alterations in caveolin-1-eNOS protein interactions are associated with ED.

Much of the present data on eNOS-caveolin interactions has arisen from two independent groups. However, their methods for co-immunoprecipitation are similar. (Feron *et al.*, 1996; Garcia-Cardena *et al.*, 1996a; Michel *et al.*, 1997a; Michel *et al.*, 1997b; Feron *et al.*, 1998a; Feron *et al.*, 1998b). From careful analysis of the literature it became clear that co-immunoprecipitation critically depends on the method of lysis, in particular the type of detergent used. Strong ionic detergents such as SDS will destroy protein-protein interactions. Therefore mild, non-ionic detergents (e.g. NP-40, Triton X-100 or octylglucoside) are required which should still be strong enough to solubilise the proteins of interest. For this reason I began this series of analytical experiments by testing different types of buffers in order to establish which would provide optimal co-immunoprecipitation conditions.

Another important point to note is that, to my knowledge, co-immunoprecipitation of eNOS-caveolin complexes has not been reported in tissue until very recently (Murata *et al.*, 2002). Most reports have performed co-immunoprecipitation on cultured cells (e.g. cardiac myocytes, bovine aortic endothelial cells (BAEC), bovine lung microvascular endothelial cells (BLMEC) or transfected COS-7 cells). Therefore, it was decided to optimise the co-immunoprecipitation protocol using cultured endothelial cells and then extend this to tissue and caveolin-rich domains samples.

3.2.6.1 eNOS and caveolin interact in isolated endothelial cells

HUVECS were used to optimise co-immunoprecipitation of eNOS-caveolin complexes using two different types of detergent, Nonidet P-40 (NP-40) and octylglucoside (OG). Cells were lysed in either NP-40 buffer or OG buffer followed

by immunoprecipitation with either caveolin-1 or eNOS antibodies (refer to sections 2.3.2 & 2.3.4). Resulting immune complexes were immunoblotted with complementary antibodies to assess for eNOS-caveolin interactions. For example, antibodies directed against eNOS were used for caveolin immunoprecipitates whilst antibodies directed against caveolin were used for eNOS immunoprecipitates. Figure 3-15 shows the results of immunoprecipitating HUVECS lysates (solubilised in NP-40 or OG) with caveolin antibodies followed by immunoblotting for eNOS. The success of immunoprecipitation was assessed by firstly probing the immunoprecipitates with antibodies towards caveolin (figure 3-15a). Enrichment of the caveolin signal appeared only in those samples which were incubated with anti-caveolin antibodies (C). On the other hand, omission of immune antibody resulted in no caveolin signal (-). A similar result was achieved regardless of the type of lysis buffer used. Immunoblotting of the same immunoprecipitates was then performed using eNOS antibodies to determine if caveolin and eNOS interact in these cellular preparations. The immunoblot shown in figure 3-15b reveals that immunoprecipitation of caveolin (C) did indeed result in co-precipitation of eNOS. However, the signal was extremely weak particularly for OG lysates. Again, immunoprecipitation without immune antibody (-) did not result in detection of eNOS. It should be noted that these experiments were repeated five different times. On two occasions no interaction between eNOS and caveolin were observed which suggests that this technique is highly variable between preparations.

A complementary experiment was then performed in which lysates were immunoprecipitated with eNOS antibodies followed by immunoblotting with caveolin. Again, immunoprecipitation was firstly evaluated by immunoblotting with eNOS antibodies (figure 3-16a). As with caveolin, a strong signal for eNOS appeared only in those samples which were precipitated with anti-eNOS antibodies (E) and not in those in which immune antibody had been omitted (-). However, this time there was a significant difference in the intensity of the signal depending on the lysis

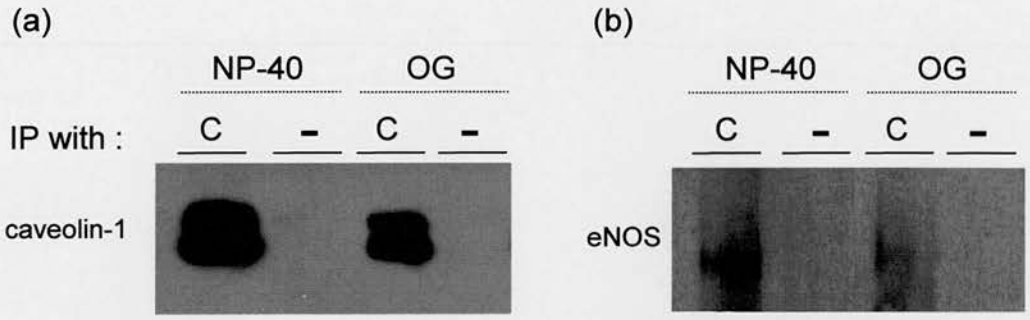

Figure 3-15. Immunoprecipitation of HUVEC lysates with caveolin-1 antibodies. HUVEC NP-40 or OG lysates were immunoprecipitated with either caveolin-1 antibodies (C) or without immune antibody (-) and then immunoblotted with (a) caveolin-1 or (b) eNOS antibodies. The blots shown are representative of three independent experiments.

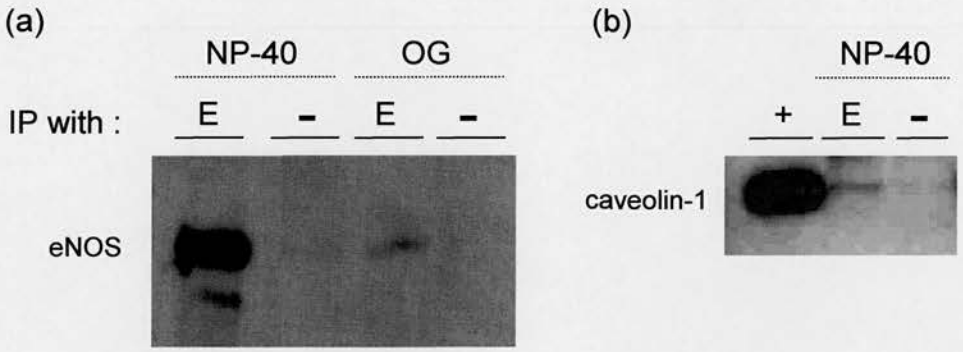

Figure 3-16. Immunoprecipitation of HUVEC lysates with eNOS antibodies. HUVEC NP-40 or OG lysates were immunoprecipitated with either eNOS antibodies (E) or without immune antibody (-) and then immunoblotted with (a) eNOS or (b) caveolin antibodies. A positive control (+) for caveolin is included in (b). The blots shown are representative of two independent experiments.

buffer used. NP-40 buffer resulted in increased precipitation of eNOS compared to OG buffer. The eNOS-precipitated NP-40 lysates were then immunoblotted for caveolin (figure 3-16b) and confirmed that caveolin co-precipitated with eNOS although again the signal was extremely low. This is obvious by comparing the signal to the positive control shown in figure 3-16b which was taken from a non-precipitated sample.

Therefore, although eNOS-caveolin interactions were observed in HUVEC lysates, the quantity of protein participating in these interactions appeared to be very low. This series of experiments also demonstrated that of the two buffers tested, lysis with NP-40 produced the more encouraging result. Therefore, this lysis buffer was used in further experiments.

3.2.6.2 eNOS-caveolin interactions cannot be detected in lung tissue

In order to determine if eNOS-caveolin interactions also exist *in vivo*, the co-immunoprecipitation technique described for HUVECS was applied to lung homogenates. Lung was chosen due to the abundance of eNOS and caveolin in this tissue. Whole lung homogenates were prepared in NP-40 lysis buffer and immunoprecipitated with anti-eNOS antibodies. Resulting immunocomplexes were immunoblotted for eNOS and caveolin as shown in figure 3-17. eNOS was again enriched following eNOS immunoprecipitation and analysis of the supernatants following immunoprecipitation revealed that the majority of eNOS had been captured in these samples (figure 3-17a). However, on no occasion did eNOS immunoprecipitation result in the co-precipitation of caveolin (figure 3-17b). Instead, all caveolin appeared in the corresponding supernatant (S/E). These results imply that in these lung samples eNOS and caveolin did not physically interact.

3.2.6.3 eNOS-caveolin interactions cannot be detected in caveolin-rich domains

Proteins interactions were also investigated in caveolin-rich domains. However, despite the abundance of caveolin and eNOS in these caveolar preparations, it was not possible to detect any interaction between the proteins.

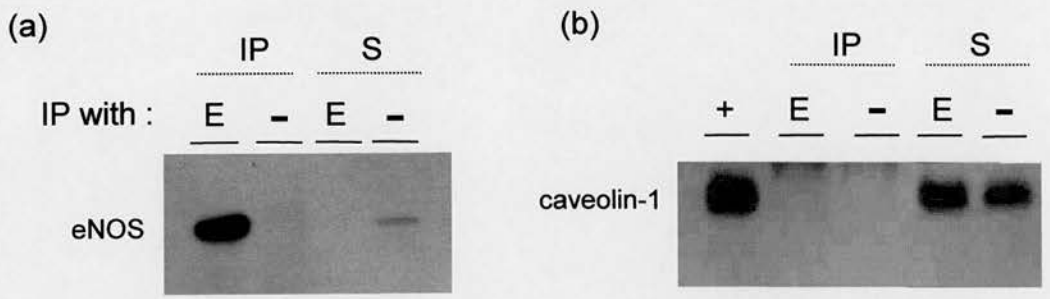

Figure 3-17. Immunoprecipitation of lung NP-40 lysates with eNOS antibodies. Lung lysates were immunoprecipitated with either eNOS antibodies (E) or without immune antibody (-). Immunocomplexes (IP) and their corresponding supernatants remaining after pelleting (S) were immunoblotted with (a) eNOS or (b) caveolin antibodies. A positive control (+) for caveolin is included in (b). The blots shown are representative of three independent experiments.

3.2.7 Quantification of eNOS-caveolin interaction in isolated endothelial cells

The previous set of experiments demonstrated that although eNOS and caveolin interacted in endothelial cells, the amount of interacting protein was very small. Furthermore, given that no interactions were observed in either lung or caveolin-rich domains, it was decided to investigate what proportion of cellular eNOS is in fact bound to caveolin in HUVECS. Therefore, to quantify the eNOS-caveolin interaction a similar series of experiments to those described above were performed. However, as well as analysing the proteins which were immunoprecipitated by either eNOS or caveolin, the supernatants remaining after immunopreciptation were also analysed. This gives an indication of the proportion of protein that has not been immunoprecipitated. eNOS immunoprecipitates were immunoblotted for eNOS and caveolin (figure 3-18). As before, eNOS immunoprecipitation resulted in enrichment of eNOS only in the sample which had been incubated with anti-eNOS antibody (E) and not in those in which antibody had been omitted (-) (figure 3-18a). Conversely in the corresponding supernatants, the opposite pattern was observed. Here, the majority of eNOS was found in the supernatant of the immunoprecipitates which had non-immune antibody. A fainter signal was observed in the supernatant of eNOS immunoprecipitates indicating that most eNOS had been successfully immunoprecipitated. On the other hand, when these samples were immunoblotted for caveolin (figure 3-18b), signals for the supernatants of both eNOS immunoprecipitates (E) and non-immune immunoprecipitates (-) were equally strong whereas the amount of caveolin immunoprecipitated by eNOS antibodies was extremely low in comparison. Therefore, it can be concluded that the amount of caveolin interacting with eNOS in these cellular preparations is very low compared to the total cellular caveolin pool and that the majority of caveolin does not interact with eNOS.

A similar conclusion can be drawn from analysing the amount of eNOS remaining following caveolin immunoprecipitation of HUVEC lysates (figure 3-19). Although caveolin immunoprecipitation resulted in co-precipitation of eNOS, a significant amount of eNOS remained in the corresponding supernatant.

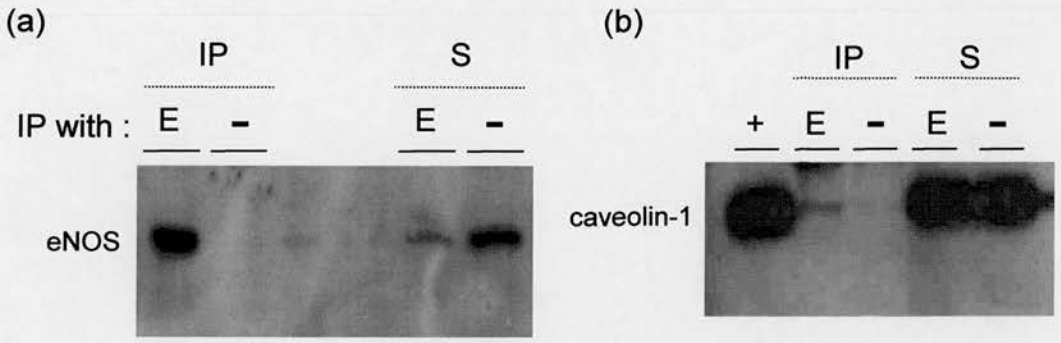

Figure 3-18. Immunoprecipitation of HUVEC NP-40 lysates with eNOS antibodies. HUVEC lysates were immunoprecipitated with either eNOS antibodies (E) or without immune antibody (-). Immunocomplexes (IP) and their corresponding supernatants remaining after pelleting (S) were immunoblotted with (a) eNOS or (b) caveolin antibodies. A positive control (+) for caveolin is included in (b). The blots shown are representative of two independent experiments.

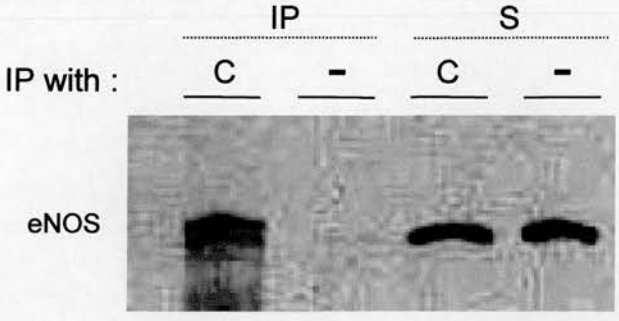

Figure 3-19. Immunoprecipitation of HUVEC NP-40 lysates with caveolin antibodies. HUVEC lysates were immunoprecipitated with either caveolin antibodies (C) or without immune antibody (-). Immunocomplexes (IP) and their corresponding supernatants remaining after pelleting (S) were immunoblotted with eNOS antibodies. The blots shown are representative of two independent experiments.

This set of experiments shows that in these cellular preparations only a small proportion of cellular eNOS and caveolin interact.

3.2.8 eNOS and caveolin do not colocalise in HUVECS by immunofluoresence

The results of the co-immunoprecipitation experiments were surprising given that previous data from Feron *et al* demonstrated that the majority of eNOS was found in association with caveolin (Feron *et al.*, 1996). In order to investigate these discrepancies further, I used fluorescent antibodies towards caveolin and eNOS to visualise intracellular localisation of these proteins in HUVECS (refer to section 2.3.9). This powerful method allows colocalisation of proteins to be detected directly. As shown in figure 3-20, caveolin (green) was found concentrated to the edges of the plasma membrane (figure 3-20a) whereas eNOS (red) was clearly confined to the cytoplasm of the cell, in particular the perinuclear and Golgi regions (figure 3-20b). Double staining of HUVECS revealed that eNOS and caveolin did not colocalise in these cells (figure 3-20c).

(a) Caveolin

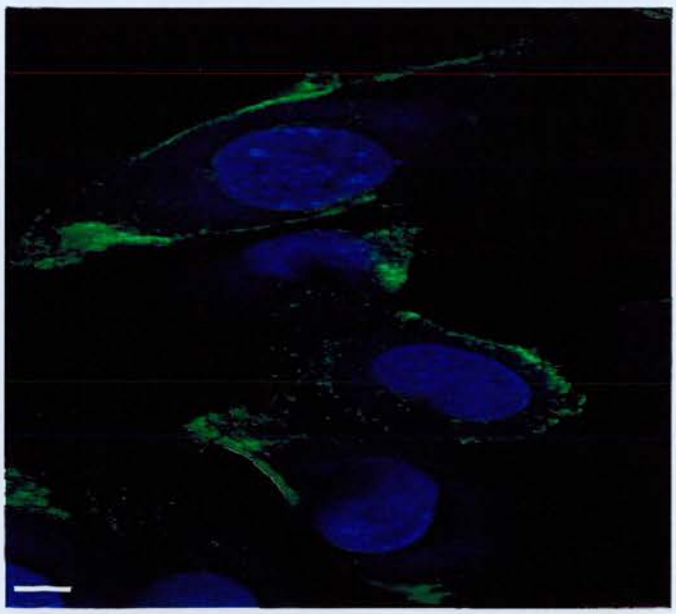

(b) eNOS

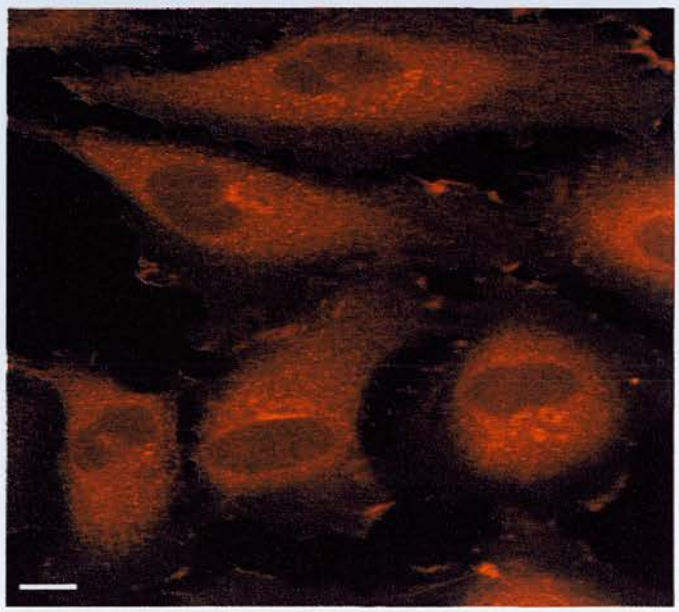

Figure 3-20. Intracellular localisation of caveolin and eNOS in HUVECS (continued overleaf). HUVECS were stained with fluorescent antibodies towards (a) caveolin (green) and (b) eNOS (red). In (a) nuclei are stained in blue. Scale bar = 10μm.

(c) Caveolin/eNOS

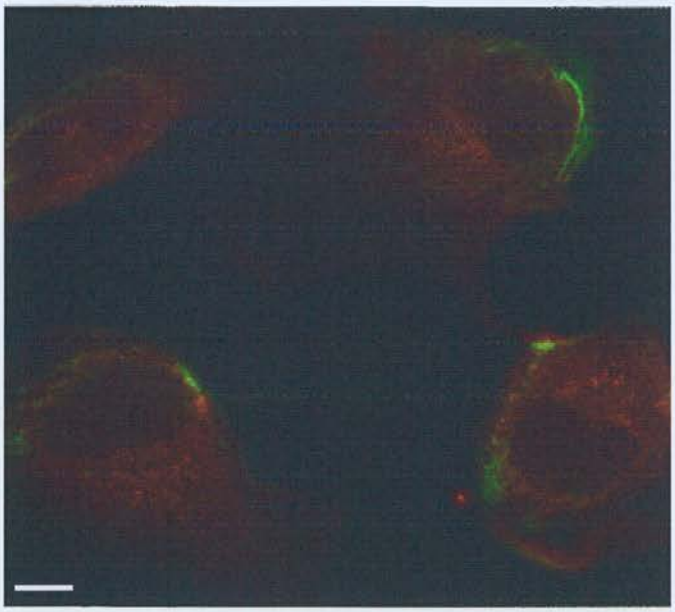

Figure 3-20. Intracellular localisation of caveolin and eNOS in HUVECS (continued). (c) Double staining of HUVECS with antibodies towards caveolin (green) and eNOS (red). Scale bar = 10μm.

3.3 DISCUSSION

In most animal models of hypertension, endothelium-dependent relaxations to ACh are impaired (Pinto & Ganten, 1998). One of these models, the SHR, has been extensively studied and collectively reports have resulted in numerous hypotheses for why the SHR develops ED. These range from the concomitant release of prostanoid constricting factors which antagonize the relaxing properties of NO (Luscher *et al.*, 1990) to overproduction of O_2^- which inactivates NO (Bauersachs *et al.*, 1998). Interestingly, many groups have documented an increase in eNOS expression in SHR compared to normotensive WKY counterparts (see below). This may at first appear contradictory given that NO availability is reduced during ED. However, eNOS-mediated NO production is a tightly regulated process and relies on several additional post-translational regulatory mechanisms, any of which may be altered during ED (refer to section 1.3). Thus, augmented eNOS expression does not necessarily signify increased NO production.

Recent studies have documented that protein-protein interactions between eNOS and regulatory protein, caveolin, may be altered in conditions such as hypercholesterolemia (Feron *et al.*, 1999) and hypertension (Murata *et al.*, 2002). Both groups reported increased numbers of eNOS-caveolin inhibitory complexes, implying that in these conditions, eNOS activity is reduced. Changes in caveolar morphology have also been observed during ED associated with hypertension (Goto *et al.*, 1990). Together, these studies prompted the hypothesis that alterations in caveolar structure, caveolar protein expression and, in particular, abnormalities in eNOS-caveolin interactions may be associated with ED. This chapter has described experiments which sought to address these questions, with particular emphasis on the kidney.

Isolation of caveolin-rich domains provided a useful tool for the analysis of eNOS and caveolin expression in SHR and WKY. These domains were highly enriched in caveolin and eNOS and are thought to represent isolated caveolae (Lisanti *et al.*,

1994). There are now several reports documenting isolation of caveolae ranging from immunopurification to flotation on OptiPrep gradients (Anderson, 1998). Initially, attempts were made to replicate a recently published method involving organ perfusion of silica beads (data not shown) (Chaney & Jacobson, 1983; Schnitzer *et al.*, 1995). Positively charged silica beads are used to coat the endothelial layers of blood vessels but are of a sufficient enough size that they do not penetrate caveolae. Due to the density of the silica, the beads, with attached membranes, can be separated from the rest of the tissue by centrifugation, followed by shearing away of non-caveolar membranes resulting in a pure caveolar population. My attempts to replicate this procedure did not yield useful results largely due to the difficulties in reproducing consistent data. Instead, a different method of caveolar isolation was employed. Sucrose density centrifugation has been widely used in the caveolar field. First described by Sargiacomo *et al* on cultured cell preparations (Sargiacomo *et al.*, 1993), it has since been applied to tissues (Lisanti *et al.*, 1994). This method exploits the resistance of solubilisation of caveolae to detergents, mainly attributed to their cholesterol and glycosphingolipid rich core. It also makes use of their light buoyant density and ability to float on sucrose gradients. I found this method of subcellular fractionation to be highly reproducible, consistently producing fractions enriched in caveolin. However, it should be noted that some reports question the property of detergent insolubility in ascribing proteins to a caveolar location (Kurzchalia *et al.*, 1995). On the other hand, some reports maintain that physical aids used during caveolar purification can, in fact, alter the molecular composition of caveolae. In particular, detergents, such as Triton-X100, may solubilise resident proteins (e.g. eNOS) thereby yielding extracted preparations of caveolae (Smart *et al.*, 1995; Shaul *et al.*, 1996). I did not find this to be the case and consistently observed that the caveolin-rich fractions were also enriched in eNOS, at least those obtained from the lung. Although caveolin-rich domains isolated from kidneys were also enriched in caveolin, eNOS was not detectable in these fractions, possibly due to limitations of the detection system.

After confirming that SHR animals displayed characteristics of ED by assessing endothelial responses to ACh, caveolin and eNOS expression in caveolin-rich domains from these animals were compared with WKY. Analysis of protein expression within these domains demonstrated that there were no differences in eNOS or caveolin levels between groups implying that alterations in eNOS and caveolin expression within caveolin-rich domains do not account for ED in the SHR.

Although caveolin expression within SHR has not been previously addressed, several reports document changes in eNOS expression in SHR. Vaziri *et al* and Nava *et al* demonstrated increased eNOS expression in SHR kidney, heart and aorta, paralleled by increased eNOS activity (Nava *et al.*, 1996; Nava *et al.*, 1998; Vaziri *et al.*, 1998; Vaziri *et al.*, 2000). However, these observations have not always been confirmed elsewhere. Chou *et al* reported downregulation of eNOS expression and activity in aortas of SHR (Chou *et al.*, 1998), a finding which was also documented by Bauersachs *et al* (Bauersachs *et al.*, 1998). These discrepancies may result from differences in the ages at which the animals were studied. Nevertheless, the results presented here agree with the former observations. In this study, analysis of eNOS expression in whole homogenates of kidney and heart clearly demonstrated that protein levels were increased in SHR compared to WKY and provides evidence supporting the view that ED in the SHR is not associated with eNOS translational abnormalities. Despite increased eNOS production, it is clear that NO bioavailability is diminished in these animals, manifested as impaired endothelium-dependent vasodilatation (Konishi & Su, 1983; Luscher & Vanhoutte, 1986; Luscher *et al.*, 1990) and lower flow induced dilatation (Qiu *et al.*, 1998). Although not directly measured in this study, eNOS activity may be reduced and may provide an explanation for reduced NO availability.

As described above, one of the potential mechanisms for altered eNOS activity in SHR could be alterations in the relationship between eNOS and it's inhibitor, caveolin. Therefore, the second aim of this chapter was to investigate whether eNOS-caveolin interactions are altered during ED. Co-immunopreciptation using antibodies

against eNOS and caveolin resulted in detection of eNOS-caveolin interactions in HUVECS. However, these data were not reproduced in lung tissue or in caveolin-rich domains. The reasons for this have not been fully elucidated. The explanation may be simply that the proteins do not interact *in vivo*. However, a recent study demonstrated eNOS-caveolin interactions within rat aorta by co-immunoprecipitation (Murata *et al.*, 2002). In addition, data from caveolin knockout mice do not support this argument (Drab *et al.*, 2001; Razani *et al.*, 2001). Another explanation is that eNOS and caveolin do interact but harsh solubilisation conditions have destroyed these interactions. As alluded to earlier the choice of detergent is critical in the detection of interacting proteins. NP-40 was chosen for the encouraging results observed in HUVECS and as NP-40 is a relatively mild detergent it is unlikely that protein-protein interactions would be destroyed. On the other hand TX-100, which was used during sucrose density centrifugation, may have had a detrimental effect on eNOS-caveolin co-precipitation. Although, in this study, eNOS expression was detected in caveolin-rich domains, some reports argue that TX-100 based methods of caveolar purification do not always allow co-isolation of eNOS (see above and (Shaul *et al.*, 1996)). Furthermore, Feron *et al* reported that two different detergents (OG and CHAPS) used for examining eNOS-caveolin interactions resulted in different outcomes depending on their abilities to solubilise the eNOS-caveolin complex (Feron *et al.*, 1998a).

Interestingly, the method of lysis may also play an important role in preserving eNOS-caveolin interactions. All of the papers documenting the presence of eNOS-caveolin complexes in cultured endothelial cells have used sonication to lyse cells. Sonication is a vigorous method of lysis using ultrasonic waves to disrupt cells by agitation. Although the data have not been shown here, a preliminary experiment using sonication instead of mechanical homogenisation to lyse HUVEC cells, resulted in a dramatic increase in the amount of eNOS co-precipitated by anti-caveolin antibodies. This may provide a reason for the discrepancies concerning the extent to which eNOS and caveolin interact. Sonication is most commonly used for small scale cell suspensions and is obviously not a practical method for the

preparation of tissue protein extracts and was therefore not attempted. Nevertheless, the report by Murata *et al* who showed interactions between eNOS and caveolin in aorta used a similar method of homogenisation to myself (Murata *et al.*, 2002). From their experimental procedures it would appear that all other components of co-immunoprecipitation were the same apart from their choice of lysis buffer. Therefore, in the future, it will be interesting to investigate if this protocol can be used to identify eNOS-caveolin interactions within the lung and kidney.

A further explanation for why eNOS-caveolin interactions were not observed in the lung, concerns the limitations of the detection method. As described above, in homogenised HUVECS eNOS co-precipitated a very small proportion of the total caveolin protein pool. The same was observed for caveolin co-precipitation of eNOS and in some preparations no interactions were observed at all. If this is a true reflection of the intracellular situation, it can be concluded that the relative quantities of interacting proteins were extremely low. Therefore, if this situation is mirrored *in vivo*, then it is possible that the number of eNOS-caveolin complexes in tissue were too few to be detected by this method.

However, it was surprising that the interactions between eNOS and caveolin observed here were extremely low considering that Feron *et al* had previously published that the majority of eNOS is found in association with caveolin (Feron *et al.*, 1996). The data presented here clearly showed that a significant proportion of eNOS remained within the supernatant after immunoprecipitation. Therefore, there appears to be some discrepancy concerning exactly what proportion of cellular eNOS is bound to caveolin. As described above these differences may be the result of differing lysis conditions (i.e. sonication versus homgenisation). Other factors may be involved, for example, the type of endothelial cells used (e.g. HUVECS versus BAEC). It is possible that different cells will exhibit different eNOS-caveolin interactions. Culturing conditions may also affect results. Not only has the degree of confluency been shown to alter eNOS-caveolin colocalisation (Sowa *et al.*, 1999), prolonged culture caused loss of caveolae in endothelial cells (Schnitzer *et al.*, 1994).

Furthermore, the same report documented that BLMECs retained 5-10 times more caveolae than BAECs. To my knowledge there are no similar data for HUVECS.

One of the major inconsistencies concerning the subject of eNOS-caveolin interactions is the lack of histochemical data supporting the biochemical evidence for the existence of this interaction. Immunofluoresence microscopy revealed that the majority of eNOS did not co-localise with caveolin intracellularly (Garcia-Cardena *et al.*, 1996b). In the present study immunofluoresence failed to show intracellular colocalisation of the proteins. Instead, eNOS was found within the perinuclear region of the cell, a finding which is in agreement with earlier studies on eNOS intracellular localisation (O'Brien *et al.*, 1995; Sessa *et al.*, 1995) and caveolin at the cell periphery. It is clear that further studies are required to investigate these discrepancies.

The lack of histochemical data showing eNOS-caveolin colocalisation throws doubt upon the physiological presence and importance of eNOS-caveolin interactions. Until recently it would have been easy to simply dismiss the biochemical observations as an artifact of the methods used in subcellular fractionation and co-immunoprecipitation. However, the recent insight into the potential physiological relevance of eNOS-caveolin interactions was discovered through the use of caveolin knockout mice (refer to section 1.3.6.4). Therefore, the importance of eNOS-caveolin interactions *in vivo* remains an attractive area of eNOS regulation.

One of the important areas to address now is how the multitude of *in vitro* studies on eNOS regulation, particularly those describing caveolin-eNOS interactions, translate to the *in vivo* situation and how eNOS is differentially regulated within different tissues, especially within the kidney. In this study, I have shown that caveolin is expressed within the kidney. However, I have not been able to prove if renal eNOS and caveolin directly interact. Furthermore, renal caveolin expression was not altered during ED, at least not within caveolin-rich domains or whole homogenates. On the other hand, renal eNOS expression was modestly increased in SHR. As mentioned

earlier, other groups have also reported elevated eNOS protein levels within SHR kidneys (Vaziri *et al.*, 1998; Vaziri *et al.*, 2000) complemented by increased renal eNOS activity (Nava *et al.*, 1996) compared to the WKY. Furthermore, Nava *et al* reported significantly higher eNOS activity in the renal medulla of the SHR and to a lesser extent in the cortex compared to the same tissue portions of the WKY (Nava *et al.*, 1996). Since medullary eNOS is thought to play a critical role in natriuresis/diuresis and lowering blood pressure, this may be a compensatory response to prolonged hypertension in SHR. However, this remains to be confirmed. Other animal models of ED also exhibit alterations in renal eNOS expression. Studies on DOCA-salt hypertensive rats revealed augmented expression of eNOS in both the renal cortex and medulla (Allcock *et al.*, 1999). In contrast, both Dahl salt sensitive and two-kidney, one-clip hypertensive rats displayed reduced renal eNOS expression compared to their normotensive counterparts (Ni *et al.*, 1999; Wickman *et al.*, 2001). Therefore, it is clear that eNOS expression is affected differentially depending on the type of hypertension. Further studies are required before any firm conclusions concerning eNOS expression and hypertension can be made.

As described in section 1.2.2.8, ET-1 and ET_B are potential major physiological activators of eNOS and natriuresis/diuresis within the kidney. One of the aims of this chapter was to determine if ET_B, like caveolin, directly interacts with eNOS, if it is localised to caveolae and if these characteristics are altered during ED (see section 1.3.7). Unfortunately, I was unable to detect the presence of ET_B in isolated caveole, whole tissue or in HUVECS due to the lack of good commercial antibodies. Since the synthesis of "in-house" antibodies was beyond the scope of this thesis, I have been unable to address the role of ET_B mediated regulation of eNOS activity by these methods. However, the remainder of this thesis describes further experiments focusing on the role of ET_B in mediating eNOS activation and NO production within the kidney using different molecular methods.

3.4 SUMMARY

In summary, this chapter has investigated whether alterations in caveolar structure are associated with ED in hypertension. The main findings were:

- Alterations in eNOS and caveolin expression within caveolin-rich domains do not account for ED in SHR.
- ED in SHR is not associated with translational abnormalities of eNOS, on the contrary eNOS expression levels are augmented in the kidney and the heart.
- Caveolin and eNOS protein interactions were detected within HUVEC lysates by co-immunoprecipitation.
- Immunofluorescence did not support intracellular co-localisation of eNOS and caveolin in HUVECS. eNOS was found to reside in the Golgi apparatus, whereas caveolin was localised to the plasma membrane.
- Caveolin and eNOS did not interact in lung preparations, raising questions concerning the extent to which these proteins interact *in vivo*.

CHAPTER 4

GENERATION OF *EDNRB* - LACZ KNOCK- IN MICE

4.1 INTRODUCTION

Due to the difficulties in analysing eNOS protein-protein interactions as described in the previous chapter, a different approach to investigating renal eNOS regulation was adopted. Instead of pursuing the nature of eNOS protein-protein interactions within the kidney and how these may be altered during ED, the remainder of the thesis focuses on the upstream mechanisms involved in eNOS activation. Much of the evidence to date implies that the renal endothelin system, in particular ET-1 and ET_B, is a major physiological activator of eNOS (see section 1.2.2.7). It is hypothesised that the inability of ET-1 to stimulate ET_B-mediated NO production may lead to ED within the kidney ultimately resulting in reduced natriuresis and elevation of blood pressure. In order to address this hypothesis first requires knowledge of the cellular and molecular mechanisms involved in ET-1 induced natriuresis through ET_B and eNOS activation. As described in section 1.2.2.8, the major site of expression of ET-1, ET_B and eNOS within the kidney is the medulla. However, confusing localisation and expression data makes it difficult to ascertain precisely which cells are involved. This has led to the conflicting proposals of both an autocrine and paracrine mechanism as discussed in section 1.2.2.8. It is particularly important to establish precise localisation of these components in order to unravel the mechanisms involved. Therefore, the aim of the next two chapters was to determine which cells within the renal medulla are responsible for sensing ET-1; in other words, which cells express ET_B.

Of course the use of conventional techniques such as autoradiography and immunohistochemistry have already led to numerous studies on ET_B localisation in the kidney. However, close analysis of the literature reveals that the results are somewhat conflicting. This may be due to the occurrence of false positives resulting from the difficulties in distinguishing localisation between adjacent cells particularly since IMCD cells and endothelial cells of the vasa recta are separated only by a basal membrane. Therefore, techniques such as immunohistochemistry and radioligand binding may have resulted in problems in identifying localisation to individual cell

types (Hagiwara *et al.*, 1993; Dean *et al.*, 1994; Yukimura *et al.*, 1996; Zhuo *et al.*, 1998). Also, techniques that rely on micro-dissection of nephrons, such as RT-PCR, may have been hampered by cross-contamination (Terada *et al.*, 1992a). These localisation studies will be discussed in more detail in chapter 5 (see section 5.3).

Therefore, in order to address the difficulties of localising ET_B to the kidney a molecular approach was adopted. This approach was based on a "knock-in" strategy using an *EDNRB*-LacZ reporter transgene. The bacterial *Escherichia coli* LacZ gene encodes for β-galactosidase (β-gal), an enzyme which produces a blue colour on staining with X-gal (5-bromo-4-chloro-3-indolyl-β-D-galactosidase). This allows LacZ expression and activity to be assayed colorimetrically (see section 2.6). Introduction of this reporter gene into the *EDNRB* locus resulted in transgenic mice that express LacZ wherever *EDNRB* are expressed and therefore provided a means of obtaining an accurate *in vivo* ET_B gene expression profile by colorimetric staining of β-gal.

This chapter documents the generation of the *EDNRB*-LacZ transgenic mice. It describes in detail the construction of the targeting cassette, targeting of the *EDNRB* locus by homologous recombination in ES cells, verification of targeted ES cells by analysing LacZ expression *in vitro* and the generation of chimeric mice and germline transmission. Chapter 5 describes analysis of these mice and determination of ET_B expression within the kidney.

4.2 RESULTS

4.2.1 Construction of *EDNRB*-LacZ transgene

4.2.1.1 The targeting construct

The targeting construct shown in figure 4-1 was based on the fusion of the LacZ reporter cassette to exon three of the *EDNRB* gene. The *EDNRB* mouse gene, found on chromosome 14, spans 26 kb and consists of 7 exons and 6 introns [1]. Previously, a genomic clone containing around 16kb of the *EDNRB* mouse sequence had been obtained by screening a λphage library (performed by Dr. A. Bagnall, University of Edinburgh). This clone encompassed the last 12 kb of intron 1 to the first 54 bp of exon 5 of the *EDNRB* sequence (see figure 2-3) and was used in the construction of the *EDNRB*-LacZ transgene. Exon 3 was chosen as the site of insertion of the LacZ cassette because it contains the unique restriction site, SphI. In addition, previous reports have documented that regulatory transcriptional elements in intron one of *EDNRB* are important for efficient transcription of the gene (Shin *et al.*, 1997). Therefore, it was important that these should remain intact. The genomic sequences of *EDNRB* located either side of exon 3 provided the 5′ and 3′ homology arms required for insertion of the transgene into the *EDNRB* locus in ES cells by homologous recombination.

A combination of other DNA elements were also present in the reporter cassette. Firstly, translation of LacZ was under the control of a picornaviral internal ribosome entry site (IRES). This sequence acts as a ribosome binding site and allows internal initiation of translation of the reporter gene regardless of the ET_B reading frame (Mountford *et al.*, 1994). Stop codons, present in all three reading frames preceding IRES, stop read-through of the ET_B protein.

---

[1] The genomic sequence of the mouse *EDNRB* gene can be found in full using Ensemble gene I.D. ENSMUSG00000022122 at http://www.ensembl.org/Mus_musculus
The cDNA sequence of the mouse *EDNRB* gene is documented at http://www.ncbi.nlm.nih.gov/Entrez/ using accession number U32329.

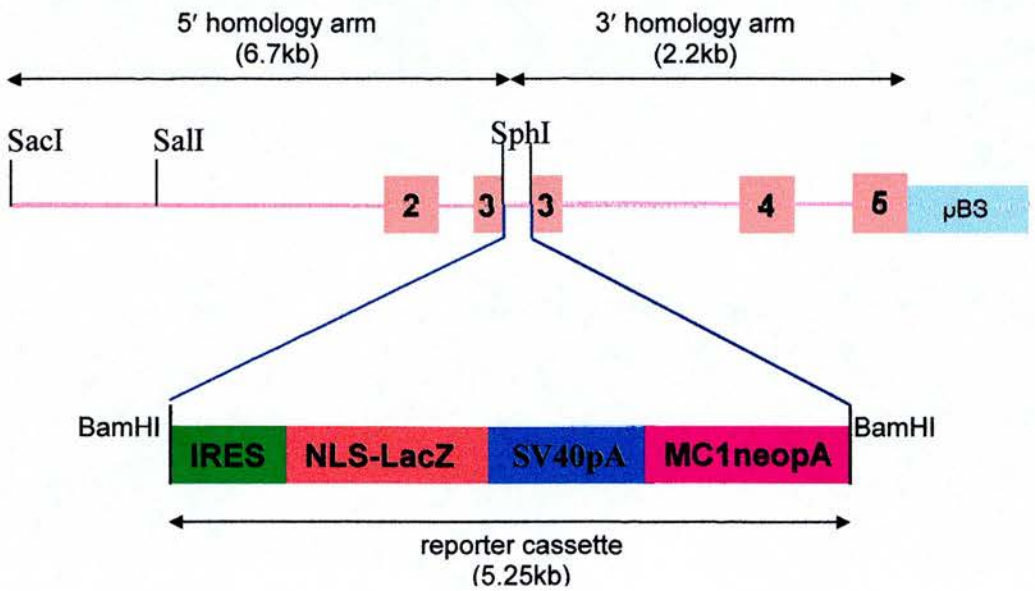

Figure 4-1. *EDNRB*-LacZ targeting construct. Abbreviations: pBS, pBluescript II SK; IRES, internal ribosome entry site; NLS, nuclear localisation signal; SV40pA, simian virus 40 polyadenylation signal; MC1neopA, promoter driven neomycin phosphotransferase resistance gene. See text for further details. Diagram is not drawn to scale.

A nuclear localisation signal (NLS) was also included. This 29 base pair sequence encodes a 10 amino acid consensus sequence as shown.

NLS 5′- GGG CCC AAG AAG AAA CGC AAA GTG GGG AG - 3′
G P K K K R K V G S

The five consecutive positively charged residues (KKKRK) are thought to aid transport into the nucleus thereby confining LacZ expression to the nucleus (Kalderon *et al.*, 1984). This sequence is identical to that used by Teichert *et al* in the eNOS promoter-reporter construct in which they observed precise LacZ expression within the nucleus (Teichert *et al.*, 2000). It is therefore anticipated that the NLS would improve localisation of LacZ staining thereby reducing the incidence of false positives.

The simian virus 40 polyadenylation signal (SV40pA), was also required to add a poly(A) tail to the 3′ end of the LacZ transcript. This is necessary to protect against 3′ degradation of the transcript.

Finally, a modified version of the neomycin phosphotransferase resistance gene, pMC1 Neo, was present in the targeting construct. The neomycin resistance gene has been used for some time in the selection of targeted ES cells during gene targeting events. However, Thomas and Capecchi recognised that the targeting of genes which are either poorly expressed or not expressed at all in ES cells, resulted in low transfection efficiencies (Thomas & Capecchi, 1987). By introducing a promoter to drive expression of the neomycin resistance gene, they improved targeting efficiency. pMC1 Neo, named after the founder, Mario Capecchi, contains the herpes simplex virus thymidine kinase (hsv-tk) promoter which drives the expression of neomycin. Also included are two repeats of the F9 polyoma enhancer which increases the efficiency of the hsv-tk promoter. Since the level of ET_B expression in ES cells is not known, the use of the MC1 promoter ensures high expression of the neomycin resistance gene regardless of the level of ET_B expression. An equivalent

promoterless construct would rely on high expression of ET_B to drive neomycin expression.

4.2.1.2 The cloning strategy – an overview

A detailed description of the cloning strategy is given below. Briefly, the plasmids pictured in figures 2-3 – 2-8 were used in the construction of the *EDNRB*-LacZ transgene. As described in section 4.2.1.1, pλPXho is a genomic clone spanning from intron 1 to part of exon 5 of the mouse *EDNRB* gene and provided the homology arms for the targeting construct. pKL53 and p1049 both encode for LacZ. In pKL53, LacZ is preceded by an NLS but it contains a promoterless neomycin resistance gene. On the other hand, p1049 has the promoter driven neomycin gene (pMC1 Neo) but lacks NLS. Therefore, these plasmids were combined by inserting the NLS signal from pKL53 into p1049 to generate p1049NLS. BamHI-digested p1049NLS was then subcloned into exon 3 of a modified version of pλPXho. In order to perform this step the BamHI site present in NLS of pKL53 was mutated to a BglII site.

All DNA digests, purification of DNA fragments and ligations were performed according to the protocols given in sections 2.4.8, 2.4.10 and 2.4.12 respectively. Recombinants obtained from ligation reactions were screened by restriction enzyme digest of mini-prep DNA (see section 2.4.13.1) unless otherwise stated.

4.2.1.3 Site-directed mutagenesis of BamHI in pKL53

In order to manipulate pKL53 more easily, the region to be mutated was first subcloned into pBS (see figure 2-6) to produce pKS. This was achieved by digesting pKL53 with KpnI and SacI. The resulting 2.1kb fragment was purified and ligated to KpnI/SacI sites in the polylinker of pBS. Resulting colonies were screened by analysis of DNA mini-preps digested with SacI/ClaI (see figure 4-2). All colonies contained the insert indicated by the presence of two bands of 4 and 1.1kb on the agarose gel in figure 4-2. One of these colonies was used for further cloning and was named pKS.

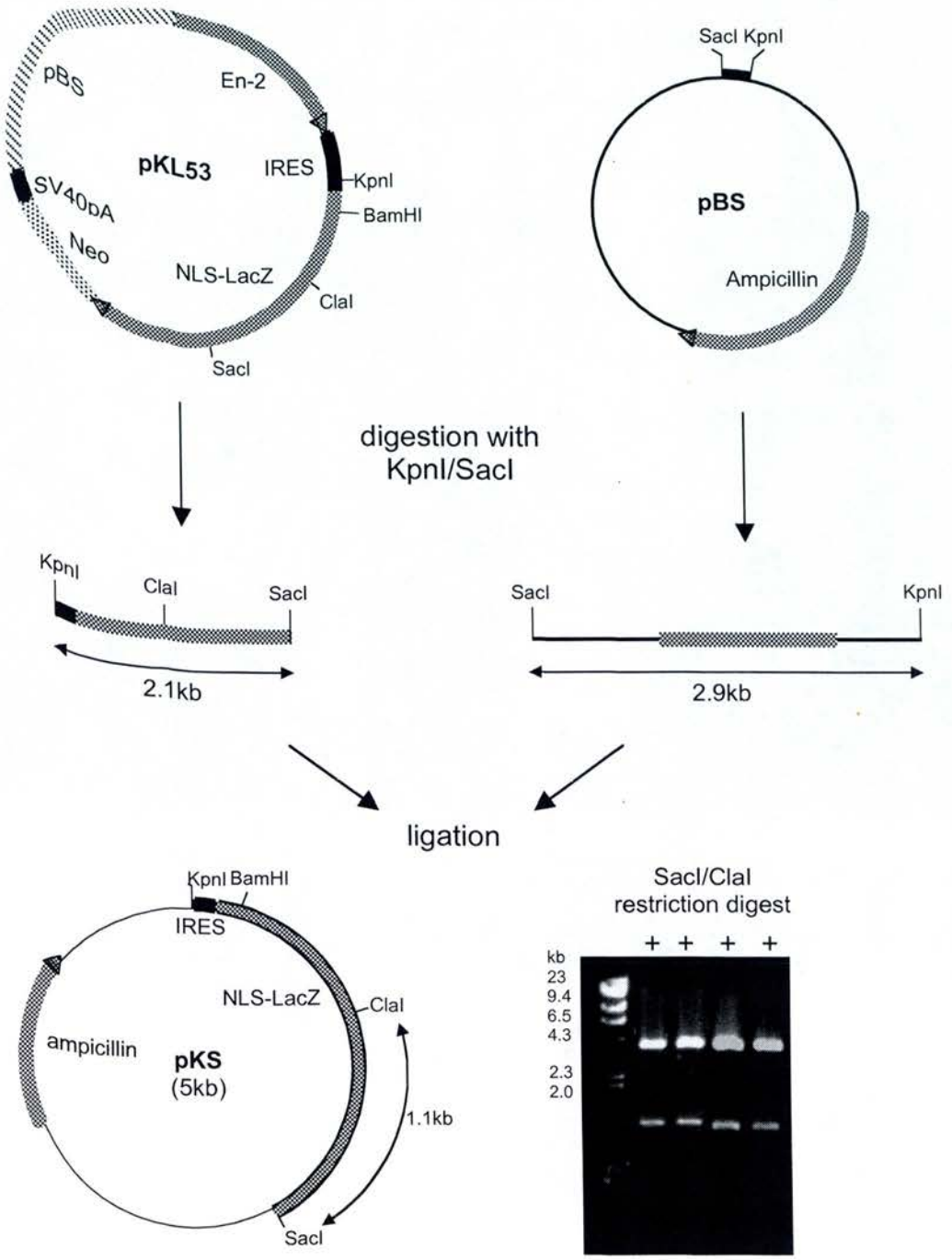

Figure 4-2. Subcloning of pKL53 into pBS. Diagram illustrating how pKL53 and pBS were used to create pKS. See text for details (section 4.2.1.3). Also pictured is a DNA gel of SacI/ClaI digested DNA prepared from pKL53/pBS recombinant colonies. Positive clones are indicated (+).

Mutation of BamHI was achieved by PCR site-directed mutagenesis using primers designed from the pKL53 sequence. The sequences and positions of the primers are shown in figure 4-3. One of the primers, NLSBgl, incorporated the base changes (G-A_{2521} and C-T_{2526}) which were necessary to mutate BamHI (**G**GATC**C**) to BglII (**A**GATC**T**). Although these sites have compatible sticky ends, which were required for subsequent cloning, ligation to each other destroys both sites. The reverse primer (KLCla) was identical to the wild type pKL53 sequence. As shown in figure 4-4 the mutations introduced into pKL53 did not dramatically alter the translated amino acid sequence. A change in amino acid from proline (P) to leucine (L) was generated. However, it was not expected to have any adverse structural effects on the protein. As described in section 2.4.9.1, PCR was performed on pKS to produce an 833bp product (see figure 4-3). PCR was performed using a Pfu proofreading enzyme to ensure that the frequency of introducing random mutations was kept to a minimum. Following PCR, the PCR products were treated to the Klenow, Kinase and Ligase reaction (see section 2.4.9.2) which resulted in the formation of concatamers (see figure 4-5). Concatamers were then prepared for ligation by digestion with BglII/ClaI. Meanwhile, the vector was prepared by digesting pKS with BamHI/ClaI and the resulting 4.2kb DNA fragment purified. Ligation of PCR products and the purified fragment was performed and resulting colonies were screened by restriction enzyme digest of mini-prep DNA using BamHI/ClaI as analytical restriction enzymes. Since BamHI was destroyed during PCR, those clones which contained the PCR product produced a single 5kb band upon BamHI/ClaI digestion. On the other hand, colonies containing the wild type plasmid generated two bands (4.2kb and 0.8kb) as the BamHI site was still present (see figure 4-5). One of the positive clones, named pKSw/oBamHI, was selected and used for further cloning.

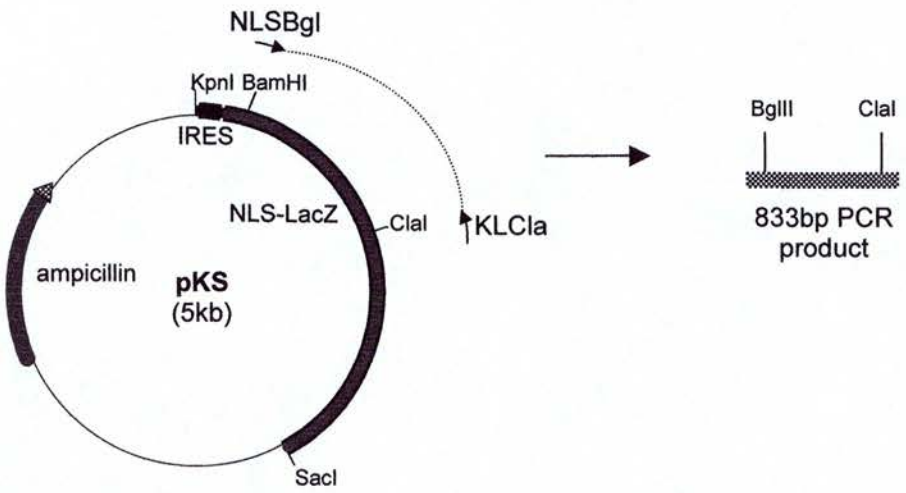

NLSBgl (2516-2542bp of pKL53)

5′ – ATG GCA GAT CTC GTC GTT TTA CAA CG – 3′

KLCla (3325-3349bp of pKL53)

5′ – ACG CTC ATC GAT AAT TTC ACC GCC – 3′

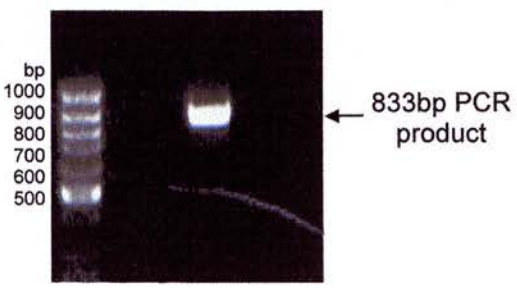

Figure 4-3. PCR site-directed mutagenesis of pKS. Mutagenesis of BamHI was performed by PCR using primers NLSBgl and KLCla. Base changes are shown in red. See text for details (section 4.2.1.3). Also pictured is a DNA gel showing the 833bp product from the PCR reaction.

Figure 4-4. Comparison of wild-type and mutated pKL53 DNA and amino acid sequences. The base changes (shown in red) introduced by site-directed mutagenesis result in a change from BamHI to BglII. Changes in amino acid sequence are shown in green.

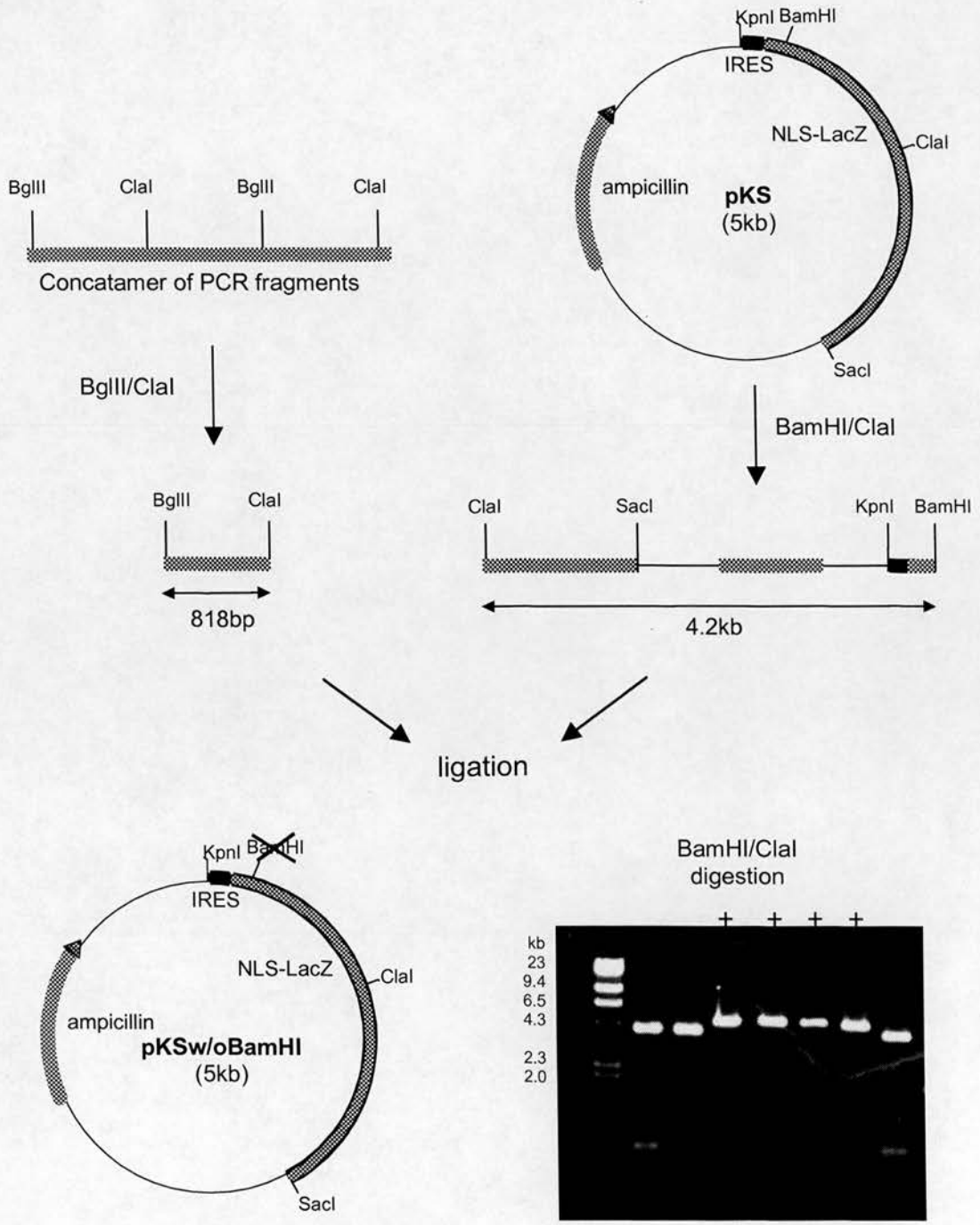

Figure 4-5. Subcloning of mutated PCR products into pKS. Diagram illustrating restriction enzyme digests of PCR concatamers and pKS and subsequent ligation to produce pKSw/oBamHI. See text for details (section 4.2.1.3). Also pictured is a DNA gel of BamHI/ClaI digested DNA prepared from PCR/pKS recombinant clones. Positive clones are indicated (+).

4.2.1.4 Introduction of NLS into p1049

The next stage was to subclone the DNA fragment from pKSw/oBamHI containing the NLS signal into p1049. This was done using KpnI/SacI to digest both plasmids followed by ligation. However, before p1049 could be digested the additional KpnI and SacI sites present in the polylinker of pBS had to be removed. Therefore, the 5.2kb cassette from p1049 was excised by BamHI digestion, purified and cloned into BamHI in the polylinker of pSP72poly3 (see figure 4-6). This vector contained no KpnI or SacI sites (see figure 2-7). Colonies were screened by restriction enzyme digestion analysis with BamHI. Those colonies which contained the insert were identifiable by the presence of the 5.2kb band upon BamHI digestion, whereas negative colonies contained only the vector (2.4kb). The resulting positive plasmid was named p1049SP72. pKSw/oBamHI and p1049SP72 were then digested with KpnI/SacI. The resulting 2.1kb fragment obtained from pKSw/oBamHI was used to replace the corresponding fragment in p1049SP72 (see figure 4-7). Colonies were screened by PCR to identify those clones which contained the NLS sequence. Primers were designed from the pKL53 sequence (see figure 4-7). One of the primers, pKL53NLS, corresponded to the NLS sequence of pKL53. A PCR product of 866bp was generated only in clones containing the NLS sequence as shown in figure 4-7. The resulting positive clone was named p1049NLS.

4.2.1.5 Sequencing of p1049NLS

Before proceeding with the final stages of insertion of p1049NLS into exon 3 of *EDNRB*, p1049NLS was extensively sequenced. The reason for this was that there was a possibility that additional mutations may have been introduced during PCR despite Pfu polymerase having an error rate of 1:10000bp. Therefore, the entire region that was subject to PCR was sequenced using overlapping primers and carefully checked for discrepancies against the pKL53 sequence. Two additional base changes were found (A-G_{2812} and T-C_{3073}). It is possible that this was simply a mistake in the sequencing of either p1049NLS or the original pKL53 sequence. Nevertheless, both mutations occurred in the third position of the codon and therefore did not alter the translated sequence.

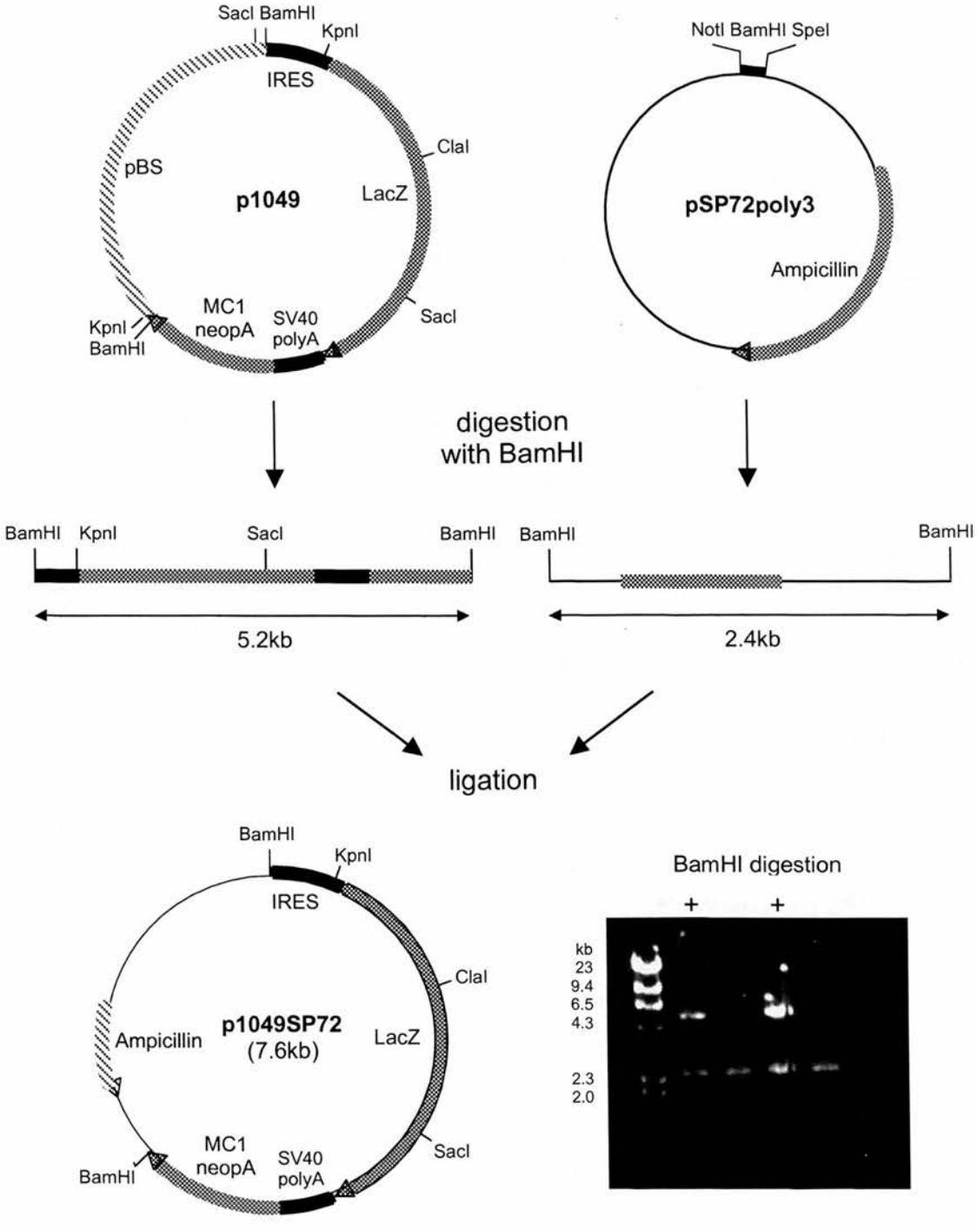

Figure 4-6. Subcloning of p1049 into pSP72poly3. Diagram illustrating how p1049 and pSP72poly3 were used to create p1049SP72. See text for details (section 4.2.1.4). Also pictured is a DNA gel of BamHI digested DNA prepared from p1049/pSP72poly3 recombinant clones. Positive clones are indicated (+).

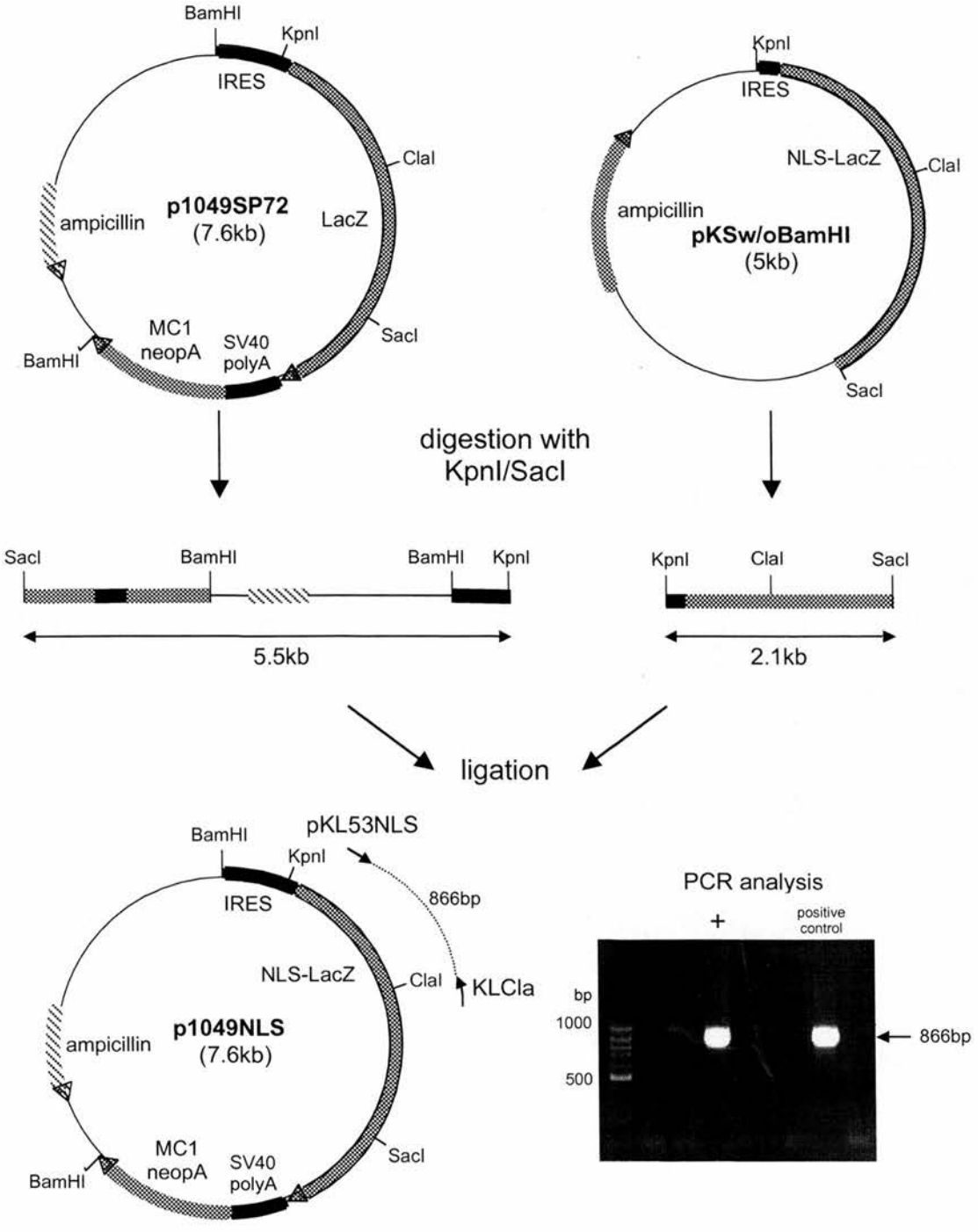

pKL53NLS (2483-2506 of pKL53) 5′ – ATG GGG CCC AAG AAG AAA CGC AAA – 3′
KLCla (3325-3349bp of pKL53) 5′ – ACG CTC ATC GAT AAT TTC ACC GCC – 3′

Figure 4-7. Subcloning of NLS from pKSw/oBamHI into p1049SP72. Diagram illustrating how pKSw/oBamHI and p1049SP72 were used to create p1049NLS. See text for details (section 4.2.1.4). Also pictured is a DNA gel of the PCR reaction used to screen pKSw/oBamHI/p1049SP72 recombinant clones. Positive clones are indicated (+).

4.2.1.6 Shortening of the 5′ homology arm of pλPXho

The penultimate step before inserting the cassette from p1049NLS into exon 3 of the *EDNRB* locus was to modify pλPXho. pλPXho contains a very large section of *EDNRB* intron 1 exceeding 10kb in size. Since this contributes to part of the 5′ homology arm it would have proven extremely difficult to develop an efficient 5′ screening strategy for homologous recombination. Therefore, it was decided to modify pλPXho to produce a plasmid (pλPXhoS) with a shorter homology arm of approximately 6.7kb. This was achieved by digesting pλPXho with SacI. The resulting 9kb DNA fragment was purified and subcloned into SacI-digested pBS (see figure 4-8). Resulting colonies were screened by restriction enzyme digestion analysis of DNA mini-preps using SalI. One colony was found to contain the insert as indicated by the appearance of a larger band shown on the gel in figure 4-8 and was named pλPXhoS. All other colonies contained only the pBS vector.

4.2.1.7 Insertion of cassette from p1049NLS into exon 3 of pλPXho

To complete the construct, the modified cassette from p1049NLS was inserted into pλPXhoS. The 5.2kb fragment generated from BamHI-digested p1049NLS was purified and the ends blunt-ended using T4 DNA polymerase as described in section 2.4.11. pλPXhoS was digested with SphI and also blunt-ended with T4 DNA polymerase followed by ligation to the 5.2kb insert to produce p*EDNRB*NLS+ (see figure 4-9). Since blunt-ended ligations have a lower success rate compared to sticky-end ligations, it was deemed necessary to screen a greater number of colonies than usual. An efficient method of doing this is by colony lift and hybridisation using a radioactive probe complementary to the insert DNA (see section 2.4.13.2). This allows several hundred colonies to be screened at once. Only those colonies containing the insert will be identified by the probe. Therefore, colony lifts and hybridisation were performed. The probe was isolated as an EcoRI fragment from p1049 as shown in figure 4-10 and used to screen the recombinant colonies. Several colonies were found to contain the insert, the presence of which was confirmed by

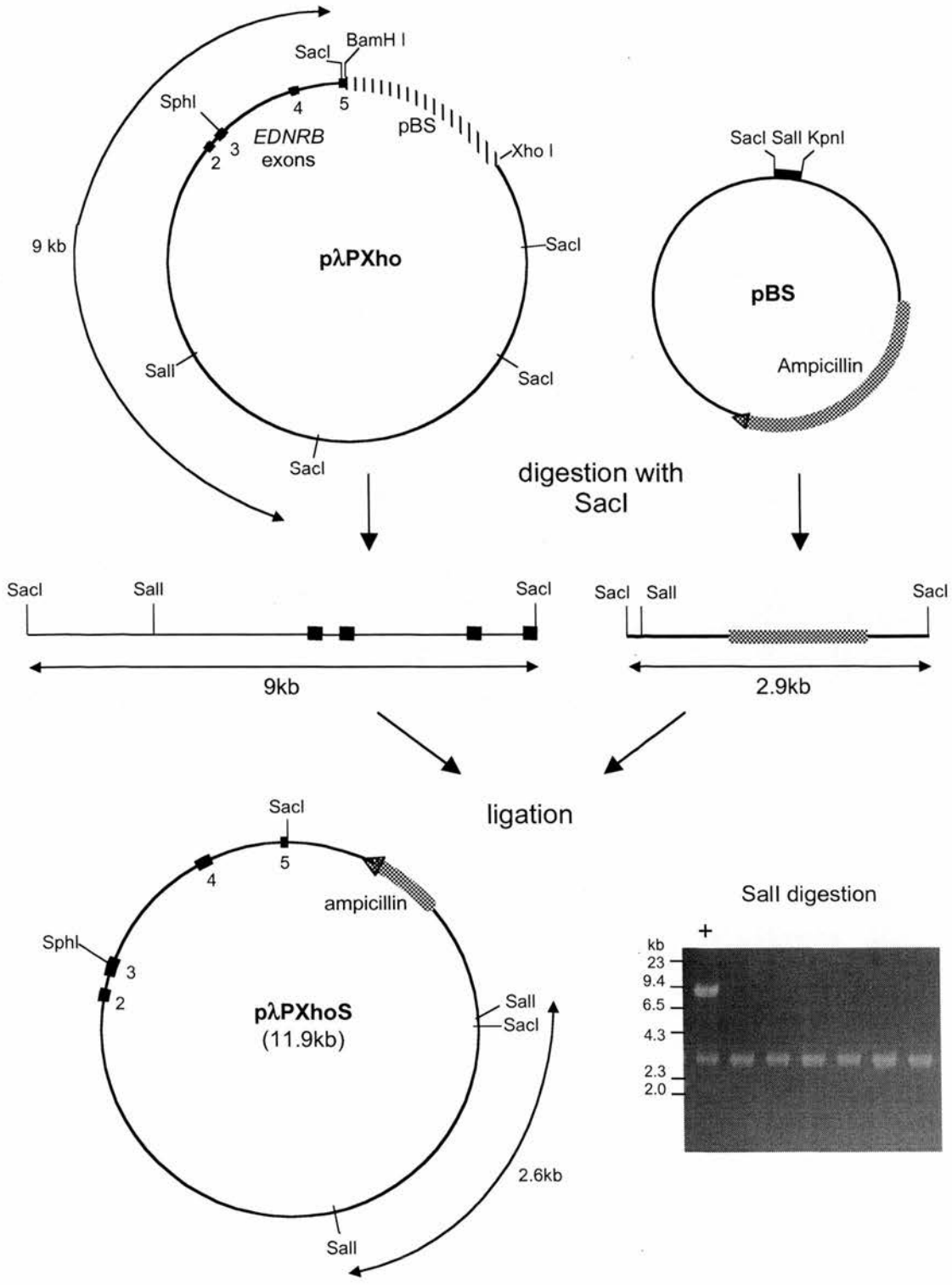

Figure 4-8. Shortening of 5′ homology arm of pλPXho. Diagram illustrating how pλPXho and pBS were used to create pλPXhoS. See text for details (section 4.2.1.6). Also pictured is a DNA gel of SalI digested DNA prepared from pλPXho/pBS recombinant colonies. Positive clones are indicated (+).

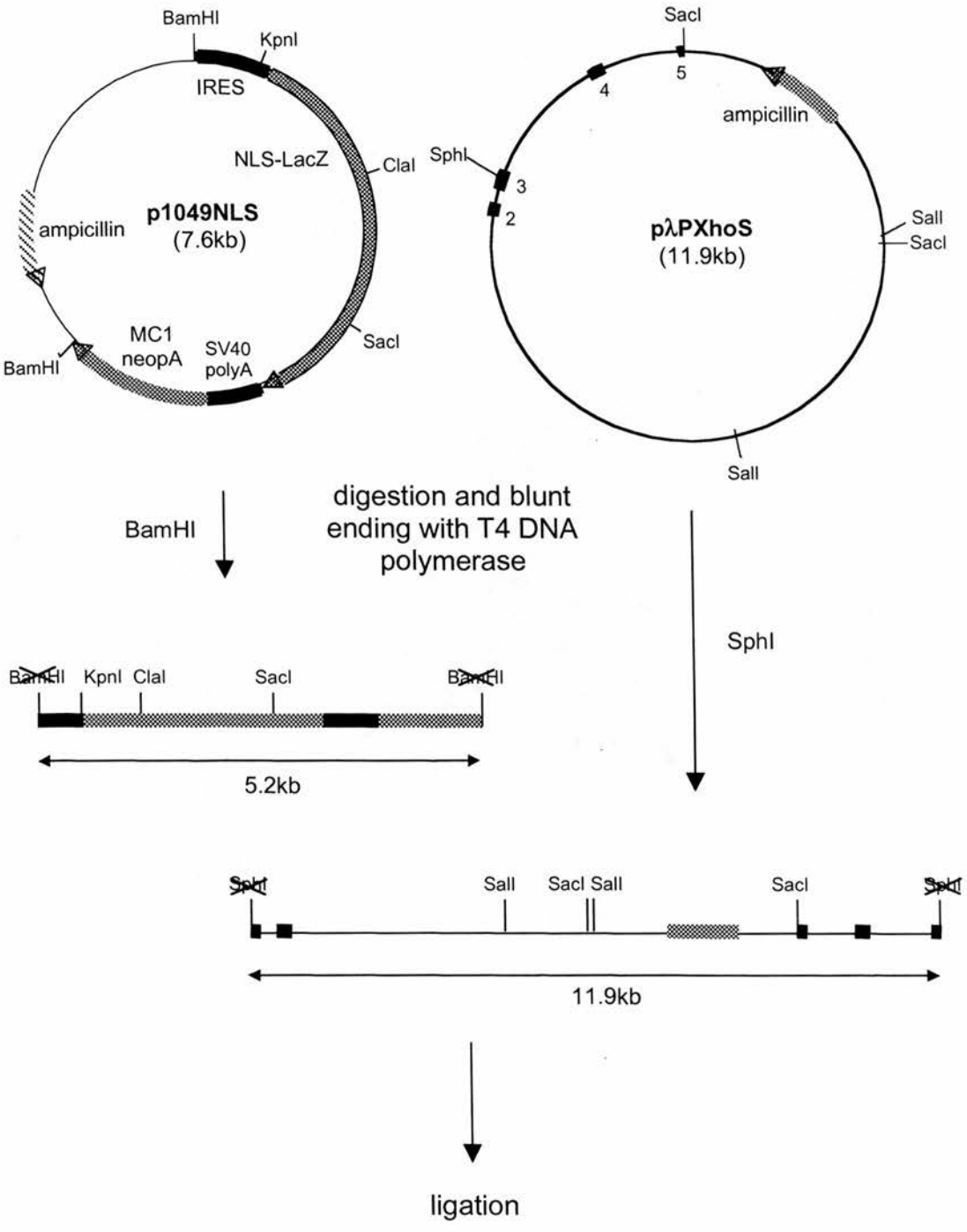

Figure 4-9. Generation of p*EDNRB*NLS+ (continued overleaf). Diagram illustrating digestion of p1049NLS and pλPXhoS to generate the DNA fragments which were used to make p*EDNRB*NLS+. See text for details (section 4.2.1.7).

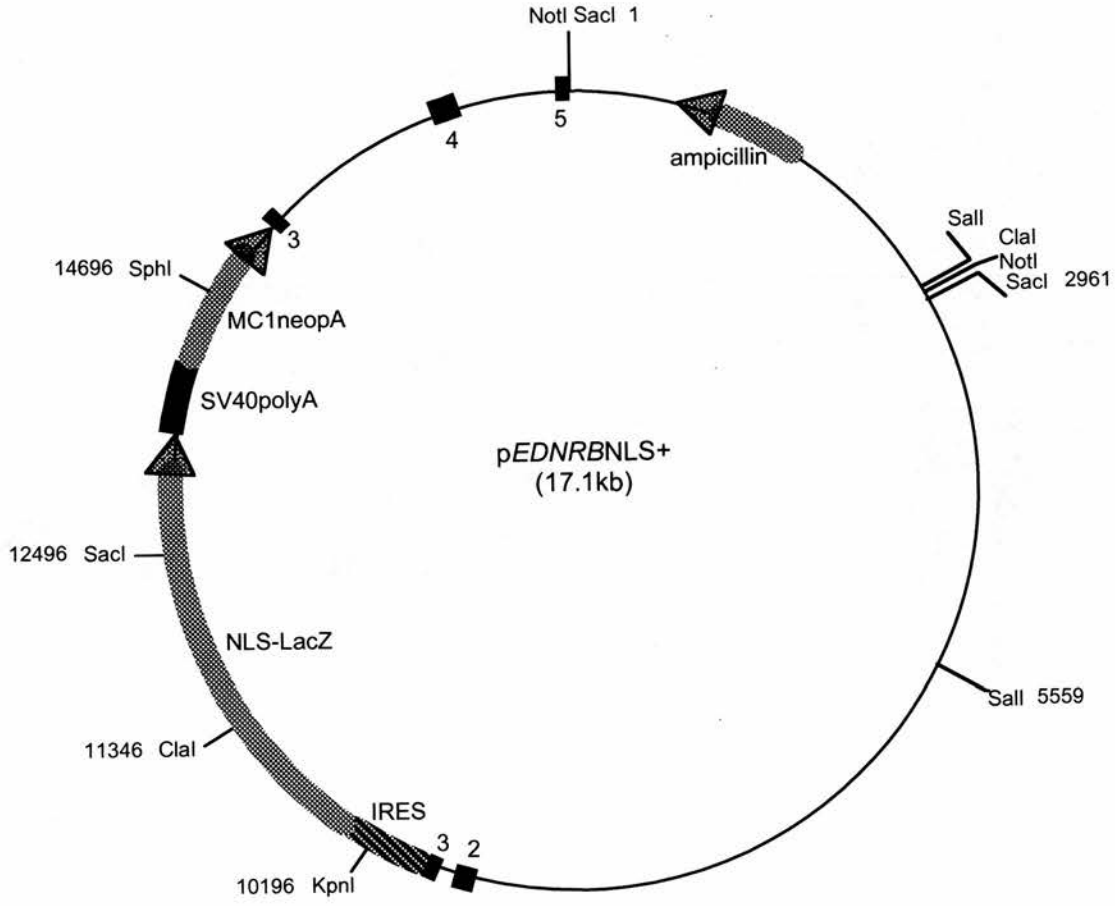

Figure 4-9. Generation of p*EDNRB*NLS+ (continued).

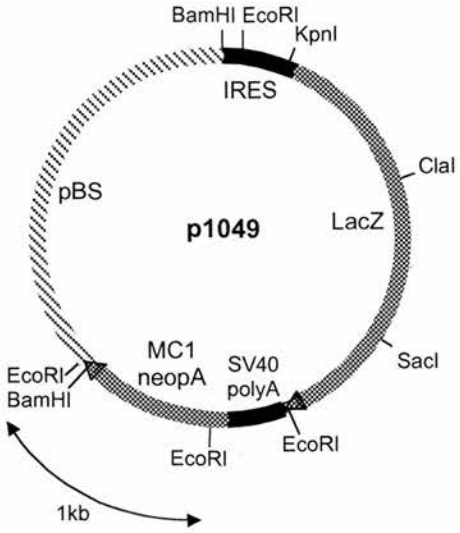

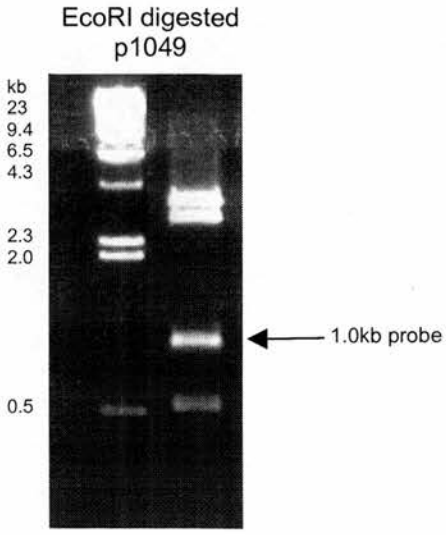

Figure 4-10. Preparation of probe for colony lifts. A 1kb fragment was isolated from EcoRI-digested p1049 for use as the probe in p1049NLS/ pλPXhoS recombinant colony lifts. See text for details (section 4.2.1.7).

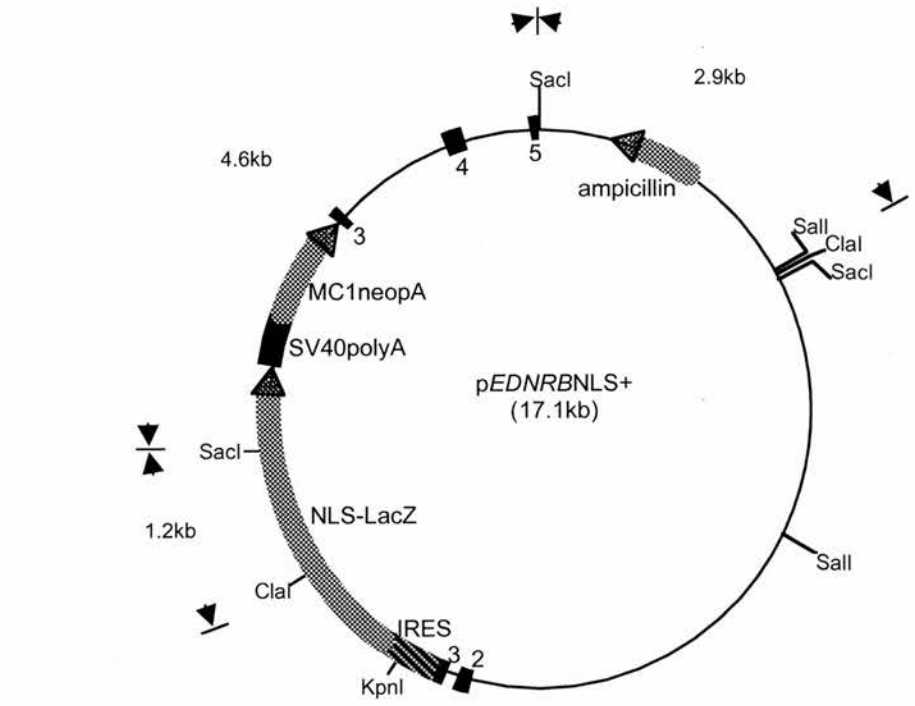

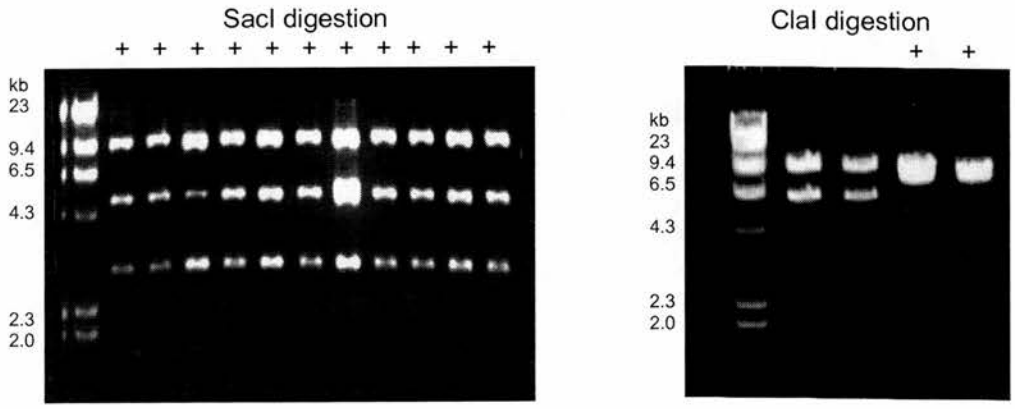

Figure 4-11. Restriction enzyme digests of p*EDNRB*NLS+. The presence of the insert was confirmed by SacI digestion. Correct orientation was determined by ClaI digestion. See text for details (section 4.2.1.7). Positive clones are indicated (+).

analysis with SacI which generated fragments of 9.6kb, 4.6kb and 2.9kb (see figure 4-11). Orientation of the insert was analysed by ClaI digestion. Colonies containing the insert in the correct orientation generated fragments of 8.7 and 8.4kb upon ClaI digestion (see figure 4-11). On the other hand, incorrect orientation yielded fragments of 10.7 and 6.4kb.

4.2.1.8 Sequencing across the junction of the cassette and exon 3 of EDNRB

As a final verification that p*EDNRB*NLS+ had been correctly constructed, the junction between the cassette and the 3′ end of *EDNRB* exon 3 was sequenced using a primer designed from the Stratagene pMC1neopA sequence 1441-1466bp (p*EDNRB*NLSNeoF 5′- GCG AAT GGG CTG ACC GCT TCC TCG - 3′). The resulting sequence was then compared to the pMC1neopA and the *EDNRB* cDNA sequences. Alignment of these sequences is shown in figure 4-12 where a dot represents homology between the sequences. It should be noted that homology between pMC1neopA and p*EDNRB*NLS+ stopped at the BamHI site indicating the end of the cassette and entry into exon 3 of *EDNRB* (figure 4-12a). Likewise, alignment of *EDNRB* cDNA and p*EDNRB*NLS+ sequences resulted in homology only after the SphI site in exon 3 of *EDNRB* cDNA (figure 4-12b). Homology ceased at the start of exon 4 in the cDNA and intron 3 in p*EDNRB*NLS+. This provided further evidence that the reporter cassette had been cloned into exon 3 of *EDNRB* in the correct orientation.

(a) Alignment of pMC1neopA (top) with p*EDNRB*RNLS+ (bottom)

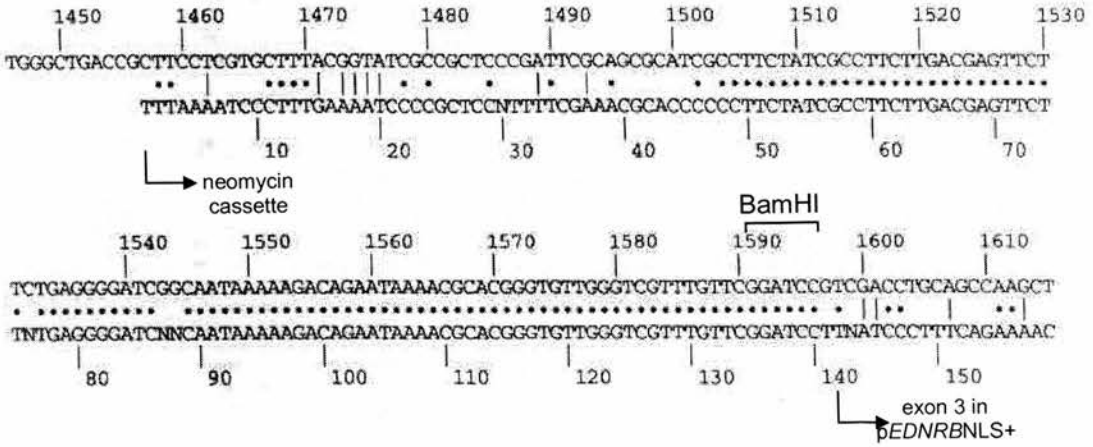

(b) Alignment of *EDNRB* cDNA (top) with p*EDNRB*NLS+ (bottom)

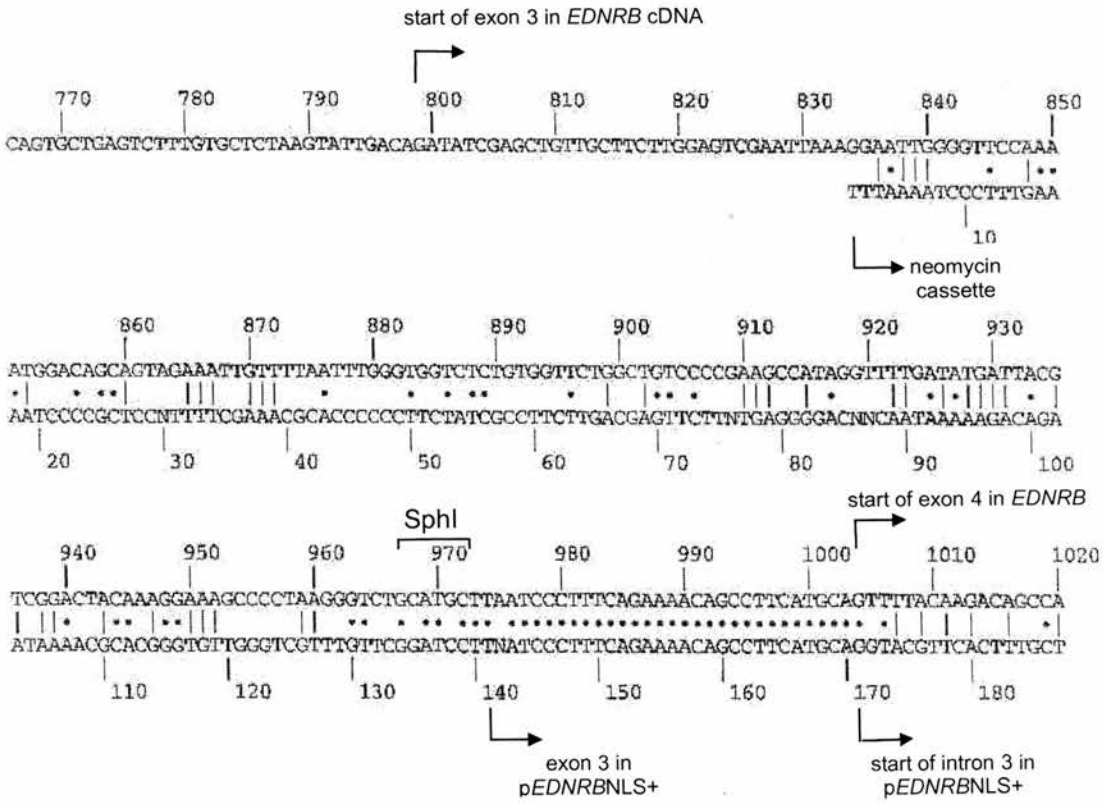

Figure 4-12. Sequence analysis of p*EDNRB*NLS+. p*EDNRB*NLS+ was aligned with (a) pMC1neopA and (b) *EDNRB* cDNA. See text for details (section 4.2.1.8).

4.2.2 Targeting of the *EDNRB* locus with p*EDNRB*NLS+

*4.2.2.1 Introduction of p*EDNRB*NLS+ into ES cells*

The construct was introduced into the *EDNRB* locus by homologous recombination in ES cells. p*EDNRB*NLS+ was linearised with NotI and was electroporated into ES cells as described in section 2.5.5. Twenty-four hours after electroporation, selection was started by adding G418 to the medium. Only those cells which had taken up the construct expressed neomycin and were able to survive in the presence of G418. All other cells died. After selection in G418 for 7-8 days, clones were picked and expanded in 96 well plates for either freezing or for DNA preparation (see section 2.5.6). Altogether 960 colonies were picked. The next stage was to distinguish between clones in which the targeting construct had been inserted randomly and those in which homologous recombination had occurred. Colonies were screened by either Southern blot analysis (section 4.2.2.2) or PCR (section 4.2.2.3).

4.2.2.2 Southern blot analysis of G418-resistant clones

In order to determine if homologous recombination had taken place in any of the colonies, all colonies were screened by Southern blot analysis (see section 2.5.9). Rare-cutting restriction enzymes, SacI and SphI, were used to digest genomic DNA isolated from the ES cells followed by detection of homologously targeted loci with radioactive probes complementary to the *EDNRB* locus. SacI and SphI sites were chosen based on information obtained from the *EDNRB* genomic sequence (see footnote on page138). The probes were positioned outwith the ends of the 5′ and 3′ homology arms of the construct and therefore only identified clones which were homologously targeted to the *EDNRB* locus and not clones in which the construct had been randomly integrated. A diagram of the Southern screening strategy is depicted in figure 4-13 and predicted fragment sizes from targeted and wild type *EDNRB* genes are summarised in table 4-1.

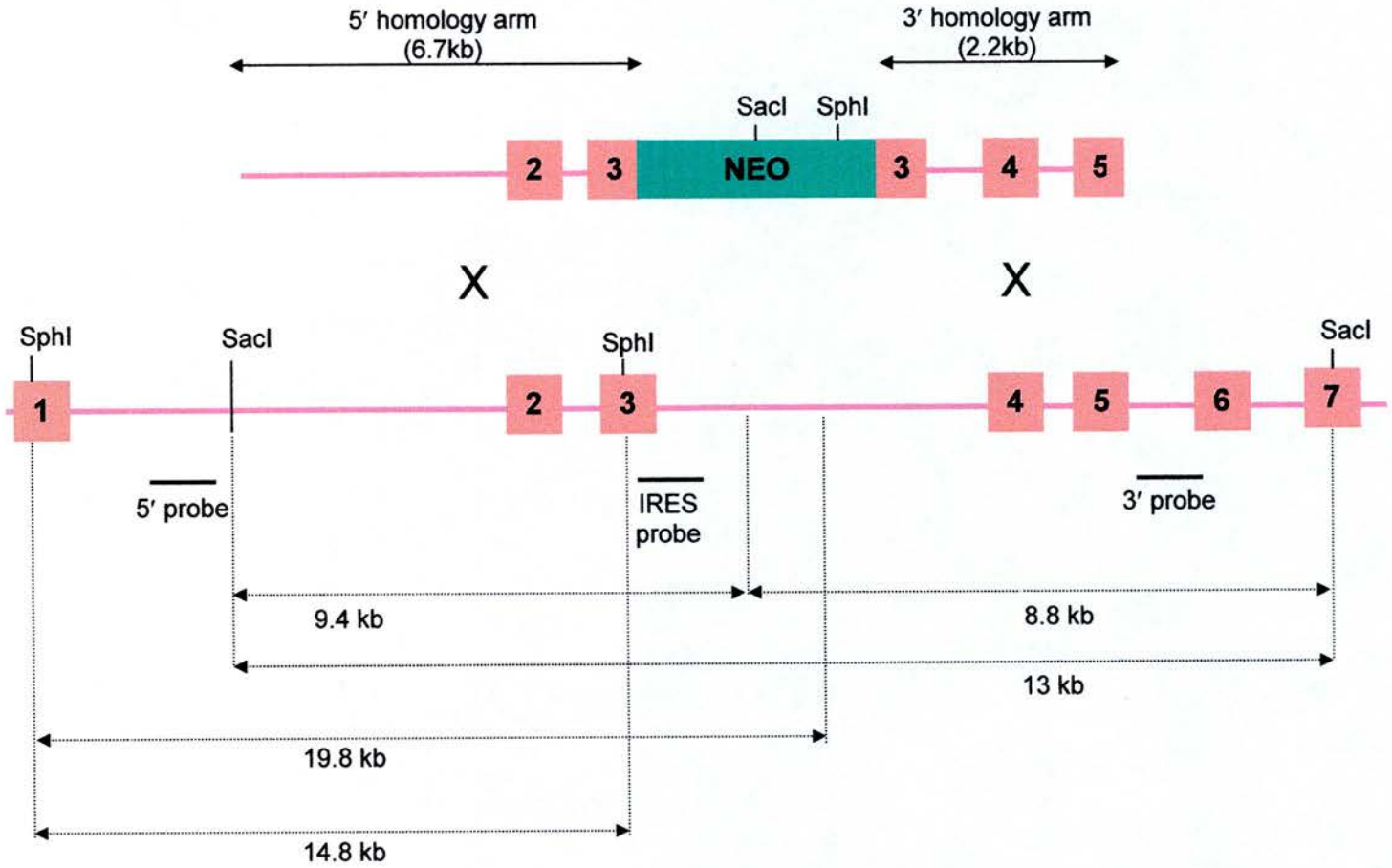

Figure 4-13. Southern blot screening strategy. Diagram of Southern blot strategy for screening for homologous recombination at the *EDNRB* locus in G418-resistant ES cell colonies. Diagram is not drawn to scale. See text for details (section 4.3.2.2).

Table 4-1. Predicted sizes for wild type and targeted bands in Southern blot analysis.

Digest and probe used	Wild type (*EDNRB*)	Targeted (LacZ)
SacI and 3′ probe	13kb	8.8kb
SphI and 5′ probe	14.8kb	19.8kb
SacI and IRES probe	——	9.4kb

The 5′ and 3′ probes were prepared from plasmids pλPxho (see figure 2-3) and pCRII-6.18 (see figure 2-8) respectively as shown in figure 4-14. The 5′ probe was prepared by PCR of pλPXho using primers designed from the *EDNRB* genomic sequence. This generated a 1.2kb fragment. The 3′ probe was prepared from BamHI-digested pCRII-6.18 and subsequent purification of the resulting 1kb fragment.

DNA digestion, separation of DNA on agarose gels and Southern blots were all performed in a 96 well format in order to speed up the screening process. Initially 3′ Southern analysis was performed by SacI digestion followed by probing with the 3′ probe. As expected, the wild type band of 13kb was present in all colonies (figure 4-15). However, out of 960 colonies screened only two appeared to be targeted to the *EDNRB* locus indicated by the presence of a shorter band (see figure 4-15c, clones 10D8 and 2G11). Curiously, the bands from these clones were of different sizes. Since the targeted band should have been approximately 8.8kb, it would appear that clone 10D8 was probably correct. 5′ Southern analysis was then performed on these two clones. DNA was digested with SphI followed by Southern blotting using the 5′ probe which resulted in a wild type band of 14.8kb (see figure 4-16). However, only one of the clones, 2G11 was targeted correctly at the 5′ end shown by the presence of a larger band corresponding to the predicted size of 19.8kb. Therefore, only clone 2G11 appeared to be targeted to the *EDNRB* locus at both the 5′ and 3′ ends.

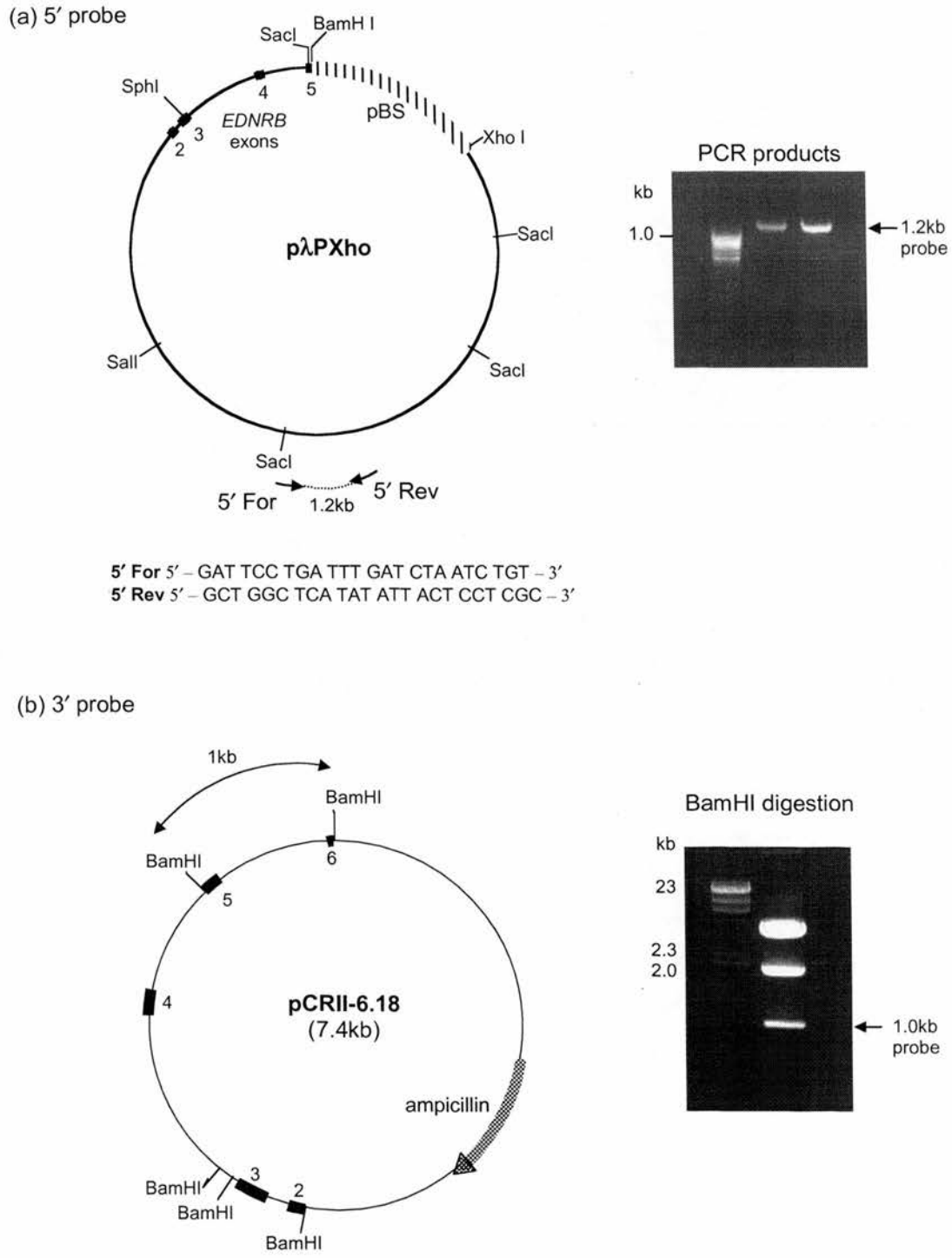

Figure 4-14. Preparation of 5′ and 3′ probes for Southern blotting. pλPXho and pCRII-6.18 were used to make the 5′ and 3′ probes respectively. (a) PCR of pλPXho using the primers shown generated a 1.2kb fragment. (b) Digestion of pCRII-6.18 with BamHI yielded a 1kb fragment. 25ng of each probe was used for each Southern blot. Refer to text for details (section 4.2.2.2).

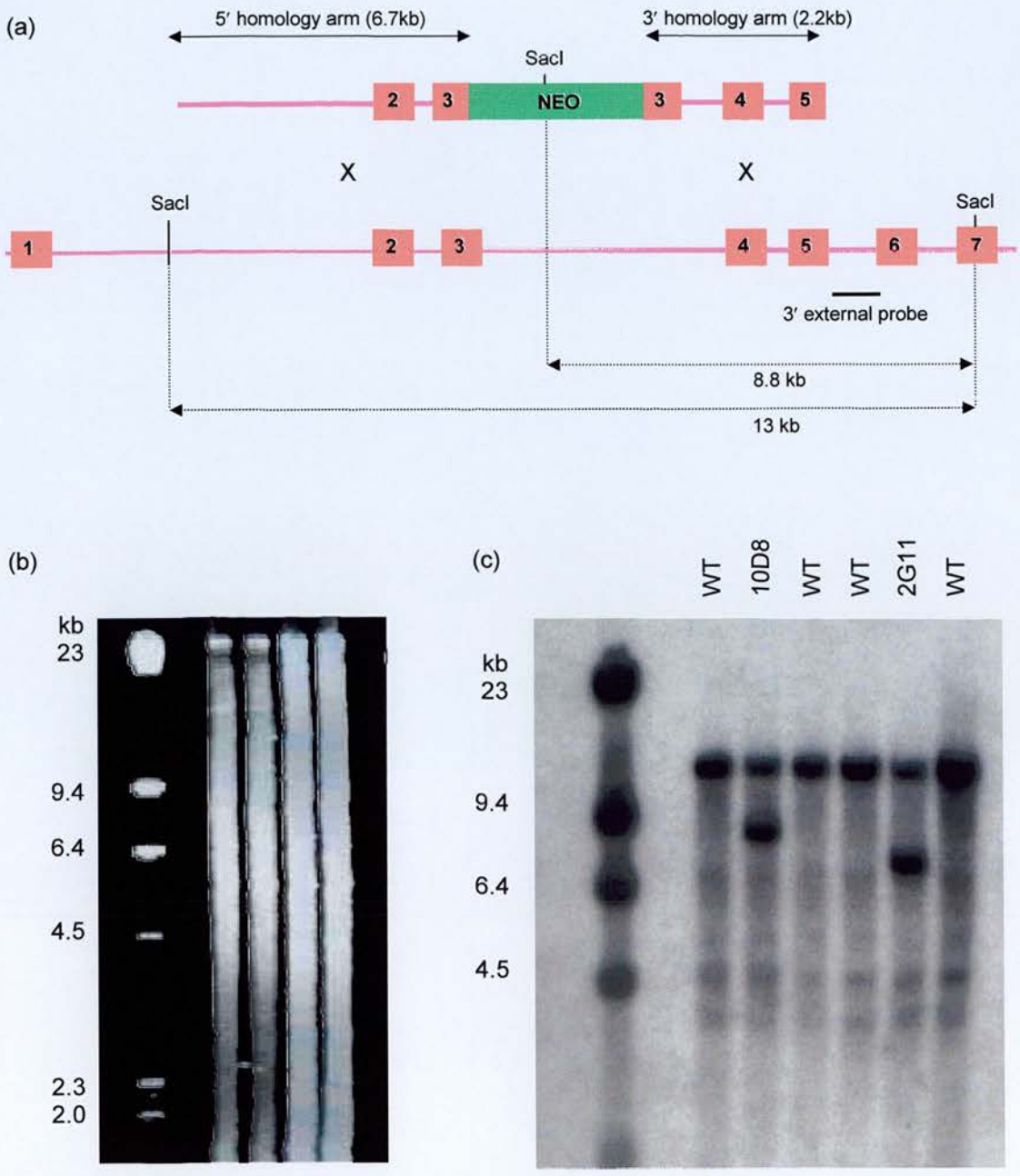

Figure 4-15. 3′ Southern analysis of G418-resistant ES cell colonies. In order to identify homologously targeted clones, genomic DNA isolated from ES cells was digested with restriction enzyme, SacI and probed with the 3′ probe. (a) 3′ Southern screening strategy, (b) DNA gel of digested genomic DNA, (c) Southern blot of SacI-digested DNA using 3′ probe. WT, wild type. See text for further details (section 4.2.2.2).

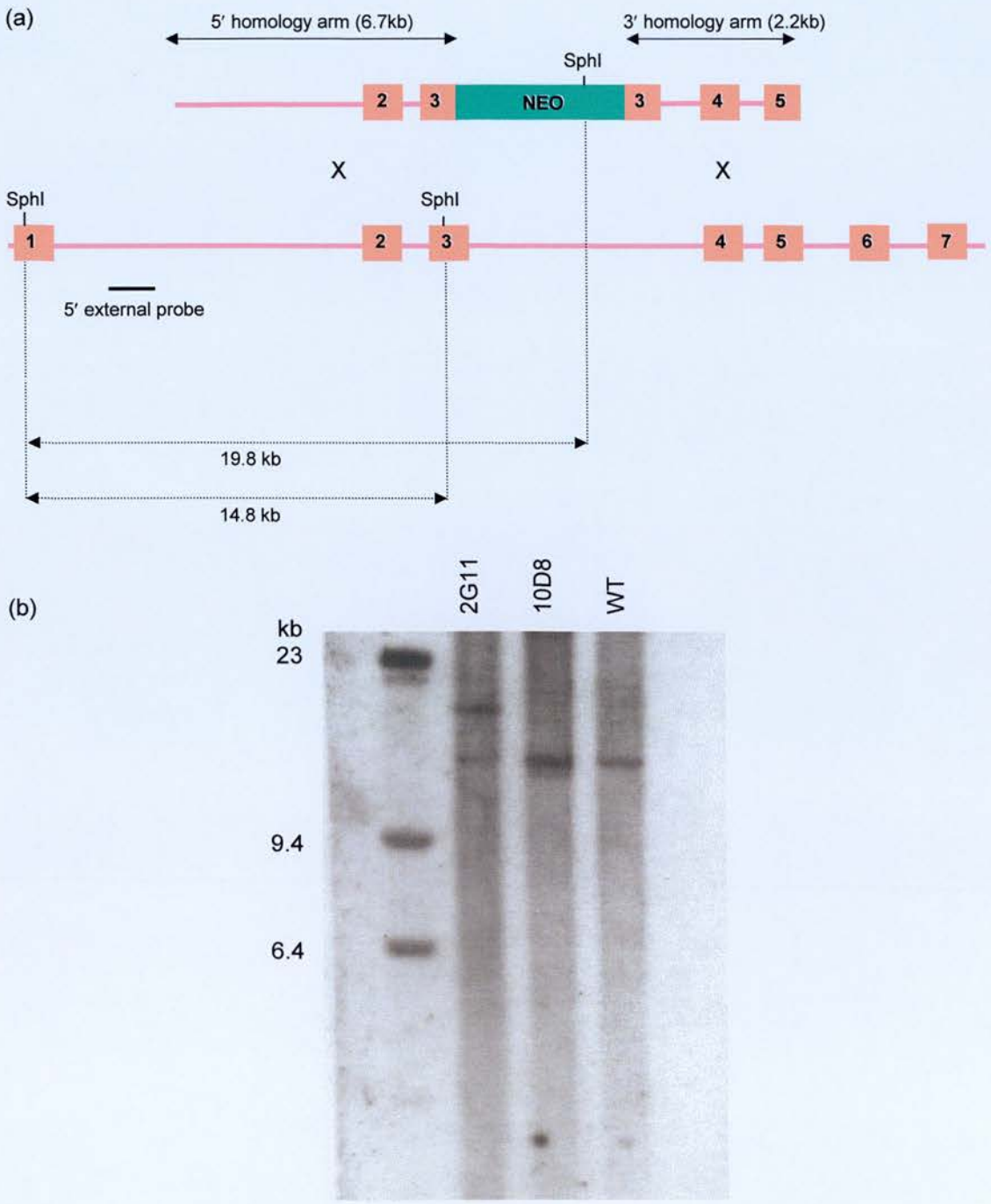

Figure 4-16. 5′ Southern analysis of G418-resistant ES cell colonies. Genomic DNA isolated from ES cells was digested with restriction enzyme, SphI and probed with the 5′ probe. (a) 5′ Southern screening strategy, (b) Southern blot of SphI-digested DNA using 5′ probe. WT, wild type. See text for further details (section 4.2.2.2).

In order to further characterise clone 2G11, an additional Southern blot was performed using a probe complementary to the cassette. The IRES probe was prepared from p1049 digested with KpnI and BamHI (see figure 4-17a). The resulting 0.5kb band was purified and used as the probe for SacI-digested 2G11 DNA. As predicted this resulted in a band of 9.4kb (see figure 4-13 and 4-17b). This also confirmed that only one copy of the transgene had been integrated into the *EDNRB* locus.

4.2.2.3 Analysis of G418-resistant clones by PCR screening

In order to speed up the screening process, a PCR-based screening strategy was used in parallel with Southern analysis. The Expand Long Template PCR System is specifically designed to amplify long templates and was used in conjunction with a 96-well PCR block to screen G418-resistant colonies (see section 2.5.10). Screening was only attempted at the 3′ end of homology since the 5′ end was too long to develop a reliable PCR protocol. A diagram of this strategy showing primer positions and expected sizes of bands is shown in figure 4-18. Primer sequences are also documented there. Three separate sets of primers were used (see table 4.2). Two sets of primers, NeoF/417R and 78F/5to4R, acted as internal controls to confirm that the PCR was optimal. The third set of primers, NeoF/5to4R, only produced a band of 2.5kb in homologously recombined clones since the 5to4R primer lay outwith the end of the 3′ homology arm.

Table 4-2. Primer pairs and predicted sizes for wild type and targeted bands in PCR analysis.

Primers	Predicted size	Comment
NeoF / 417R	1.5kb	positive control for presence of transgene
78F / 5 to 4R	2.5kb	positive control for wild type allele
NeoF / 5 to 4R	2.5kb	will produce PCR product only in homologously targeted clones

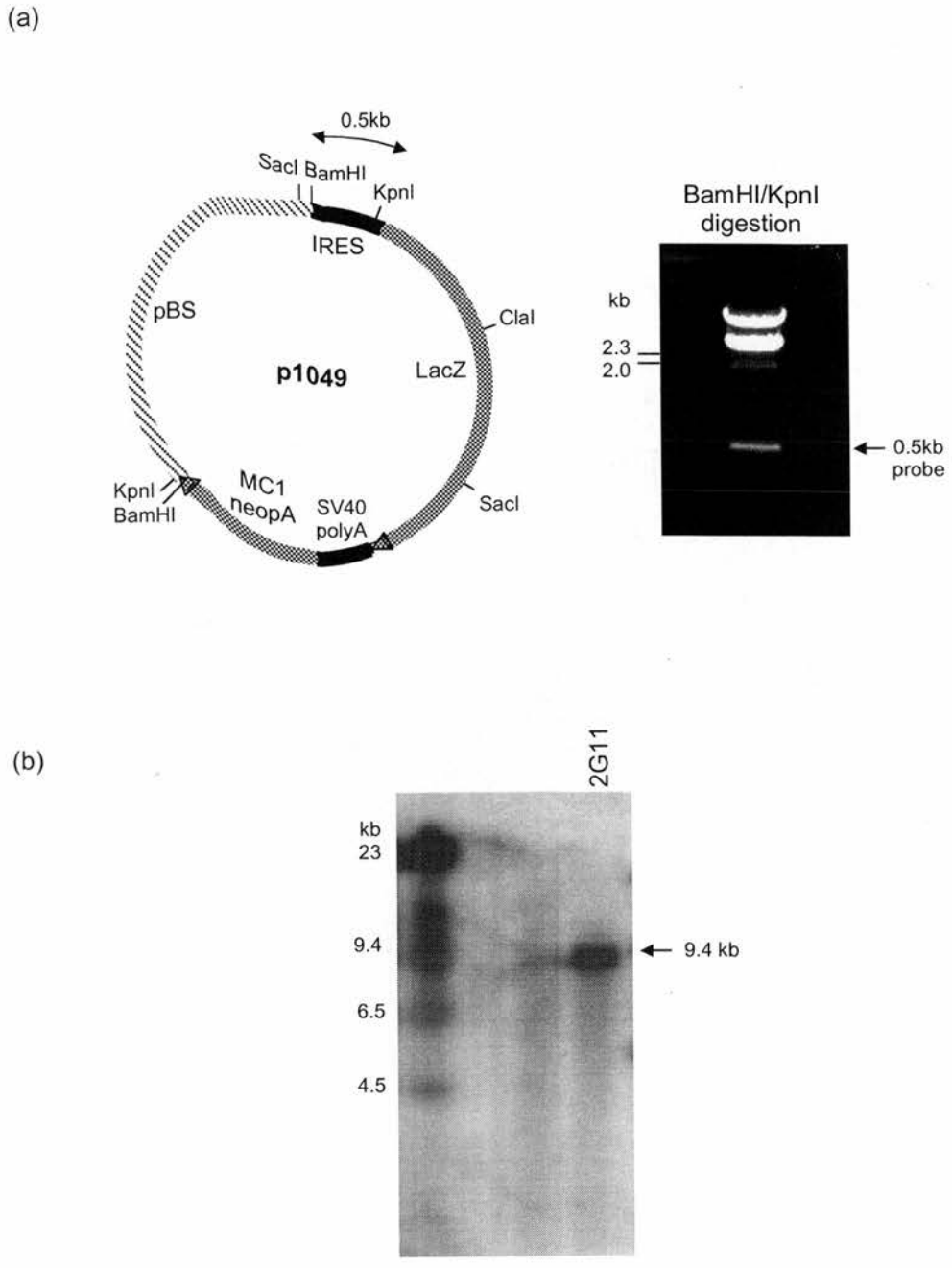

Figure 4-17. Southern blotting of clone 2G11 using IRES probe. (a) A probe was prepared from p1049 digested with KpnI/BamHI. The 0.5kb fragment was purified and used in Southern blotting. (b) Southern blot of SacI-digested 2G11 DNA using IRES probe. Refer to figure 4-13 for predicted size of band and see section 4.2.2.2 for further details.

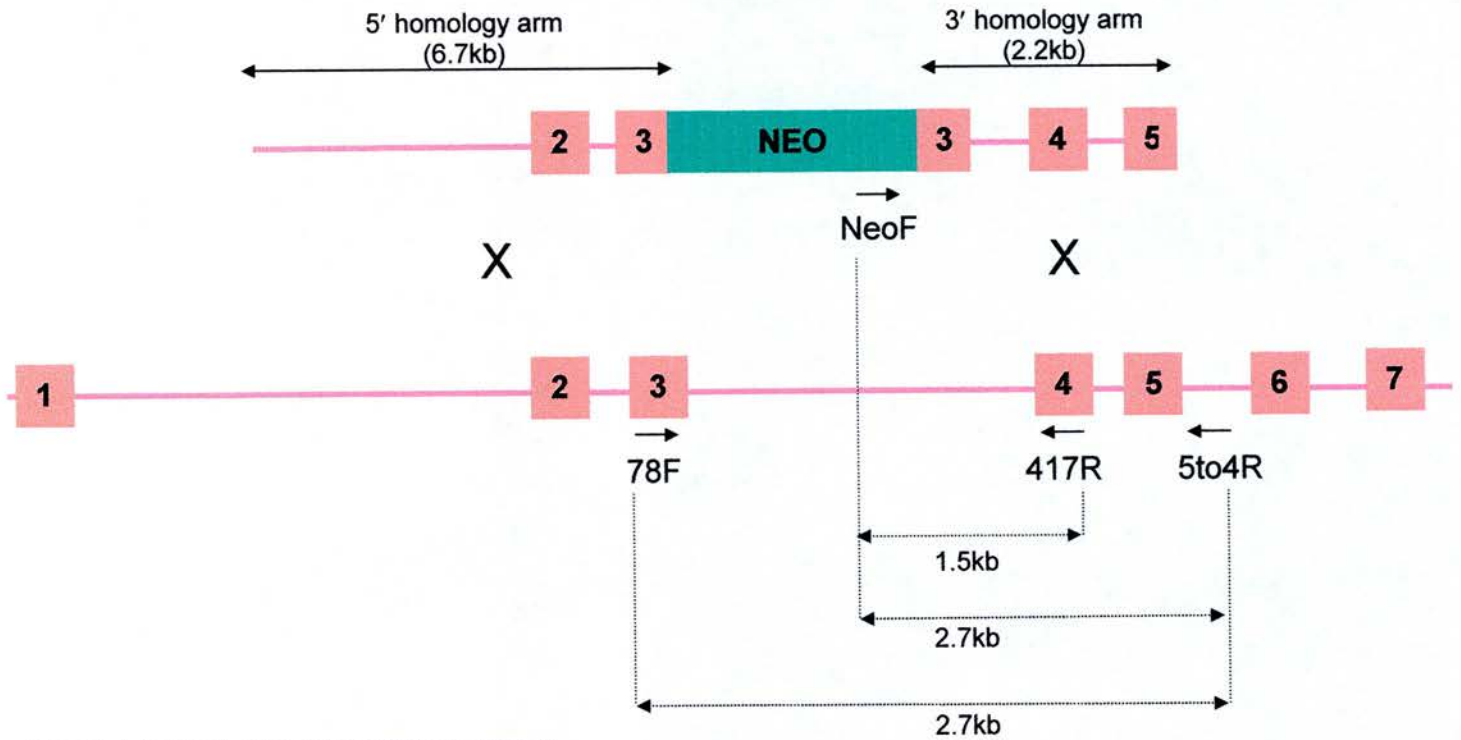

NeoF	5′ GCG AAT GGG CTG ACC GCT TCC TCG 3′
78F	5′ TTT GGG TGG TCT CTG TGG TTC TGG 3′
417R	5′ GTA GAA ACT GAA CAG CCA CCA ATC 3′
5to4R	5′ GAA CAG CTG CCA CGT CTC CT 5′

Figure 4-18. PCR screening strategy. Diagram of PCR strategy for screening for homologous recombination at the *ENDRB* locus in G418-resistant ES cell colonies. Also shown are primer sequences. NeoF was designed from the Stratagene pMC1neopA sequence 1441-1466bp. 78F and 417R were designed from *EDNRB* mouse cDNA 877-899bp and 1023-1046bp respectively. 5to4R was designed from *EDNRB* mouse genomic sequence (intron 5-6, 95012993-95013013bp). Diagram is not drawn to scale. See text for further details (section 4.2.2.3).

Several colonies were screened by this method and two, 10D8 and 1H3, were found to produce the correct band with NeoF/5 to 4R primers (see figure 4-19). Clone 10D8 had already been identified by 3′ Southern analysis (see section 4.2.2.2). However clone 2G11, which was also identified as being positive by 3′ Southern analysis, was not amplified by PCR suggesting that the 3′ arm of this clone was not completely correct. This may account for the shorter band produced during 3′ Southern analysis (see section 4.2.2.2).

A summary of the results of screening for homologous recombination by Southern blotting and PCR analysis is shown in table 4-3. Unfortunately clone 1H3 did not survive defrosting. Of the two remaining targeted clones 2G11 appeared to be the best candidate for microinjection, the primary reason being that this was the only clone that was correctly targeted at the 5′ end. The 5′ end of integration is essential for driving *EDNRB* and consequently LacZ expression.

Table 4-3. Summary of targeted clones and methods used to identify them.

Method of screening	No. of colonies screened	Clone ID	% positive
3′ Southern	960	2G11, 10D8	0.2
3′ PCR	480	10D8, 1H3	0.4
5′ Southern [1]	N/A	2G11	N/A

[1] 5′ Southern analysis was only performed on clones which were found to be positive by 3′ Southern analysis (i.e. clone 2G11 and clone 10D8). Other clones were also included as wild type controls.

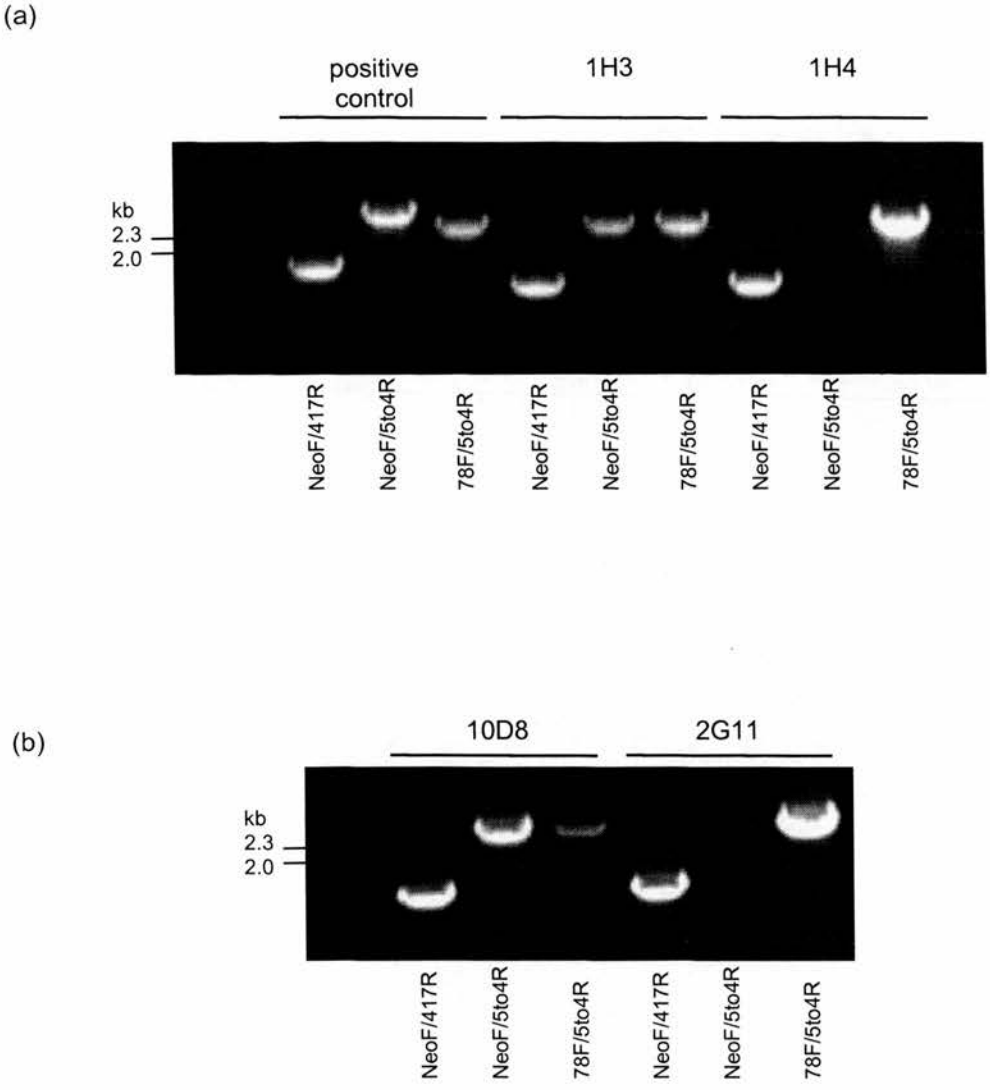

Figure 4-19. PCR analysis of G418-resistant ES cell clones for 3′ homologous recombination. (a) Clone 1H3 was identified as being homologously targeted to the *EDNRB* locus as shown by the presence of a 2.7kb band for NeoF/5to4R primers. (b) Two clones, 10D8 and 2G11 previously identified as being targeted to the *EDNRB* locus by 3′ Southern analysis were analysed by PCR. Only clone 10D8 produced bands for each set of primers and therefore was identified as being homologously targeted to the 3′ end of the *EDNRB* locus. Refer to figure 4-18 for predicted sizes of bands and see section 4.2.2.3 for further details.

4.2.3 Clone 2G11 expresses LacZ *in vitro*

Prior to microinjection of clone 2G11 into blastocysts, it was decided to confirm expression of the transgene *in vitro*. Since ET_B is probably not highly expressed in ES cells, a simple differentiation assay was designed. 2G11 and non-transfected ES cells were cultured as hanging drops to produce embryoid bodies which have the potential to differentiate into a number of different cell types (see section 2.5.12.1). Embryoid bodies were allowed to differentiate for several days before being stained for β-gal activity. Figure 4-20a & b clearly shows that clone 2G11 expressed LacZ as indicated by the presence of blue cells. On the other hand, wild type, non-transfected cells did not express LacZ (figure 4-20c). Although these results confirmed that clone 2G11 expresses LacZ *in vitro* it was impossible to deduce which type of cells were expressing LacZ and also if expression was confined to the nucleus given the presence of the nuclear localisation signal in the transgene. This was largely due to the nature in which the cells grow when cultured as embyroid bodies (i.e. in close contact with each other). Therefore, to further investigate expression of the transgene *in vitro* a complementary set of differentiation experiments was performed. 2G11 ES cells were cultured on collagen IV-coated plates in the presence and absence of LIF in order to produce an endothelial cell population as described in section 2.5.12.2. Since endothelial cells express ET_B, it was anticipated that LacZ expression would be visible at a subcellular level within these cells. Resulting cells were also compared to those grown on a gelatin matrix. Flow cytometry analysis (see section 2.5.12.3) of cells grown on collagen in the absence of LIF revealed that approximately 13% of total cells counted ($1x10^4$) were positive for the endothelial marker, Flk-1, compared to 5.2% of cells grown on gelatin (see figure 4-21a). Visually, cells grown by this method were more spread out compared to the embryoid bodies making it easier to identify individual cells. However when assayed for β-gal activity, the absence of blue staining suggested that none of these cells expressed LacZ (figure 4-21b).

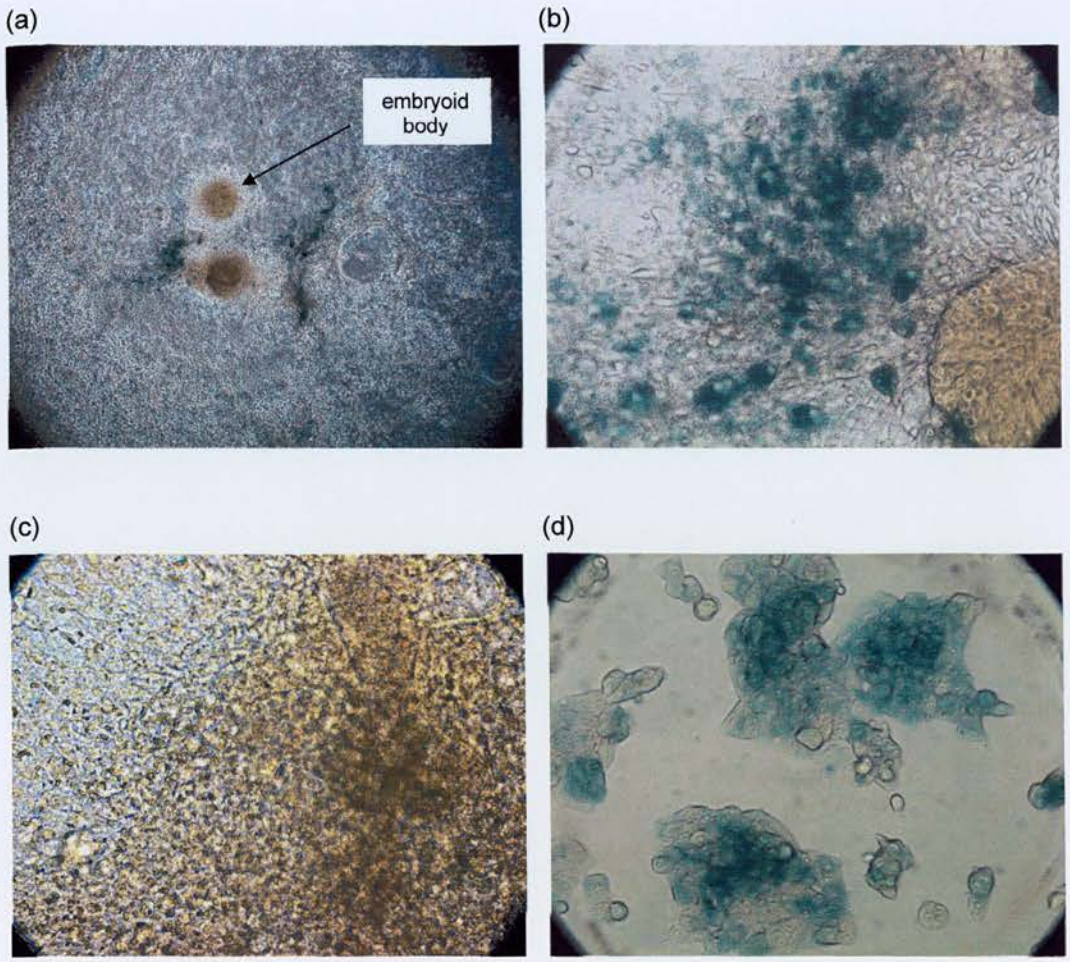

Figure 4-20. Differentiation of ES cells as hanging drops and analysis of LacZ expression. 2G11 and non-transfected ES cells were cultured as hanging drops to produce embryoid bodies and stained for β-gal activity. The conversion of the substrate, X-gal, to a visible blue product is indicative of β-gal activity. (a) Low magnification of 2G11 cells which express LacZ (x50), (b) High magnification of (a) (x200), (c) Non-transfected ES cells do not express LacZ (x50), (d) Positive control for LacZ expression (x200). See text for further details (section 4.2.3).

(a)

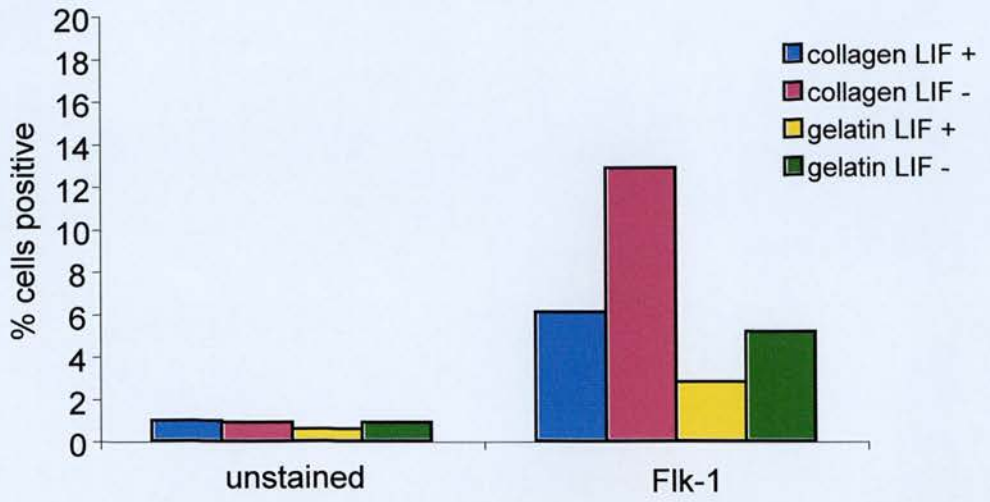

(b)

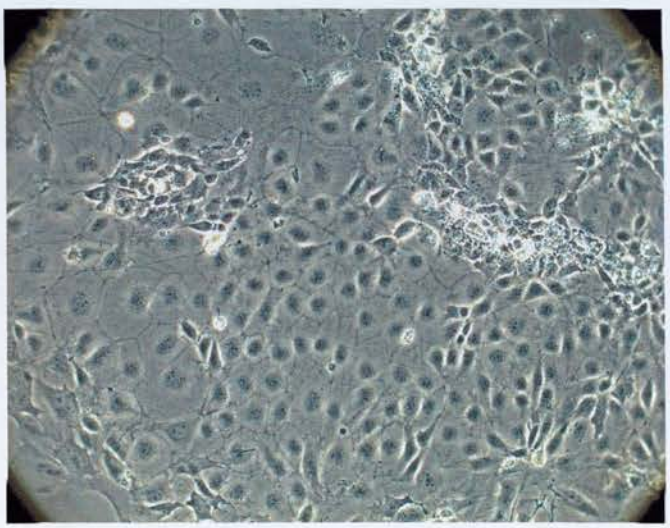

Figure 4-21. Differentiation of ES cells on collagen IV and analysis of LacZ expression. 2G11 and non-transfected ES cells were cultured on collagen IV and gelatin coated plates in the absence and presence of LIF. The resulting cell population was analysed by flow cytometry and stained for β-gal activity. (a) FACS analysis of cells stained with anti-Flk-1 antibodies. (b) Staining of cells for β-gal activity. Differentiated cells do not express LacZ. See text for further details (section 4.2.3).

Despite the lack of LacZ expression in collagen IV differentiated 2G11 ES cells, this clone was shown to be correctly targeted to the *EDNRB* locus by Southern blotting and did express LacZ when differentiated under the correct conditions (i.e. as embryoid bodies). Therefore, this clone was used in the generation of *EDNRB*-LacZ transgenic mice as described below.

4.2.4 Generation of chimeric mice and germline transmission

Clone 2G11 was successfully defrosted and expanded. ES cells were microinjected into C57BL/6J mouse blastocysts and implanted into a pseudopregnant mouse as described in section 2.5.13. In total, one male chimera and one female chimera were born. Chimeric pups were comprised of cells from two different mouse strains and therefore were identified by the presence of beige coloured patches amidst the normal black fur (see figure 4-22a). Beige patches originated from ES cell-derived 129 cells, whilst the dark fur was derived from the host C57BL/6J blastocyst cells. Chimeras were backcrossed with BKW mice in an attempt to achieve germline transmission of the targeted gene. Only the male chimera produced offspring suggesting that the female chimera was probably sterile. Again, offspring were assessed by coat colour (figure 4-22b). Generation of black pups indicated inheritance of C57BL/6J chromosomes derived from the parent blastocyst and therefore did not carry the targeted gene. In contrast, beige coloured pups indicated inheritance of chromosomes derived from 129 ES cells and had a 1 in 2 chance of carrying the targeted allele. Germline transmission was confirmed by PCR analysis of tail tip DNA (refer to section 2.5.14). The primers used were designed from the LacZ gene of the pKL53 sequence and are documented in figure 4-23. From one litter, 5 out of 8 beige mice contained the targeted gene as indicated by the presence of a 701bp band (figure 4-23).

(a)

(b)

Figure 4-22. Chimeric mouse and germline transmission of targeted *EDNRB* gene. (a) A male chimera derived from 129 ES cells from clone 2G11 (beige) and host C57BL/6J blastocyst derived cells (black). This chimera was mated with a female BKW mouse and produced offspring of 2 different colours (b). Black pups were derived from chromosomes inherited from C57BL/6J whilst beige pups were derived from chromosomes inherited from 129 ES cells and therefore had a 1 in 2 chance of carrying the targeted gene.

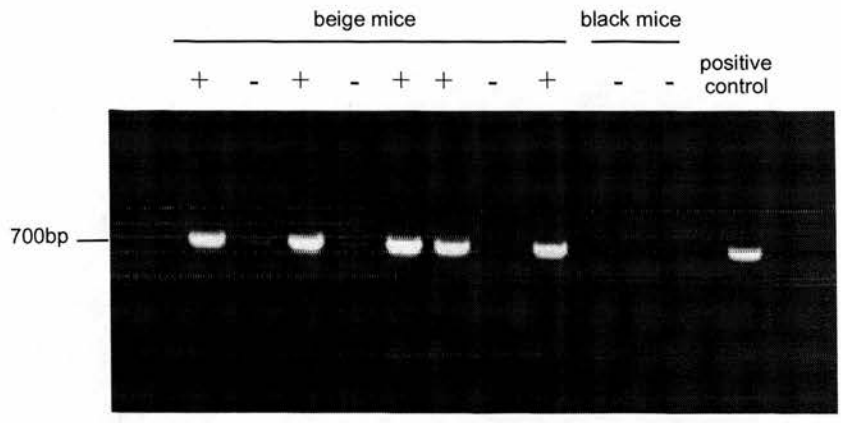

p1049NLS-PCRF (2648-2671bp of pKL53)

5′ – CAA CAG TTG CGC AGC CTG AAT GGC – 3′

KLCla (3325-3349bp of pKL53)

5′ – ACG CTC ATC GAT AAT TTC ACC GCC – 3′

Figure 4-23. Germline transmission of LacZ gene to F1 progeny of chimera/BKW crosses. Tail tip DNA from the offspring of chimera/BKW crosses were analysed for germline transmission of the targeted *EDNRB* gene. 5 out of 8 beige mice produced a PCR product of 701bp using primers corresponding to the LacZ sequence (sequences are shown). The other 3 beige mice and black mice were negative for germline transmission.

4.2.5 A second strain of *EDNRB*-LacZ mice – *EDNRB*-LacZ(2)

At around the time of completing ES cell targeting, I became aware that Dr. Myung Shin in Philadelphia, USA had generated a very similar mouse strain to the one described here. His work is, as yet, unpublished. This strain also contained the LacZ reporter gene knocked-in to the *EDNRB* locus although his targeting construct was slightly different to mine. Instead of fusion to exon 3, LacZ had been used to replace exon 1 and part of intron 1 of *EDNRB* (see figure 4-24). This construct also lacked an IRES and an NLS. Due to the risks involved in the completion of generating my own transgenic mice (e.g. failure to breed chimeras or failure to achieve germline transmission), it was decided to request mice from Dr. Shin. This would still allow me to address the aim of this project even if my own mice were not generated. He very generously agreed and two male mice were transported to our animal house. These mice were heterozygous for the targeted gene and were immediately bred to wild type female mice in order to generate our own colony. Genotyping of the progeny was performed by PCR analysis of tail tip DNA as described in section 2.5.14. An example of the PCR genotyping and the primer sequences which were used is shown in figure 4-24. The targeted gene was identified by the presence of a 270bp band with primers Ednrb5/Lac4. Heterozygotes were then intercrossed to produce offspring homozygous for the targeted gene. In the remainder of this thesis, these mice are known as *EDNRB*-LacZ(2).

Since my own *EDNRB*-LacZ mice were only born one month before the submission of this thesis, much of the data described in the remainder of the thesis have been the result of analysing *EDNRB*-LacZ(2) mice.

(a)

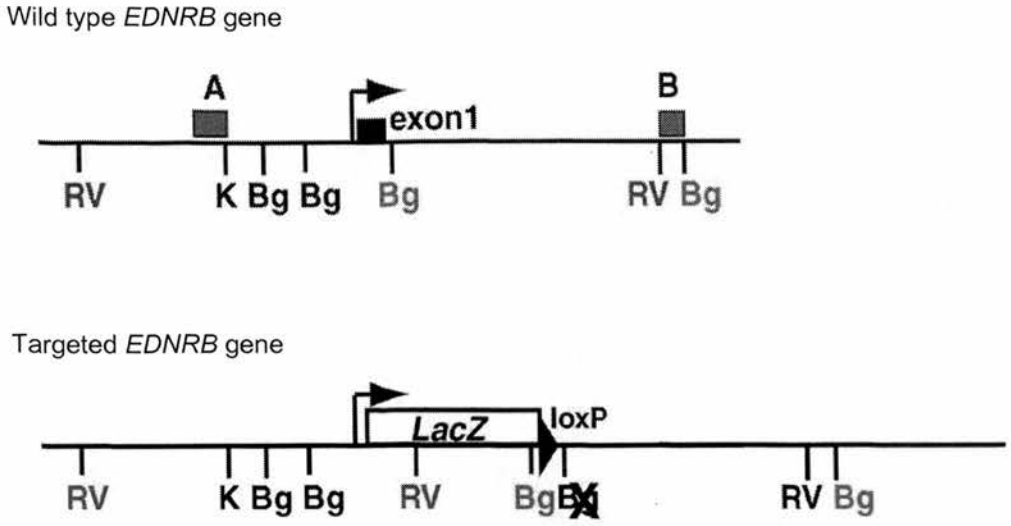

(b)

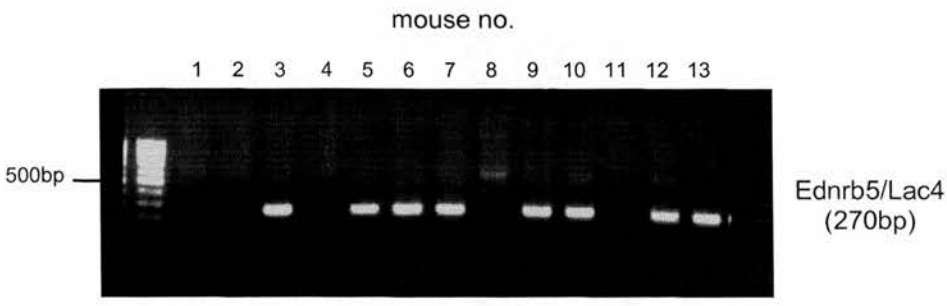

Ednrb5 5′- AGA CTG AAA ACA GCA GAG CGG CTA -3′

Lac4 5′- CTG TTG GGA AGG GCG ATC GGT GC -3′

Figure 4-24. *EDNRB*-LacZ(2) knock-in mice. (a) Targeting construct used by Dr. M. Shin to generate *EDNRB*-LacZ(2) knock-in mice, (b) *EDNRB*-LacZ(2) mice were genotyped using the primers Ednrb5/Lac4 which resulted in amplification of the targeted *EDNRB* locus only in *EDNRB*-LacZ(2) heterozygotes to produce a 270bp PCR product. Primers sequences are shown. Ednrb5 were designed from the mouse *EDNRB* cDNA sequence, 151-176bp and Lac4 was designed from 2631-2654bp of pKL53.

4.3 DISCUSSION

This chapter documents the generation of the *EDNRB*-LacZ knock-in mice. The primary reason for making these mice was to achieve precise localisation of ET_B expression within the kidney. Although analysis of renal ET_B expression has been attempted by other groups using more conventional methods, the results have not yielded conclusive data (discussed in section 5.3). Therefore, it was decided to use the reporter gene, LacZ, to create a knock-in transgenic animal in which β-gal is expressed wherever ET_B is expressed thus providing a precise picture of *in vivo* ET_B expression.

Reporter genes such as LacZ and green fluorescent protein (GFP) are now widely used in molecular biology (reviewed in (Alam & Cook, 1990; Spergel *et al.*, 2001)). By linking reporter genes to endogenous genes of interest, gene expression can be visualised as a result of enzymatic activity or fluorescence. They therefore provide powerful tools for visualisation of *in vivo* gene expression in the embryo through to the adult. β-gal catalyses the conversion of the chromogenic substrate, X-gal, to the visible blue product 5,5'-dibromo-4,4'-dichloroindigo (Pearson *et al.*, 1961; Horwitz *et al.*, 1964). Each molecule of enzymatic reporter protein catalyses the reaction of many molecules of substrate to product and therefore makes this a more sensitive detector of gene expression than non-enzymatic reporter genes. In addition, β-gal activity can be quantified using fluorescent and chemiluminescent assays. There are also commercial antibodies available for the detection of β-gal in fixed tissues. Therefore, the use of the LacZ reporter gene offers many possibilities.

LacZ was introduced into the coding region (exon 3) of *EDNRB* locus by homologous recombination in ES cells using homology arms of 6.7 and 2.2kb corresponding to the *EDNRB* sequence. Also included in the targeting construct was an IRES which allows translation of the reporter gene by binding the ribosome directly and eliminates the need to introduce the reporter gene "in-frame" with the ET_B coding region (Mountford *et al.*, 1994). Another important feature of the

construct was the inclusion of an NLS sequence (Kalderon *et al.*, 1984). Many reporter genes are now used in conjunction with subcellular localisation signals. In this case, the use of an NLS sequence will allow precise differentiation between expressing and non-expressing cells by confining expression of LacZ to the nucleus. Finally, expression of the neomycin phosphotransferase gene within ES cells was enhanced by the presence of the MC1 promoter (pMC1 Neo) (Thomas & Capecchi, 1987). Although not directly compared to a promoterless construct, pMC1 Neo ensured high expression of neomycin phosphotransferase within ES cells regardless of the expression of ET_B and therefore improved survival of targeted ES cells when exposed to G418. The final construct (see figure 4-1) was generated by a complex, multi-step cloning strategy involving a combination of PCR manipulation and subcloning. Before introduction into ES cells the construct was extensively sequenced and checked by analytical restriction enzyme digests.

Following introduction of the transgene into ES cells by electroporation, a 96-well targeting strategy was adopted (Ramirez-Solis *et al.*, 1992; Udy & Evans, 1994). This involved culturing G418-resistant colonies in 96-well tissue culture plates until confluent. These plates were then split and replica plates produced. For one set of plates the cells were lysed and DNA prepared for screening for homologous recombination. The other plates were frozen until screening was complete. If any positively targeted clones were identified during screening, the "frozen" plate was defrosted and the corresponding positive clone revived. Screening was also performed using a 96-well format. Restriction digests were set up in 96-well plates and DNA was carefully loaded onto 96-well gels using multi-channel pipettes followed by Southern blotting. This method of targeting has several advantages over the more conventional 24-well procedures. The major advantage is the simultaneous analysis of multiple samples thereby reducing the time taken to screen large numbers of colonies. In many cases involving gene targeting, including this one, recombination frequency can be very low. Therefore, a large number of colonies have to be screened in order to identify homologously targeted clones. By screening 96 samples at once, this maximises efficiency and allows several hundreds of

colonies to be screened in a matter of weeks. However, there are also disadvantages to this approach. In some cases, DNA yields from cells grown in 96-well plates are limited. Therefore, if several Southern blots need to be performed on the same sample or if a Southern blot fails and has to be repeated, there may not be enough DNA. In addition, there may be an increased chance of cells grown in 96-well plates to die after defrosting. Indeed, one of the positive clones described here was not viable following freeze-thawing. In cases where recombination frequency is low, this can be a major disadvantage.

As well as screening by the conventional method of Southern blotting, a PCR-based screening strategy was also attempted. The PCR system that was used is specifically designed to amplify long templates (Cheng *et al.*, 1994). PCR was also performed in a 96-well format using a 96-well PCR block. Although initial results using this system looked promising and two colonies were identified as being correctly targeted at the 3′ end, it was later found to be highly variable between runs. After several attempts at optimisation, this method was deemed unreliable and the remainder of the screening was achieved by Southern blotting.

In total, 3 clones were found to be targeted to the *EDNRB* locus (see table 4-3). 2G11 and 10D8 were targeted at the 3′ end as shown by Southern blotting. 10D8 was also positive by 3′ PCR screening. However, only 2G11 was targeted correctly at the 5′ end. In addition a further clone, 1H3, was identified by PCR to be targeted correctly at the 3′ end. Unfortunately this clone did not survive defrosting. Given that the 5′ end of integration is responsible for driving *EDNRB* and subsequently LacZ expression, it was decided that 2G11, which had a correctly targeted 5′ end, was the best candidate to proceed with blastocyst microinjection. Usually more than one clone would be injected to increase the chance of generating chimeras. However, given the low frequency of recombination (0.1%) this was not possible. Due to time constraints it was not possible to repeat the targeting experiment. Therefore, it was decided to proceed with clone 2G11.

Other researchers have also found the *EDNRB* locus difficult to target (M. Yanagisawa, University of Texas Southwestern Medical Center at Dallas, Texas, personal communication). The reasons for why certain loci are more problematic to manipulate by gene targeting are unknown. It may be due to the secondary structure of the chromosome or inaccessibility of the *EDNRB* gene during recombination. The extent of homology between donor and target DNA should also be taken into account. Many reports provide evidence that increased donor-target homology increases the targeting frequency (Deng & Capecchi, 1992). Indeed, Dr. A. Bagnall achieved a 6% targeting efficiency for the *EDNRB* locus using 5′ and 3′ homology arms of 12.1 and 2.2 kb respectively (A. Bagnall, University of Edinburgh, personal communication). This is compared to the 0.1% targeting efficiency observed here using a shorter 5′ homology arm of 6.7kb.

In vitro differentiation of clone 2G11 by culturing ES cells as hanging drops confirmed that this clone contained a functional LacZ gene. Growth of ES cells as hanging drops gives rise to a variety of different cell types and so it was impossible to determine what specific cell types were expressing LacZ without further analysis. Instead a different method of differentiation was used to investigate if the gene was expressed in endothelial cells derived from ES cells cultured on collagen IV. This extracellular matrix provides the correct environment to promote differentiation of endothelial cells from ES cells (Nishikawa *et al.*, 1998). The rationale behind this experiment was that since endothelial cells express ET_B, these cells should also express LacZ. Furthermore, since cells cultured by this method grow as a single cell layer rather than in tight groups of cells as in embryoid bodies, it was expected to be able to visualise LacZ expression intracellularly (i.e. within the nucleus). Flow cytometry revealed that some of these cells were positive for the endothelial cell marker, Flk-1. However, when assessed for β-gal activity, no blue staining was observed. While disappointing, it is possible to speculate as to why no staining was seen. Although a Flk-1 positive population was present, it was not known what type of endothelial cells were represented here. It is possible that different populations of endothelial cells express genes differentially depending on their location. For

example, endothelial cells from the kidney may not necessarily be phenotypically identical to endothelial cells from the heart. Therefore, it could be that the endothelial cells studied here simply did not express LacZ. It is also possible that ET_B is expressed at a later stage of endothelial differentiation. Flk-1 is an early marker of endothelial cell progenitors (Yamaguchi *et al.*, 1993) and therefore these immature endothelial cells might not have expressed ET_B. It may have been interesting to look for LacZ expression at later stages of differentiation. Finally, it may be that expression levels were simply too low to be detected by this assay. This could have been easily investigated by RT-PCR analysis. However, since expression of LacZ in clone 2G11 had already been documented by the previous method, it was felt that this was not within the aims of this project and was therefore not pursued.

Nevertheless, this set of experiments did raise concerns over the sensitivity of the β-gal assay. If ET_B was indeed expressed by these cells but at a level undetectable by the assay, would the same situation arise *in vivo*. It is possible that the reason that LacZ expression was observed in embryoid bodies was that these cells were found in large clusters, possibly consisting of hundreds of cells. Therefore, the LacZ signal would be greatly intensified compared to what it might be at a single cell level. Since the aim of this project is to localise ET_B to specific cells within the kidney, the potential lack of sensitivity is an important point to bear in mind. However, there are now scientific tools which could help in these situations (e.g. anti-β-gal antibodies combined with highly sensitive chemiluminescent detection systems).

Clone 2G11 was used to generate two chimeric mice, one of which produced progeny in which the transgene had been transmitted to the germline. These mice are now being bred to generate a colony of *EDNRB*-LacZ knock-in mice which will be used to analyse ET_B expression patterns. As described in section 4.2.5, a second strain of *EDNRB*-LacZ mice, *EDNRB*-LacZ(2), was obtained from Dr. M. Shin. These are essentially the same as my mice in that the LacZ gene has been inserted into the *EDNRB* locus. It will therefore be extremely interesting to compare the ET_B expression patterns obtained from both strains of mice. However, it should not be

overlooked that the targeting constructs used to make both strains of mice were very different and may therefore lead to different outcomes. In particular, it is worth noting that in Dr. Shin's construct a large region of intron one was replaced with the LacZ cassette. However, Shin *et al* have also reported previously that intron one may have a regulatory role in *EDNRB* transcription (Shin *et al.*, 1997). Removal of this sequence may have a detrimental effect on *EDNRB* and LacZ expression. It is also anticipated that the inclusion of an NLS signal in my construct will help in identifying individual cells and therefore improve specific cellular localisation within the kidney. These issues will be discussed further in chapter 5.

4.4 SUMMARY

In summary, this chapter has described the generation of *EDNRB*-LacZ knock-in mice which will be used to investigate expression of ET_B within the kidney.

- Homologous recombination in ES cells enabled the reporter gene, LacZ, to be introduced into the *EDNRB* locus.
- One ES cell clone, 2G11, was identified as being correctly targeted to the *EDNRB* gene.
- Functional expression of LacZ within this clone was confirmed *in vitro*.
- Clone 2G11 was used to generate chimeras and produce *EDNRB*-LacZ knock-in mice.
- Together with strain *EDNRB*-LacZ(2), these mice will be used to analyse ET_B expression as described in the following chapter.

CHAPTER 5

LOCALISATION OF ET_B USING *EDNRB*-LACZ KNOCK-IN MICE

5.1 INTRODUCTION

As described in section 4.1, the main purpose for developing knock-in mice harbouring an *EDNRB*-LacZ transgene was to determine the expression profile of ET_B within the kidney. Establishing precisely which cells within the inner medulla express ET_B will help to elucidate the cellular mechanisms involved in ET_B-mediated natriuresis as described in section 1.2.2.8. In this thesis it is hypothesised that the major site of medullary ET_B expression is the endothelium of the vasa recta. This is in line with the paracrine mechanism of action of ET-1 as described in section 1.2.2.8 and figure 1-5. In contrast, the alternative autocrine pathway implies that ET_B is predominantly expressed by IMCD cells. Therefore, the main aim of this chapter was to determine whether ET_B is predominantly localised to the vasa recta or to IMCD cells.

It is also anticipated that the information obtained from *EDNRB*-LacZ mice will provide a more accurate picture of renal ET_B expression compared to conventional methods, which have not led to conclusive data mainly due to technical limitations (refer to section 4.1). Although most of the literature is in agreement that the highest expression of ET_B is found in the renal medulla and papilla, clearly shown by macroautoradiography (Davenport *et al.*, 1989; Yukimura *et al.*, 1996; Zhuo *et al.*, 1998), precise cellular ET_B localisation has generated conflicting results. However, of the many localisation reports those using *in vitro* and *in vivo* radioligand ($[^{125}I]$-ET-1) electron microscopy appear to present the most convincing findings (Dean *et al.*, 1994; Yukimura *et al.*, 1996). These studies showed the majority of $[^{125}I]$-ET-1 binding was localised to glomeruli, peritubular capillaries and vasa recta. In contrast there was very low binding in medullary collecting duct cells and tubules. However, this technique is also limited by technical difficulties since binding sites may be inaccessible to intravascularly administered $[^{125}I]$-ET-1. Furthermore Kohan *et al* reported high ET_B expression in cultured IMCD cells (Kohan *et al.*, 1992). Therefore, even the most credible results are contradicted by others. It is clear that further localisation studies are required.

Therefore, *EDNRB*-LacZ mice were used to determine ET_B localisation within the kidney. Due to the lack of availability of my own animals at this time, *EDNRB*-LacZ(2) were used (see section 4.2.5). This chapter describes the histological analysis of transgene expression in kidney sections obtained from *EDNRB*-LacZ(2) knock-in animals. The results are discussed in the context of existing studies and data examined in terms of the proposed ET-1 paracrine hypothesis.

5.2 RESULTS

5.2.1 Histological staining of the *EDNRB*-LacZ(2) transgene

LacZ expression can be visualised by the formation of a blue precipitate resulting from hydrolysis of substrate 5-bromo-4-chloro-indolyl-β-D-galactoside (X-gal). Therefore, organs from *EDNRB*-LacZ(2) mice were cryosectioned to obtain sections 10-15μm in thickness, stained with X-gal and counterstained with eosin as described in section 2.6.2. Both male and female mice were used and no obvious differences were observed between sexes. Furthermore, LacZ expression was absent in all corresponding organs of transgene negative littermates. Staining was performed on several mice (n>5) and consistent staining was observed between animals.

Heterozygous adult *EDNRB*-LacZ(2) mice (8-10 weeks old) were initially used for staining. As expected all mice appeared phenotypically normal since only one allele of the *EDNRB* locus had been disrupted. The other allele remained intact and previous studies from ET_B heterozygous knockout mice have shown that these animals do not experience haploinsufficiency (Hosoda *et al.*, 1994). As well as studying heterozygotes, homozygous *EDNRB*-LacZ(2) mice were also analysed. These mice were recognisable by their piebald appearance resulting from a lack of epidermal melanocytes. In addition, homozygous ET_B knockout mice have an abnormal enteric nervous system. Although viable at birth, they die from aganglionic megacolon at around 3 weeks of age (Hosoda *et al.*, 1994), Therefore, *EDNRB*-LacZ(2) homozygotes were studied at 2.5 weeks of age.

5.2.2 *EDNRB*-LacZ(2) expression in lung tissue

Due to the high expression of ET_B in lung, this tissue was used as a positive control to determine if LacZ expression could be detected by this method. Representative frozen lung sections from heterozygous *EDNRB*-LacZ(2) transgenic mice are shown in figure 5-1. As can be clearly seen, blue staining was abundant in these sections. Staining was observed in pulmonary parenchyma and alveoli. High expression was also present within large airways such as bronchioles where staining was confined to the smooth muscle layer (figure 5-1c). Similar results were obtained with homozygous *EDNRB*-LacZ(2) mice although, as expected, staining was significantly brighter compared to heterozygotes (figure 5-2), the reason being that in these mice both *EDNRB* alleles contained LacZ.

These findings were consistent with previous localisation studies examining ET_B expression within the lung, albeit in different species (i.e. rat and pig) (Nakamichi *et al.*, 1992; Goldie *et al.*, 1996; Soma *et al.*, 1999), and therefore provided convincing evidence that the LacZ expression observed here was an accurate reflection of ET_B expression.

5.2.3 *EDNRB*-LacZ(2) expression in kidney

5.2.3.1 Analysis of heterozygotes

Renal cryosections were then examined for expression of the *EDNRB*-LacZ(2) transgene in heterozygotes. As expected, staining was localised to glomeruli (figure 5-3a), afferent and efferent arterioles (figure 5-3b) and large blood vessels within the cortex (figure 5-3c). As alluded to in section 5.1, previous localisation studies have reported extremely high radioligand binding of [^{125}I]-ET-1 within the medulla and papilla (Dean *et al.*, 1994; Yukimura *et al.*, 1996; Zhuo *et al.*, 1998). Therefore, it was surprising that staining for β-gal activity within the medulla was not in line with these reports. Instead, weak staining was observed in the inner medulla manifested as tiny spots running alongside collecting tubules (figure 5-4a & b). From these images it was impossible to determine the identity of these cells. In addition, faint staining was noticeable in the papilla (not shown).

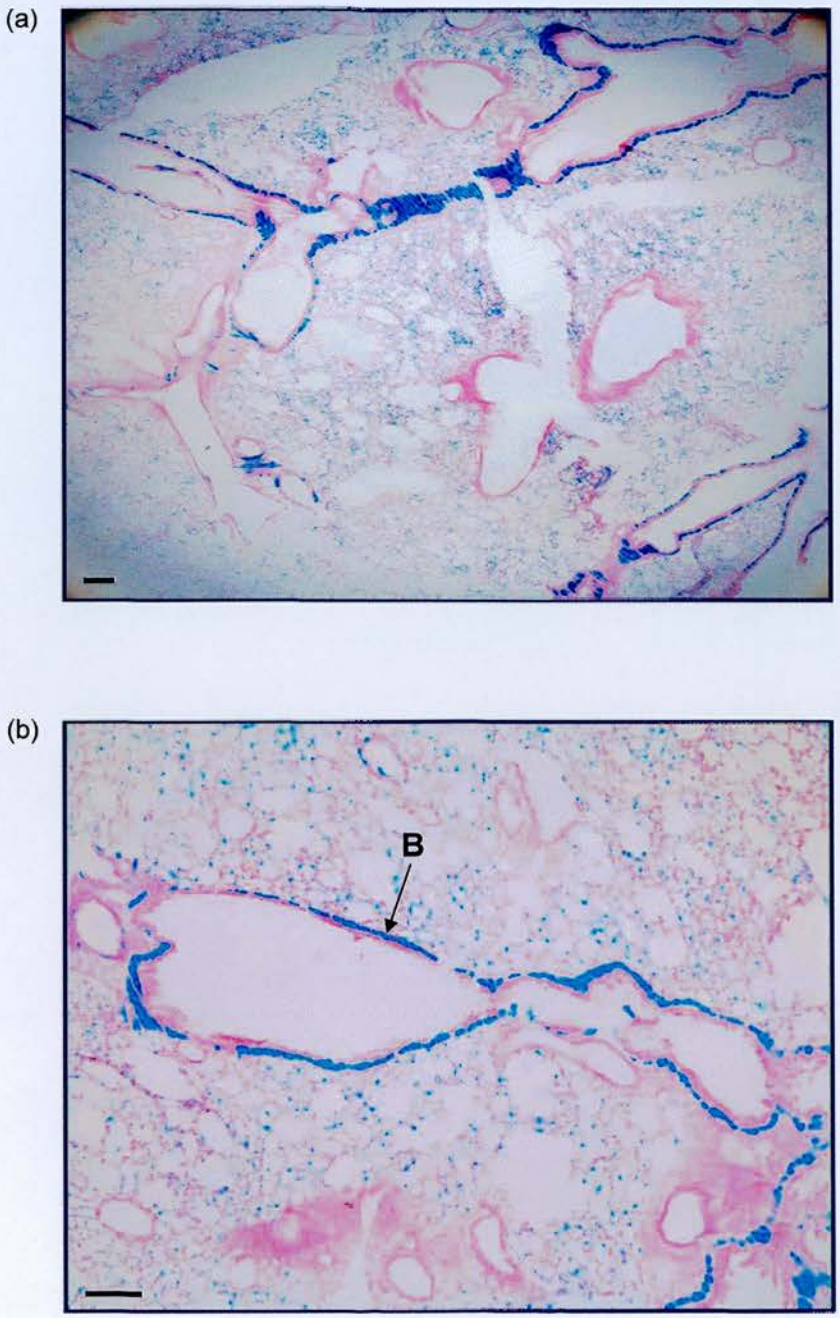

Figure 5-1. LacZ expression in lung tissue from *EDNRB*-LacZ(2) heterozygous mice (continued overleaf). Representative cryosections of lungs from *EDNRB*-LacZ(2) heterozygous mice stained for β-gal activity (blue) and counterstained with eosin (pink). See text for further details (section 5.2.2) (a) Low magnification of lung section (x40). Scale bar = 0.2mm. LacZ expression in bronchioles and pulmonary parenchyma. (b) Higher magnification of (a) (x100) Scale bar = 0.1mm. Abbreviations: B, bronchiole.

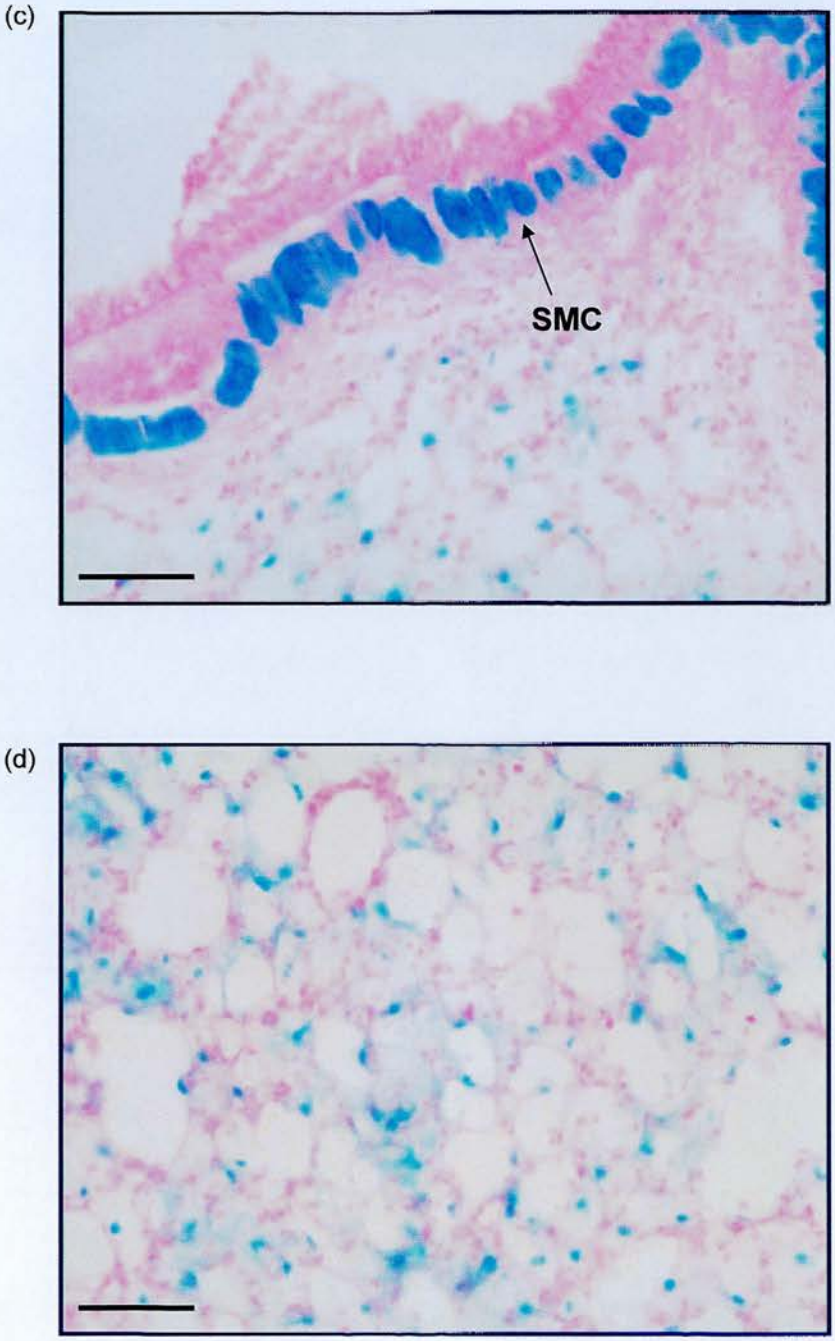

Figure 5-1. LacZ expression in lung tissue from *EDNRB*-LacZ(2) heterozygous mice (continued). (c) High magnification of bronchiole (x400). LacZ expression is confined to the smooth muscle layer. (d) High magnification of lung tissue (parenchyma and alveolar network) (x400). Scale bar = 0.05mm. Abbreviations: SMC, smooth muscle cells.

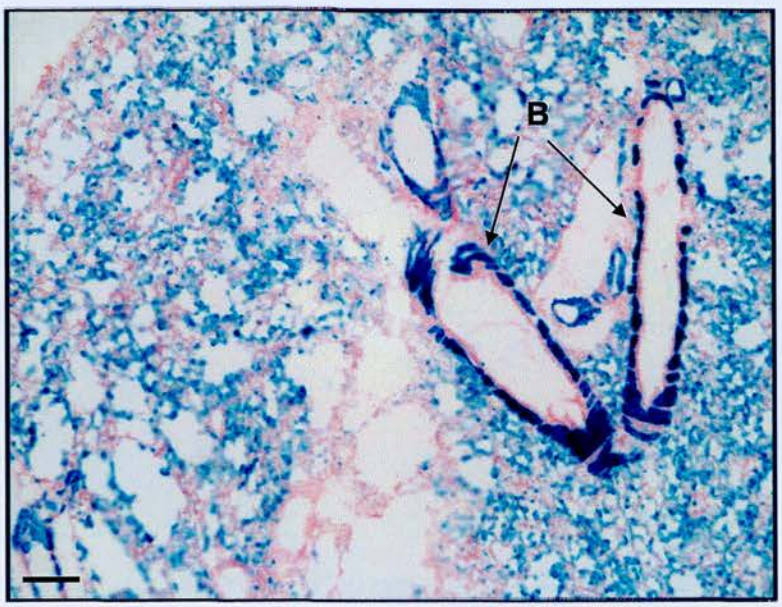

Figure 5-2. LacZ expression in lung tissue from *EDNRB*-LacZ(2) homozygous mice. Representative cryosection of lung from *EDNRB*-LacZ(2) homozygous mice stained for β-gal activity (blue) and counterstained with eosin (pink). See text for further details (section 5.2.2). LacZ expression is abundant in bronchioles and lung parenchyma (x100). Scale bar = 0.1mm. Abbreviations: B, bronchiole.

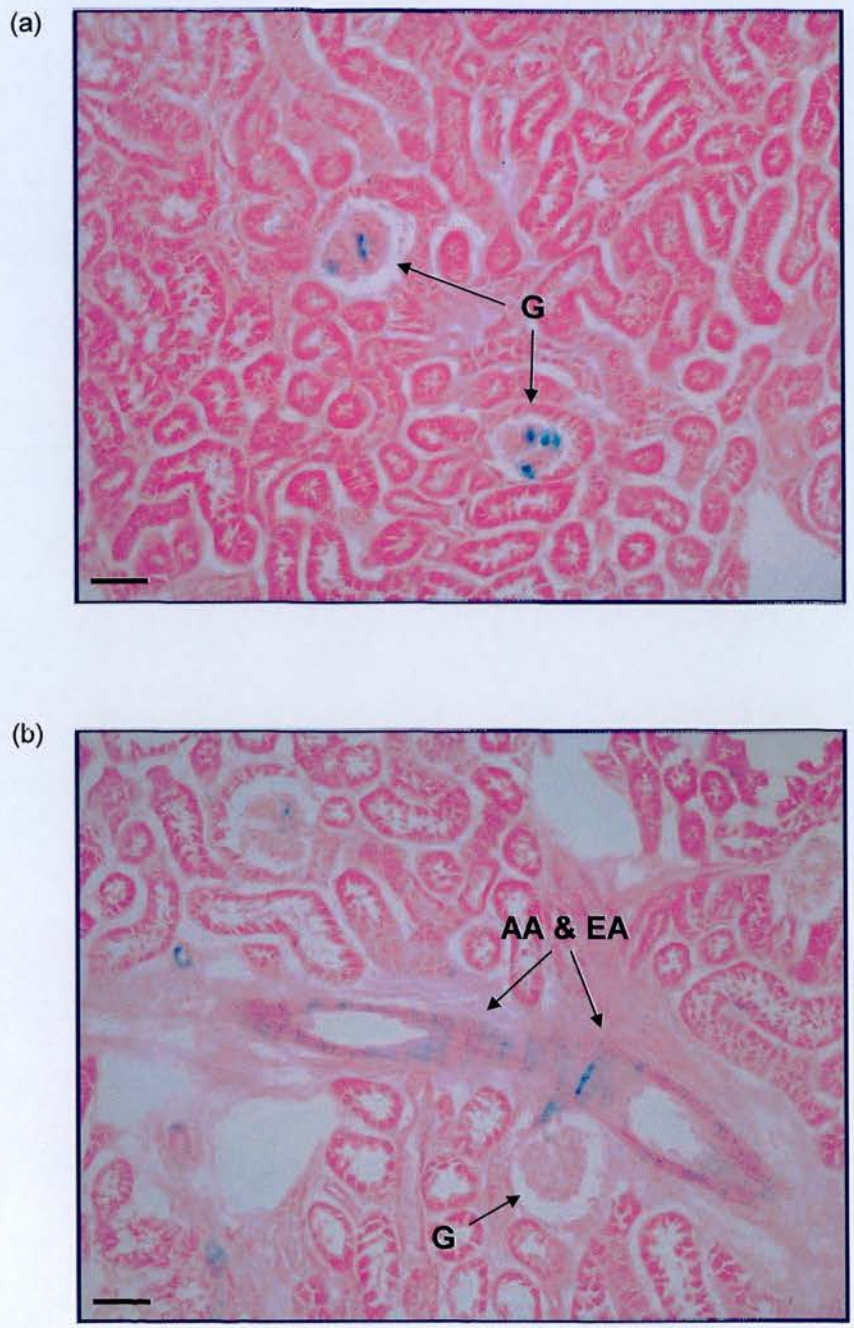

Figure 5-3. LacZ expression in renal cortex of *EDNRB*-LacZ(2) heterozygous mice (continued overleaf). Representative cryosections of kidneys from *EDNRB*-LacZ(2) heterozygous mice stained for β-gal activity (blue) and counterstained with eosin (pink). See text for further details (section 5.2.3.1). (a) LacZ expression confined to glomeruli (x200). (b) LacZ expression in afferent and efferent arterioles (x200). Scale bar = 0.05mm. Abbreviations: G, glomerulus; AA, afferent arteriole; EA, efferent arteriole.

(c)

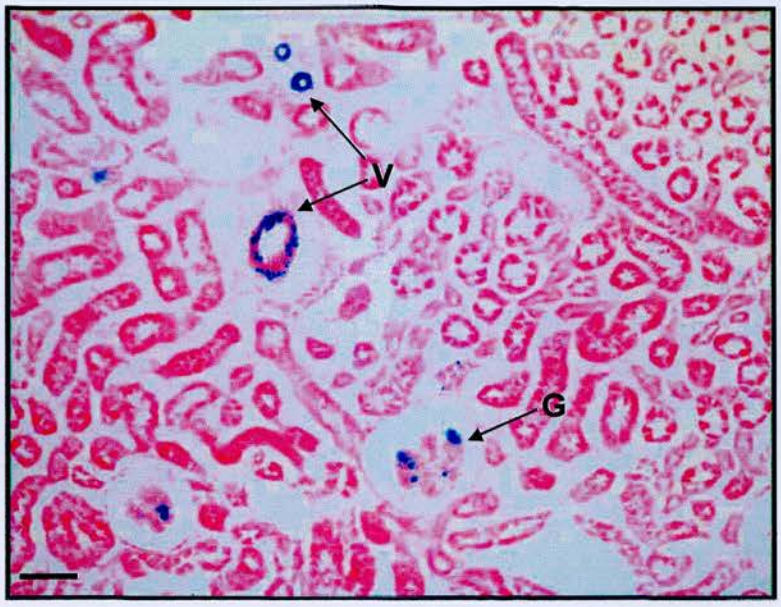

Figure 5-3. LacZ expression in renal cortex of *EDNRB*-LacZ(2) heterozygous mice (continued). (c) LacZ expression in large blood vessels and glomeruli (x200). Scale bar = 0.05mm. Abbreviations: G, glomerulus; V, vessel.

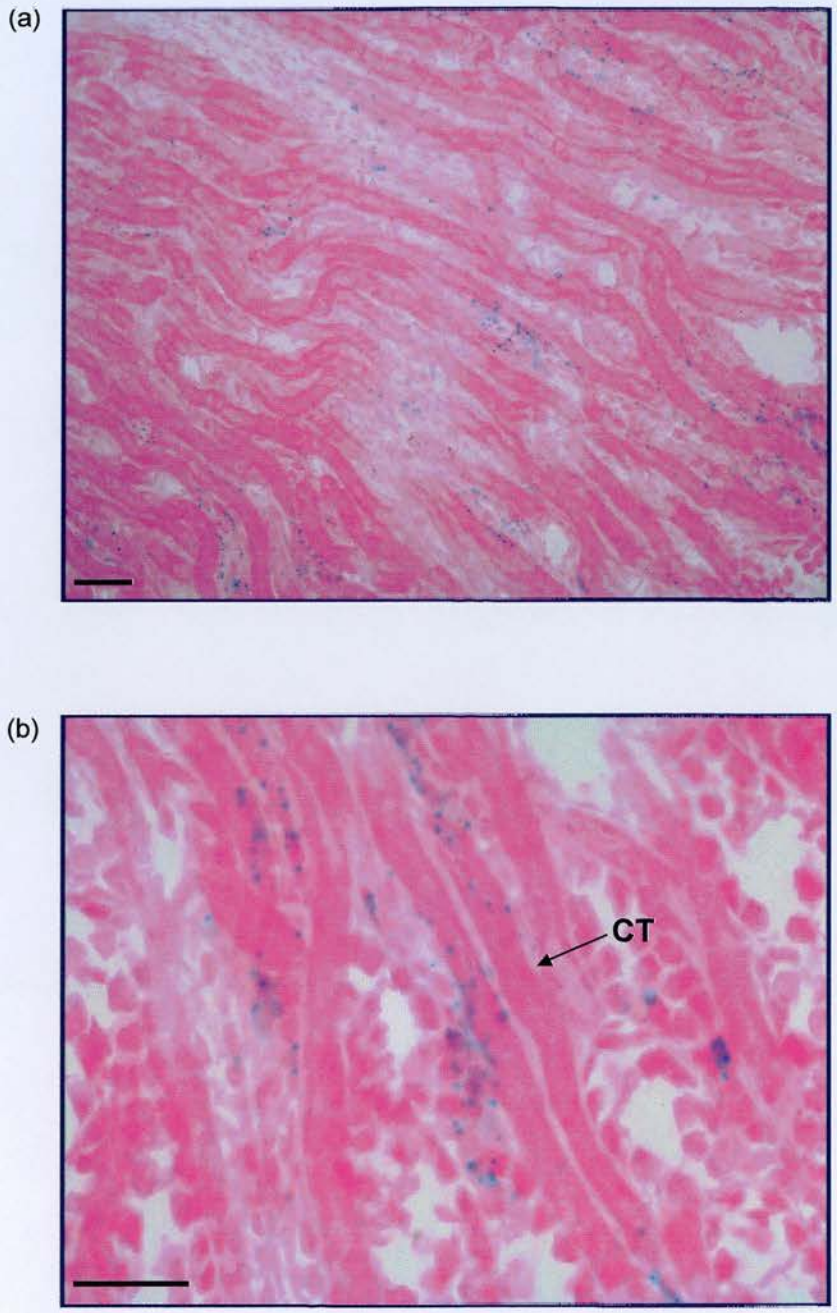

Figure 5-4. LacZ expression in renal medulla of *EDNRB*-LacZ(2) heterozygous mice (continued overleaf). Representative longitudinally cut cryosections of kidneys from *EDNRB*-LacZ(2) heterozygous mice stained for β-gal activity (blue) and counterstained with eosin (pink). See text for further details (section 5.2.3.1). (a) LacZ expression in medulla (x200). Scale bar = 0.05mm. (b) Higher magnification of (a) (x400). Scale bar = 0.05mm. Abbreviations: CT, collecting tubule.

5.2.3.2 Analysis of homozygotes

Staining of β-gal activity in renal sections obtained from *EDNRB*-LacZ(2) homozygous mice produced a much more comprehensive picture of ET_B localisation. LacZ expression was considerably higher than in heterozygotes and staining appeared more consistent throughout each section. Figure 5-5 shows a representative image of a whole kidney longitudinal section from an *EDNRB*-LacZ(2) homozygous mouse. Intense staining was localised to glomeruli, the inner medulla and the papillae. Staining was also found in longitudinal bands in the inner stripe of the outer medulla. In contrast, the outer stripe of the outer medulla exhibited relatively low LacZ expression.

The increased intensity of staining and improved morphology made it easier to determine specific cellular sites of expression compared to heterozygotes. Figures 5-6 and 5-7 contain high resolution images of figure 5-5 in which specific cellular structures within the cortex and medulla are clearly visible. In the cortex the majority of staining was localised to glomeruli and large blood vessels (figure 5-6a & b). Higher magnification revealed LacZ expression confined to specific cells within glomeruli (figure 5-6c). Although it is difficult to be certain, these cells probably represent glomerular capillary endothelial cells or mesangial cells. Upon closer inspection of vessels, it was clear that staining was present in both the endothelial layer and smooth muscle layer (figure 5-6d). However, due to the intensity of staining, it is difficult to distinguish between the layers. Overall intensity of LacZ expression increased dramatically within the medulla (figure 5-7), although renal tubules appeared not to be stained. Instead, staining was mainly present in the spaces between tubules identified as large blood vessels and capillary endothelial cells. There was also strong LacZ expression within the papillae (figure 5-7e & f).

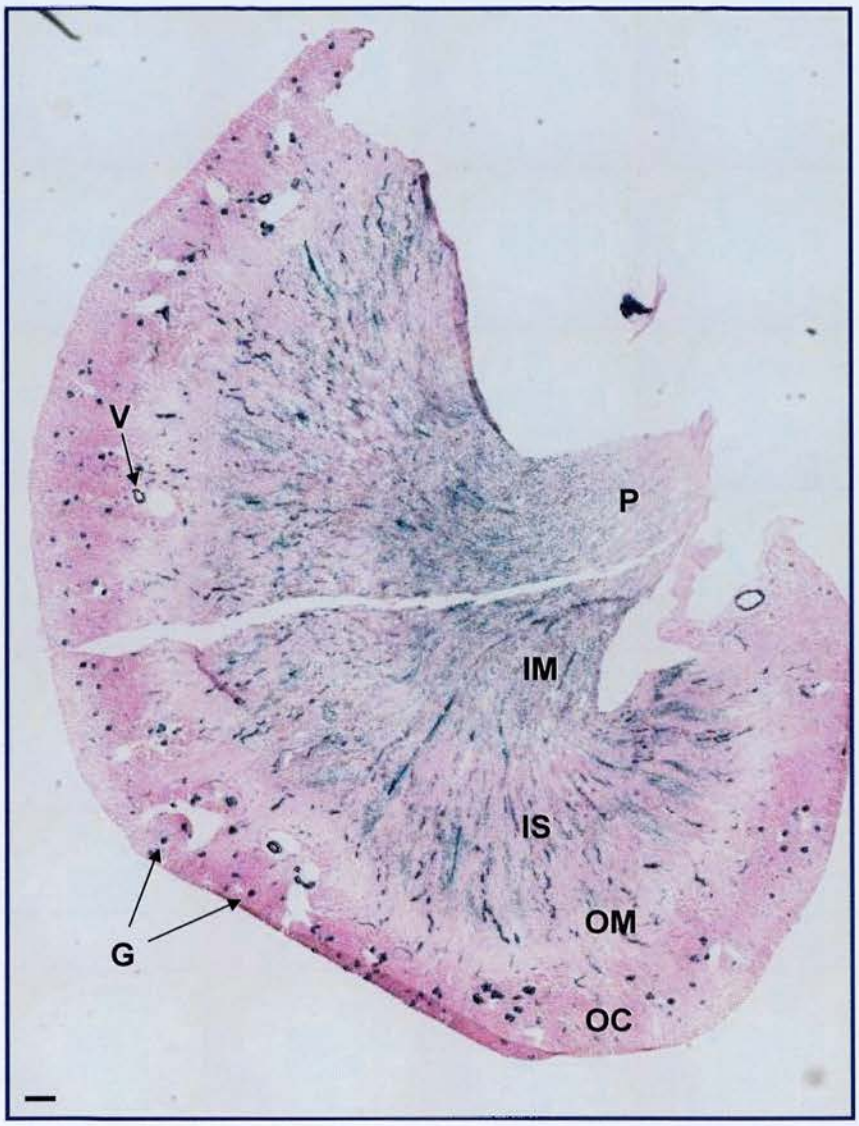

Figure 5-5. Renal LacZ expression in *EDNRB*-LacZ(2) homozygous mice. A representative longitudinally cut cryosection from an *EDNRB*-LacZ(2) homozygote mouse kidney stained for β-gal activity (blue) and counterstained with eosin (pink). See text for further details (section 5.2.3.2). Magnification is x40. Scale bar = 0.2mm. Abbreviations: G, glomerulus; V, vessel; OC, outer cortex; OM, outer medulla; IS, inner stripe of outer medulla; IM, inner medulla; P, papilla.

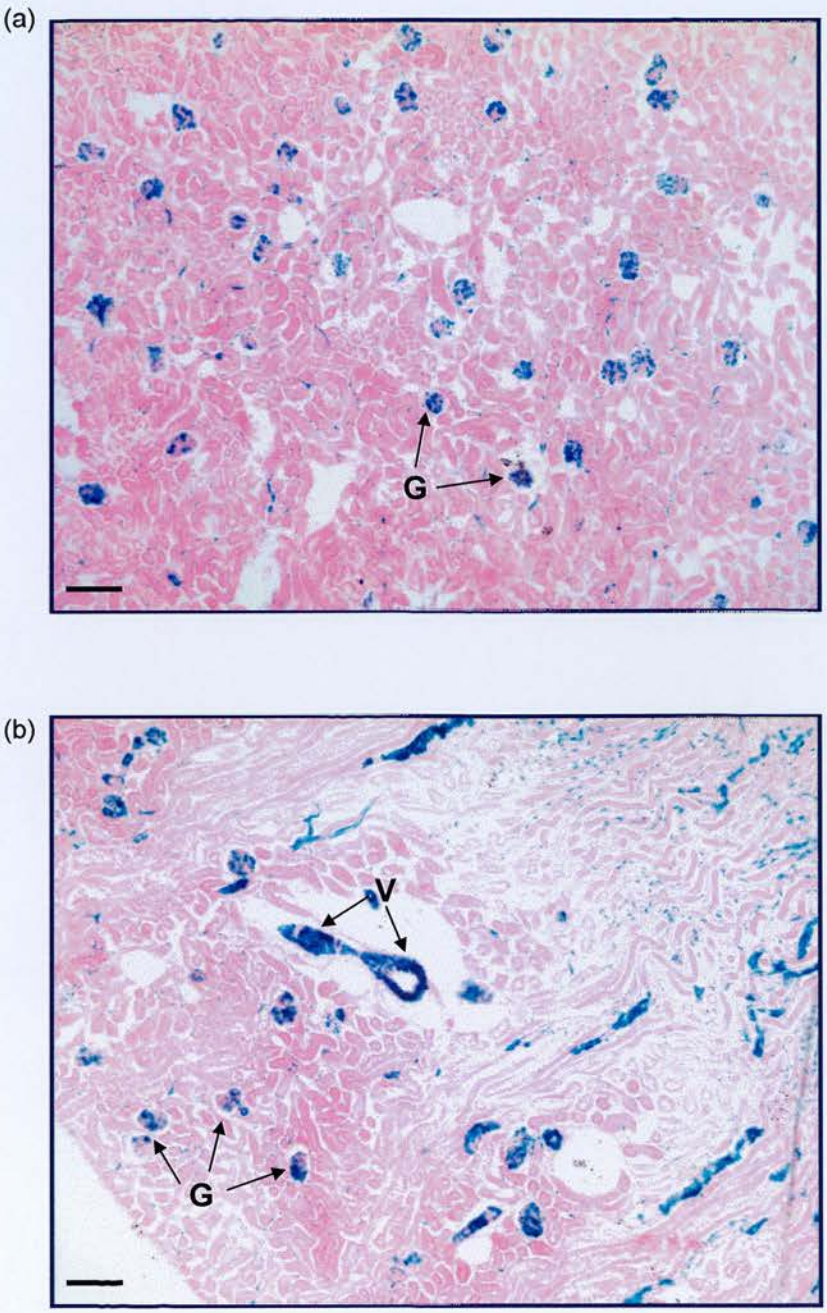

Figure 5-6. LacZ expression in renal cortex of *EDNRB*-LacZ(2) homozygous mice (continued overleaf). Representative longitudinally cut cryosections from an *EDNRB*-LacZ(2) homozygous mouse kidney stained for β-gal activity (blue) and counterstained with eosin (pink). See text for further details (section 5.2.3.2). (a) LacZ expression in the outer cortex (x100). (b) Low magnification of cortex (x100). Scale bar = 0.1mm. Abbreviations: G, glomerulus; V, vessel.

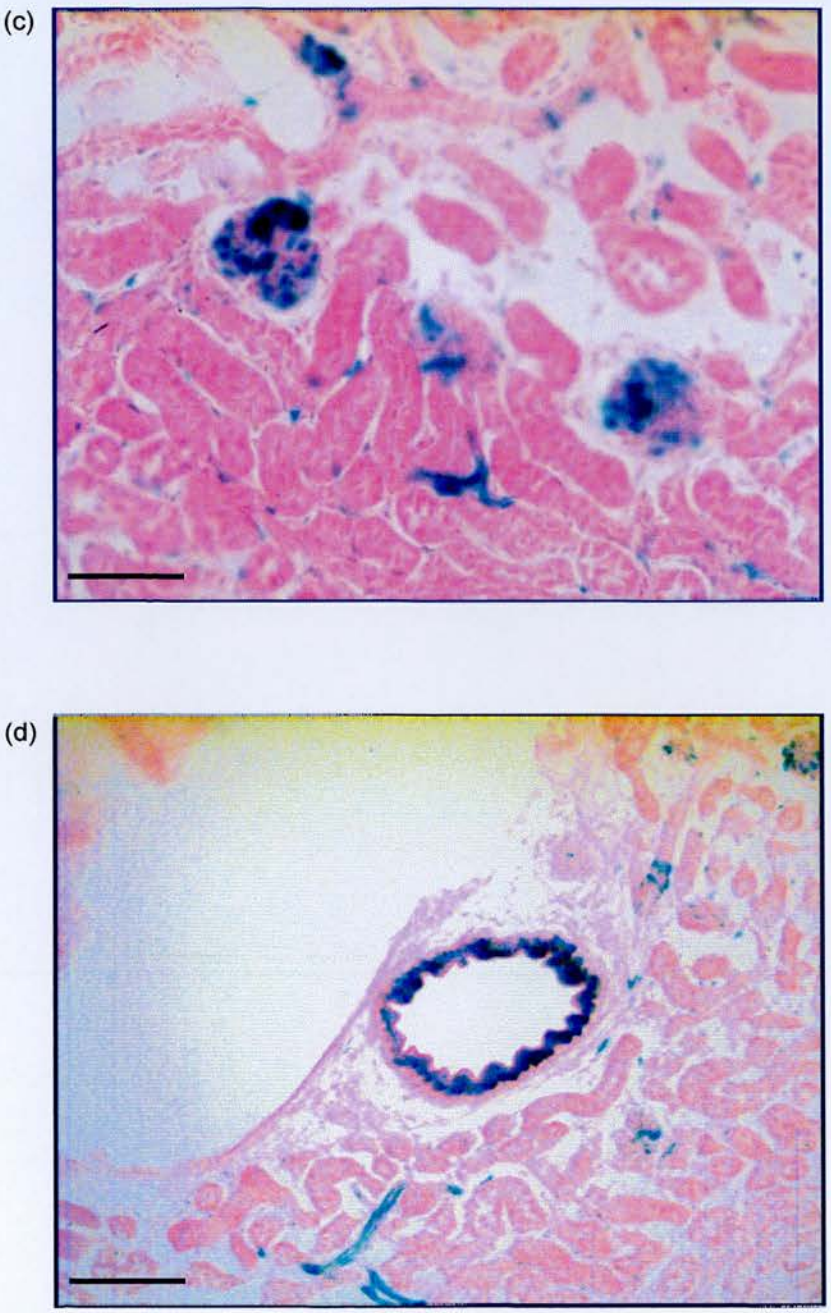

Figure 5-6. LacZ expression in renal cortex of *EDNRB*-LacZ(2) homozygous mice (continued). (c) LacZ expression in glomeruli (x400). (d) LacZ expression in endothelium and smooth muscle layer of blood vessel (x400). Scale bar = 0.05mm.

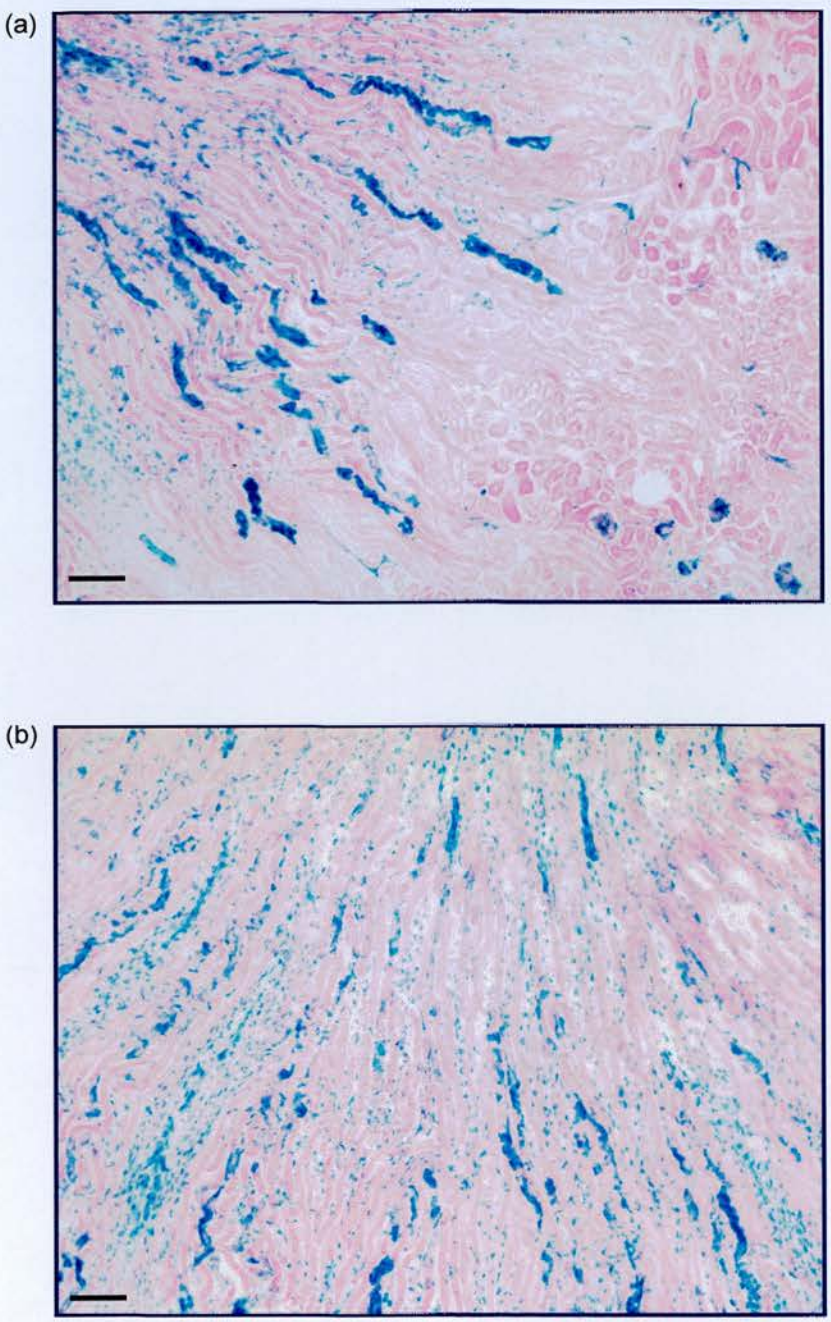

Figure 5-7. LacZ expression in renal medulla of *EDNRB*-LacZ(2) homozygous mice (continued overleaf). Representative longitudinally cut cryosections from an *EDNRB*-LacZ(2) homozygous mouse kidney stained for β-gal activity (blue) and counterstained with eosin (pink). See text for further details (section 5.2.3.2). (a) & (b) Low magnification of medulla (x100). LacZ expression is confined to the spaces between tubules. Tubules are negative for LacZ expression. Scale bar = 0.1mm.

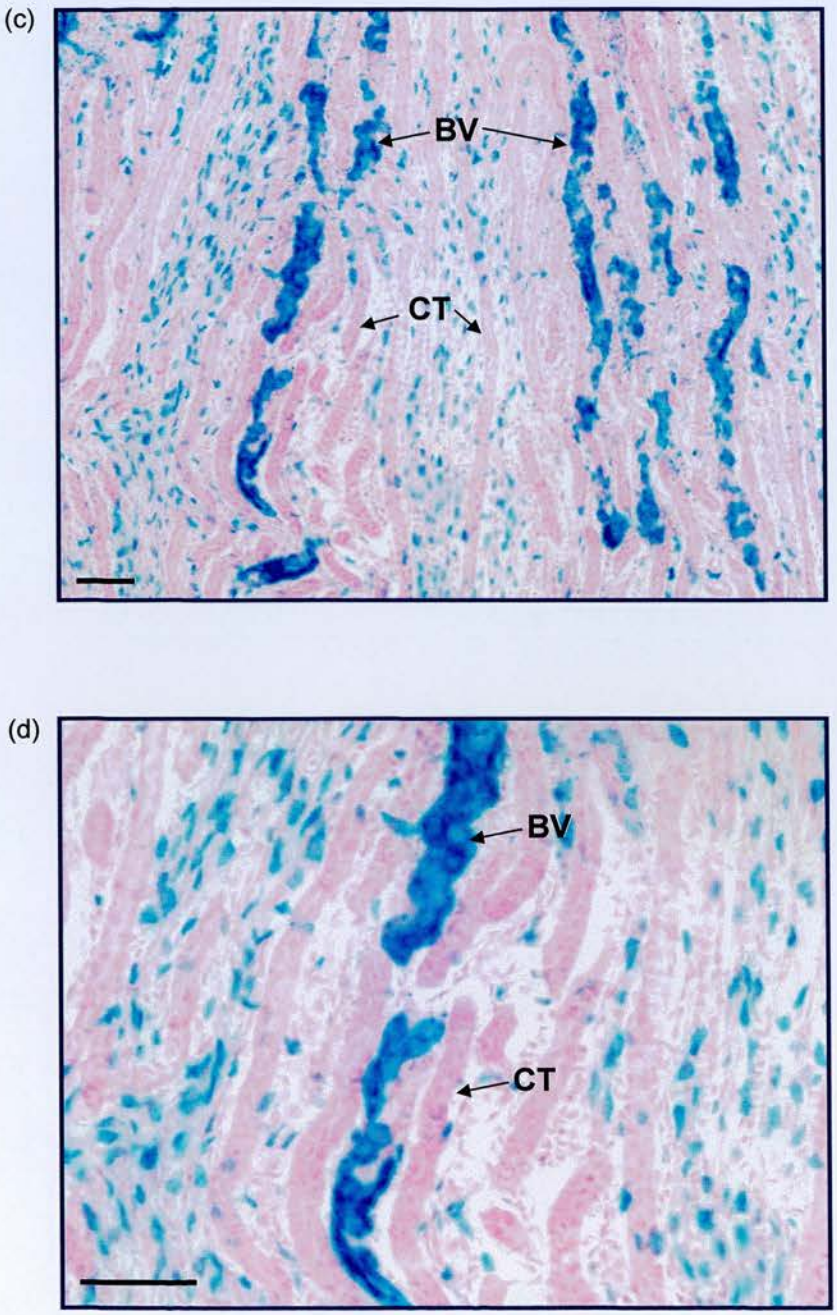

Figure 5-7. LacZ expression in renal medulla of *EDNRB*-LacZ(2) homozygous mice (continued). (c) & (d) Higher magnification of medulla, x200 and x400 respectively. Scale bar = 0.05mm. Abbreviations: CT, collecting tubules; BV, large blood vessels.

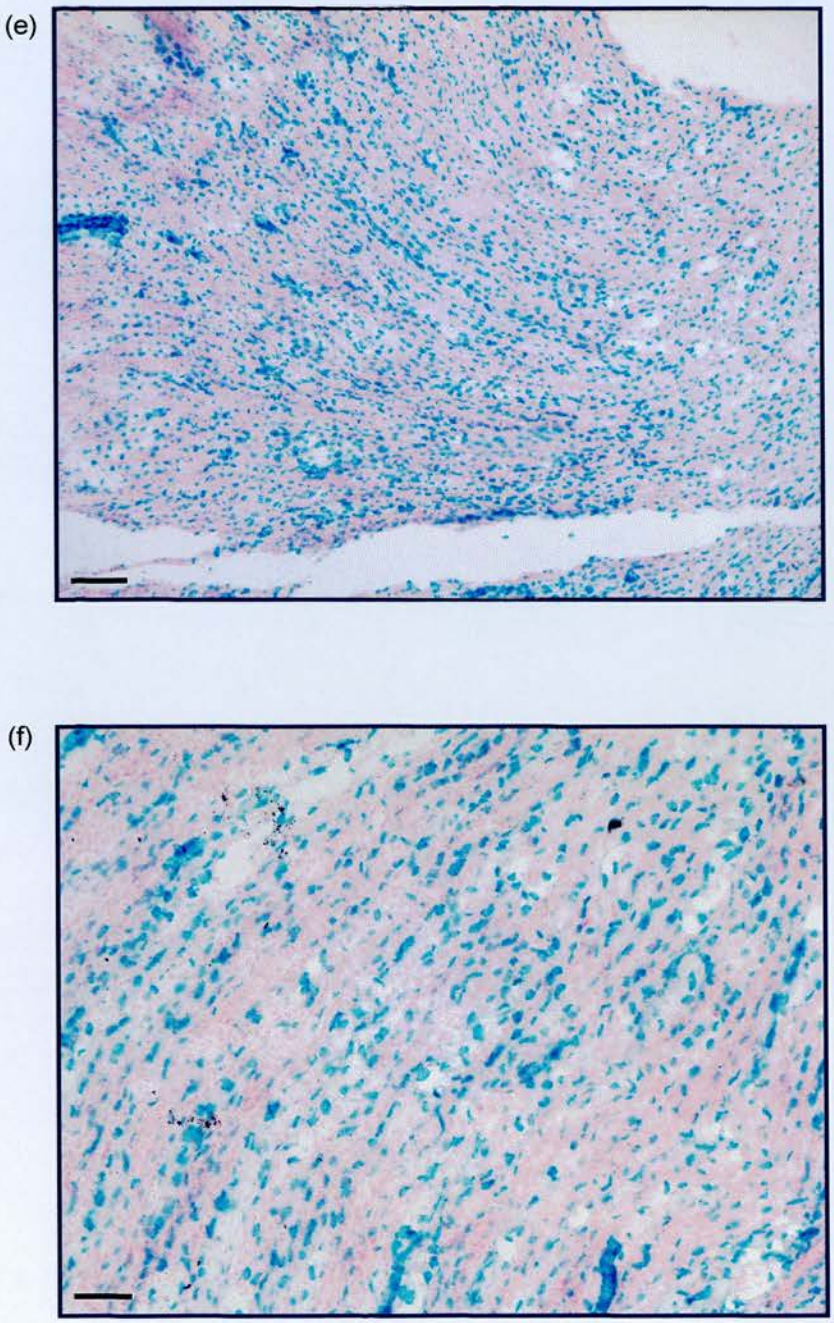

Figure 5-7. LacZ expression in renal medulla of *EDNRB*-LacZ(2) homozygous mice (continued). (e) LacZ expression in papilla (x100) Scale bar = 0.1mm. (f) Higher magnification of (e) (x200). Scale bar = 0.05mm.

To obtain a clearer picture, kidneys were also sectioned transversely as shown in figure 5-8. Here, collecting tubules were visualised more clearly and were devoid of LacZ expression. On the other hand, staining was observed in the spaces surrounding the tubules corresponding to capillaries (figure 5-8c & d). Larger vessels were also stained. Again, the papilla was strongly stained (figure 5-8e & f).

5.2.4 Preliminary analysis of *EDNRB*-LacZ mice

Until recently all localisation analysis was performed on *EDNRB*-LacZ(2) mice provided by Dr. Myung Shin. However, towards the end of the project my own mice became available and I was able to analyse LacZ expression in *EDNRB*-LacZ heterozygotes. However, it should be noted that analysis was in the early stages and required further optimisation. Analysis of these mice is ongoing. Figure 5-9 shows LacZ expression in lung sections taken from *EDNRB*-LacZ heterozygote mice. Staining was localised to the smooth muscle layer of large airways (e.g. bronchioles) and, as expected, appeared to be localised to the nucleus due to the presence of the NLS.

A summary of staining for β-gal activity is shown in table 5-1.

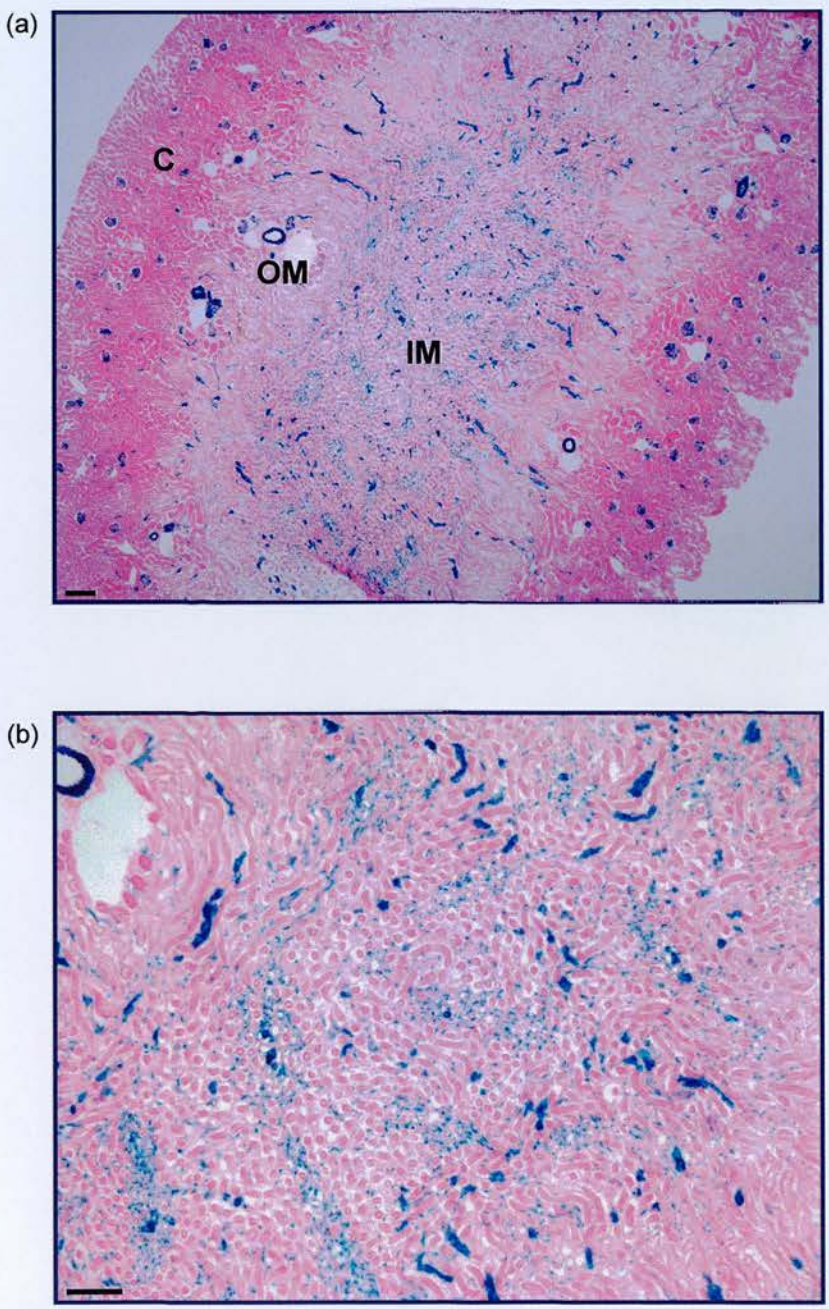

Figure 5-8. Renal LacZ expression in *EDNRB*-LacZ(2) homozygous mice (continued overleaf). Representative transversely cut cryosections from an *EDNRB*-LacZ(2) homozygous mouse kidney stained for β-gal activity (blue) and counterstained with eosin (pink). See text for further details (section 5.2.3.2). (a) Low magnification of kidney section (x40). Scale bar = 0.2mm. (b) Low magnification of renal medulla (x100). Scale bar = 0.1mm. Abbreviations: C, cortex; OM, outer medulla; IM, inner medulla.

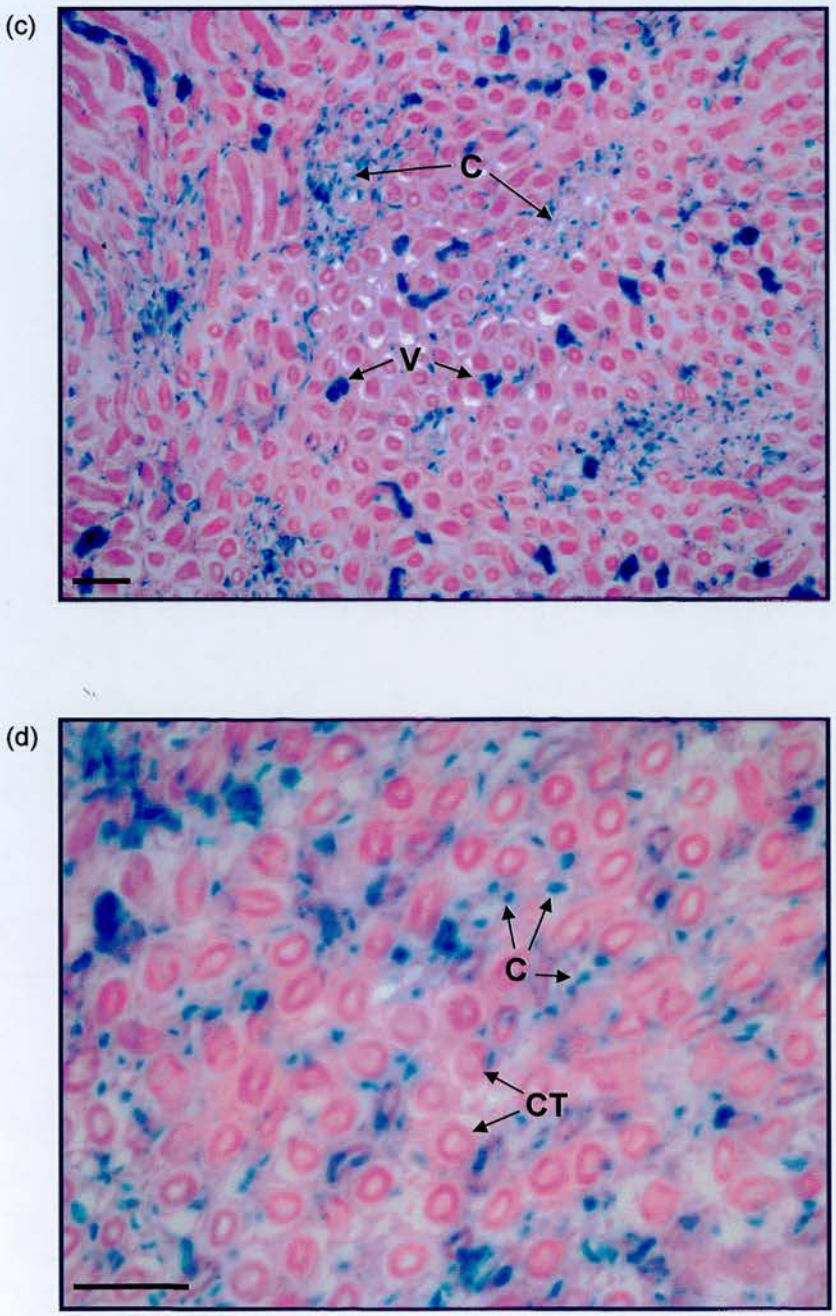

Figure 5-8. Renal LacZ expression in *EDNRB*-LacZ(2) homozygous mice (continued). (c) & (d) High magnification of renal medulla, x200 and x400 respectively. LacZ expression is confined to the spaces surrounding tubules. Tubules are negative for LacZ expression. Scale bar = 0.05mm. Abbreviations: C, capillaries; V, blood vessels; CT, collecting tubules.

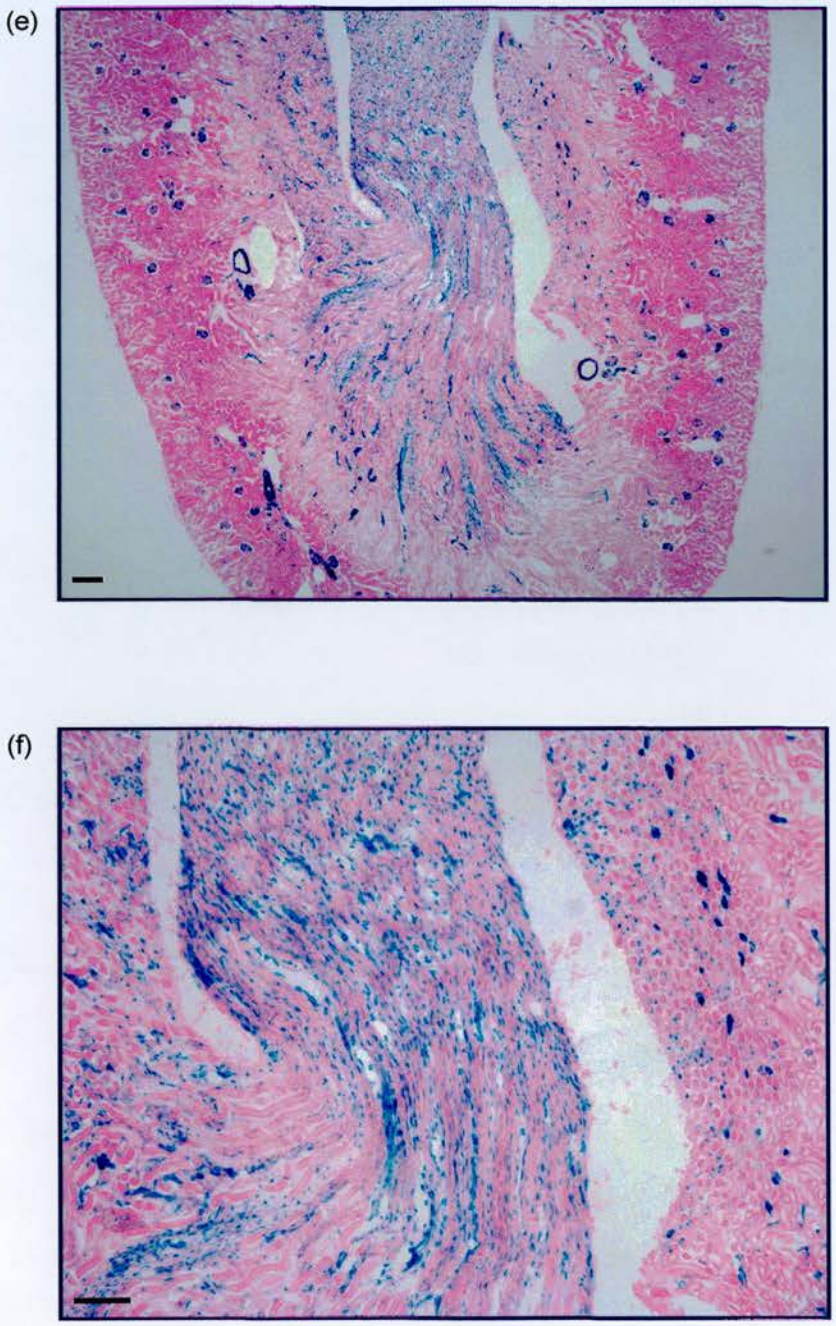

Figure 5-8. Renal LacZ expression in *EDNRB*-LacZ(2) homozygous mice (continued). (e) LacZ expression in papilla (x40). Scale bar = 0.2mm. (f) Higher magnification of (e) (x100). Scale bar = 0.1mm.

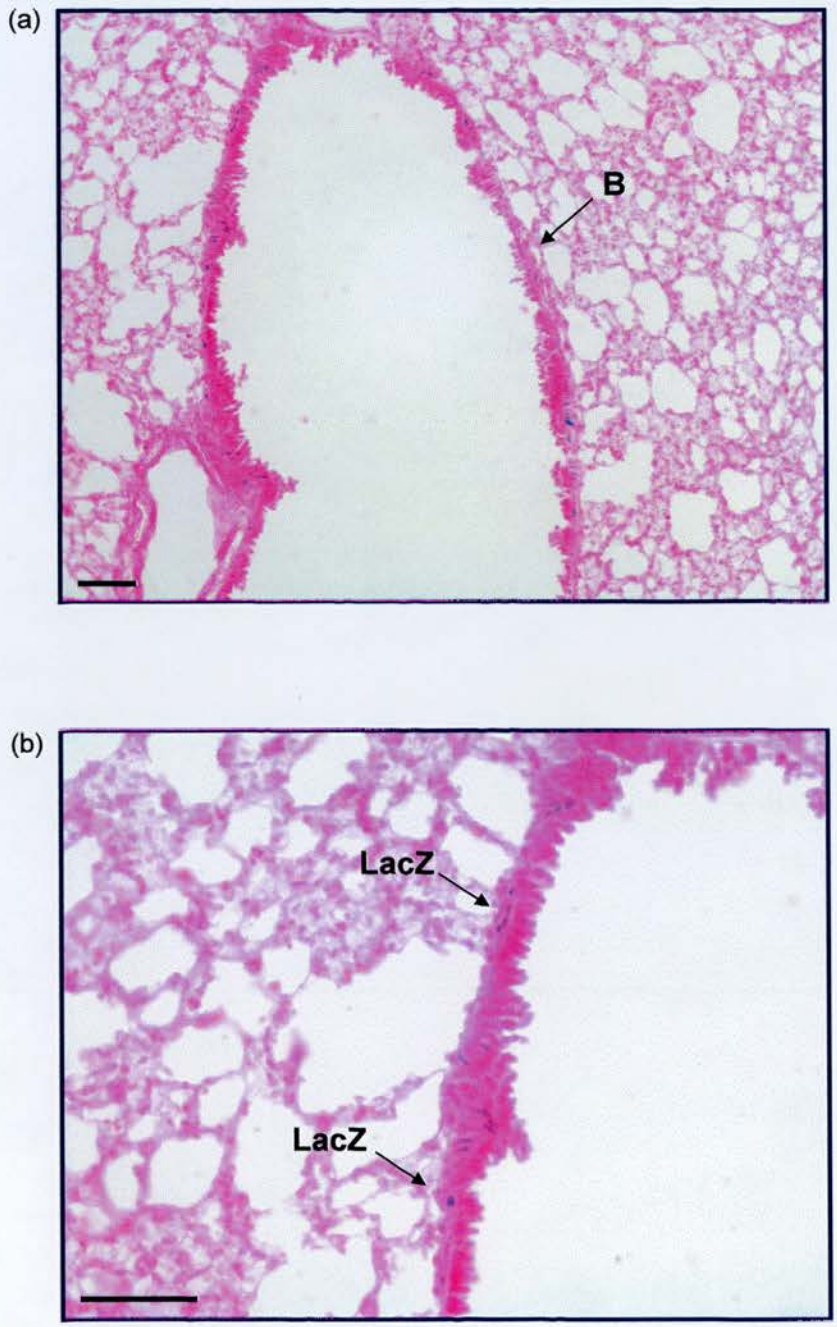

Figure 5-9. LacZ expression in lung tissue from *EDNRB*-LacZ heterozygous mice. Representative cryosections of lungs from *EDNRB*-LacZ heterozygote mice which were generated during the course of this project, stained for β-gal activity (blue) and counterstained with eosin (pink). See text for further details (section 5.2.4). (a) Low magnification of lung section (x200). Scale bar = 0.05mm. (b) Nuclear localised LacZ expression in smooth muscle layer of bronchiole (x400). Scale bar = 0.05mm. Abbreviations: B, bronchiole.

	Localisation of β-gal activity	Figure reference
***EDNRB*-LacZ(2)**		
Lung		
Heterozygotes	smooth muscle of bronicholes (++), pulmonary parenchyma (++)	5.1
Homozygotes	smooth muscle of bronchioles (+++), pulmonary parenchyma (+++)	5.2
***EDNRB*-LacZ(2)**		
Kidney		
Heterozygotes	Cortex: glomeruli (++), afferent/efferent arterioles (++), peritubular capillaries (++)	5.3
	Medulla: vasa recta (+), papillae (+), collecting tubules (NP)	5.4
Homozygotes	Cortex: glomeruli (+++), afferent/efferent arterioles (+++), peritubular capillaries (+++)	5.6
	Medulla: vasa recta (+++), papillae (++), collecting tubules (NP)	5.7, 5.8
***EDNRB*-LacZ**		
Lung		
Heterozygotes	smooth muscle of bronicholes (+)	5.9

Table 5.1. Summary of staining for β-gal activity in *EDNRB*-LacZ(2) and *EDNRB*-LacZ mice. +++, high staining; ++, moderate staining; +, low staining; NP, not present.

5.3 DISCUSSION

One of the fundamental questions when studying any biological pathway *in vivo* is to determine cellular localisation of the components involved. Cellular localisation of ET_B in the kidney is important for the understanding of the mechanisms involved in ET-1 regulation of salt and water homeostasis. The quest to identify ET-1 binding sites began shortly after the discovery of ET-1 in 1989. These early studies were hampered by the unavailability of specific ET receptor agonists and antagonists and therefore made it impossible to distinguish between binding to ET_A or ET_B. However, they did provide vital information regarding the importance of the renal endothelin system by reporting that some of the highest binding of [^{125}I]-ET-1 within the whole animal occurred within the kidney, in particular within the inner medulla (Kitamura *et al.*, 1989a; Kitamura *et al.*, 1989b; Koseki *et al.*, 1989).

At around the same time the first autoradiographic localisation studies revealed images showing intense [^{125}I]-ET-1 binding in glomeruli, inner medulla and papilla (Davenport *et al.*, 1989; Jones *et al.*, 1989; Kohzuki *et al.*, 1989). Electron microscopic autoradiography offered more specific cellular localisation of intravenously injected [^{125}I]-ET-1 within the medulla (Furuya *et al.*, 1992; Dean *et al.*, 1994). There was strong binding reported in peritubular capillaries and to a lesser extent in vasa recta whilst binding to renal tubules was undetectable (Dean *et al.*, 1994). A similar pattern was reported by Furuya *et al* (Furuya *et al.*, 1992). However, this group also reported that the extent of [^{125}I]-ET-1 binding was greatly dependent on the duration of [^{125}I]-ET-1 infusion. Furthermore, some binding sites may have been inaccessible to intravenously administered [^{125}I]-ET-1. *In vitro* electron microscopic autoradiography showed binding predominantly on endothelial cells of the vasa recta (Yukimura *et al.*, 1996). Unlike the other reports, binding was also observed on IMCD cells. However, it was still unknown which endothelin receptor subtype the binding corresponded to. Indeed it was reported that cultured IMCD cells expressed both ET_B and ET_A as shown by RT-PCR (Kohan *et al.*, 1992).

The development of ET_B antibodies provided some insight into receptor subtypes showing staining of glomeruli and capillaries within the inner medulla. No positive staining was observed in collecting ducts (Hagiwara *et al.*, 1993). On the other hand, *in situ* RT-PCR identified ET_B mRNA exclusively in the epithelial cells of collecting ducts, whereas ET_A was observed in medullary interstitial cells and vasa recta (Chow *et al.*, 1995). However, due to the proximity of capillaries and collecting duct cells, distinguishing one cell from another using these techniques may have proven to be problematic. Localisation by RT-PCR was also attempted on microdissected rat nephrons (Terada *et al.*, 1992a). Large signals were obtained for ET_B in glomeruli, IMCD cells, cortical collecting ducts and a weaker signal for vasa recta bundles. However, given the sensitivity of RT-PCR, the possibility of cross-contamination cannot be ruled out in techniques relying on micro-dissection despite the appropriate controls being in place. Furthermore, RT-PCR provides information only about ET_B transcription and gives no indication of ET_B protein expression.

More recent autoradiography studies have made use of endothelin receptor agonists and antagonists to distinguish between ET_B and ET_A. By blocking ET_A sites with antagonist 97-139, binding of [^{125}I]-ET-1 to ET_B was determined. Although binding was still observed in the cortex and inner medulla, no comments were given on specific structures and it is difficult for the reader to determine this from the pictures given (Yukimura *et al.*, 1996). Dean *et al* reported inhibition of [^{125}I]-ET-1 binding by sarafotoxin 6c, an ET_B agonist and BQ123, an ET_A antagonist (Dean *et al.*, 1996). Whereas, sarafotoxin 6c abolished [^{125}I]-ET-1 binding throughout the kidney except for renomedullary interstitial cells of the inner medulla, BQ123 had little effect on overall binding. This indicated that ET_A was localised to renomedullary interstitial cells of the inner medulla whilst the remaining [^{125}I]-ET-1 binding represented ET_B sites. High resolution light microscopy and electron microscopy of the medulla revealed these sites to be the vascular endothelium, in particular glomerular and peritubular capillaries. As with the *in vivo* autoradiography described above, the authors reported no binding within renal tubular cells. However, again this is not

particularly clear from the autoradiograph pictures. Therefore, the precise cellular sites of renal ET_B expression *in vivo* have yielded conflicting and unconvincing data.

This chapter reports precise ET_B localisation within the kidney by analysing the expression profile of an *EDNRB*-LacZ transgene. Analysis of *EDNRB*-LacZ homozygote mice revealed strong expression in glomeruli, the inner medulla and papilla. The overall staining pattern was similar to those obtained using [^{125}I]-ET-1 radioligand macroautoradiography (Davenport *et al.*, 1989; Jones *et al.*, 1989; Kohzuki *et al.*, 1989; Dean *et al.*, 1994; Yukimura *et al.*, 1996; Zhuo *et al.*, 1998). At higher resolution, staining within the cortex was confined to glomerular endothelial and mesangial cells and blood vessels, including afferent and efferent arterioles. However, as mentioned in section 5.1, the main aim of this chapter was to identify which cells within the medulla express ET_B. I have clearly shown that the endothelial cells of medullary capillaries (i.e. vasa recta) expressed LacZ whilst tubular cells (i.e. IMCD cells) were negative for transgene expression. The lack of LacZ expression in IMCD cells contradicts previous studies documenting ET_B expression within these tubular cells (Kohan *et al.*, 1992; Terada *et al.*, 1992a; Yukimura *et al.*, 1996). However, several criticisms can be made of these reports as described earlier. To my knowledge, this is the first study to demonstrate localisation of ET_B within the renal medulla to this degree of precision without being hampered by technical difficulties such as cross-contamination and the occurrence of false positives.

However, localisation of proteins using transgene technology also carries with it inherent criticisms. For example, in order to knock-in a reporter gene also involves the "knocking out" of one or both alleles of the targeted gene, in this case *EDNRB*. It is impossible to know what effect this will have on expression levels of the gene. The lack of functional ET_B may initiate a negative feedback mechanism in which transcription and translation of the gene is upregulated. This may be a potential reason for the observed differences between heterozygote and homozygote expression levels. It was expected that LacZ expression of homozygous mice would simply be twice the intensity of heterozygote mice. However, it is clear that this was

not the case. LacZ expression in kidneys from homozygote mice was several times higher than in kidneys from heterozygote mice. It is possible that complete abolition of ET_B protein in homozygote mice may be responsible for increased ET_B promoter activity and thus augmented LacZ expression. In contrast, heterozygous mice still express functional ET_B protein and so negative feedback upregulation of gene expression may not be initiated. Although this is a valid explanation, it is probably unlikely that this is the case. As described above, previous localisation data suggest that ET_B is highly expressed within the kidney implying that the pattern obtained from homozygote mice is a more accurate reflection of actual ET_B expression than that obtained from heterozygote mice. Furthermore, even if knocking-out of ET_B had some compensatory effect on expression levels, it is unlikely that this would alter localisation in terms of which cells were expressing LacZ. In other words, it is not anticipated that knocking out of ET_B would result in *de novo* expression of ET_B in cells that do not usually express the protein.

In addition to knocking-out functional protein expression, gene targeting may also interfere with regulatory DNA sequences required for gene transcription. Transcriptional gene expression usually relies on functional activity of the promoter, as well as regulatory DNA sequences involved in binding transcription factors and upstream enhancer elements. Little is known about transcriptional control of *EDNRB* (Aria *et al.*, 1993). However, Shin *et al* have previously reported that a mutation in intron 1 of the *EDNRB* locus resulted in truncated RNA transcripts (Shin *et al.*, 1997). In the *EDNRB*-LacZ(2) targeting construct, the LacZ reporter gene was used to replace intron 1 which may have adverse effects on *EDNRB* and LacZ transcription. It is not clear whether *EDNRB*-LacZ(2) failed to be expressed in IMCD cells because important cell-specific transcriptional control elements were lacking. Although speculative, it is an important factor to be considered during the analysis of the localisation data. In contrast to *EDNRB*-LacZ(2), the *EDNRB*-LacZ targeting construct did not involve removal of any region of the genomic *EDNRB* sequence upstream of exon 3. It will therefore be interesting to compare renal localisation from

the *EDNRB*-LacZ(2) strain with the *EDNRB*-LacZ strain once renal staining of these animals has been optimised.

Another explanation for the differences observed between heterozygote and homozygote mice could be the age at which the animals were studied. As described in section 5.2.1, heterozygote mice were analysed at 8-10 weeks of age, whereas homozygote mice were only 2.5 weeks old. It is possible that LacZ expression was easier to detect in kidneys from younger mice. Kidneys from younger mice were significantly smaller than those from older mice and may have been more accessible to penetration of fixative solutions. Whatever the reason for these differences, it is clear that further investigation is required. In particular, analysis of 2.5 week old heterozygote mice is required. Unfortunately, due to time constraints it was not possible to analyse young heterozygote mice but this will be undertaken in the future.

Although not yet fully analysed for transgene expression within the kidney, initial studies on my own *EDNRB*-LacZ mice provided promising results for future analysis. Despite reduced LacZ expression in the lung compared to *EDNRB*-LacZ(2) mice, staining was clearly localised to the nucleus and appeared to correspond to the staining observed in lungs from *EDNRB*-LacZ(2) mice, at least within the smooth muscle layer of bronchioles. It is anticipated that optimisation of the staining protocol will improve LacZ staining. It is well known that the duration of paraformaldehyde fixation can dramatically affect β-gal activity (refer to section 2.6.2). β-gal activity can be completely suppressed if incubation periods are too long. It should also be emphasised that my transgene and Dr Shin's transgene are different (see section 4.2.5) and this may account for the differences in LacZ expression (e.g. IRES driven translation may result in lower protein expression). Once staining is optimised for my own mice, it will be interesting to compare localisation patterns within the kidney with that of *EDNRB*-LacZ(2), as well as investigating the involvement of *EDNRB* intron 1 in regulating LacZ expression (see above). It is also anticipated that localisation of LacZ expression to the nucleus via expression of NLS, will provide further useful information.

Despite the concerns described above, the *EDNRB*-LacZ(2) renal localisation data observed here are in line with the report by Dean *et al* which, in my opinion, presents the most accurate account of ET_B localisation to date (Dean *et al.*, 1996) and therefore appears to represent an accurate picture of *in vivo* expression of ET_B.

Localisation of ET_B to capillary endothelial cells but not to IMCD cells is an important step towards understanding the intracellular mechanisms involved in ET-1 and ET_B renal signalling and their physiological role in natriuresis/diuresis. As discussed in section 1.2.2.7, ET-1 appears to exert its natriuretic effect through the stimulation of NO release. ET-1 and NO modulate sodium transport in the same regions of the nephron (Plato *et al.*, 1999; Plato *et al.*, 2000a). L-NAME inhibits the natriuretic effects of ET-1 (Hoffman *et al.*, 2000; Plato *et al.*, 2000a). Plato *et al* also reported that these effects are mediated by ET_B and eNOS (Plato *et al.*, 2000a; Plato *et al.*, 2000b). ET-1 and NO are thought to enhance sodium and water excretion by directly inhibiting sodium transport in IMCD cells. Previously, an autocrine model of ET-1 action in the medulla was proposed based on IMCD *in vitro* studies in which both ET-1 and ET_B were expressed (Kohan & Padilla, 1992). However, culturing of IMCD cells firstly requires micro-dissection of tubules devoid of vasa recta bundles and therefore introduces the possibility of cross-contamination. Furthermore, as with any cell culture, it is not known how the phenotype of IMCD cells is affected during prolonged culturing. The results presented here would suggest that the autocrine signalling pathway is not valid since ET_B is not expressed by IMCD cells *in vivo*. Instead, the localisation data provide evidence in support of a paracrine mechanism of action in which ET-1 released from IMCD cells binds to ET_B located on the vasa recta (see section 1.2.2.8 and figure 1-5). Additional physiological experiments documented that eNOS was the major isoform involved in ET-1/ ET_B mediated NO production (Plato *et al.*, 2000b). In order for ET_B to activate eNOS, both components have to be expressed in the same cell. Teichert *et al* reported the highest site of renal eNOS expression within the medulla occurred in endothelial cells of the vasa recta

(Teichert *et al.*, 2000). This lends further support to a paracrine mechanism of ET-1 action.

Vasa recta are specialised peritubular capillaries that extend deep into the medulla. They lie adjacent to the renal tubules of the juxtamedullary nephrons (see figure 1-4), which make up approximately 20-30% of total nephrons and play an important role in concentrating urine. The ability of the kidney to excrete concentrated urine is largely dependent on the counter-current mechanism in the loop of Henle which establishes a high osmolarity of interstitial fluid in the medulla due to the accumulation of solutes reabsorbed from the thin ascending loop of Henle but not reabsorption of water. In the presence of ADH, this osmotic gradient causes water in the collecting ducts to diffuse into the renal interstitium and vasa recta, thereby concentrating urine. Positioned at the terminal portion of the nephron, IMCD cells are the final site for processing urine before excretion and are therefore responsible for the final decision regarding urine output of water and salts. Thus, the endothelin/NO system could play a critical role in the fine-tuning of sodium and water excretion.

There are two major mechanisms which lead to increased sodium and water excretion. The first is a reduction in tubular sodium transport. As alluded to above, both ET-1 and NO have been reported to directly inhibit sodium transport, independent of alterations in renal blood flow (Stoos *et al.*, 1995; Plato *et al.*, 1999; Plato *et al.*, 2000a). It has been reported that ET-1 can inhibit sodium reabsorption by downregulating ENaC activity (Gallego & Ling, 1996; Gariepy *et al.*, 2000) and by inhibiting Na^+-K^+-ATPase activity (Zeidel *et al.*, 1989). It has also been suggested that NO blocks sodium channels through a cGMP-kinase dependent phosphorylation pathway (Light *et al.*, 1990; Lahera *et al.*, 1993). ET-1 may also inhibit water reabsorption by blocking ADH activity, thereby reducing water permeability in the collecting duct (Tomita *et al.*, 1990; Nadler *et al.*, 1992). Increased sodium and water excretion can also result from augmented blood flow to the medulla. Compared to the cortex, blood flow to the vasa recta is low, accounting for only 1-2% of total

renal blood flow. Physiologically, low renal blood flow minimises washout of the solute gradient established by the counter-current mechanism (see above). On the other hand, high blood flow through the vasa recta, dissipates solutes, reduces the ability of the kidney to concentrate urine and leads to increased natriuresis/diuresis (Cowley, 1997). As well as exerting direct effects on sodium transport, ET-1 and NO also regulate medullary blood flow (Gurbanov *et al.*, 1996; Mattson & Wu, 2000a). By increasing blood flow through the vasa recta, ET-1 and NO indirectly initiate natriuresis/diuresis.

In summary, the localisation data presented here and physiological data from other reports, suggest that, by binding to ET_B on the vasa recta, ET-1 activates eNOS. NO released from medullary capillary endothelial cells, acts simultaneously on IMCD cells to decrease sodium transport and on the vasa recta to enhance renal blood flow. This dual action has the net effect of reducing sodium reabsorption and promoting natriuresis/diuresis thus helping to maintain systemic blood pressure within the normal, healthy range.

It should be clear that abnormalities in the system described above, resulting in reduced NO release, may have a detrimental effect on sodium transport and may lead to sodium retention and hypertension. Indeed, urinary excretion of NO metabolites (NO_2 and NO_3) were significantly lower in hypertensive patients (Sierra *et al.*, 1998). ED within the kidney has been described in a number of models of hypertension (refer to section 1.2.3). As discussed in chapter 3, reduced NO availability may result from changes in several different factors. In particular, components of the pathway described above may be altered. At present there is no convincing evidence supporting a reduction in renal eNOS expression. In contrast, many of the reports to date, including data reported in chapter 3 of this thesis, would suggest that renal eNOS expression is elevated during hypertension. Instead, reduced activation of eNOS and NO release by the renal endothelin system may be a potential mechanism in the pathogenesis of ED. As discussed in section 1.2.3, daily urinary excretion of ET-1 was significantly decreased in hypertensive patients compared to normotensive

subjects (Hoffman *et al.*, 1994). Furthermore, when hypertensive patients were given high sodium diets, the salt-sensitive subset excreted less urinary ET-1 than the salt-resistant subset. More direct evidence for diminished medullary ET-1 production in hypertension comes from animal models. Levels of ET-1 mRNA and immunoreactive ET-1 in the inner medulla were decreased in SHR compared to WKY rats (Kitamura *et al.*, 1989b; Hughes *et al.*, 1992). This is further supported by the observation that ET-1 production was significantly lower in IMCD cells isolated from SHR (Hughes *et al.*, 1992). Likewise, ET_B mRNA expression was downregulated in DOCA-salt sensitive hypertensive rats. In addition, these animals produced less NO in response to ET-1 perfusion (Hirata *et al.*, 1995b). However, no information was given regarding precise sites of altered ET_B expression. The importance of ET_B in maintaining normal blood pressure is further emphasised by the observation that animals deficient in ET_B developed salt-sensitive hypertension (Ohuchi *et al.*, 1999b; Gariepy *et al.*, 2000). Furthermore, collecting duct specific knockouts of ET-1 excrete less sodium and are hypertensive (Ahn *et al.*, 2002). Together, these data imply that reduced activity of the renal endothelin system may be a contributing factor to diminished NO availability within the kidney and that renal ED may play a crucial role in the development and maintenance of hypertension.

5.4 SUMMARY

In summary, this chapter has described the precise localisation of ET_B within the kidney using *EDNRB*-LacZ(2) knock-in mice. The main findings were:

- The *EDNRB*-LacZ transgene was highly expressed within the inner medulla.
- LacZ expression was confined to medullary capillaries (i.e. vasa recta).
- Tubular cells within the inner medulla (i.e. IMCD cells) were negative for transgene expression.

- These data support the hypothesis that ET-1 acts as a paracrine natriuretic hormone where it is released from IMCD cells and binds to ET_B located on the vasa recta. Activation of ET_B initiates eNOS to release NO which blocks sodium transport and increases medullary blood flow, thereby promoting natriuresis/diuresis.

CHAPTER 6

ALTERATION IN ET_B EXPRESSION FOLLOWING SALT LOADING OF *EDNRB*-LACZ(2) MICE

6.1 INTRODUCTION

In the previous chapter, renal ET_B localisation in *EDNRB*-LacZ(2) mice was described and the results discussed in the context of the cellular and molecular mechanisms underlying ET-1/ET_B mediated natriuresis/diuresis. To further investigate the role of ET_B in sodium transport, *EDNRB*-LacZ(2) mice were used in physiological salt loading experiments.

Several studies have examined renal endothelin regulation in response to salt loading. Pollock *et al* reported that urinary ET-1 excretion was significantly higher in wild type rats fed a high salt (10% NaCl) diet than those on a low sodium diet, implying that ET-1 renal production is increased in response to high salt intake (Pollock & Pollock, 2001). Similar findings have been reported in mice. Melo *et al* used a radioimmunoassay to measure ET-1 levels in kidney extracts from mice fed an 8% NaCl diet for one week (Melo *et al.*, 1998). Compared to mice on a sodium deficient diet, they detected significantly increased renal ET-1. In support of this finding, Ohuchi *et al* reported upregulation of renal preproET-1 mRNA by RT-PCR in mice fed high salt diets for 3 weeks (Ohuchi *et al.*, 1999b). These findings are in keeping with *in vitro* experiments showing that one of the main stimuli for ET-1 production is increased osmolality. Increasing the sodium concentration of IMCD cell media resulted in an increase in preproET-1 mRNA accompanied by increased ET-1 production (Yang *et al.*, 1993; Migas *et al.*, 1995). In addition, some animal models with salt sensitive hypertension have activated endothelin systems. For example, in both the DOCA-salt hypertensive rat and the Dahl salt sensitive rat, renal prepro-ET-1 mRNA expression is increased (Deng *et al.*, 1996; Ikeda *et al.*, 1999). However, it is important to remember at this point that the renal vasculature and the renal tubule react differently to ET-1. Within the vasculature, increases in ET-1 predominantly results in vasoconstriction, thereby promoting a hypertensive effect. On the other hand, increased ET-1 in the nephron enhances sodium and water excretion and consequently lowers blood pressure. In the hypertensive animal studies described above, no indication is given regarding specific cellular sites of ET-1

upregulation and therefore these results must be interpreted cautiously. Elevated renal expression of ET-1 in the vasculature of these animal models of hypertension may, in fact, be a pathological feature of hypertension and not a physiological adaptation to increased salt intake.

Nevertheless, the studies performed on wild type animals provide strong evidence that renal ET-1 expression and release is stimulated during conditions of high salt intake and volume expansion. However, not all studies agree with this outcome. Morita *et al* reported a 50% reduction in renal ET-1 in mice fed an 8% NaCl diet compared with mice fed a normal diet for 4 weeks (Morita *et al.*, 1998). These discrepancies may arise from the methods used to measure ET-1 or from differences in the duration of administration of the high salt diet. Furthermore, in most of the studies mentioned here, ET-1 measurements were obtained from whole kidney extracts. As described above, details of the intrarenal cellular sources of ET-1 (i.e. vascular or tubular) are necessary to fully interpret these data. More direct measurements of the source of renal ET-1 production are required to help resolve the situation.

There are few complementary studies investigating alterations in renal ET_B during salt loading. It is not known if increased salt intake is also a stimulus for ET_B expression, as it is for ET-1. Studies on salt sensitive animal models reported the opposite result. DOCA-salt hypertensive rats exhibited lower ET_B mRNA levels in whole kidney homogenates (Hirata *et al.*, 1995b). Likewise, Dahl salt sensitive rats had decreased ET_B protein expression in large renal arteries. However, no information was given regarding the renal medulla (Kakoki *et al.*, 1999). Again, as described above, these results must be viewed with caution as decreased ET_B levels may be a causative factor in the development of hypertension in these models. This is further emphasised by the observation that ET_B deficient animals develop salt sensitive hypertension (Ohuchi *et al.*, 1999b; Gariepy *et al.*, 2000). It is clear that further studies regarding the effects on salt loading on renal ET_B expression are required.

Given the role of ET_B in promoting natriuresis/diuresis and the evidence described above regarding upregulation of ET-1 during salt loading, it is hypothesised that under physiological conditions, an increase in salt intake will also perpetuate an increase in renal ET_B expression. In turn, NO production and subsequent excretion of excess salt and water will be enhanced. Therefore, the aim of this study was to investigate the effects of salt loading on renal ET_B expression in *EDNRB*-LacZ(2) mice. Because homozygote mice die at an early age (see section 5.2.1), heterozygote mice were used.

6.2 RESULTS

6.2.1 General parameters of salt loading

EDNRB-LacZ(2) heterozygote male mice (10 weeks old) were fed high (8%) or standard (0.8%) NaCl diets for 3 weeks (see section 2.6.4). There were no significant differences in body weights between groups at the start and end of the experimental time period (Table 6-1). Kidney to body weight ratios were also comparable between groups. Mice on the high salt diet ate considerably more food (figure 6-1a), possibly due to increased energy expenditure or simply due to taste preferences. Consequently, mice on high salt diets drank significantly increased amounts of water (figure 6-1b) and as a result, urine output was approximately 3 times greater from mice on high salt diets (figure 6-1c). However, it should be noted that urine was only collected over a period of 12 hours, due to Home Office regulations, and was therefore not as accurate as the more commonly measured 24 hour collection period.

Table 6-1. General parameters of salt loading.

Group	BW start (g)	BW end (g)	Kidney/BW ratio
Standard salt (n=5)	27.2 ± 1.0	26.7 ± 1.0	0.0088 ± 0.0004
High salt (n=5)	29.8 ± 1.2	28.2 ± 1.0	0.0104 ± 0.0007

Values are given as mean ± S.E.M. Abbreviations: BW, body weight.

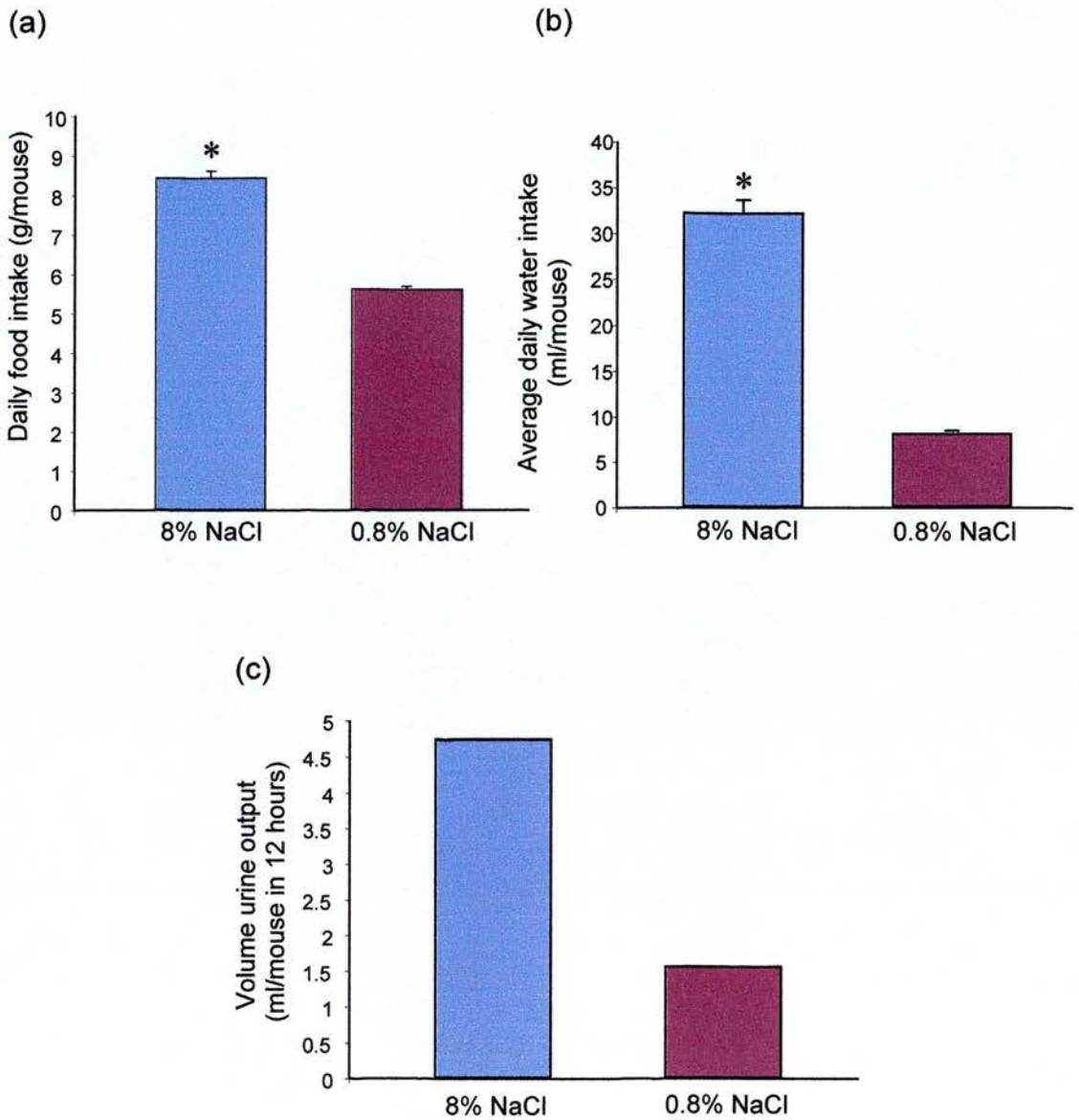

Figure 6-1. Food and water intake and urine volume from mice on high or standard sodium diets. (a) Daily food intake (n=5). (b) Daily water intake (n=5). (c) Volume of urine output over a 12 hour period. For urine collection, animals were divided into separate metabolic cages and urine volumes combined for each group. * $P<0.05$ versus 0.8% NaCl group.

6.2.2 ET_B expression during salt loading

ET_B expression was assessed by measuring β-gal activity in whole kidney extracts. β-gal activity was quantified in tissue extracts using an assay based on the methylumbelliferone fluorescence method which measures the hydrolysis of 4-methylumbelliferyl-β-D-galactoside catalysed by β-gal. This reaction yields 4-methylumbelliferone (MU), a fluorescent product that emits fluorescence at 460nm when excited at 365nm (see section 2.6.3). Figure 6-2a shows the results of β-gal activity in kidney extracts from mice fed high salt or normal salt diets. *EDNRB*-LacZ(2) mice which were fed high salt exhibited slightly higher β-gal activity although significance was not reached (P=0.21). However, it should also be noted from figure 6-2a that wild type mice (i.e. those mice which were negative for the *EDNRB*-LacZ(2) transgene) also had high levels of β-gal activity. The reasons for this are unclear but it has been documented elsewhere and appears to be unique to the kidney (Pelisek *et al.*, 2000). Lung extracts from wild type mice did not exhibit the same high β-gal background activity (figure 6-2b). It was possible that the high background was masking the effect of salt loading on ET_B expression. Therefore, 3 different protocols were used in an attempt to reduce the activity of endogenous β-gal activity. The first was to use a pull down assay, similar to the co-immunoprecipitation assay described in section 2.3.4, to extract exogenous β-gal. An antibody specific to bacterial β-gal, together with protein G sepharose were used to capture exogenous β-gal. The β-gal activity of this sample was then measured. The second approach was to selectively inhibit the activity of endogenous β-gal by heat treatment, thereby intensifying the activity of the exogenous reporter gene. Young *et al* have previously reported that heat treatment at 50°C inactivated endogenous β-gal activity without affecting the activity of bacterial β-gal (Young *et al.*, 1993). The final approach was similar to the second. Instead of using heat to inactivate endogenous β-gal, increased pH was used (from pH 7.5 to pH 8.5). Again, this is reported to decrease endogenous activity (Kantachuvesiri, 1999). However, bacterial β-gal activity may also be reduced by up to 50%. Unfortunately, none of these methods produced satisfactory results. The result was either complete abolition of

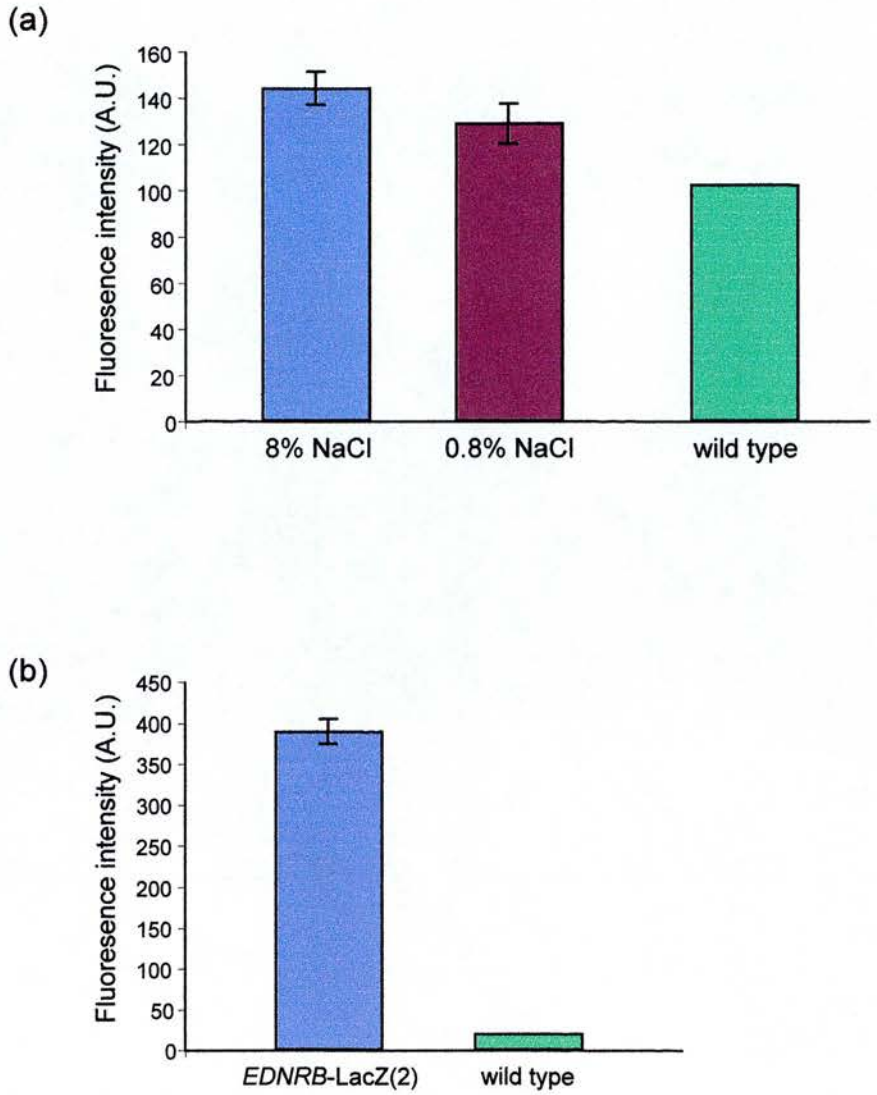

Figure 6-2. β-gal activity in kidney extracts from mice on high or normal salt diets. (a) β-gal activity in kidneys from mice on high and normal diets. Also shown is β-gal activity from a wild type mouse. (b) β-gal activity in lung extracts from *EDNRB*-LacZ(2) and wild type mice. n=5 in each group, except wild type (n=1).

β-gal activity or no increased difference in activity between *EDNRB*-LacZ(2) and wild type animals. Further investigations are therefore required to resolve these technical problems.

6.3 DISCUSSION

As discussed in section 6-1, the majority of studies examining the regulation of the endothelin system in response to salt loading, indicate that renal ET-1 expression increases. Based on these observations and the proposed mechanism of ET-1 induced natriuresis/diuresis described in chapter 5, it was hypothesised that increased levels of ET-1 may result in augmented renal NO production via activation of ET_B and eNOS. The downstream result would be increased natriuresis/diuresis thereby excreting excess dietary salt and maintaining normal blood pressure. Although some studies indicate that renal eNOS expression and NO production are increased during salt loading (Schultz & Tolins, 1993; Mattson & Higgins, 1996), no such studies exist for ET_B. This chapter has described a preliminary investigation on the effects of salt loading on renal ET_B expression.

I have used the *EDNRB*-LacZ(2) knock-in mice described in chapters 4 and 5 to perform salt loading experiments. By measuring β-gal activity in renal extracts from heterozygote *EDNRB*-LacZ(2) mice fed normal and high salt diets, I was able to quantify the level of renal ET_B expression. Initial results suggest that renal ET_B expression is increased by high salt intake. However, it should be noted that the numbers of animals used in this study were low (n=5). It is therefore important that this experiment should be repeated using increased numbers of animals (e.g. n=10-15) before making any firm conclusions. Furthermore, high endogenous β-gal activity was observed in these kidney samples which may be masking part of the effect. I attempted a variety of methods to try and reduce background β-gal activity in kidney homogenates, but to no avail. It is also possible that exogenous β-gal activity in these samples was simply too low to quantify accurately. As described in chapter 5 (see section 5.2.3.1), LacZ expression in kidney sections taken from

EDNRB-LacZ(2) heterozygote mice was extremely low. This low expression became more apparent when compared to β-gal expression in 2.5 week old homozygote *EDNRB*-LacZ(2) mice in which β-gal expression was significantly higher. It is hypothesised that these differences in expression may be a result of the age at which the mice were studied. It is also possible that endogenous β-gal activity increases with age. Therefore, future salt loading experiments may yield clearer data if performed on younger mice. It is unfortunate that homozygote *EDNRB*-LacZ(2) mice, which have significantly increased renal β-gal expression compared to heterozygotes, cannot be used in this type of study since they die at an early age (Hosoda *et al.*, 1994). Furthermore, ET_B knockout animals are hypertensive on a normal salt diet which is augmented during salt loading (Ohuchi *et al.*, 1999b; Gariepy *et al.*, 2000). This would therefore complicate findings. Although there are no data describing salt loading of heterozygote ET_B knockout mice, they are not hypertensive on a normal sodium diet. It may also be possible to quantify LacZ gene expression on kidney sections. Not only will this give information regarding overall changes in ET_B expression, it should also provide data on how ET_B expression is altered during salt loading within specific cells in the kidney.

In the future it will be desirable to include a positive control for the upregulation of ET_B expression. However, there are few reports investigating which physiological factors upregulate or downregulate renal ET_B expression. *In vitro* studies suggest that cytokines and growth factors downregulate ET_B expression in HUVECS (Smith *et al.*, 1998). Kanno *et al* reported that angiotensin II dose dependently upregulated ET_B mRNA (Kanno *et al.*, 1993). However, this was performed in cultured rat cardiomyocytes. The equivalent study has not been reported for renal cells. Indirect evidence showing that renin and angiotensin II levels drop during salt loading, imply that angiotensin II is not an activator of renal ET_B expression (Melo *et al.*, 1998).

Increased ET_B expression during salt loading is in line with existing data on alterations in ET-1 and eNOS expression in response to high salt intake. Pollock *et al* reported increased renal ET-1 production in rats fed high salt diets (Pollock &

Pollock, 2001). Likewise, Melo *et al* documented augmented ET-1 expression in whole kidney homogenates as well as higher eNOS expression in salt-loaded mice (Melo *et al.*, 1998). Increased eNOS expression was also observed in the inner medulla of rats on high salt diets (Mattson & Higgins, 1996). Taken together, these data suggest that increased levels of ET-1, ET_B and eNOS may be a physiological adaptation to increased dietary salt intake aimed at counteracting the pressor effect of high salt by facilitating increased medullary sodium transport and increasing medullary blood flow, both of which promote natriuesis/diuresis (see section 5.3). The main aim now is to elucidate in which renal vascular or tubular segments these changes take place.

The kidneys have an enormous capacity to alter sodium excretion in response to changes in sodium intake. In physiological conditions this occurs with relatively small changes in extracellular fluid volume and thus maintains normal blood pressure. The results presented in this chapter and reports by others suggest that the endothelin system may play an important role in regulating sodium homeostasis. However, other systems also play their part.

The basic mechanisms of how increased salt intake can initiate increased natriuresis/diuresis have been well described for some time (reviewed in (Guyton & Hall, 2000b)). As sodium intake increases, the osmolality of the extracellular fluid also increases. This is one of the major stimuli for the sensation of thirst. If water is in abundant supply, water intake also increases. In the study described here, animals on high salt diets drank around 4-5 times more water than animals on normal salt diets. Increased sodium and water intake leads to an increase in extracellular fluid volume which in turn triggers various mechanisms to increase sodium and water excretion. Firstly, the increase in fluid volume causes a small rise in blood pressure initiating pressure natriuresis/diuresis to excrete excess sodium and water. In addition, anti-natriuretic/diuretic systems are suppressed. Of these, the renin-angiotensin system is the most important. By blocking renin release, and consequently angiotensin II and aldosterone production, sodium and water retention

are reduced. Finally, increased extracellular fluid volume can stimulate natriuretic system such as atrial natriuretic peptide and possibly the endothelin system described above, which contribute further to increased sodium and water excretion. Therefore, by suppressing water and sodium retaining systems and by activating natriuretic/diuretic systems, the kidney can respond to increased salt intake by promoting sodium and water excretion through the production of large volumes of urine. All this occurs with only slight changes in extracellular fluid volume and blood pressure.

Despite the ability of the kidney to control sodium homeostasis with such fine precision, high salt diets have been implicated in the pathogenesis of hypertension. Indeed, a large percentage of human hypertensive patients are salt sensitive. However, the underlying mechanisms are largely unknown. There is now growing evidence that aberrations in the renal endothelin and NO systems may play a role in abnormal sodium homeostasis and contribute to the development of salt-induced hypertension. This concept will be discussed further in chapter 7. Further knowledge of the mechanisms involved is awaited with much anticipation.

6.4 SUMMARY

In summary, this chapter has described preliminary investigations into alterations in ET_B expression during physiological salt loading of *EDNRB*-LacZ(2) mice. The main points are:

- It is possible to measure β-gal activity in tissues isolated from *EDNRB*-LacZ(2) mice using a methylumbelliferone fluorescent assay. However, high endogenous β-gal expression in kidneys makes it difficult to measure low levels of exogenous transgene activity.
- When fed a high salt diet, *EDNRB*-LacZ(2) mice had slightly increased β-gal activity in whole renal homogenates compared to mice fed a normal salt diet

suggesting that renal ET_B expression may be upregulated by increased salt intake.

- Further studies are necessary to establish precise cellular sites of increased ET_B expression.

CHAPTER 7

FINAL DISCUSSION

7.1 SUMMARY

The importance of the kidney in regulation of blood pressure was highlighted by Guyton many years ago (Guyton *et al.*, 1972). He emphasised the central role played by pressure natriuresis in opposing incremental increases in blood pressure. Any increase in blood pressure is compensated by an increase in renal excretion of salt and water. Thus, any alteration in the mechanisms regulating renal sodium excretion could provoke the development of hypertension. Since hypertension is a major risk factor for atherosclerosis, stroke and other cardiovascular diseases, elucidation of the mechanisms involved in sodium homeostasis may have important therapeutic implications.

This thesis has explored the concept that renal NO plays a vital role in regulating sodium homeostasis and that aberrations in the pathways controlling NO production may result in renal ED, sodium retention and contribute to the pathogenesis of hypertension (see figure 7-1). Much of the evidence to date implicates eNOS as the major enzyme responsible for NO-mediated inhibition of sodium reabsorption (reviewed in section 1.2.2.1), although little is known of the cellular and molecular mechanisms involved in regulating eNOS activity within the kidney. Since eNOS-mediated NO generation encompasses a wide array of regulatory mechanisms, I chose to investigate two distinct areas. In the first part of this thesis, regulation of eNOS activity through interactions with regulatory proteins and how these may alter during ED was investigated. In the second part of the thesis the focus shifted to the mechanisms involved in the activation of renal eNOS, in particular interactions with the endothelin system. The main findings will be summarised in this chapter. The potential contributions to the enhanced understanding of the basic cellular and molecular mechanisms involved in renal eNOS regulation and clinical relevance will also be discussed.

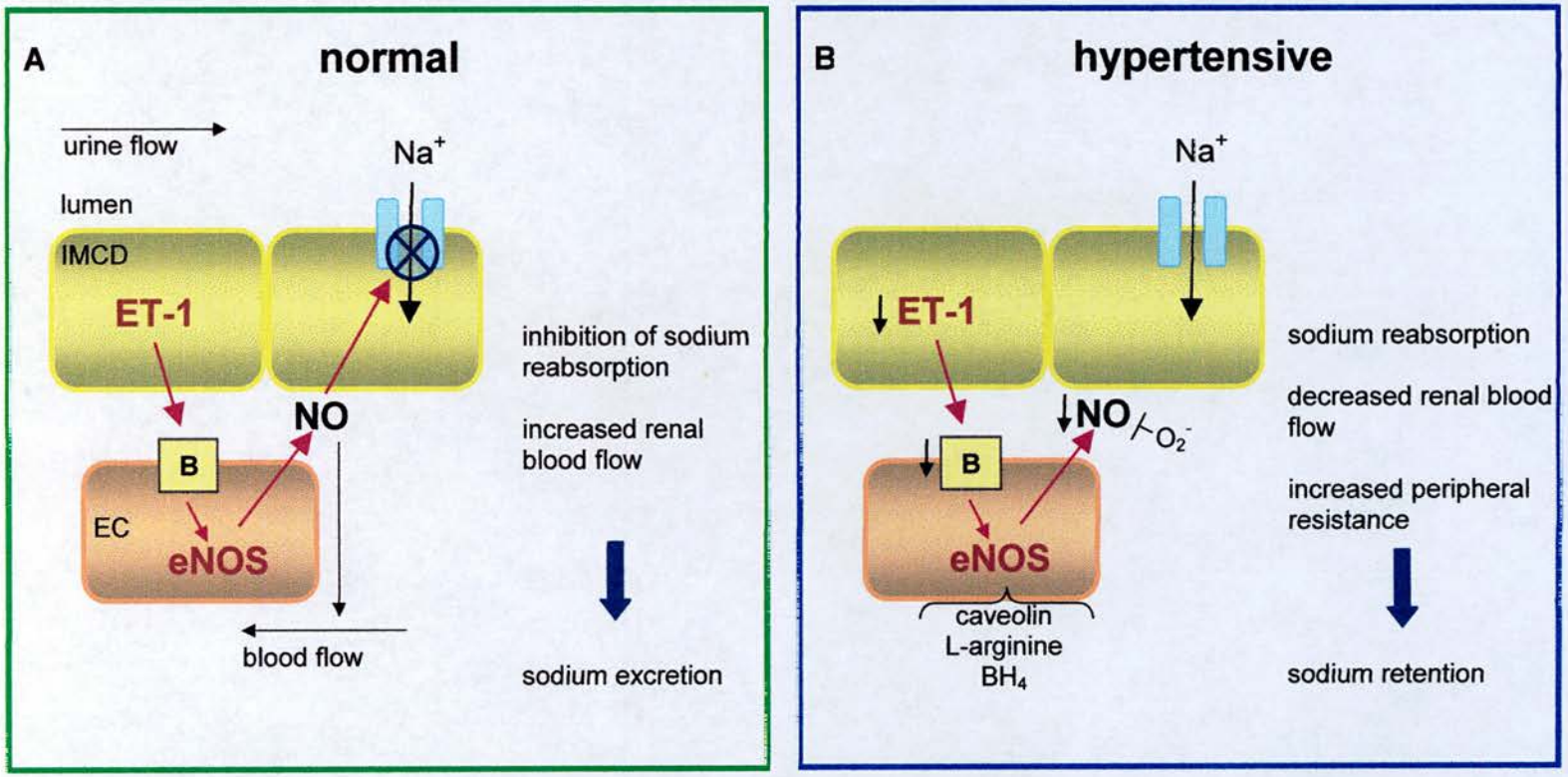

Figure 7-1. Hypothetical regulation of NO-mediated sodium transport in normal subjects and hypertensive patients. In normotensives, IMCD cells produce large amounts of ET-1, which act through ET_B in endothelial cells of the vasa recta, thereby activating eNOS to generate NO. NO acts simultaneously to inhibit sodium reasborption and increase medullary blood flow resulting in marked natriuresis and diuresis. In hypertensives, NO availability is decreased as a result of depressed ET-1 production or abnormal eNOS regulation. The end result is increased sodium reabsorption, decreased renal blood flow and increased peripheral resistance leading to an overall effect of sodium retention.

7.2 GENERAL DISCUSSION AND FUTURE WORK

7.2.1 Regulation of renal eNOS activity

Several studies have investigated whether diminished eNOS expression is responsible for reduced NO bioavailability in the SHR. Although some studies have reported decreased eNOS expression (Cuevas *et al.*, 1996; Chou *et al.*, 1998), the majority of reports, including the results presented here, have found that eNOS expression is, in fact, augmented in the SHR compared to normotensive, WKY rats (Bauersachs *et al.*, 1998; Nava *et al.*, 1998; Vaziri *et al.*, 1998; Vaziri *et al.*, 2000). The data presented in chapter 3 revealed that eNOS expression in the heart and kidney of SHR was upregulated suggesting that ED in the SHR is not associated with translational abnormalities of eNOS expression. On the contrary, it is hypothesised by others that eNOS expression may be increased as a result of elevated blood pressure (Nava *et al.*, 1998; Vaziri *et al.*, 1998). However, determination of protein expression does not provide information on the ability of the tissue to generate NO. Several other factors control eNOS-mediated NO release. One of these factors, eNOS-caveolin interactions, was investigated. No differences in caveolin expression levels were observed between SHR and WKY. Nevertheless, one of the aims of this chapter was to investigate if alterations in eNOS-caveolin protein interactions were associated with ED in the SHR. Unfortunately, this was not fully addressed due to technical difficulties. Despite these problems, the failure to observe eNOS-caveolin protein interactions within tissue did raise important questions concerning the extent to which these proteins interact *in vivo*.

The majority of the investigations on eNOS-caveolin interactions have been performed *in vitro*. Only recently has there been a report documenting *in vivo* interactions in rat aortas (Murata *et al.*, 2002). It will therefore be of interest to determine if these data are reproducible in different tissues using the exact conditions for co-immunoprecipitation documented in this report. Once established, these conditions can be used to address the original aim of whether eNOS-caveolin interactions are altered during ED.

Another important area which requires further investigation is the lack of histochemical data supporting the biochemical evidence for the existence of eNOS-caveolin interactions (see section 3.3). Therefore, future studies may involve analysis of eNOS and caveolin localisation within fixed tissue sections by immunohistochemisty. Although this will not provide much information on intracellular localisation, it will help to elucidate if these proteins are at least found within the same cells. In particular, it will be interesting to use this technique to establish if eNOS and caveolin co-localise to the same cells within the kidney.

eNOS has also been reported to interact with a number of other proteins (e.g. bradykinin receptor, angiotensin receptor, ET_B, hsp90, NOSIP, NOSTRIN (Garcia-Cardena *et al.*, 1998; Ju *et al.*, 1998; Marrero *et al.*, 1999; Dedio *et al.*, 2001; Zimmermann *et al.*, 2002)). Again, these data are the result of several *in vitro* studies and remain to be confirmed *in vivo*. Furthermore, the physiological relevance of these eNOS protein-protein interactions is awaited with much anticipation.

One of the major flaws of this study was that NOS activity was not measured. Determination of NOS activity in SHR kidneys would have provided information on whether renal eNOS regulation was abnormal in these animals. However, a previous study suggests that NOS activity is actually augmented in SHR kidneys compared to WKY (Nava *et al.*, 1996). These animals were of a similar age to those used in this study. Elevated NOS activity has also been reported in other tissues of the SHR (Nava *et al.*, 1998; Vaziri *et al.*, 1998). In addition, some reports documented that urinary excretion and plasma concentration of NO metabolites (NO_2 and NO_3) are also increased in SHR (Nava *et al.*, 1998; Vaziri *et al.*, 1998). Together these data imply that ED in the SHR is not associated with diminished eNOS activity or NO production. Instead the NO pathway appears to be activated suggesting that ED is a result of some mechanism other than reduced eNOS activity. Indeed, there are numerous reports providing alternative reasons for why the SHR develops ED. These include inactivation of NO by superoxide (Bauersachs *et al.*, 1998; Vaziri *et al.*, 2000), downregulation of sGC expression (Bauersachs *et al.*, 1998; Ruetten *et al.*,

1999), an inability of NO to activate sGC/cGMP (Nava *et al.*, 1998) and release of endothelial derived contracting factors which counteract the effects of NO (Luscher & Vanhoutte, 1986; Luscher *et al.*, 1990). It would appear that development of ED in the SHR cannot be attributed to a single mechanism but is a multifactorial process. It is also clear from the literature that ED in the SHR manifests itself differently depending on the tissue of interest and the age of the animal. This therefore makes data difficult to interpret.

This is also true of other animal models of hypertension where ED presents different characteristics depending on the model being studied. For example, unlike the SHR, the Dahl salt sensitive hypertensive rat has reduced expression of eNOS in the kidney compared to normotensive control rats (Ni *et al.*, 1999). This is accompanied by decreased NOS activity (Luscher *et al.*, 1987). A similar observation has been reported for the two-kidney, one-clip hypertensive rat (Wickman *et al.*, 2001). It may therefore be of interest to further investigate alterations in eNOS and caveolin expression in different models of ED, particularly those in which eNOS activity is depressed.

The array of studies on animal models of hypertension highlights the many different mechanisms which are involved in the pathogenesis of ED. A similar situation probably occurs in hypertensive patients and therefore presents a challenging prospect in further elucidation of the cellular and molecular mechanisms underlying ED in hypertension.

7.2.2 Regulation of renal eNOS activation

One of the important aspects of this thesis was to highlight the importance of eNOS within the kidney. The pathways that control renal eNOS activity have not yet been clarified. One of the major questions that remains unanswered is what is the major physiological activator of eNOS within the kidney. Much of the evidence to date implicates the endothelin system as a major stimulator of renal eNOS ((Hoffman *et al.*, 2000; Plato *et al.*, 2000a; Plato *et al.*, 2000b) and reviewed in section 1.2.2.7).

The second part of this thesis investigated the cellular mechanisms involved in ET-1/ ET_B mediated activation of eNOS by localising ET_B to specific cells within the kidney. This was achieved using a transgenic mouse in which a LacZ reporter gene was under the control of *EDNRB* transcription. The main finding was that the *EDNRB*-LacZ(2) transgene was highly expressed within the inner medulla of homozygote mice. LacZ gene expression was confined to the endothelial cells of the vasa recta, whereas tubular cells were negative for LacZ gene expression. This indicated that the major site of medullary ET_B expression is within the capillaries of the inner medulla and supports the hypothesis that ET-1, released from IMCD cells, binds ET_B on endothelial cells and therefore acts as a paracrine substance.

Although localisation of LacZ gene expression was confirmed by an expert renal histologist, there are additional studies which could be performed to strengthen these results. In particular, the use of antibodies directed against endothelial cell markers (e.g. CD31, Flk-1) would help to confirm the presence of endothelial ET_B expression. Double staining of kidney sections with these antibodies and anti-β-gal antibodies will further help in the precise localisation of ET_B. In addition, antibodies specific for IMCD cells could be used to prove that these cells are negative for LacZ gene expression.

One of the main areas in which further investigation is warranted is to clarify the reasons for the differences observed in LacZ gene expression between heterozygote and homozygote *EDNRB*-LacZ(2) mice. In theory, LacZ gene expression in heterozygote mice should be half that of homozygote mice. However, heterozygote mice displayed significantly reduced LacZ gene expression. It is hypothesised that the reason for this discrepancy is the differences in ages at which these animals were studied. Therefore, staining of young heterozygote mice (aged 2-3 weeks) is required to investigate this possibility. These studies are ongoing.

In addition, further experiments will include analysis of the *EDNRB*-LacZ mice. Unfortunately, the final *EDNRB*-LacZ mice were born only a few weeks before the

submission of this thesis. Due to time constraints and low numbers of animals, full investigation of LacZ gene expression within the kidney was not possible. However, preliminary investigations within the lung offered promising results and analysis of renal LacZ gene expression in these mice is underway. It will be interesting to compare renal expression between the different strains, bearing in mind that the targeting constructs used to generate the two strains of mice were different.

The knock-in mice also offer opportunities for a wide array of physiological studies. Chapter 6 described a preliminary experiment investigating how salt loading affects ET_B expression by measuring β-gal activity in whole kidney homogenates. Initial results were promising showing a slight increase in renal β-gal activity in mice fed high salt diets and suggest that ET_B expression may be upregulated during increased salt intake. This provides further support for the proposal that ET_B is involved in mediating sodium transport. However, in order to validate these data will require higher numbers of animals. In addition, it will be important to establish precisely which intrarenal cellular sites are responsible for increased ET_B expression. One possibility would be to measure β-gal activity separately within the cortex and medulla. Alternatively, more precise localisation of altered ET_B expression could be achieved by staining kidney sections as performed in chapter 5. Obviously this is a more challenging idea as strict criteria will have to be used for counting cells in order for the researcher to remain objective. However, under the correct conditions this may yield valuable information.

The *EDNRB*-LacZ mice are also a valuable resource for investigating regulation of ET_B expression under other physiological and pathophysiological challenges (e.g. changes in osmotic pressure, coronary artery ligation and heart failure, hypoxia and pulmonary hypertension). However, it should be noted that β-gal has been reported to be a very stable protein which limits the use of these mice only to studies in which upregulation of ET_B expression will occur. Nevertheless, the opportunities for further work are vast.

7.3 CLINICAL IMPLICATIONS

Hypertension is prevalent in the western world and is a major risk factor for atherosclerosis, stroke and other cardiovascular diseases. A common feature of human hypertension is sodium retention where hypertensive patients are unable to excrete salt and water at normal blood pressure levels. Instead, abnormal renal function means that these patients are only able to excrete salt and water at high levels of arterial pressure. In other words, the pressure-natriuresis curve has been shifted to the right, towards higher pressures. In addition, a large percentage of human hypertensive patients are salt sensitive where high salt intake exacerbates hypertension. However, the underlying molecular mechanisms of sodium retention and salt sensitivity in hypertension are unknown. Much of the evidence discussed in this thesis suggests that aberrations in the renal NO and endothelin systems may play a role in the pathogenesis of hypertension. Hypertensive patients have diminished renal excretion of NO metabolites (NO_2 and NO_3) (Sierra *et al.*, 1998). Systemic infusion of L-arginine showed the existence of a blunted renal vasodilatation in hypertensive patients compared to normotensives (Higashi *et al.*, 1995). This renal ED may result from decreased activation of NO production by ET-1. Indeed, daily urinary excretion of ET-1 was significantly decreased in hypertensive patients compared to normotensive subjects (Hoffman *et al.*, 1994). Furthermore, when hypertensive patients were given high sodium diets, a salt-sensitive subset excreted less urinary ET-1 than the salt-resistant subset. It should be clear from the data discussed in this thesis that diminished medullary ET-1 production and NO availability may cause impaired sodium and water excretion and impaired renal blood flow thus promoting sodium retention (summarised in figure 7-1). Therefore, decreased NO and ET-1 synthesis may be contributing factors in hypertension and salt sensitivity.

However, interpretation of these data is complicated by the dual nature of ET-1 within the kidney. Within the renal vasculature, ET-1 action results in vasoconstriction via activation of ET_A. Enhanced renal vasoconstriction reduces

renal blood flow and glomerular filtration rate and subsequently decreases sodium and water excretion. Therefore, enhanced levels of ET-1 within the renal vasculature or alterations in vascular sensitivity to ET-1 may be contributing factors to hypertension. Nevertheless, investigations designed to address these possibilities have not led to satisfactory conclusions. Although the endothelin system may be activated in experimental animal models of hypertension (e.g. DOCA-salt rats, Dahl salt-sensitive rats) (reviewed in (Schiffrin, 1999)), similar studies in humans have not demonstrated a clear association between hypertension and high circulating endothelin levels (Goddard & Webb, 2000). However, this does not rule out the possibility that local production of ET-1 may be increased in hypertension.

It is therefore difficult to establish the role of the endothelin system in hypertension due to the opposing actions (i.e. vasoconstriction versus natriuresis/diuresis) of renal ET-1. Furthermore, the dual action of ET-1 must be carefully assessed when considering the use of endothelin receptor antagonists as therapeutic agents.

Selective ET_A antagonists and combined ET_A/ET_B antagonists are currently undergoing clinical trials and may represent a new category of drugs that are useful in treating patients with hypertension (reviewed in (Benigni & Remuzzi, 1999)). Indeed, Bosentan, a non-selective antagonist, was shown to lower blood pressure in hypertensive patients (Krum *et al.*, 1998) and is already in clinical use as a treatment for pulmonary hypertension (Rubin *et al.*, 2002). However, since ET_B activation is physiologically thought to have an overall hypotensive effect, blockade of ET_B, particularly within the kidney, may not be desirable and could theoretically worsen ET_A-induced renal vasoconstriction. Therefore, endothelin receptor selectivity of antagonists for therapeutic purposes must be considered with extreme caution.

7.4 CONCLUDING REMARKS

In conclusion, the work described in this thesis has contributed to an enhanced understanding of the basic cellular and molecular mechanisms involved in the regulation and activation of renal eNOS. The salient finding has been the observation that ET_B is highly expressed within the capillaries of the renal medulla, corresponding to the major site of eNOS expression and provides further evidence in favour of the proposal that ET-1 is one of the main physiological activators of renal eNOS. Further elucidation of how this pathway and other factors involved in the regulation of renal eNOS are affected during renal ED, may provide important information regarding the mechanisms involved in the pathogenesis of hypertension.

BIBLIOGRAPHY

Ahn, D., Stricklett, P. K., Nelson, R. D., Gill, P., Yanagisawa, M., Kishore, B., Westenfelder, C., Baranowski, R. & Kohan, D. E. (2002). Abstract "Collecting duct-specific knockout of endothelin-1 in mice causes hypertension and impaired fluid excretion". American Society of Nephrology 35th Annual Meeting. Philadelphia, USA.

Aisaka, K., Gross, S. S., Griffith, O. W. & Levi, R. (1989). "NG-methylarginine, an inhibitor of endothelium-derived nitric oxide synthesis, is a potent pressor agent in the guinea pig: does nitric oxide regulate blood pressure in vivo?" *Biochem Biophys Res Commun* **160**(2): 881-886.

Alam, J. & Cook, J. (1990). "Reporter genes: application to the study of mammalian gene transcription." *Anal Biochem* **188**(2): 245-254.

Allcock, G., Hukkanen, M., Polak, J., Pollock, J. S. & Pollock, D. M. (1999). "Increased nitric oxide synthase-3 expression in kidneys of deoxycorticosterone acetate-salt hypertensive rats." *J Am Soc Nephrol* **10**(11): 2283-2289.

Alonso, J., Sanchez de Miguel, L., Monton, M., Casado, S. & Lopez-Farre, A. (1997). "Endothelial cytosolic proteins bind to the 3' untranslated region of endothelial nitric oxide synthase mRNA: regulation by tumor necrosis factor alpha." *Mol Cell Biol* **17**(10): 5719-5726.

Anderson, R. G. (1998). "The caveolae membrane system." *Annu Rev Biochem* **67**: 199-225.

Andries, L., Brutsaert, D. & Sys, S. (1998). "Nonuniformity of endothelial constitutive nitric oxide synthase distribution in cardiac endothelium." *Circ Res* **82**: 195-203.

Aria, H., Nakao, K., Takaya, K., Hosoda, K., Ogawa, Y., Nakanishi, S. & Imura, H. (1993). "The human endothelin-B receptor gene. Structural organization and chromosomal assignment." *J Biol Chem* **268**(5): 3463-3470.

Arnal, J. F., Clamens, S., Pechet, C., Negre-Salvayre, A., Allera, C., Girolami, J. P., Salvayre, R. & Bayard, F. (1996). "Ethinylestradiol does not enhance the expression of nitric oxide synthase in bovine endothelial cells but increases the release of bioactive nitric oxide by inhibiting superoxide anion production." *Proc Natl Acad Sci U S A* **93**(9): 4108-4113.

Arnal, J. F., Yamin, J., Dockery, S. & Harrison, D. G. (1994). "Regulation of endothelial nitric oxide synthase mRNA, protein, and activity during cell growth." *Am J Physiol* **267**(5 Pt 1): C1381-1388.

Arnet, U. A., McMillan, A., Dinerman, J. L., Ballermann, B. & Lowenstein, C. J. (1996). "Regulation of endothelial nitric-oxide synthase during hypoxia." *J Biol Chem* **271**(25): 15069-15073.

Bachmann, S., Bosse, H. & Mundel, P. (1995). "Topography of nitric oxide synthesis by localizing constitutive NO synthases in mammalian kidney." *Am J Physiol* **268**(5Pt2): F885-898.

Bauersachs, J., Bouloumie, A., Mulsch, A., Wiemer, G., Fleming, I. & Busse, R. (1998). "Vasodilator dysfunction in aged spontaneously hypertensive rats: changes in NO synthase III and soluble guanylyl cyclase expression, and in superoxide anion production." *Cardiovasc Res* **37**: 772-779.

Bauersachs, J., Fleming, I., Scholz, D., Popp, R. & Busse, R. (1997). "Endothelium-derived hyperpolarizing factor, but not nitric oxide, is reversibly inhibited by brefeldin A." *Hypertension* **30**(6): 1598-1605.

Benigni, A. & Remuzzi, G. (1999). "Endothelin antagonists." *The Lancet* **353**: 133-138.

Benjafield, A. & Morris, B. (2000). "Association analyses of endothelial nitric oxide synthase gene polymorphisms in essential hypertension." *Am J Hypertens* **13**(9): 994-998.

Blair, A., Shaul, P. W., Yuhanna, I. S., Conrad, P. & Smart, E. J. (1999). "Oxidized low density lipoprotein displaces endothelial nitric-oxide synthase (eNOS) from plasmalemmal caveolae and impairs eNOS activation." *J Biol Chem* **274**(45): 32512-32519.

Bloch, W., Forsberg, E., Lentini, S., Brakebusch, C., Martin, K., Krell, H., Weidle, U., Addicks, K. & Fassler, R. (1997). "B1 integrin is essential for teratoma growth and angiogenesis." *J Cell Biol* **139**(1): 265-278.

Bonnardeaux, A., Nadaud, S., Charru, A., Jeunemaitre, X., Corvol, P. & Soubrier, F. (1995). "Lack of evidence for linkage of the endothelial cell nitric oxide synthase gene to essential hypertension." *Circulation* **91**(1): 96-102.

Bossaller, C., Habib, G., Yamamoto, H., Williams, C., Well, S. & Henry, P. (1987). "Impaired muscarinic endothelium-dependent relaxation and cyclic guanosine 5'-monophosphate formation in atherosclerotic human coronary artery and rabbit aorta." *J Clin Invest* **79**(1): 170-174.

Bouloumie, A., Bauersachs, J., Linz, W., Scholkens, B., Wiemer, G., Fleming, I. & Busse, R. (1997). "Endothelial dysfunction coincides with an enhanced nitric oxide synthase expression and superoxide anion production." *Hypertension* **30**(4): 934-941.

Bouloumie, A., Schini-Kerth, V. B. & Busse, R. (1999). "Vascular endothelial growth factor up-regulates nitric oxide synthase expression in endothelial cells." *Cardiovasc Res* **41**(3): 773-780.

Bradford, M. M. (1976). "A rapid and sensitive method for the quantitation of microgram quantities of protein utilizing the principle of protein-dye binding." *Anal Biochem* **72**: 248-254.

Bradley, A., Evans, M., Kaufman, M. & Robertson, E. (1984). "Formation of germ-line chimaeras from embryo-derived teratocarcinoma cell lines." *Nature* **309**(5965): 255-256.

Braell, W. (1991). B-galactosidase assay using the TK100 mini-fluorometer. San Francisco, Hoefer Scientific Instruments.

Breton, S., Lisanti, M. P., Tyszkowski, R., McLaughlin, M. & Brown, D. (1998). "Basolateral distribution of caveolin-1 in the kidney. Absence from H^+-ATPase-coated endocytic vesicles in intercalated cells." *J Histochem Cytochem* **46**(2): 205-214.

Bretscher, M. S. & Whytock, S. (1977). "Membrane-associated vesicles in fibroblasts." *J Ultrastruct Res* **61**(2): 215-217.

Bucci, M., Gratton, J. P., Rudic, R. D., Acevedo, L., Roviezzo, F., Cirino, G. & Sessa, W. C. (2000). "In vivo delivery of the caveolin-1 scaffolding domain inhibits nitric oxide synthesis and reduces inflammation." *Nat Med* **6**(12): 1362-1367.

Buga, G. M., Singh, R., Pervin, S., Rogers, N., Schmitz, D., Jenkinson, C., Cederbaum, S. & Ignarro, L. J. (1996). "Arginase activity in endothelial cells: inhibition by NG-hydroxy-L-arginine during high-output NO production." *Am J Physiol* **271**(5 Pt 2): H1988-1998.

Burnier, M., Centeno, G., Burki, E. & Brunner, H. R. (1994). "Confocal microscopy to analyze cytosolic and nuclear calcium in cultured vascular cells." *Am J Physiol* **266**(4 Pt 1): C1118-1127.

Busconi, L. & Michel, T. (1993). "Endothelial nitric oxide synthase. N-terminal myristoylation determines subcellular localization." *J Biol Chem* **268**(12): 8410-8413.

Busse, R., Trogisch, G. & Bassenge, E. (1985). "The role of endothelium in the control of vascular tone." *Basic Res Cardiol* **80**(5): 475-490.

Chaney, L. & Jacobson, B. (1983). "Coating cells with colloidal silica for high yield isolation of plasma membrane sheets and identification of transmembrane proteins." *J Biol Chem* **258**(16): 10062-10072.

Chen, P. & Sanders, P. (1991). "L-arginine abrogates salt-sensitive hypertension in Dahl/Rapp rats." *J Clin Invest* **88**(5): 1559-1567.

Chen, S., Cao, L., Intengan, H., Humphreys, M. & Gardner, D. (2002). "Osmoregulation of endothelial nitric-oxide synthase gene expression in inner medullary collecting duct cells. Role in activation of the type A natriuretic peptide receptor." *J Biol Chem* **277**(36): 32498-32504.

Cheng, S., Fockler, C., Barnes, W. & Higuchi, R. (1994). "Effective amplification of long targets from cloned inserts and human genomic DNA." *Proc Natl Acad Sci USA* **91**(12): 5695-5699.

Chou, T., Yen, M., Li, C. & Ding, Y. (1998). "Alterations in nitric oxide synthase expression with aging and hypertension in rats." *Hypertension* **31**: 643-648.

Chow, L., Subramanian, S., Nuovo, G., Miller, F. & Nord, E. (1995). "Endothelin receptor mRNA expression in renal medulla identified by in situ RT-PCR." *Am J Physiol* **269**(3Pt2): F449-457.

Chun, M., Liyanage, U. K., Lisanti, M. P. & Lodish, H. F. (1994). "Signal transduction of a G protein-coupled receptor in caveolae: colocalization of endothelin and its receptor with caveolin." *Proc Natl Acad Sci U S A* **91**(24): 11728-11732.

Cieslik, K., Lee, C. M., Tang, J. L. & Wu, K. K. (1999). "Transcriptional regulation of endothelial nitric-oxide synthase by an interaction between casein kinase 2 and protein phosphatase 2A." *J Biol Chem* **274**(49): 34669-34675.

Clavell, A. L., Stingo, A. J., Margulies, K. B., Brandt, R. R. & Burnett, J. C., Jr. (1995). "Role of endothelin receptor subtypes in the in vivo regulation of renal function." *Am J Physiol* **268**(3 Pt 2): F455-460.

Clowes, A. W., Reidy, M. A. & Clowes, M. M. (1983). "Kinetics of cellular proliferation after arterial injury. I. Smooth muscle growth in the absence of endothelium." *Lab Invest* **49**(3): 327-333.

Cooke, J. P., Stamler, J., Andon, N., Davies, P. F., McKinley, G. & Loscalzo, J. (1990). "Flow stimulates endothelial cells to release a nitrovasodilator that is potentiated by reduced thiol." *Am J Physiol* **259**(3 Pt 2): H804-812.

Corson, M. A., James, N. L., Latta, S. E., Nerem, R. M., Berk, B. C. & Harrison, D. G. (1996). "Phosphorylation of endothelial nitric oxide synthase in response to fluid shear stress." *Circ Res* **79**(5): 984-991.

Couet, J., Li, S., Okamoto, T., Ikezu, T. & Lisanti, M. P. (1997). "Identification of peptide and protein ligands for the caveolin- scaffolding domain. Implications for the interaction of caveolin with caveolae-associated proteins." *J Biol Chem* **272**(10): 6525-6533.

Cowley, A. W. (1997). "Role of the renal medulla in volume and arterial pressure regulation." *Am J Physiol* **273**: R1-15.

Creager, M., Gallagher, S., Girerd, X., Coleman, S., Dzau, V. & Cooke, J. P. (1992). "L-arginine improves endothelium-dependent vasodilation in hypercholesterolemic humans." *J Clin Invest* **90**(4): 1248-1253.

Cuevas, P., Garcia-Calvo, M., Carceller, F., Reimers, D., Dazo, M., Cuevas, B., Munoz-Willery, I., Martinez-Coso, F., Lamas, S. & Gimenez-Gallego, G. (1996). "Correction of hypertension by normalization of endothelial level of fibroblast growth factor and nitric oxide synthase in spontaneously hypertensive rats." *Proc Natl Acad Sci USA* **93**: 11996-12001.

Davenport, A. P., Nunez, D. J. & Brown, M. J. (1989). "Binding sites for 125I-labelled endothelin-1 in the kidneys: differential distribution in rat, pig and man demonstrated by using quantitative autoradiography." *Clinical Science* **77**: 129-131.

de Nucci, G., Thomas, R., D'Orleans-Juste, P., Antunes, E., Walder, C., Warner, T. D. & Vane, J. R. (1988). "Pressor effects of circulating endothelin are limited by its removal in the pulmonary circulation and by the release of prostacyclin and endothelium-derived relaxing factor." *Proc Natl Acad Sci U S A* **85**(24): 9797-9800.

de Weerd, W. F. & Leeb-Lundberg, L. M. (1997). "Bradykinin sequesters B2 bradykinin receptors and the receptor-coupled Galpha subunits Galphaq and Galphai in caveolae in DDT1 MF-2 smooth muscle cells." *J Biol Chem* **272**(28): 17858-17866.

Dean, R., Zhuo, J., Alcorn, D., Casley, D. & Mendelsohn, F. A. (1994). "Cellular distribution of 125I-endothelin-1 binding in rat kidney following in vivo labeling." *Am J Physiol* **267**(5 Pt 2): F845-852.

Dean, R., Zhuo, J., Alcorn, D., Casley, D. & Mendelsohn, F. A. (1996). "Cellular localization of endothelin receptor subtypes in the rat kidney following in vitro labelling." *Clin Exp Pharm Physio* **23**: 524-531.

Dedio, J., Konig, P., Wohlfart, P., Schroeder, C., Kummer, W. & Muller-Esterl, W. (2001). "NOSIP, a novel modulator of endothelial nitric oxide synthase activity." *FASEB J* **15**(79-89.).

Deng, C. & Capecchi, M. (1992). "Reexamination of gene targeting frequency as a function of the extent of homology between the targeting vector and the target locus." *Mol Cell Biol* **12**(8): 3365-3371.

Deng, L., Day, R. & Schiffrin, E. (1996). "Localization of sites of enhanced expression of endothelin-1 in the kidney of DOCA-salt hypertensive rats." *J Am Soc Nephrol* **7**(8): 1158-1164.

Dietzen, D. J., Hastings, W. R. & Lublin, D. M. (1995). "Caveolin is palmitoylated on multiple cysteine residues. Palmitoylation is not necessary for localization of caveolin to caveolae." *J Biol Chem* **270**(12): 6838-6842.

Dimmeler, S., Fleming, I., Fisslthaler, B., Hermann, C., Busse, R. & Zeiher, A. M. (1999). "Activation of nitric oxide synthase in endothelial cells by Akt- dependent phosphorylation." *Nature* **399**(6736): 601-605.

Drab, M., Verkade, P., Elger, M., Kasper, M., Lohn, M., Lauterbach, B., Menne, J., Lindschau, C., Mende, F., Luft, F. C., Schedl, A., Haller, H. & Kurzchalia, T. V. (2001). "Loss of caveolae, vascular dysfunction, and pulmonary defects in caveolin-1 gene-disrupted mice." *Science* **293**(5539): 2449-2452.

Draznin, M. B., Rapoport, R. M. & Murad, F. (1986). "Myosin light chain phosphorylation in contraction and relaxation of intact rat thoracic aorta." *Int J Biochem* **18**(10): 917-928.

Drummond, G. R., Cai, H., Davis, M. E., Ramasamy, S. & Harrison, D. G. (2000). "Transcriptional and posttranscriptional regulation of endothelial nitric oxide synthase expression by hydrogen peroxide." *Circ Res* **86**(3): 347-354.

Dupree, P., Parton, R. G., Raposo, G., Kurzchalia, T. V. & Simons, K. (1993). "Caveolae and sorting in the trans-Golgi network of epithelial cells." *Embo J* **12**(4): 1597-1605.

Feron, O., Belhassen, L., Kobzik, L., Smith, T. W., Kelly, R. A. & Michel, T. (1996). "Endothelial nitric oxide synthase targeting to caveolae. Specific interactions with caveolin isoforms in cardiac myocytes and endothelial cells." *J Biol Chem* **271**(37): 22810-22814.

Feron, O., Dessy, C., Moniotte, S., Desager, J.-P. & Balligand, J.-L. (1999). "Hypercholesterolemia decreases nitric oxide production by promoting the interaction of caveolin and endothelial nitric oxide synthase." *J Clin Invest* **103**(6): 897-905.

Feron, O., Michel, J. B., Sase, K. & Michel, T. (1998a). "Dynamic regulation of endothelial nitric oxide synthase: Complementary roles of dual acylation and caveolin interactions." *Biochemistry* **37**: 193-200.

Feron, O., Saldana, F., Michel, J. B. & Michel, T. (1998b). "The endothelial nitric-oxide synthase-caveolin regulatory cycle." *J Biol Chem* **273**(6): 3125-3128.

Filep, J. G., Battistini, B., Cote, Y. P., Beaudoin, A. R. & Sirois, P. (1991). "Endothelin-1 induces prostacyclin release from bovine aortic endothelial cells." *Biochem Biophys Res Commun* **177**(1): 171-176.

Fire, A. (1992). "Histochemical techniques for locating Escherichia coli beta-galactosidase activity in transgenic organisms." *Genet Anal Tech Appl* **9**(5-6): 151-158.

Fleming, I. & Busse, R. (1999). "Signal transduction of eNOS activation." *Cardiovasc Res* **43**(3): 532-541.

Fleming, I. & Busse, R. (2003). "Molecular mechanisms involved in the regulation of the endothelial nitric oxide synthase." *Am J Physiol Regul Integr Comp Physiol* **284**(1): R1-12.

Fleming, I., Fisslthaler, B., Dimmeler, S., Kemp, B. E. & Busse, R. (2001). "Phosphorylation of Thr(495) regulates Ca(2+)/calmodulin-dependent endothelial nitric oxide synthase activity." *Circ Res* **88**(11): E68-75.

Flowers, M. A., Wang, Y., Stewart, R. J., Patel, B. & Marsden, P. A. (1995). "Reciprocal regulation of endothelin-1 and endothelial constitutive NOS in proliferating endothelial cells." *Am J Physiol* **269**(6 Pt 2): H1988-1997.

Forbes, M. S., Rennels, M. L. & Nelson, E. (1979). "Caveolar systems and sarcoplasmic reticulum in coronary smooth muscle cells of the mouse." *J Ultrastruct Res* **67**(3): 325-339.

Forstermann, U., Boissel, J. P. & Kleinert, H. (1998). "Expressional control of the 'constitutive' isoforms of nitric oxide synthase (NOS I and NOS III)." *FASEB J* **12**(10): 773-790.

Fra, A. M., Williamson, E., Simons, K. & Parton, R. G. (1995). "De novo formation of caveolae in lymphocytes by expression of VIP21- caveolin." *Proc Natl Acad Sci U S A* **92**(19): 8655-8659.

Fujimoto, T. (1993). "Calcium pump of the plasma membrane is localized in caveolae." *J Cell Biol* **120**(5): 1147-1157.

Fukuda, S., Takaichi, S., Naritomi, H., Hashimoto, N., Nagata, I., Nozaki, K. & Kikuchi, H. (1995). "Ultrastructural localization and translocation of nitric oxide synthase in the endothelium of the human cerebral artery." *Brain Res* **696**(1-2): 30-36.

Fulton, D., Fontana, J., Sowa, G., Gratton, J. P., Lin, M., Li, K. X., Michell, B., Kemp, B. E., Rodman, D. & Sessa, W. C. (2002). "Localization of endothelial nitric-oxide synthase phosphorylated on serine 1179 and nitric oxide in Golgi and plasma membrane defines the existence of two pools of active enzyme." *J Biol Chem* **277**(6): 4277-4284.

Fulton, D., Gratton, J. P., McCabe, T. J., Fontana, J., Fujio, Y., Walsh, K., Franke, T. F., Papapetropoulos, A. & Sessa, W. C. (1999). "Regulation of endothelium-derived nitric oxide production by the protein kinase Akt." *Nature* **399**(6736): 597-601.

Fulton, D., Gratton, J. P. & Sessa, W. C. (2001). "Post-translational control of endothelial nitric oxide synthase: why isn't calcium/calmodulin enough?" *J Pharmacol Exp Ther* **299**(3): 818-824.

Furchgott, R. F., Khan, M. T. & Jothianandan, D. (1987). "Evidence supporting the proposal that endothelium-derived relaxing factor is nitric oxide." *Thrombosis Research* **Suppl VII**: 5.

Furchgott, R. F. & Vanhoutte, P. M. (1989). "Endothelium-derived relaxing and contracting factors." *FASEB J* **3**(9): 2007-2018.

Furchgott, R. F. & Zawadzki, J. V. (1980). "The obligatory role of endothelial cells in the relaxation of arterial smooth muscle by acetylcholine." *Nature* **288**(5789): 373-376.

Furlong, B., Henderson, A. H., Lewis, M. J. & Smith, J. A. (1987). "Endothelium-derived relaxing factor inhibits in vitro platelet aggregation." *Br J Pharmacol* **90**(4): 687-692.

Furuya, S., Naruse, S., Nakayama, T. & Nokihara, K. (1992). "Effect and distribution of intravenously injected ^{125}I-endothelin-1 in rat kidney and lung examined by electron microscopic radioautography." *Anat Embryol* **185**: 87-96.

Gallego, M. S. & Ling, B. N. (1996). "Regulation of amiloride-sensitive Na+ channels by endothelin-1 in distal nephron cells." *Am J Physiol* **271**(2 Pt 2): F451-460.

Gallis, B., Corthals, G. L., Goodlett, D. R., Ueba, H., Kim, F., Presnell, S. R., Figeys, D., Harrison, D. G., Berk, B. C., Aebersold, R. & Corson, M. A. (1999). "Identification of flow-dependent endothelial nitric-oxide synthase phosphorylation sites by mass spectrometry and regulation of phosphorylation and nitric oxide

production by the phosphatidylinositol 3-kinase inhibitor LY294002." *J Biol Chem* **274**(42): 30101-30108.

Garcia-Cardena, G., Fan, R., Shah, V., Sorrentino, R., Cirino, G., Papapetropoulos, A. & Sessa, W. (1998). "Dynamic activation of endothelial nitric oxide synthase by Hsp90." *Nature* **392**(6678): 821-824.

Garcia-Cardena, G., Fan, R., Stern, D. F., Liu, J. & Sessa, W. C. (1996a). "Endothelial nitric oxide synthase is regulated by tyrosine phosphorylation and interacts with caveolin-1." *J Biol Chem* **271**(44): 27237-27240.

Garcia-Cardena, G., Martasek, P., Masters, B. S., Skidd, P. M., Couet, J., Li, S., Lisanti, M. P. & Sessa, W. C. (1997). "Dissecting the interaction between nitric oxide synthase (NOS) and caveolin. Functional significance of the nos caveolin binding domain in vivo." *J Biol Chem* **272**(41): 25437-25440.

Garcia-Cardena, G., Oh, P., Liu, J., Schnitzer, J. E. & Sessa, W. C. (1996b). "Targeting of nitric oxide synthase to endothelial cell caveolae via palmitoylation: implications for nitric oxide signaling." *Proc Natl Acad Sci U S A* **93**(13): 6448-6453.

Gardiner, S. M., Compton, A. M., Bennett, T., Palmer, R. M. & Moncada, S. (1990). "Control of regional blood flow by endothelium-derived nitric oxide." *Hypertension* **15**(5): 486-492.

Garg, U. C. & Hassid, A. (1989). "Nitric oxide-generating vasodilators and 8-bromo-cyclic guanosine monophosphate inhibit mitogenesis and proliferation of cultured rat vascular smooth muscle cells." *J Clin Invest* **83**(5): 1774-1777.

Gariepy, C. E., Cass, D. T. & Yanagisawa, M. (1996). "Null mutation of endothelin receptor type B gene in spotting lethal rats causes aganglionic megacolon and white coat color." *Proc Natl Acad Sci U S A* **93**(2): 867-872.

Gariepy, C. E., Ohuchi, T., Williams, S. C., Richardson, J. A. & Yanagisawa, M. (2000). "Salt-sensitive hypertension in endothelin-B receptor-deficient rats." *J Clin Invest* **105**(7): 925-933.

Gariepy, C. E., Williams, S. C., Richardson, J. A., Hammer, R. E. & Yanagisawa, M. (1998). "Transgenic expression of the endothelin-B receptor prevents congenital intestinal aganglionosis in a rat model of Hirschsprung disease." *J Clin Invest* **102**(6): 1092-1101.

Geiger, R. V., Berk, B. C., Alexander, R. W. & Nerem, R. M. (1992). "Flow-induced calcium transients in single endothelial cells: spatial and temporal analysis." *Am J Physiol* **262**(6 Pt 1): C1411-1417.

Ghosh, S., Gachhui, R., Crooks, C., Wu, C., Lisanti, M. P. & Stuehr, D. J. (1998). "Interaction between caveolin-1 and the reductase domain of endothelial nitric-oxide synthase. Consequences for catalysis." *J Biol Chem* **273**(35): 22267-22271.

Glenney, J. R., Jr. (1989). "Tyrosine phosphorylation of a 22-kDa protein is correlated with transformation by Rous sarcoma virus." *J Biol Chem* **264**(34): 20163-20166.

Glenney, J. R., Jr. & Soppet, D. (1992). "Sequence and expression of caveolin, a protein component of caveolae plasma membrane domains phosphorylated on tyrosine in Rous sarcoma virus-transformed fibroblasts." *Proc Natl Acad Sci U S A* **89**(21): 10517-10521.

Goddard, J. & Webb, D. J. (2000). "Plasma endothelin concentrations in hypertension." *J Cardio Pharm* **35** (4 suppl 2): S25-31.

Goldie, R., D'Aprile, A., Self, G., Rigby, P. & Henry, P. (1996). "The distribution and density of receptor subtypes for endothelin-1 in peripheral lung of the rat, guinea-pig and pig." *Br J Pharm* **117**: 729-735.

Gonzalez, E., Kou, R., Lin, A., Golan, D. E. & Michel, T. (2002). "Subcellular targeting and agonist-induced site-specific phosphorylation of endothelial nitric-oxide synthase." *J Biol Chem* **277**(42): 39554-39560.

Goto, Y., Yoshikane, H., Honda, M., Morioka, S., Yamori, Y. & Moriyama, K. (1990). "Three-dimensional observation on sarcoplasmic reticulum and caveolae in myocardium of spontaneously hypertensive rats." *J Submicrosc Cytol Pathol* **22**(4): 535-542.

Gottlieb, M. & Chavko, M. (1987). "Silver staining of native and denatured eucaryotic DNA in agarose gels." *Anal Biochem* **165**(1): 33-37.

Govers, R., van der Sluijs, P., van Donselaar, E., Slot, J. W. & Rabelink, T. J. (2002). "Endothelial nitric oxide synthase and its negative regulator caveolin-1 localize to distinct perinuclear organelles." *J Histochem Cytochem* **50**(6): 779-788.

Gurbanov, K., Rubinstein, I., Hoffman, A., Abassi, Z., Better, O. & Winaver, J. (1996). "Differential regulation of renal regional blood flow by endothelin-1." *Am J Physiol* **271**(6Pt2): F1166-1172.

Gustafsson, E., Brakebusch, C., Hietanen, K. & Fassler, R. (2000). "Tie-1-directed expression of Cre recombinase in endothelial cells of embryoid bodies and transgenic mice." *J Cell Sci* **114**: 671-676.

Guyton, A. C., Coleman, T. G. & Cowley, A. W. J. (1972). "Arterial pressure regulation: Overriding dominance of the kidneys in long-term regulation and in hypertension." *Am J Med* **52**: 584-594.

Guyton, A. C. & Hall, J. E. (2000a). "Dominant role of the kidney in long-term regulation of arterial pressure and in hypertension: the integrated system for pressure control". Textbook of medical physiology. Philadelphia, W.B. Saunders**:** 195-209.

Guyton, A. C. & Hall, J. E. (2000b). "Integration of renal mechanisms for control of blood volume and extracellular fluid volume". Textbook of medical physiology. Philadelphia, W.B. Saunders**:** 329-345.

Guyton, A. C., Hall, J. E., Coleman, T. G. & Manning Jr, R. D. (1990). "The dominant role of the kidneys in the long-term regulation of arterial pressure in normal and hypertensive states". Hypertension: Pathophysiology, Diagnosis, and Management. Laragh, J. H.& Brenner, B. M. New York, Raven Press Ltd.**:** 1029-1052.

Hagiwara, H., Nagasawa, T., Yamamoto, T., Lodhi, K., Ito, T., Takemura, N. & Hirose, S. (1993). "Immunochemical characterization and localization of endothelin ETB receptor." *Am J Physiol* **264**: R777-783.

Hames, B. D. & Rickwood, D. (1990). Gel electrophoresis of proteins: a practical approach. New York, Oxford University Press.

Harris, P. J., Zhuo, J., Mendelsohn, F. A. & Skinner, S. L. (1991). "Haemodynamic and renal tubular effects of low doses of endothelin in anaesthetized rats." *J Physiol* **433**: 25-39.

Hayakawa, H., Hirata, Y., Suzuki, E., Sugimoto, T., Matsuoka, H., Kikuchi, K., Nagano, T., Hirobe, M. & Sugimoto, T. (1993). "Mechanisms for altered endothelium-dependent vasorelaxation in isolated kidneys from experimental hypertensive rats." *Am J Physiol* **264**(5 Pt 2): H1535-1541.

Haynes, W. G., Noon, J. P., Walker, B. R. & Webb, D. J. (1993). "Inhibition of nitric oxide synthesis increases blood pressure in healthy humans." *J Hypertens* **11**(12): 1375-1380.

Haynes, W. G. & Webb, D. J. (1998). "Endothelin as a regulator of cardiovascular function in health and disease." *J Hypertens* **16**(8): 1081-1098.

Hecker, M., Mulsch, A., Bassenge, E., Forstermann, U. & Busse, R. (1994). "Subcellular localization and characterization of nitric oxide synthase(s) in endothelial cells: physiological implications." *Biochem J* **299**(Pt 1): 247-252.

Higashi, Y., Oshima, T., Ozono, R., Watanabe, M., Matsuura, H. & Kajiyama, G. (1995). "Effects of L-arginine infusion on renal hemodynamics in patients with mild essential hypertension." *Hypertension* **25**(4 Pt 2): 898-902.

Higashi, Y., Oshima, T., Watanabe, M., Matsuura, H. & Kajiyama, G. (1996). "Renal response to L-arginine in salt sensitive patients with essential hypertension." *Hypertension* **27**(3 Pt 2): 643-648.

Hirata, K., Miki, N., Kuroda, Y., Sakoda, T., Kawashima, S. & Yokoyama, M. (1995a). "Low concentration of oxidized low-density lipoprotein and lysophosphatidylcholine upregulate constitutive nitric oxide synthase mRNA expression in bovine aortic endothelial cells." *Circ Res* **76**(6): 958-962.

Hirata, Y., Hayakawa, H., Kakoki, M., Tojo, A., Suzuki, E., Kimura, K., Goto, A., Kikuchi, K., Nagano, T., Hirobe, M. & Omata, M. (1996). "Nitric oxide release from kidneys of hypertensive rats treated with imidapril." *Hypertension* **27**(2): 672-678.

Hirata, Y., Hayakawa, H., Suzuki, E., Kimura, K., Kikuchi, K., Nagano, T., Hirobe, M. & Omata, M. (1995b). "Direct measurements of endothelium-derived nitric oxide release by stimulation of endothelin receptors in rat kidney and its alteration in salt-induced hypertension." *Circulation* **91**(4): 1229-1235.

Hoffman, A., Abassi, Z. A., Brodsky, S., Ramadan, R. & Winaver, J. (2000). "Mechanisms of big endothelin-1-induced diuresis and natriuresis : role of ET(B) receptors." *Hypertension* **35**(3): 732-739.

Hoffman, A., Grossman, E., Goldstein, D., Gill, J. J. & Keiser, H. (1994). "Urinary excretion rate of endothelin-1 in patients with essential hypertension and salt sensitivity." *Kidney Int* **45**(2): 556-560.

Horwitz, J., Chua, J., Curby, R., Tomson, A., DaRooge, M., Fisher, B., Mauricio, J. & Klundt, I. (1964). "Substrates for cytochemical demonstration of enzyme activity. I. Some substituted 3-indolyl-β-D-glycopyranosides." *J Med Chem* **7**: 574-575.

Hosoda, K., Hammer, R. E., Richardson, J. A., Baynash, A. G., Cheung, J. C., Giaid, A. & Yanagisawa, M. (1994). "Targeted and natural (piebald-lethal) mutations of endothelin-B receptor gene produce megacolon associated with spotted coat color in mice." *Cell* **79**(7): 1267-1276.

Hosoda, K., Nakao, K., Tamura, N., Arai, H., Ogawa, Y., Suga, S., Nakanishi, S. & Imura, H. (1992). "Organization, structure, chromosomal assignment, and expression of the gene encoding the human endothelin-A receptor." *J Biol Chem* **267**(26): 18797-18804.

Hu, L. & Manning Jr, R. D. (1995). "Role of nitric oxide in regulation of long-term pressure-natriuresis relationship in Dahl rats." *Am J Physiol* **268**(6 Pt 2): H2375-2383.

Huang, P. L., Huang, Z., Mashimo, H., Bloch, K. D., Moskowitz, M. A., Bevan, J. A. & Fishman, M. C. (1995). "Hypertension in mice lacking the gene for endothelial nitric oxide synthase." *Nature* **377**(6546): 239-242.

Hughes, A. K., Cline, R. & Kohan, D. E. (1992). "Alterations in renal endothelin-1 production in the spontaneously hypertensive rat." *Hypertension* **20**(5): 666-673.

Ignarro, L. J., Buga, G. M., Wood, K. S., Byrns, R. E. & Chaudhuri, G. (1987). "Endothelium-derived relaxing factor produced and released from artery and vein is nitric oxide." *Proc Natl Acad Sci U S A* **84**(24): 9265-9269.

Ignarro, L. J., Byrns, R. E. & Wood, K. S. (1986). "Pharmacological and biochemical properties of endothelium-derived relaxant factor (EDRF): Evidence that EDRF is closely related to nitric oxide (NO) radical." *Circulation* **74 (suppl II)**: 287.

Ikeda, T., Ohta, H., Okada, M., Kawai, N., Nakao, R., Siegl, P., Kobayashi, T., Maeda, S., Miyauchi, T. & Nishikibe, M. (1999). "Pathophysiological roles of endothelin-1 in Dahl salt-sensitive hypertension." *Hypertension* **34**: 514-519.

Ikenaga, H., Suzuki, H., Ishii, N., Itoh, H. & Saruta, T. (1993). "Role of NO on pressure-natriuresis in Wistar-Kyoto and spontaneously hypertensive rats." *Kidney Int* **43**(1): 205-211.

Inoue, N., Venema, R. C., Sayegh, H. S., Ohara, Y., Murphy, T. J. & Harrison, D. G. (1995). "Molecular regulation of the bovine endothelial cell nitric oxide synthase by transforming growth factor-beta 1." *Arterioscler Thromb Vasc Biol* **15**(8): 1255-1261.

Jaffe, E. A., Nachman, R. L., Becker, C. G. & Minick, C. R. (1973). "Culture of human endothelial cells derived from umbilical veins. Identification by morphologic and immunologic criteria." *J Clin Invest* **52**(11): 2745-2756.

Janssens, S. P., Shimouchi, A., Quertermous, T., Bloch, D. B. & Bloch, K. D. (1992). "Cloning and expression of a cDNA encoding human endothelium-derived relaxing factor/nitric oxide synthase." *J Biol Chem* **267**(21): 14519-14522.

Joannides, R., Haefeli, W. E., Linder, L., Richard, V., Bakkali, E. H., Thuillez, C. & Luscher, T. F. (1995). "Nitric oxide is responsible for flow-dependent dilatation of human peripheral conduit arteries in vivo." *Circulation* **91**(5): 1314-1319.

Jones, C., Hiley, C., Pelton, J. & Miller, R. (1989). "Autoradiographic localisation of endothelin binding sites in kidney." *Eur J Pharm* **163**: 379-382.

Ju, H., Venema, V. J., Marrero, M. B. & Venema, R. C. (1998). "Inhibitory interactions of the bradykinin B2 receptor with endothelial nitric-oxide synthase." *J Biol Chem* **273**(37): 24025-24029.

Ju, H., Zou, R., Venema, V. J. & Venema, R. C. (1997). "Direct interaction of endothelial nitric-oxide synthase and caveolin-1 inhibits synthase activity." *J Biol Chem* **272**(30): 18522-18525.

Kakoki, M., Hirata, Y., Hayakawa, H., Tojo, A., Nagata, D., Suzuki, E., Kimura, K., Goto, A., Kikuchi, K., Nagano, T. & Omata, M. (1999). "Effects of hypertension, diabetes mellitus, and hypercholesterolemia on endothelin type B receptor-mediated nitric oxide release from rat kidney." *Circulation* **99**: 1242-1248.

Kalderon, D., Roberts, B., Richardson, W. & Smith, A. (1984). "A short amino acid sequence able to specify nuclear location." *Cell* **39**(3Pt2): 499-509.

Kanno, K., Hirata, Y., Tsujino, M., Imai, T., Shichiri, M., Ito, H. & Marumo, F. (1993). "Up-regulation of ETB receptor subtype mRNA by angiotensin II in rat cardiomyocytes." *Biochem Biophys Res Commun* **194**(3): 1282-1287.

Kantachuvesiri, S. (1999). Thesis "Genetics of malignant hypertension and pathophysiology study in transgenic rats with inducible hypertension." Centre for Genome Research, University, University of Edinburgh: 64.

Kim, F., Gallis, B. & Corson, M. A. (2001). "TNF-alpha inhibits flow and insulin signaling leading to NO production in aortic endothelial cells." *Am J Physiol Cell Physiol* **280**(5): C1057-1065.

Kitamura, K., Tanaka, T., Kato, J., Eto, T. & Tanaka, K. (1989a). "Regional distribution of immunoreactive endothelin in porcine tissue: abundance in inner medulla of kidney." *Biochem Biophys Res Commun* **161**(1): 348-352.

Kitamura, K., Tanaka, T., Kato, J., Ogawa, T., Eto, T. & Tanaka, K. (1989b). "Immunoreactive endothelin in rat kidney inner medulla: marked decrease in spontaneously hypertensive rats." *Biochem Biophys Res Commun* **162**(1): 38-44.

Kleinert, H., Wallerath, T., Euchenhofer, C., Ihrig-Biedert, I., Li, H. & Forstermann, U. (1998). "Estrogens increase transcription of the human endothelial NO synthase gene: analysis of the transcription factors involved." *Hypertension* **31**(2): 582-588.

Kohan, D. E. (1997). "Endothelins in the normal and diseased kidney." *Am J Kidney Dis* **29**(1): 2-26.

Kohan, D. E. & Fiedorek, F. T., Jr. (1991). "Endothelin synthesis by rat inner medullary collecting duct cells." *J Am Soc Nephrol* **2**(2): 150-155.

Kohan, D. E., Hughes, A. K. & Perkins, S. L. (1992). "Characterization of endothelin receptors in the inner medullary collecting duct of the rat." *J Biol Chem* **267**(17): 12336-12340.

Kohan, D. E. & Padilla, E. (1992). "Endothelin-1 is an autocrine factor in rat inner medullary collecting ducts." *Am J Physiol* **263**(4 Pt 2): F607-612.

Kohzuki, M., Johnston, C., Chai, S., Casley, D. & Mendelsohn, F. A. (1989). "Localization of endothelin receptors in rat kidney." *Eur J Pharm* **160**: 193-194.

Konishi, M. & Su, C. (1983). "Role of endothelium in dilator responses of spontaneously hypertensive rat arteries." *Hypertension* **5**(6): 881-886.

Koseki, C., Imai, M., Hirata, Y., Yanagisawa, M. & Masaki, T. (1989). "Autoradiographic distribution in rat tissues of binding sites for endothelin: a neuropeptide?" *Am J Physiol* **256**: R858-866.

Kotelevtsev, Y. & Webb, D. J. (2001). "Endothelin as a natriuretic hormone: the case for a paracrine action mediated by nitric oxide." *Cardiovasc Res* **51**(3): 481-488.

Krum, H., Viskoper, R., Lacourciere, Y., Budde, M. & Charlon, V. (1998). "Bosentan Hypertension Investigators. The effect of an endothelin-receptor antagonist, bosentan, on blood pressure in patients with essential hypertension." *N Engl J Med* **338**: 784-790.

Kubes, P., Suzuki, M. & Granger, D. N. (1991). "Nitric oxide: an endogenous modulator of leukocyte adhesion." *Proc Natl Acad Sci U S A* **88**(11): 4651-4655.

Kurihara, Y., Kurihara, H., Suzuki, H., Kodama, T., Maemura, K., Nagai, R., Oda, H., Kuwaki, T., Cao, W. H., Kamada, N. & et al. (1994). "Elevated blood pressure and craniofacial abnormalities in mice deficient in endothelin-1." *Nature* **368**(6473): 703-710.

Kurtz, A. & Wagner, C. (1998). "Role of nitric oxide in the control of renin secretion." *Am J Physiol* **275**: F849-862.

Kurzchalia, T. V., Dupree, P., Parton, R. G., Kellner, R., Virta, H., Lehnert, M. & Simons, K. (1992). "VIP21, a 21-kD membrane protein is an integral component of trans-Golgi- network-derived transport vesicles." *J Cell Biol* **118**(5): 1003-1014.

Kurzchalia, T. V., Hartmann, E. & Dupree, P. (1995). "Guilt by insolubility - does a protein's detergent insolubility reflect a caveolar location?" *Trends in Cell Biol* **5**: 187-189.

Lahera, V., Navarro, J., Biondi, M., Ruilope, L. & Romero, J. C. (1993). "Exogenous cGMP prevents decrease in diuresis and natriuresis induced by inhibition of NO synthesis." *Am J Physiol* **264**: F344-347.

Lahera, V., Salom, M. G., Fiksen-Olsen, M. J., Raij, L. & Romero, J. C. (1990). "Effects of NG-monomethyl-L-arginine and L-arginine on acetylcholine renal response." *Hypertension* **15**(6 Pt 1): 659-663.

Lahera, V., Salom, M. G., Fiksen-Olsen, M. J. & Romero, J. C. (1991a). "Mediatory role of endothelium-derived nitric oxide in renal vasodilatory and excretory effects of bradykinin." *Am J Hypertens* **4**(3 Pt 1): 260-262.

Lahera, V., Salom, M. G., Miranda-Guardiola, F., Moncada, S. & Romero, J. C. (1991b). "Effects of NG-nitro-L-arginine methyl ester on renal function and blood pressure." *Am J Physiol* **261**(6 Pt 2): F1033-1037.

Lamas, S., Marsden, P. A., Li, G. K., Tempst, P. & Michel, T. (1992). "Endothelial nitric oxide synthase: molecular cloning and characterization of a distinct constitutive enzyme isoform." *Proc Natl Acad Sci U S A* **89**(14): 6348-6352.

Larson, T. & Lockhart, J. (1995). "Restoration of vasa recta hemodynamics and pressure natriuresis in SHR by L-arginine." *Am J Physiol* **268**(5 Pt 2): F907-912.

Li, S., Couet, J. & Lisanti, M. P. (1996). "Src tyrosine kinases, Galpha subunits, and H-Ras share a common membrane-anchored scaffolding protein, caveolin. Caveolin binding negatively regulates the auto-activation of Src tyrosine kinases." *J Biol Chem* **271**(46): 29182-29190.

Li, S., Okamoto, T., Chun, M., Sargiacomo, M., Casanova, J. E., Hansen, S. H., Nishimoto, I. & Lisanti, M. P. (1995). "Evidence for a regulated interaction between heterotrimeric G proteins and caveolin." *J Biol Chem* **270**(26): 15693-15701.

Liao, J. K., Shin, W. S., Lee, W. Y. & Clark, S. L. (1995). "Oxidized low-density lipoprotein decreases the expression of endothelial nitric oxide synthase." *J Biol Chem* **270**(1): 319-324.

Lifton, R. P. (1996). "Molecular genetics of human blood pressure variation." *Science* **272**: 676-680.

Light, D., Corbin, J. & Stanton, B. (1990). "Dual ion-channel regulation by cyclic GMP and cyclic GMP-dependent protein kinase." *Nature* **344**(6264): 336-339.

Lisanti, M. P., Scherer, P. E., Vidugiriene, J., Tang, Z., Hermanowski-Vosatka, A., Tu, Y. H., Cook, R. F. & Sargiacomo, M. (1994). "Characterization of caveolin-rich

membrane domains isolated from an endothelial-rich source: implications for human disease." *J Cell Biol* **126**(1): 111-126.

Liu, J., Garcia-Cardena, G. & Sessa, W. C. (1996). "Palmitoylation of endothelial nitric oxide synthase is necessary for optimal stimulated release of nitric oxide: implications for caveolae localization." *Biochemistry* **35**(41): 13277-13281.

Liu, J., Hughes, T. E. & Sessa, W. C. (1997). "The first 35 amino acids and fatty acylation sites determine the molecular targeting of endothelial nitric oxide synthase into the Golgi region of cells: a green fluorescent protein study." *J Cell Biol* **137**(7): 1525-1535.

Lu, J. L., Schmiege, L. M., 3rd, Kuo, L. & Liao, J. C. (1996). "Downregulation of endothelial constitutive nitric oxide synthase expression by lipopolysaccharide." *Biochem Biophys Res Commun* **225**(1): 1-5.

Luscher, T. F., Aarhus, L. L. & Vanhoutte, P. M. (1990). "Indomethacin improves the impaired endothelium-dependent relaxations in small mesenteric arteries of the spontaneously hypertensive rat." *Am J Hypertens* **3**(1): 55-58.

Luscher, T. F., Raij, L. & Vanhoutte, P. M. (1987). "Endothelium-dependent vascular responses in normotensive and hypertensive Dahl rats." *Hypertension* **9**: 157-163.

Luscher, T. F. & Vanhoutte, P. M. (1986). "Endothelium-dependent contractions to acetylcholine in the aorta of the spontaneously hypertensive rat." *Hypertension* **8**(4): 344-348.

Marrero, M. B., Venema, V. J., Ju, H., He, H., Liang, H., Caldwell, R. B. & Venema, R. C. (1999). "Endothelial nitric oxide synthase interactions with G-protein-coupled receptors." *Biochem J* **343 Pt 2**: 335-340.

Mattson, D. & Higgins, D. (1996). "Infuence of dietary sodium intake on renal medullary nitric oxide synthase." *Hypertension* **27**(2): 688-692.

Mattson, D. L. & Wu, F. (2000a). "Control of arterial blood pressure and renal sodium excretion by nitric oxide synthase in the renal medulla." *Acta Physiol Scand* **168**(1): 149-154.

Mattson, D. L. & Wu, F. (2000b). "Nitric oxide synthase activity and isoforms in rat renal vasculature." *Hypertension* **35**(1 Pt 2): 337-341.

McCabe, T. J., Fulton, D., Roman, L. J. & Sessa, W. C. (2000). "Enhanced electron flux and reduced calmodulin dissociation may explain "calcium-independent" eNOS activation by phosphorylation." *J Biol Chem* **275**(9): 6123-6128.

McDonald, K., Zharikov, S., Block, E. & Kilberg, M. (1997). "A caveolar complex between the cationic amino acid transporter 1 and endothelial nitric-oxide synthase may explain the "arginine paradox"." *J Biol Chem* **272**(50): 31213-31216.

McGuire, P. & Twietmeyer, T. (1985). "Transcytosis of ferritin and increased production of subendothelial matrix components by aortic endothelial cells during the development of hypertension." *Microcirculation, Endothelium and Lymphatics* **2**(2): 129-149.

McQuillan, L. P., Leung, G. K., Marsden, P. A., Kostyk, S. K. & Kourembanas, S. (1994). "Hypoxia inhibits expression of eNOS via transcriptional and posttranscriptional mechanisms." *Am J Physiol* **267**(5 Pt 2): H1921-1927.

Melo, L., Veress, A., Chong, C., Pang, S., Flynn, T. & Sonnenberg, H. (1998). "Salt-sensitive hypertension in ANP knockout mice: potential role of abnormal plasma renin activity." *Am J Physiol* **274**: R255-261.

Michel, J. B., Feron, O., Sacks, D. & Michel, T. (1997a). "Reciprocal regulation of endothelial nitric-oxide synthase by Ca2+- calmodulin and caveolin." *J Biol Chem* **272**(25): 15583-15586.

Michel, J. B., Feron, O., Sase, K., Prabhakar, P. & Michel, T. (1997b). "Caveolin versus calmodulin. Counterbalancing allosteric modulators of endothelial nitric oxide synthase." *J Biol Chem* **272**(41): 25907-25912.

Michel, T., Li, G. K. & Busconi, L. (1993). "Phosphorylation and subcellular translocation of endothelial nitric oxide synthase." *Proc Natl Acad Sci U S A* **90**(13): 6252-6256.

Michell, B., Griffiths, J., Mitchelhill, K., Rodriguez-Crespo, I., Tiganis, T., Bozinovski, S., de Montellano, P., Kemp, B. E. & Pearson, R. (1999). "The Akt kinase signals directly to endothelial nitric oxide synthase." *Curr Biol* **9**(15): 845-848.

Migas, I., Backer, A., Meyer-Lehnert, H. & Kramer, H. J. (1995). "Endothelin synthesis by porcine inner medullary collecting duct cells. Effects of hormonal and osmotic stimuli." *Am J Hypertens* **8**(7): 748-752.

Miyamoto, Y., Saito, Y., Kajiyama, N., Yoshimura, M., Shimasaki, Y., Nakayama, M., Kamitani, S., Harada, M., Ishikawa, M., Kuwahara, K., Ogawa, E., Hamanaka, I., Takahashi, N., Kaneshige, T., Teraoka, H., Akamizu, T., Azuma, N., Yoshimasa, Y., Yoshimasa, T., Itoh, H., Masuda, I., Yasue, H. & Nakao, K. (1998). "Endothelial nitric oxide synthase gene is positively associated with essential hypertension." *Hypertension* **32**(1): 3-8.

Moncada, S., Palmer, R. M. & Higgs, E. A. (1991). "Nitric oxide: physiology, pathophysiology, and pharmacology." *Pharmacol Rev* **43**(2): 109-142.

Morita, H., Kurihara, H., Kurihara, Y., Shindo, T., Kuwaki, T., Kumada, M. & Yazaki, Y. (1998). "Systemic and renal response to salt loading in endothelin-1 knockout mice." *J Cardiovasc Pharmacol* **31**(Suppl 1): S557-560.

Mountford, P., Zevnik, B., Duwel, A., Nichols, J., Li, M., Dani, C., Robertson, M., Chambers, I. & Smith, A. (1994). "Dicistronic targeting constructs: Reporters and modifiers of mammalian gene expression." *Proc Natl Acad Sci U S A* **91**: 4303-4307.

Mourlon-Le Grand, M., Benessiano, J. & Levy, B. (1992). "cGMP pathway and mechanical properties of carotid artery wall in WKY rats and SHR: role of endothelium." *Am J Physiol* **263**(1 Pt 2): H61-67.

Mugge, A., Elwell, J., Peterson, T., Hofmeyer, T., Heistad, D. & Harrison, D. G. (1991). "Chronic treatment with polyethylene-glycolated superoxide dismutase partially restores endothelium-dependent vascular relaxations in cholesterol-fed rabbits." *Circ Res* **69**(5): 1293-1300.

Murata, T., Sato, K., Hori, M., Ozaki, H. & Karaki, H. (2002). "Decreased endothelial nitric-oxide synthase (eNOS) activity resulting from abnormal interaction between eNOS and its regulatory proteins in hypoxia-induced pulmonary hypertension." *J Biol Chem* **277**(46): 44085-44092.

Nadler, S., Zimpelmann, J. & Hebert, R. (1992). "Endothelin inhibits vasopressin-stimulated water permeability in rat terminal inner medullary collecting duct." *J Clin Invest* **90**(4): 1458-1466.

Nakamichi, K., Ihara, M., Kobayashi, M., Saeki, T., Ishikawa, K. & Yano, M. (1992). "Different distribution of endothelin receptor subtypes in pulmonary tissues revealed by the novel selective ligands BQ-123 and [Ala1,3,11,15]ET-1." *Biochem Biophys Res Commun* **182**(1): 144-150.

Nakayama, T., Soma, M., Takahashi, Y., Izumi, Y., Kanmatsuse, K. & Esumi, M. (1997). "Association analysis of CA repeat polymorphism of the endothelial nitric oxide synthase gene with essential hypertension in Japanese." *Clin Genet* **51**(1): 26-30.

Nava, E., Farre, A. L., Moreno, C., Casado, S., Moreau, P., Cosentino, F. & Luscher, T. F. (1998). "Alterations to the nitric oxide pathway in the spontaneously hypertensive rat." *J Hypertens* **16**(5): 609-615.

Nava, E., Llinas, M., Gonzalez, J. & Salazar, F. (1996). "Nitric oxide synthase activity in renal cortex and medulla of normotensive and spontaneously hypertensive rats." *Am J Hypertens* **9**: 1236-1239.

Ni, Z., Oveisi, F. & Vaziri, N. D. (1999). "Nitric oxide synthase isotype expression in salt-sensitive and salt resistant Dahl rats." *Hypertension* **34**(4Pt1): 552-557.

Nishida, K., Harrison, D. G., Navas, J. P., Fisher, A. A., Dockery, S. P., Uematsu, M., Nerem, R. M., Alexander, R. W. & Murphy, T. J. (1992). "Molecular cloning and characterization of the constitutive bovine aortic endothelial cell nitric oxide synthase." *J Clin Invest* **90**(5): 2092-2096.

Nishikawa, S. I., Nishikawa, S., Hirashima, M., Matsuyoshi, N. & Kodama, H. (1998). "Progressive lineage analysis by cell sorting and culture identifies FLK1+VE-cadherin+ cells at a diverging point of endothelial and hemopoietic lineages." *Development* **125**(9): 1747-1757.

Niu, X. F., Smith, C. W. & Kubes, P. (1994). "Intracellular oxidative stress induced by nitric oxide synthesis inhibition increases endothelial cell adhesion to neutrophils." *Circ Res* **74**(6): 1133-1140.

O'Brien, A. J., Young, H. M., Povey, J. M. & Furness, J. B. (1995). "Nitric oxide synthase is localized predominantly in the Golgi apparatus and cytoplasmic vesicles of vascular endothelial cells." *Histochem Cell Biol* **103**(3): 221-225.

Ohuchi, T., Kuwaki, T., Ling, G. Y., Dewit, D., Ju, K. H., Onodera, M., Cao, W. H., Yanagisawa, M. & Kumada, M. (1999a). "Elevation of blood pressure by genetic and pharmacological disruption of the ETB receptor in mice." *Am J Physiol* **276**(4 Pt 2): R1071-1077.

Ohuchi, T., Laghmani, K., Yamada, T., Gariepy, C. E., Preisig, P., Alpern, R. & Yanagisawa, M. (1999b). Abstract "Salt-sensitive hypertension in endothelin B receptor-deficient mice due to impaired renal salt excretion". Sixth International Conference on Endothelin, Montreal, Canada.

Okamoto, K. & Aoki, K. (1963). "Development of a strain of spontaneously hypertensive rats." *Jpn Circ J* **27**: 282-293.

Palade, G. E. (1953). "Fine structure of blood capillaries." *Journal of Applied Physics* **24**: 1424-1436.

Palmer, R. M., Ashton, D. S. & Moncada, S. (1988a). "Vascular endothelial cells synthesize nitric oxide from L-arginine." *Nature* **333**(6174): 664-666.

Palmer, R. M., Ferrige, A. G. & Moncada, S. (1987). "Nitric oxide release accounts for the biological activity of endothelium-derived relaxing factor." *Nature* **327**(6122): 524-526.

Palmer, R. M. & Moncada, S. (1989). "A novel citrulline-forming enzyme implicated in the formation of nitric oxide by vascular endothelial cells." *Biochem Biophys Res Commun* **158**(1): 348-352.

Palmer, R. M., Rees, D. D., Ashton, D. S. & Moncada, S. (1988b). "L-arginine is the physiological precursor for the formation of nitric oxide in endothelium-dependent relaxation." *Biochem Biophys Res Commun* **153**(3): 1251-1256.

Panza, J., Garcia, C. E., Kilcoyne, C., Quyyumi, A. & Cannon, R. (1995). "Impaired endothelium-dependent vasodilation in patients with essential hypertension. Evidence that nitric oxide abnormality is not localized to a single signal tranduction pathway." *Circulation* **91**(6): 1732-1738.

Patel, A., Layne, S., Watts, D. & Kirchner, K. (1993). "L-arginine administration normalizes pressure natriuresis in hypertensive Dahl rats." *Hypertension* **22**(6): 863-869.

Pearson, B., Andrews, M. & Grose, F. (1961). "Histochemical demonstration of mammalian glucosidase by means of 3-(5-bromoindolyl)-beta-D-glucopyranoside." *Proc Soc Exptl Biol Med* **108**: 619-623.

Pelisek, J., Armeanu, S. & Nikol, S. (2000). "Evaluation of β-Galactosidase activity in tissue in the presence of blood." *J Vasc Res* **37**: 585-593.

Piech, A., Dessy, C., Havaux, X., Feron, O. & Balligand, J.-L. (2003). "Differential regulation of nitric oxide synthases and their allosteric regulators in heart and vessels of hypertensive rats." *Cardiovasc Res* **57**: 456-467.

Pieper, G. (1997). "Acute amelioration of diabetic endothelial dysfunction with a derivative of the nitric oxide synthase cofactor, tetrahydrobiopterin." *J Cardiovasc Pharmacol* **29**(1): 8-15.

Pieper, G. & Peltier, B. (1995). "Amelioration by L-arginine of a dysfunctional arginine/nitric oxide pathway in diabetic endothelium." *J Cardiovasc Pharmacol* **25**(3): 397-403.

Pinto, Y. & Ganten, D. (1998). "Lessons from rat models of hypertension: from Goldblatt to genetic engineering." *Cardiovasc Res* **39**: 77-88.

Plato, C. F. & Garvin, J. L. (1999). "Nitric oxide, endothelin and nephron transport: potential interactions." *Clin Exp Pharmacol Physiol* **26**(3): 262-268.

Plato, C. F., Pollock, D. M. & Garvin, J. L. (2000a). "Endothelin inhibits thick ascending limb chloride flux via ET(B) receptor-mediated NO release." *Am J Physiol Renal Physiol* **279**(2): F326-333.

Plato, C. F., Shesely, E. G. & Garvin, J. L. (2000b). "eNOS mediates L-arginine-induced inhibition of thick ascending limb chloride flux." *Hypertension* **35**(1 Pt 2): 319-323.

Plato, C. F., Stoos, B. A., Wang, D. & Garvin, J. L. (1999). "Endogenous nitric oxide inhibits chloride transport in the thick ascending limb." *Am J Physiol* **276**(1 Pt 2): F159-163.

Pohl, U., Holtz, J., Busse, R. & Bassenge, E. (1986). "Crucial role of endothelium in the vasodilator response to increased flow in vivo." *Hypertension* **8**(1): 37-44.

Pollock, D. & Pollock, J. (2001). "Evidence for endothelin involvement in the response to high salt." *Am J Physiol Renal Physiol* **281**: F144-150.

Pollock, J. S., Forstermann, U., Mitchell, J. A., Warner, T. D., Schmidt, H. H., Nakane, M. & Murad, F. (1991). "Purification and characterization of particulate endothelium-derived relaxing factor synthase from cultured and native bovine aortic endothelial cells." *Proc Natl Acad Sci U S A* **88**(23): 10480-10484.

Pou, S., Pou, W., Bredt, D. S., Snyder, S. & Rosen, G. (1992). "Generation of superoxide by purified brain nitric oxide synthase." *J Biol Chem* **267**(34): 24173-24176.

Prabhakar, P., Cheng, V. & Michel, T. (2000). "A chimeric transmembrane domain directs endothelial nitric-oxide synthase palmitoylation and targeting to plasmalemmal caveolae." *J Biol Chem* **275**(25): 19416-19421.

Prabhakar, P., Thatte, H. S., Goetz, R. M., Cho, M. R., Golan, D. E. & Michel, T. (1998). "Receptor-regulated translocation of endothelial nitric-oxide synthase." *J Biol Chem* **273**(42): 27383-27388.

Qiu, H. Y., Henrion, D., Benessiano, J., Heymes, C., Tournier, B. & Levy, B. I. (1998). "Decreased flow-induced dilation and increased production of cGMP in spontaneously hypertensive rats." *Hypertension* **32**(6): 1098-1103.

Radomski, M. W., Palmer, R. M. & Moncada, S. (1987a). "Comparative pharmacology of endothelium-derived relaxing factor, nitric oxide and prostacyclin in platelets." *Br J Pharmacol* **92**(1): 181-187.

Radomski, M. W., Palmer, R. M. & Moncada, S. (1987b). "Endogenous nitric oxide inhibits human platelet adhesion to vascular endothelium." *Lancet* **2**(8567): 1057-1058.

Ramirez-Solis, R., Rivera-Perez, J., Wallace, J., Wims, M., Zheng, H. & Bradley, A. (1992). "Genomic DNA microextraction: a method to screen numerous samples." *Anal Biochem* **201**(2): 331-335.

Rapoport, R. M., Draznin, M. B. & Murad, F. (1983). "Endothelium-dependent relaxation in rat aorta may be mediated through cyclic GMP-dependent protein phosphorylation." *Nature* **306**(5939): 174-176.

Raposo, G., Dunia, I., Marullo, S., Andre, C., Guillet, J. G., Strosberg, A. D., Benedetti, E. L. & Hoebeke, J. (1987). "Redistribution of muscarinic acetylcholine receptors on human fibroblasts induced by regulatory ligands." *Biol Cell* **60**(2): 117-123.

Razani, B., Engelman, J. A., Wang, X. B., Schubert, W., Zhang, X. L., Marks, C. B., Macaluso, F., Russell, R. G., Li, M., Pestell, R. G., Di Vizio, D., Hou, H., Jr., Kneitz, B., Lagaud, G., Christ, G. J., Edelmann, W. & Lisanti, M. P. (2001). "Caveolin-1 null mice are viable but show evidence of hyperproliferative and vascular abnormalities." *J Biol Chem* **276**(41): 38121-38138.

Rees, D. D., Palmer, R. M. & Moncada, S. (1989). "Role of endothelium-derived nitric oxide in the regulation of blood pressure." *Proc Natl Acad Sci U S A* **86**(9): 3375-3378.

Rees, D. D., Palmer, R. M., Schulz, R., Hodson, H. F. & Moncada, S. (1990). "Characterization of three inhibitors of endothelial nitric oxide synthase in vitro and in vivo." *Br J Pharmacol* **101**(3): 746-752.

Reiner, M., Bloch, W. & Addicks, K. (2001). "Functional interaction of caveolin-1 and eNOS in myocardial capillary endothelium revealed by immunoelectron microscopy." *J Histochem Cytochem* **49**(12): 1605-1609.

Rizzo, V., McIntosh, D., Oh, P. & Schnitzer, J. E. (1998). "*In situ* flow activates endothelial nitric oxide synthase in luminal caveolae of endothelium with rapid caveolin dissociation and calmodulin association." *J Biol Chem* **273**(52): 34724-34729.

Robinson, L. J., Busconi, L. & Michel, T. (1995). "Agonist-modulated palmitoylation of endothelial nitric oxide synthase." *J Biol Chem* **270**(3): 995-998.

Robinson, L. J. & Michel, T. (1995). "Mutagenesis of palmitoylation sites in endothelial nitric oxide synthase identifies a novel motif for dual acylation and subcellular targeting." *Proc Natl Acad Sci U S A* **92**(25): 11776-11780.

Rothberg, K. G., Heuser, J. E., Donzell, W. C., Ying, Y. S., Glenney, J. R. & Anderson, R. G. (1992). "Caveolin, a protein component of caveolae membrane coats." *Cell* **68**(4): 673-682.

Rubanyi, G. M. & Polokoff, M. A. (1994). "Endothelins: molecular biology, biochemistry, pharmacology, physiology, and pathophysiology." *Pharmacol Rev* **46**(3): 325-415.

Rubanyi, G. M., Romero, J. C. & Vanhoutte, P. M. (1986). "Flow-induced release of endothelium-derived relaxing factor." *Am J Physiol* **250**(6 Pt 2): H1145-1149.

Rubin, L. J., Badesch, D. B., Barst, R. J., Gaile, N., Black, C. M., Keogh, A., Pulido, T., Frost, A., Roux, S., Leconte, I., Landzberg, M & Simonneau, G. (2002) "Bosentan therapy for pulmonary aterial hypertension." *N Engl J Med* **346**(12): 896-903.

Ruetten, H., Zabel, U., Linz, W. & Schmidt, H. H. (1999). "Downregulation of soluble guanylyl cyclase in young and aging spontaneously hypertensive rats." *Circ Res* **85**: 534-541.

Sakamoto, A., Yanagisawa, M., Sakurai, T., Takuwa, Y., Yanagisawa, H. & Masaki, T. (1991). "Cloning and functional expression of human cDNA for the ETB endothelin receptor." *Biochem Biophys Res Commun* **178**(2): 656-663.

Sakoda, T., Hirata, K., Kuroda, R., Miki, N., Suematsu, M., Kawashima, S. & Yokoyama, M. (1995). "Myristoylation of endothelial cell nitric oxide synthase is important for extracellular release of nitric oxide." *Mol Cell Biochem* **152**(2): 143-148.

Salom, M. G., Lahera, V., Miranda-Guardiola, F. & Romero, J. C. (1992). "Blockade of pressure natriuresis induced by inhibition of renal synthesis of nitric oxide in dogs." *Am J Physiol* **262**(5 Pt 2): F718-722.

Sambrook, J., Fritch, E. F. & Maniatis, T. (1989). Molecular Cloning. A Laboratory Manual. New York, Cold Spring Harbor Laboratory Press.

Sargiacomo, M., Scherer, P. E., Tang, Z., Kubler, E., Song, K. S., Sanders, M. C. & Lisanti, M. P. (1995). "Oligomeric structure of caveolin: implications for caveolae membrane organization." *Proc Natl Acad Sci U S A* **92**(20): 9407-9411.

Sargiacomo, M., Sudol, M., Tang, Z. & Lisanti, M. P. (1993). "Signal transducing molecules and GPI-linked proteins form a caveolin-rich insoluble complex in MDCK cells." *J Cell Biol* **122**: 789-807.

Scherer, P. E., Okamoto, T., Chun, M., Nishimoto, I., Lodish, H. F. & Lisanti, M. P. (1996). "Identification, sequence, and expression of caveolin-2 defines a caveolin gene family." *Proc Natl Acad Sci U S A* **93**(1): 131-135.

Scherer, P. E., Tang, Z., Chun, M., Sargiacomo, M., Lodish, H. F. & Lisanti, M. P. (1995). "Caveolin isoforms differ in their N-terminal protein sequence and

subcellular distribution. Identification and epitope mapping of an isoform-specific monoclonal antibody probe." *J Biol Chem* **270**(27): 16395-16401.

Schiffrin, E. L. (1999). "Role of endothelin-1 in hypertension." *Hypertension* **34**(2): 876-881.

Schlegel, A. & Lisanti, M. P. (2000). "A molecular dissection of caveolin-1 membrane attachment and oligomerization. Two separate regions of the caveolin-1 C-terminal domain mediate membrane binding and oligomer/oligomer interactions in vivo." *J Biol Chem* **275**(28): 21605-21617.

Schlegel, A., Schwab, R. B., Scherer, P. E. & Lisanti, M. P. (1999). "A role for the caveolin scaffolding domain in mediating the membrane attachment of caveolin-1. The caveolin scaffolding domain is both necessary and sufficient for membrane binding in vitro." *J Biol Chem* **274**(32): 22660-22667.

Schnitzer, J. E., Oh, P., Jacobson, B. & Dvorak, A. (1995). "Caveolae from luminal plasmalemma of rat lung endothelium: microdomains enriched in caveolin, Ca2+-ATPase, and inositol trisphosphate receptor." *Proc Natl Acad Sci U S A* **92**: 1759-1763.

Schnitzer, J. E., Siflinger, A., DelVecchio, P. & Malik, A. (1994). "Segmental differentiation of permeability, protein glycosylation, and morphology of cultured bovine lung vascular endothelium." *Biochem Biophys Res Commun* **199**: 11-19.

Schultz, P. & Tolins, J. (1993). "Adaptation to increased dietary salt intake in the rat: role of endogenous nitric oxide." *J Clin Invest* **91**: 642-650.

Segal, S., Brett, S. & Sessa, W. C. (1999). "Codistribution of NOS and caveolin throughout peripheral vasculature and skeletal muscle of hamsters." *Am J Physiol* **277**: H1167-1177.

Sessa, W. C., Barber, C. M. & Lynch, K. R. (1993). "Mutation of N-myristoylation site converts endothelial cell nitric oxide synthase from a membrane to a cytosolic protein." *Circ Res* **72**(4): 921-924.

Sessa, W. C., Garcia-Cardena, G., Liu, J., Keh, A., Pollock, J. S., Bradley, J., Thiru, S., Braverman, I. M. & Desai, K. M. (1995). "The Golgi association of endothelial nitric oxide synthase is necessary for the efficient synthesis of nitric oxide." *J Biol Chem* **270**(30): 17641-17644.

Sessa, W. C., Harrison, J. K., Barber, C. M., Zeng, D., Durieux, M. E., D'Angelo, D. D., Lynch, K. R. & Peach, M. J. (1992). "Molecular cloning and expression of a cDNA encoding endothelial cell nitric oxide synthase." *J Biol Chem* **267**(22): 15274-15276.

Sessa, W. C., Pritchard, K., Seyedi, N., Wang, J. & Hintze, T. H. (1994). "Chronic exercise in dogs increases coronary vascular nitric oxide production and endothelial cell nitric oxide synthase gene expression." *Circ Res* **74**(2): 349-353.

Shaul, P. W., Smart, E. J., Robinson, L. J., German, Z., Yuhanna, I. S., Ying, Y., Anderson, R. G. & Michel, T. (1996). "Acylation targets endothelial nitric-oxide synthase to plasmalemmal caveolae." *J Biol Chem* **271**(11): 6518-6522.

Shesely, E. G., Maeda, N., Kim, H. S., Desai, K. M., Krege, J. H., Laubach, V. E., Sherman, P. A., Sessa, W. C. & Smithies, O. (1996). "Elevated blood pressures in mice lacking endothelial nitric oxide synthase." *Proc Natl Acad Sci U S A* **93**(23): 13176-13181.

Shin, M., Russell, L. & Tilghman, S. (1997). "Molecular characterization of four induced alleles at the Ednrb locus." *Proc Natl Acad Sci USA* **94**: 13105-13110.

Sierra, M., Gonzalez, A., Gomez-Alamillo, C., Monreal, I., Huarte, E., Gil, A., Sanchez-Casajus, A. & Diez, J. (1998). "Decreased excretion of nitrate and nitrite in essential hypertensives with renal vasoconstriction." *Kidney Int Suppl* **68**: S10-13.

Simionescu, N., Simionescu, M. & Palade, G. E. (1972). "Permeability of intestinal capillaries. Pathway followed by dextrans and glycogens." *J Cell Biol* **53**(2): 365-392.

Smart, E. J., Ying, Y., Mineo, C. & Anderson, R. G. (1995). "A detergent-free method for purifying caveolae membrane from tissue culture cells." *Proc Natl Acad Sci U S A* **92**: 10104-10108.

Smith, P. J., Teichert-Kuliszewska, K., Monge, J. & Stewart, D. (1998). "Regulation of endothelin-B receptor mRNA expression in human endothelial cell by cytokines and growth factors." *J Cardio Pharm* **31**(Suppl 1): S158-160.

Solzbach, U., Hornig, B., Jeserich, M. & Just, H. (1997). "Vitamin C improves endothelial dysfunction of epicardial coronary arteries in hypertensive patients." *Circulation* **96**(5): 1513-1519.

Soma, S., Takahashi, H., Muramatsu, M., Oka, M. & Fukuchi, Y. (1999). "Localization and distribution of endothelin receptor subtypes in pulmonary vasculature of normal and hypoxia-exposed rats." *Am J Respir Cell Mol Biol* **20**: 620-630.

Southern, E. M. (1975). "Detection of specific sequences among DNA fragments separated by gel electrophoresis." *J Mol Biol* **98**(3): 503-517.

Sowa, G., Liu, J., Papapetropoulos, A., Rex-Haffner, M., Hughes, T. E. & Sessa, W. C. (1999). "Trafficking of endothelial nitric-oxide synthase in living cells.

Quantitative evidence supporting the role of palmitoylation as a kinetic trapping mechanism limiting membrane diffusion." *J Biol Chem* **274**(32): 22524-22531.

Spergel, D., Kruth, U., Shimshek, D., Sprengel, R. & Seeburg, P. (2001). "Using reporter genes to label selected neuronal populations in transgenic mice for gene promoter, anatomical, and physiological studies." *Progress in Neurobiology* **63**: 673-686.

Stanboli, A. & Morin, A. M. (1994). "Nitric oxide synthase in cerebrovascular endothelial cells is inhibited by brefeldin A." *Neurosci Lett* **171**(1-2): 209-212.

Stauss, H. M., Nafz, B., Mrowka, R. & Persson, P. B. (2000). "Blood pressure control in eNOS knock-out mice: comparison with other species under NO blockade." *Acta Physiol Scand* **168**(1): 155-160.

Stoos, B. A., Garcia, N. H. & Garvin, J. L. (1995). "Nitric oxide inhibits sodium reabsorption in the isolated perfused cortical collecting duct." *J Am Soc Nephrol* **6**(1): 89-94.

Stroes, E., Kastelein, J., Cosentino, F., Erkelens, W., Wever, R., Koomans, H., Luscher, T. F. & Rabelink, T. J. (1997). "Tetrahydrobiopterin restores endothelial function in hypercholesterolemia." *J Clin Invest* **99**(1): 41-46.

Stuehr, D. J. (1999). "Mammalian nitric oxide synthases." *Biochim Biophys Acta* **1411**(2-3): 217-230.

Tamai, O., Oka, N., Kikuchi, T., Koda, Y., Soejima, M., Wada, Y., Fujisawa, M., Tamaki, K., Kawachi, H., Shimizu, F., Kimura, H., Imaizumi, T. & Okuda, S. (2001). "Caveolae in mesangial cells and caveolin expression in mesangial proliferative glomerulonephritis." *Kidney Int* **59**(2): 471-480.

Tang, Z., Scherer, P. E., Okamoto, T., Song, K., Chu, C., Kohtz, D. S., Nishimoto, I., Lodish, H. F. & Lisanti, M. P. (1996). "Molecular cloning of caveolin-3, a novel member of the caveolin gene family expressed predominantly in muscle." *J Biol Chem* **271**(4): 2255-2261.

Teichert, A. M., Miller, T. L., Tai, S. C., Wang, Y., Bei, X., Robb, G. B., Phillips, M. J. & Marsden, P. A. (2000). "In vivo expression profile of an endothelial nitric oxide synthase promoter-reporter transgene." *Am J Physiol Heart Circ Physiol* **278**(4): H1352-1361.

Terada, Y., Tomita, K., Nonoguchi, H. & Marumo, F. (1992a). "Different localization of two types of endothelin receptor mRNA in microdissected rat nephron segments using reverse transcription and polymerase chain reaction assay." *J Clin Invest* **90**: 107-112.

Terada, Y., Tomita, K., Nonoguchi, H. & Marumo, F. (1992b). "Polymerase chain reaction localization of constitutive nitric oxide synthase and soluble guanylate cyclase messenger RNAs in microdissected rat nephron segments." *J Clin Invest* **90**(2): 659-665.

Thomas, K. & Capecchi, M. (1987). "Site-directed mutagenesis by gene targeting in mouse embryo-derived stem cells." *Cell* **51**: 503-512.

Tomita, K., Nonoguchi, H. & Marumo, F. (1990). "Effects of endothelin on peptide-dependent cyclic adenosine monophosphate accumulation along the nephron segments of the rat." *J Clin Invest* **85**(6): 2014-2018.

Toya, Y., Schwencke, C., Couet, J., Lisanti, M. P. & Ishikawa, Y. (1998). "Inhibition of adenylyl cyclase by caveolin peptides." *Endocrinology* **139**(4): 2025-2031.

Udy, G. & Evans, M. (1994). "Microplate DNA preparation, PCR screening and cell freezing for gene targeting in embryonic stem cells." *Biotechniques* **17**(5): 887-894.

Uwabo, J., Soma, M., Nakayama, T. & Kanmatsuse, K. (1998). "Association of a variable number of tandem repeats in the endothelial constitutive nitric oxide synthase gene with essential hypertension in Japanese." *Am J Hypertens* **11**(1Pt1): 125-128.

Vallance, P., Collier, J. & Moncada, S. (1989). "Effects of endothelium-derived nitric oxide on peripheral arteriolar tone in man." *Lancet* **2**(8670): 997-1000.

Vallance, P., Leone, A., Calver, A., Collier, J. & Moncada, S. (1992). "Accumulation of an endogenous inhibitor of nitric oxide synthesis in chronic renal failure." *Lancet* **339**(8793): 572-575.

Vaziri, N. D., Ni, Z. & Oveisi, F. (1998). "Upregulation of renal and vascular nitric oxide synthase in young spontaneously hypertensive rats." *Hypertension* **31**(6): 1248-1254.

Vaziri, N. D., Ni, Z., Oveisi, F. & Trnavsky-Hobbs, D. L. (2000). "Effect of antioxidant therapy on blood pressure and NO synthase expression in hypertensive rats." *Hypertension* **36**(6): 957-964.

Vaziri, N. D. & Wang, X. Q. (1999). "cGMP-mediated negative-feedback regulation of endothelial nitric oxide synthase expression by nitric oxide." *Hypertension* **34**(6): 1237-1241.

Venema, R. C., Nishida, K., Alexander, R. W., Harrison, D. G. & Murphy, T. J. (1994). "Organization of the bovine gene encoding the endothelial nitric oxide synthase." *Biochim Biophys Acta* **1218**(3): 413-420.

Wang, X. Q. & Vaziri, N. D. (1999). "Erythropoietin depresses nitric oxide synthase expression by human endothelial cells." *Hypertension* **33**(3): 894-899.

Way, M. & Parton, R. G. (1995). "M-caveolin, a muscle-specific caveolin-related protein." *FEBS Lett* **376**(1-2): 108-112.

Whittle, B. J., Lopez-Belmonte, J. & Rees, D. D. (1989). "Modulation of the vasodepressor actions of acetylcholine, bradykinin, substance P and endothelin in the rat by a specific inhibitor of nitric oxide formation." *Br J Pharmacol* **98**(2): 646-652.

Wickman, A., Andersson, I., Jia, J., Hedin, L. & Bergstrom, G. (2001). "Endothelial nitric oxide synthase protein is reduced in the renal medulla of two-kidney, one-clip hypertensive rats." *J Hypertens* **19**(9): 1665-1673.

Wong, N., Wong, B. & Tsui, J. (2000). "Vasopressin regulates endothelin-B receptor in rat inner medullary collecting duct." *Am J Physiol Renal Physiol* **278**(3): F369-374.

Wu, F., Park, F., Cowley, A. W., Jr. & Mattson, D. L. (1999). "Quantification of nitric oxide synthase activity in microdissected segments of the rat kidney." *Am J Physiol* **276**(6 Pt 2): F874-881.

Yamada, E. (1955). "The fine structure of the gall bladder epithelium of the mouse." *Journal of Biophysical and Biochemical Cytology* **1**: 445-469.

Yamaguchi, T., Dumont, D., Conlon, R., Breitman, M. & Rossant, J. (1993). "flk-1, an flt-related receptor tyrosine kinase is an early marker for endothelial cell precursors." *Development* **118**(2): 489-498.

Yanagisawa, M., Kurihara, H., Kimura, S., Tomobe, Y., Kobayashi, M., Mitsui, Y., Yazaki, Y., Goto, K. & Masaki, T. (1988). "A novel potent vasoconstrictor peptide produced by vascular endothelial cells." *Nature* **332**(6163): 411-415.

Yang, T., Terada, Y., Nonoguchi, H., Ujiie, K., Tomita, K. & Marumo, F. (1993). "Effect of hyperosmolality on production and mRNA expression of ET-1 in inner medullary collecting duct." *Am J Physiol* **264**(4 Pt 2): F684-689.

Yoshizumi, M., Perrella, M. A., Burnett, J. C., Jr. & Lee, M. E. (1993). "Tumor necrosis factor downregulates an endothelial nitric oxide synthase mRNA by shortening its half-life." *Circ Res* **73**(1): 205-209.

Young, D., Kingsley, S., Ryan, K. & Dutko, F. (1993). "Selective inactivation of eukaryotic B-galactosidase in assays for inhibitors of HIV-1 TAT using bacterial B-galactosidase as a reporter enzyme." *Analytical Biochemistry* **215**: 24-30.

Yukimura, T., Notoya, M., Mizojiri, K., Mizuhira, V., Matsuura, T., Ebara, T., Miura, K., Kim, S., Iwao, H. & Song, K. (1996). "High resolution localization of endothelin receptors in rat renal medulla." *Kidney Int* **50**(1): 135-147.

Zeidel, M., Brady, H., Kone, B., Gullans, S. & Brenner, B. M. (1989). "Endothelin, a peptide inhibitor of Na(+)-K(+)-ATPase in intact renaltubular epithelial cells." *Am J Physiol* **257**(6Pt1): C1101-1107.

Zhuo, J., Dean, R., Maric, C., Aldred, P. G., Harris, P., Alcorn, D. & Mendelsohn, F. A. (1998). "Localization and interactions of vasoactive peptide receptors in renomedullary interstitial cells of the kidney." *Kidney Int Suppl* **67**: S22-28.

Zimmermann, K., Opitz, N., Dedio, J., Renne, C., Muller-Esterl, W. & Oess, S. (2002). "NOSTRIN: A protein modulating nitric oxide and subcellular distribution of endothelial nitric oxide synthase." *Proc Natl Acad Sci USA* **99**(26): 17167-17172.

APPENDIX

Additional publication

The following publication arose from a 10 week project carried out during the first year of my 4 year Ph.D. under the supervision of Professor Jonathan Bard, Department of Biomedical Sciences, University of Edinburgh.

Bard, J. B. L., Gordon, A., Sharp, L. & Sellers, W. I. (2001). "Early nephron formation in the developing mouse kidney." *J Anat* **199:** 385-92.